Picking the best isoform

Picking the best isoform

PDE4D isoforms as therapeutic targets in Alzheimer's disease

Dean Paes

ISBN: 978-94-6469-525-0
Picking the best isoform: PDE4D isoforms as therapeutic targets in Alzheimer's disease

Cover design by Dean Paes

Image of 4WZI (Cedervall P, Aulabaugh A, Geoghegan KF, McLellan TJ, Pandit J. (2015) Engineered stabilization and structural analysis of the autoinhibited conformation of PDE4. Proc Natl Acad Sci U S A. Mar 24;112(12):E1414-22. doi: 10.1073/pnas.1419906112. created with The PyMOL Molecular Graphics System, Schrödinger, LLC. Background image by Max Griss.

Printed by Ipskamp Printing

Picking the best isoform

PDE4D isoforms as therapeutic targets in Alzheimer's disease

PROEFSCHRIFT

Ter verkrijging van de graad van doctor aan de Universiteit Maastricht,

op gezag van de Rector Magnificus, Prof. dr. P. Habibović

en

de graad van doctor in de Biomedische wetenschappen door de Universiteit Hasselt/tUL, op gezag van de Rector, Prof. dr. Bernard Vanheusden

volgens het besluit van het College van Decanen

in het openbaar te verdedigen op

vrijdag 17 november 2023 om 10.00 uur

door

Dean Paes

Promotores
Prof. dr. Daniël van den Hove (Maastricht University)
Dr. Tim Vanmierlo (Hasselt University)

Co-promotor
Prof. dr. Niels Hellings (Hasselt University)

Assessment committee
Prof. dr. Bart Rutten (chair, Maastricht University)
Prof. dr. Ilse Dewachter (Hasselt University)
Dr. Robbert Havekes (University of Groningen)
Dr. David Henderson (Mironid Ltd., Glasgow, United Kingdom)

The research described in this thesis was financially supported by:

Table of Contents

Chapter 1

General Introduction

A visualized, non-expert version of this introductory chapter can be accessed using the following QR-code or hyperlink. Both link to a 3-minute, Dutch spoken video in which I explain the background and general aim of this thesis: Video Summary

Memory, dementia, and Alzheimer's

At this very moment, whilst reading this text, your body is processing a tremendous amount of information unrelated to the reading to get a sense of what is happening on the inside and outside. Although the focus may be on the visual information coming from these words, other stimuli, for example tactile information coming from holding this booklet or electronic device, is constantly being sent to the brain. The brain receives all incoming information, but only focuses on those stimuli that are deemed important. Evolutionary, it is beneficial to be able to recognize and prioritize situations or states of being, that are deemed important, in order to respond to or handle them in a manner that ensures survival and/or the production of offspring. The ability to form and store memories ensures that experiences can be 'captured' and that an individual can respond aptly to future, similar situations. One could argue that one's memory, in part, creates one's personality as it determines how someone behaves in and responds to specific similar or related situations. At the personal level, memory formation and storage allows to keep, in a literal sense, cheerful moments and loved ones in mind. If this information stays 'out of mind' ('demens' in Latin), a person may suffer from dementia. Clearly, memory impairments cause a tremendous burden on patients suffering from dementia, their family members, and caregivers.

The most common cause of dementia is Alzheimer's disease (AD). AD is associated with progressive memory impairments and is characterized by the toxic buildup and aggregation of amyloid-β (Aβ) and tau, the aggregates of which are referred to as plaques and tangles, respectively. While the pathological

characteristics are similar, a distinction can be made between familial and sporadic AD. Familial AD typically develops earlier in life than sporadic AD and is associated with mutations in the amyloid precursor protein (*APP*) and presenilin (*PSEN1* and *PSEN2*) genes (Bertram and Tanzi, 2008). In contrast, sporadic AD, which is more prevalent, is not associated with mutations in these genes, but can be linked to other genetic risk factors (described in detail by Bellenguez et al. (2022) and Bertram and Tanzi (2008)). Next to genetic aspects, environmental and lifestyle factors can influence the development and progression of AD (reviewed by Stozická et al. (2007)). Although the different forms of AD and the associated neuropathology can involve different underlying causal mechanisms, similar consequences are being observed within the brains of AD patients. Overall, Aβ plaques and tau tangles are associated with neuro-inflammation as the brain reacts to these neurotoxic buildups with an immunological response. This inflammatory environment and the plaques and tangles themselves negatively impact neuronal function and survival and the ability of neurons and other cell types to promote (neuro)plasticity. Neuroplasticity can be described as the brain's ability to effectively respond and adapt to incoming stimuli by promoting mitosis (e.g. neurogenesis), phenotypic changes (e.g. cell differentiation), and morphological changes (e.g. the number of synaptic connections and the growth and/or extension of neuronal axons and dendrites). These neuroplasticity mechanisms are crucial for effective memory consolidation. In AD, neuroplasticity has been shown to be impaired as AD brains exhibit neurodegeneration and neurons with less complex morphologies (Teter and Ashford, 2002). It has been widely found that Aβ exposure reduces neurite outgrowth in cell culture experiments, which indicates the direct effect of AD pathology on neuronal morphology (e.g. (Kwon et al., 2010)). Neurite outgrowth is just one process that is affected in AD, but also the number of dendrites, dendritic length, and dendritic spine density have been found to be reduced by Aβ exposure (Cui et al., 2019).

As AD progresses, the pathological Aβ plaques and tau tangles become more abundant and widespread throughout the brain causing increased neuro-inflammation and impaired neuroplasticity (Braak and Braak, 1991). Brain regions important in memory functioning (e.g. the basal forebrain and hippocampus) appear to be particularly sensitive to AD-associated pathology (Brueggen et al., 2015; Schmitz et al., 2016). The hippocampus is a crucial brain structure in consolidating information in long-term memory. In addition, the basal forebrain signals to the hippocampus using the neurotransmitter acetylcholine to facilitate memory consolidation. Hence, degeneration of both the basal forebrain and hippocampus in response to AD-associated pathology has detrimental effects on the ability to store memories.

Based on the rationale that acetylcholine signaling from the basal forebrain is diminished in AD, several types of medication have been developed in an effort to compensate for decreased cholinergic signaling. At the time of writing, five molecules have been approved for the treatment of AD: donepezil, rivastigmine, galantamine, memantine, and (in the United States only) aducanumab. The first three molecules belong to the class of acetylcholinesterase inhibitors (AChEI) and increase cholinergic signaling by inhibiting the enzymatic breakdown of acetylcholine. Memantine blocks the N-methyl-D-aspartate (NMDA) receptor and thereby can reduce neurotoxicity by preventing 'overexcitation' of neurons that may be caused by an imbalanced excitatory/inhibitory neuron ratio. Noteworthy, memantine has also been reported to block specific acetylcholine receptors (i.e. α7 nicotinic acetylcholine receptors) (Aracava et al., 2005), which is a mechanism that can also promote memory-enhancing effects as reported by myself and my research group, and others in cell and animal studies (Hahn et al., 2011; van Goethem et al., 2019). Aducanumab, which has only recently been approved by the Food and Drug Administration (FDA), yet rejected by the European Medicines Agency (EMA), has been developed to reduce Aβ plaques in the brain, but its clinical efficacy and safety

are, despite its approval, still under debate (Sevigny et al., 2016). Clearly, functional memory improvements of current AD medication are only modest and often associated with severe side effects, e.g. diarrhea (AChEI), obstipation (memantine), nausea and vomiting (AChI and memantine), or brain swelling and brain bleeding (aducanumab) (Casey et al., 2010; Seibert et al., 2021). Hence, novel approaches are crucial for efficacious and safe treatment of memory impairments in AD.

'Memory molecules'

To facilitate the discovery and development of new pharmacological compounds, understanding the molecular signaling cascades underlying memory consolidation is essential. In other words, which molecules are important for memory formation? Fundamental insights into these 'memory molecules' have been gathered through the seminal work of Eric Kandel and Paul Greengard (Kandel, 2012; Walaas and Greengard, 1991). It has now been well-established that upon binding of neurotransmitters, specific signaling cascades can be initiated in neurons. Many of these cascades, including those elicited by cholinergic signaling, involve the conversion of adenosine triphosphate (ATP) into the signaling molecule cyclic adenosine monophosphate (cAMP) by the enzyme adenylate cyclase (AC). cAMP can then activate, among other molecules, protein kinase A (PKA), which by itself can induce changes by phosphorylating target proteins. For example, phosphorylation by PKA can lead to sensitization of neurotransmitter receptors, which facilitates the connectivity between two neurons. Particularly important for long-term memory formation is PKA-mediated phosphorylation of the transcription factor cAMP response element-element binding protein (CREB) (Kandel, 2012). Upon its phosphorylation, CREB induces the transcription of several genes that promote neuroplasticity. Through these transcription-dependent mechanisms, several changes that strengthen synaptic connections between neurons are being induced. These changes comprise, for example, physiological changes owing to the synthesis

of neurotransmitter receptors and morphological changes via the formation of axons and dendrites.

Thus, the cAMP-PKA-CREB signaling cascade is of utmost important for functional memory consolidation. This notion is also supported by the observation that cAMP-PKA-CREB signaling is decreased in AD (reviewed in: (Kelly, 2018)). As such, pharmacological modulation of this pathway provides opportunities to restore memory functioning in AD. While the synthesis of cAMP occurs specifically by AC, its hydrolytic degradation is regulated exclusively via members of the superfamily of phosphodiesterase (PDE) enzymes. Hence, these PDEs provide interesting targets to specifically modulate cAMP levels and associated signaling.

The PDE superfamily consists of 11 gene families (PDE1-PDE11), which are categorized based on functional protein domains and substrate selectively (Baillie et al., 2019; Bender and Beavo, 2006; Chapter 2: Paes et al., 2021). Next to hydrolyzing cAMP, certain members of the PDE enzyme family degrade the closely related cyclic guanosine monophosphate (cGMP). In fact, the gene families PDE1, PDE2, PDE3, PDE10, and PDE11 can degrade both cAMP and cGMP. PDE5, PDE6, and PDE9 specifically break down cGMP, whilst PDE4, PDE7, and PDE8 are selective towards cAMP. Given the importance of cAMP in memory consolidation signaling, the cAMP-selective PDE families are interesting targets to modulate this signaling. By inhibiting these PDE enzymes in the brain, cAMP degradation can be diminished, leading to stimulation of memory consolidation processes.

PDE4 enzymes and PDE4-macology

Historically, most research has been conducted on the PDE4 family, as for a long time, no selective PDE7 and PDE8 inhibitors were available. In studies as early as in 1976, the archetypical PDE4 inhibitor rolipram was used to identify and inhibit cAMP-specific PDE activity (Schwabe et al., 1976). Rolipram was also found to be able to inhibit activity of the Drosophila enzyme encoded by the *dunce* gene, which plays

a pivotal role in learning and memory (Davis et al., 1989; Dudai, 1988). Subsequently, rolipram-sensitive PDE4 enzyme orthologues of *dunce* were discovered in rats and humans and observed to be expressed in brain tissue (Bolger et al., 1993; Davis et al., 1989; Schwabe et al., 1976; Swinnen et al., 1989a; b). These findings, together with clinical studies using rolipram as a potential antidepressant, strongly suggested that PDE4 inhibition has effects in the mammalian brain. Accordingly, several studies found that PDE4 inhibition is able to preserve intact memory and restore impaired memory in rodents (Egawa et al., 1997; Rutten et al., 2007; Vanmierlo et al., 2016). In addition, PDE4 inhibition has been shown to reduce neuroinflammation and protect against neuronal death (Pearse and Hughes, 2016; Vilhena et al., 2021). As both neuroinflammation and neuronal death are hallmarks of AD, PDE4 inhibitors are promising candidates to prevent, slow down or halt the progression of AD (Guerriero et al., 2017).

Consequently, the therapeutic potential of PDE4 inhibition to treat AD has been examined in preclinical studies. In different animal models of AD, inhibition of PDE4 was found to restore neuroplasticity, reduce neuroinflammation and/or improve memory performance (Gong et al., 2004; Guo et al., 2017; Shi et al., 2021; Vitolo et al., 2002; Zhang et al., 2004). Furthermore, the PDE4 inhibitor roflumilast was found to enhance verbal learning in both young and old healthy individuals (Blokland et al., 2019; Van Duinen et al., 2018). Despite these beneficial effects, clinical use of PDE4 inhibitors has been hampered so far due to the occurrence of adverse side effects including nausea, emesis, headache, and diarrhea (Compton et al., 2001). PDE4 enzymes, as pivotal regulators of cAMP signaling, are expressed in many organs and in different cell types, which can produce unwanted effects additional to the therapeutic actions in the brain. Hence, PDE4 inhibition as a therapeutic strategy should be optimized in order to improve efficacy and safety.

The memory-modulating PDE4D subtype

The PDE4 gene family comprises multiple members. Four different PDE4 genes exist (PDE4A-D). These various genes encode subtypes of PDE4 enzymes with distinct amino acid sequences (Bolger et al., 1993; Bolger, 1994; Johnson et al., 2010; Milatovich et al., 1994). Hence, targeting specific PDE4 subtypes may provide a promising opportunity to enhance memory functioning while minimizing or preventing side effects. Using PDE4 subtype-selective inhibitors, Zhang et al. identified that inhibition of PDE4D, rather than PDE4B, displayed most potent memory-enhancing effects in rodents (Zhang et al., 2017). Additional support for a role of PDE4D in cognition has been provided by the fact that mutations in PDE4D are associated with the neurodevelopmental disorder acrodysostosis (Lee et al., 2012). Moreover, genetic variation in the *PDE4D* gene has been associated with human cognitive performance (Gurney, 2019). In addition, expression of PDE4D was found to correlate negatively with cognitive performance in an aging study using monozygotic twins (Mohammadnejad et al., 2021). In patients suffering from mild cognitive impairment and AD, polymorphisms in the *PDE4D* gene were found to affect the functional network brain activity (Xiang et al., 2020).

Thus, given its involvement in cognition, PDE4D may provide a more specific target for pharmacological interventions to treat memory problems in AD. As a result, efforts have been made to develop PDE4D-selective inhibitors, which show pro-cognitive effects in animal studies (Brullo et al., 2016; Bruno et al., 2011; Bruno et al., 2009; Burgin et al., 2010; Ricciarelli et al., 2017; Sierksma et al., 2014; Wang et al., 2020; Zhang et al., 2018). Despite the efficacy of PDE4D-selective inhibition, PDE4D inhibition seems to induce emetic side effects elicited through α_2-adrenoceptor-mediated mechanisms in the brainstem, which would hamper their clinical use (Robichaud et al., 2001; Robichaud et al., 2002). Recently, studies by the Richter laboratory have indicated that other side effects observed upon PDE4 inhibition (i.e. hypothermia and gastroparesis) are not predominantly mediated by PDE4D but are

rather a result of inhibition or more than one PDE4 subtype (Boyd et al., 2021; McDonough et al., 2020a; McDonough et al., 2020b). Thus, compared to the complete side effect profile of non-specific PDE4 inhibitors, PDE4D selective inhibitors may show fewer or less intense side effects. Indeed, certain PDE4D inhibitors have shown to be less emetic than non-specific PDE4 inhibitors (Bruno et al., 2011; Ricciarelli et al., 2017; Zhang et al., 2018), which may be a result of the fact that the PDE4D-selective inhibition elicits effects in the brainstem (emesis) but does not impact the stomach (gastroparesis). However, considering the role of PDE4D in brainstem-mediated emetic side effects, these side effects may have to be prevented or circumvented in order to fully exploit PDE4D inhibition as a safe and efficacious treatment strategy to ameliorate memory problems in AD.

The importance of isoforms

Interestingly, the *PDE4D* gene encodes different transcript variants that translate into different protein isoforms. As PDE4D subtypes and isoforms are expressed in a tissue-dependent and cell-type-specific manner (Miró et al., 2002a; Miró et al., 2002b; Pérez-Torres et al., 2000), inhibition of specific isoforms can produce different physiological and/or behavioral effects. Hence, inhibition of specific PDE4D isoforms may produce memory-enhancing effects while minimizing adverse PDE4-mediated side effects.

Although it has been well-established that different PDE4 subtypes and isoforms are cell-type specifically expressed and localize to specific intracellular compartments (Blackman et al., 2011), the role of specific PDE4D isoforms in memory processes has only sporadically been described. One study using very few samples has reported PDE4D isoform expression in post-mortem brain material of AD patients and healthy individuals (McLachlan et al., 2007). Another study found no difference in PDE4D expression in brain material of AD patients and controls, but in this study the expression of the individual PDE4D isoforms was not specified (Ugarte

et al., 2015). Therefore, it remains unknown which isoforms are important for memory processes and would thus be appropriate targets for the treatment of memory problems associated with AD. Identification of the PDE4D isoforms involved in memory processes (in AD) will allow for target specification so that treatment efficacy can be maintained whilst minimizing side effects.

Alternatively, approaches to reduce the therapeutic dose of PDE4(D) inhibitors will decrease the risk of PDE4-mediated adverse side effects. Given the fact that multiple PDE gene families can degrade cAMP and that they localize to specific intracellular compartments, inhibition of PDE4(D) and other cAMP-degrading PDEs can have synergistic effects. Using this synergistic treatment, the therapeutic dose of PDE4(D) could be lowered, which would reduce the occurrence of possible side effects.

Goals and outline of the thesis

With the purpose of finding new treatment strategies to efficaciously and safely inhibit PDE4(D), in order to stimulate memory consolidation processes as a treatment for AD, the goals of this thesis are:

- To identify which PDE4D isoforms are involved in neuroplasticity processes that are impaired by AD-associated pathology
- To investigate the therapeutic potential of using combined treatments to reduce the therapeutic dose of PDE4(D) inhibitors

By means of literature research and *in vivo*, *in vitro*, and *in silico* experimental approaches, these goals were pursued as outlined in the following chapters.

Chapter 2 provides a comprehensive review on a myriad of aspects of PDE4 enzymes as pharmacological targets. Firstly, all currently known PDE4 subtypes,

transcript variants, and isoforms in humans and rodents are defined. To determine which PDE4(D) isoform should be picked as optimal therapeutic target in AD, an understanding those PDE4(D) isoforms existing is crucial. Both in the scientific literature and in online databases, inconsistencies in classification appear. Specifically, mRNA molecules that are different in sequence, but stem from the same gene would be referred to as transcript variants. As these different mRNA species differ in sequence, they can encode for protein products with distinct amino acid sequences that would be referred to as (protein) isoforms. Difficulties arise in classifying and comparing these transcript variants and isoforms as online databases (e.g. Ensembl and NCBI Gene) use different annotations. Additional discrepancies exist in the naming of orthologues across species (e.g. the rodent equivalents of human PDE4A isoforms are named differently). Hence, it is crucial to have a proper understanding of how the four distinct PDE4 genes encode the different transcript variants that translate to different protein isoforms for different species. The obtained understanding of PDE4D gene, mRNA, and protein sequences is critical for translational experiments described in **Chapter 3** and **Chapter 4**. Secondly, the effects of inherent, structural features of the different PDE4 isoforms on their enzymatic activity are being described. Furthermore, per isoform, the consequences of post-translational modifications and their interactions with other proteins, on enzyme activity and inhibitor binding are outlined. Specific post-translational modifications are investigated *in silico* in more detail in **Chapter 5**. This information is followed up by a detailed description of a large list of PDE4 inhibitors and their affinity for PDE4 subtypes, isoforms, and conformations. Insights acquired from this overview are then discussed in light of PDE4 inhibitor screening pipelines and are used to better put preclinical findings into context in **Chapter 6**. Next, strategies for target specification and approaches to develop subtype- and isoform-specific PDE4 inhibitors are described. Lastly, PDE4 inhibitors are compared regarding their ability

to elicit side effects and potential molecular mechanisms underlying these side effects are pointed out.

Chapter 3 presents an experimental study that investigated which PDE4D isoforms display altered transcriptional regulation in AD and may therefore be (more) suitable therapeutic targets. In this study, human post-mortem temporal lobe brain material of AD patients and healthy controls is used, in which the epigenetic signature of the *PDE4D* gene is measured. In addition, mRNA expression levels of PDE4D isoforms are determined. Both the epigenetic and transcriptional profiles are correlated with the degrees of AD-associated pathology in the tissue and the subject's degree of cognitive decline.

Complementing and following up on the previous chapter, **Chapter 4** demonstrates a series of experiments in which PDE4D isoform expression changes are determined in the hippocampus and frontal cortex of transgenic AD mice. Furthermore, the effects of pharmacological PDE4D inhibition on neurite outgrowth of neuronal cells in both the presence and absence of amyloid-β are described. Most importantly, the potential of PDE4D isoform-specific inhibition targeted at facilitating neurite outgrowth and protecting against amyloid-β is examined by means of *in vitro* CRISPR-Cas9-mediated knockout experiments.

In **Chapter 5**, a computational model of PDE4 isoform-mediated cAMP signaling is presented. The model was used to simulate how different PDE4 isoforms dynamically control cAMP levels and downstream signaling over time. By implementing isoform-specific feedback mechanisms (as also reviewed in **Chapter 2**), the importance of specific PDE4 isoform types in cAMP regulation is being highlighted.

Beyond the context of AD and as an alternative to increasing treatment-specificity by targeting PDE4D isoforms, **Chapter 6** presents the potential of combined PDE2-PDE4 inhibition to promote neuroplasticity processes *in vitro* and enhance memory consolidation *in vivo*. It is revealed that PDE2 and PDE4 inhibitors

work synergistically, thereby requiring lower doses of each, which likely minimizes the occurrence of adverse side effects.

In the concluding **Chapter 7**, the acquired insights from the previous chapters are being put into perspective, considering experimental strengths and limitations. Ultimately, an outlook is provided for future research to be explored in order to eventually let AD patients benefit from efficacious and safe (isoform-specific) PDE4(D) inhibitors.

REFERENCES

Aracava Y, Pereira EFR, Maelicke A and Albuquerque EX (2005) Memantine Blocks α7[*] Nicotinic Acetylcholine Receptors More Potently Than N-Methyl-D-aspartate Receptors in Rat Hippocampal Neurons. *Journal of Pharmacology and Experimental Therapeutics* **312**:1195-1205.

Baillie GS, Tejeda GS and Kelly MP (2019) Therapeutic targeting of 3',5'-cyclic nucleotide phosphodiesterases: inhibition and beyond. *Nat Rev Drug Discov* **18**:770-796.

Bellenguez C, Küçükali F, Jansen IE, Kleineidam L, Moreno-Grau S, Amin N, Naj AC, Campos-Martin R, Grenier-Boley B, Andrade V, Holmans PA, Boland A, Damotte V, van der Lee SJ, Costa MR, Kuulasmaa T, Yang Q, de Rojas I, Bis JC, Yaqub A, Prokic I, Chapuis J, Ahmad S, Giedraitis V, Aarsland D, Garcia-Gonzalez P, Abdelnour C, Alarcón-Martín E, Alcolea D, Alegret M, Alvarez I, Álvarez V, Armstrong NJ, Tsolaki A, Antúnez C, Appollonio I, Arcaro M, Archetti S, Pastor AA, Arosio B, Athanasiu L, Bailly H, Banaj N, Baquero M, Barral S, Beiser A, Pastor AB, Below JE, Benchek P, Benussi L, Berr C, Besse C, Bessi V, Binetti G, Bizarro A, Blesa R, Boada M, Boerwinkle E, Borroni B, Boschi S, Bossù P, Bråthen G, Bressler J, Bresner C, Brodaty H, Brookes KJ, Brusco LI, Buiza-Rueda D, Bûrger K, Burholt V, Bush WS, Calero M, Cantwell LB, Chene G, Chung J, Cuccaro ML, Carracedo Á, Cecchetti R, Cervera-Carles L, Charbonnier C, Chen H-H, Chillotti C, Ciccone S, Claassen JAHR, Clark C, Conti E, Corma-Gómez A, Costantini E, Custodero C, Daian D, Dalmasso MC, Daniele A, Dardiotis E, Dartigues J-F, de Deyn PP, de Paiva Lopes K, de Witte LD, Debette S, Deckert J, del Ser T, Denning N, DeStefano A, Dichgans M, Diehl-Schmid J, Diez-Fairen M, Rossi PD, Djurovic S, Duron E, Düzel E, Dufouil C, Eiriksdottir G, Engelborghs S, Escott-Price V, Espinosa A, Ewers M, Faber KM, Fabrizio T, Nielsen SF, Fardo DW, Farotti L, Fenoglio C, Fernández-Fuertes M, Ferrari R, Ferreira CB, Ferri E, Fin B, Fischer P, Fladby T, Fließbach K, Fongang B, Fornage M, Fortea J, Foroud TM, Fostinelli S, Fox NC, Franco-Macías E, Bullido MJ, Frank-García A, Froelich L, Fulton-Howard B, Galimberti D, García-Alberca JM, García-González P, Garcia-Madrona S, Garcia-Ribas G, Ghidoni R, Giegling I, Giorgio G, Goate AM, Goldhardt O, Gomez-Fonseca D, González-Pérez A, Graff C, Grande G, Green E, Grimmer T, Grünblatt E, Grunin M, Gudnason V, Guetta-Baranes T, Haapasalo A, Hadjigeorgiou G, Haines JL, Hamilton-Nelson KL, Hampel H, Hanon O, Hardy J, Hartmann AM, Hausner L, Harwood J, Heilmann-Heimbach S, Helisalmi S, Heneka MT, Hernández I, Herrmann MJ, Hoffmann P, Holmes C, Holstege H, Vilas RH, Hulsman M, Humphrey J, Biessels GJ, Jian X, Johansson C, Jun GR, Kastumata Y, Kauwe J, Kehoe PG, Kilander L, Ståhlbom AK, Kivipelto M, Koivisto A, Kornhuber J, Kosmidis MH, Kukull WA, Kuksa PP, Kunkle BW, Kuzma AB, Lage C, Laukka EJ, Launer L, Lauria A, Lee C-Y, Lehtisalo J, Lerch O, Lleó A, Longstreth W, Lopez O, de Munain AL, Love S, Löwemark M, Luckcuck L, Lunetta KL, Ma Y, Macías J, MacLeod CA, Maier W, Mangialasche F, Spallazzi M, Marquié M, Marshall R, Martin ER, Montes AM, Rodríguez CM, Masullo C, Mayeux R, Mead S, Mecocci P, Medina M, Meggy A, Mehrabian S, Mendoza S, Menéndez-González M, Mir P, Moebus S, Mol M, Molina-Porcel L, Montrreal L, Morelli L, Moreno F, Morgan K, Mosley T, Nöthen

MM, Muchnik C, Mukherjee S, Nacmias B, Ngandu T, Nicolas G, Nordestgaard BG, Olaso R, Orellana A, Orsini M, Ortega G, Padovani A, Paolo C, Papenberg G, Parnetti L, Pasquier F, Pastor P, Peloso G, Pérez-Cordón A, Pérez-Tur J, Pericard P, Peters O, Pijnenburg YAL, Pineda JA, Piñol-Ripoll G, Pisanu C, Polak T, Popp J, Posthuma D, Priller J, Puerta R, Quenez O, Quintela I, Thomassen JQ, Rábano A, Rainero I, Rajabli F, Ramakers I, Real LM, Reinders MJT, Reitz C, Reyes-Dumeyer D, Ridge P, Riedel-Heller S, Riederer P, Roberto N, Rodriguez-Rodriguez E, Rongve A, Allende IR, Rosende-Roca M, Royo JL, Rubino E, Rujescu D, Sáez ME, Sakka P, Saltvedt I, Sanabria Á and Sánchez-Arjona MB (2022) New insights into the genetic etiology of Alzheimer's disease and related dementias. *Nature Genetics* **54**:412-436.

Bender AT and Beavo JA (2006) Cyclic nucleotide phosphodiesterases: molecular regulation to clinical use. *Pharmacol Rev* **58**:488-520.

Bertram L and Tanzi RE (2008) Thirty years of Alzheimer's disease genetics: the implications of systematic meta-analyses. *Nature reviews Neuroscience* **9**:768-778.

Blackman BE, Horner K, Heidmann J, Wang D, Richter W, Rich TC and Conti M (2011) PDE4D and PDE4B function in distinct subcellular compartments in mouse embryonic fibroblasts. *J Biol Chem* **286**:12590-12601.

Blokland A, Van Duinen MA, Sambeth A, Heckman PRA, Tsai M, Lahu G, Uz T and Prickaerts J (2019) Acute treatment with the PDE4 inhibitor roflumilast improves verbal word memory in healthy old individuals: a double-blind placebo-controlled study. *Neurobiol Aging* **77**:37-43.

Bolger G, Michaeli T, Martins T, St John T, Steiner B, Rodgers L, Riggs M, Wigler M and Ferguson K (1993) A family of human phosphodiesterases homologous to the dunce learning and memory gene product of Drosophila melanogaster are potential targets for antidepressant drugs. *Mol Cell Biol* **13**:6558-6571.

Bolger GB (1994) Molecular biology of the cyclic AMP-specific cyclic nucleotide phosphodiesterases: a diverse family of regulatory enzymes. *Cell Signal* **6**:851-859.

Boyd A, Aragon IV, Rich J, McDonough W, Oditt M, Irelan D, Fiedler E, Abou Saleh L and Richter W (2021) Assessment of PDE4 Inhibitor-Induced Hypothermia as a Correlate of Nausea in Mice. *Biology* **10**.

Braak H and Braak E (1991) Neuropathological stageing of Alzheimer-related changes. *Acta Neuropathol* **82**:239-259.

Brueggen K, Dyrba M, Barkhof F, Hausner L, Filippi M, Nestor PJ, Hauenstein K, Klöppel S, Grothe MJ, Kasper E and Teipel SJ (2015) Basal Forebrain and Hippocampus as Predictors of Conversion to Alzheimer's Disease in Patients with Mild Cognitive Impairment - A Multicenter DTI and Volumetry Study. *J Alzheimers Dis* **48**:197-204.

Brullo C, Ricciarelli R, Prickaerts J, Arancio O, Massa M, Rotolo C, Romussi A, Rebosio C, Marengo B, Pronzato MA, van Hagen BTJ, van Goethem NP, D'Ursi P, Orro A, Milanesi L, Guariento S, Cichero E, Fossa P, Fedele E and Bruno O (2016) New insights into selective PDE4D inhibitors: 3-(Cyclopentyloxy)-4-methoxybenzaldehyde O-(2-(2,6-dimethylmorpholino)-2-oxoethyl) oxime (GEBR-7b) structural development and promising activities to restore memory impairment. *Eur J Med Chem* **124**:82-102.

Bruno O, Fedele E, Prickaerts J, Parker LA, Canepa E, Brullo C, Cavallero A, Gardella E, Balbi A, Domenicotti C, Bollen E, Gijselaers HJ, Vanmierlo T, Erb K, Limebeer CL, Argellati F, Marinari UM, Pronzato MA and Ricciarelli R (2011) GEBR-7b, a novel PDE4D selective inhibitor that improves memory in rodents at non-emetic doses. *Br J Pharmacol* **164**:2054-2063.

Bruno O, Romussi A, Spallarossa A, Brullo C, Schenone S, Bondavalli F, Vanthuyne N and Roussel C (2009) New selective phosphodiesterase 4D inhibitors differently acting on long, short, and supershort isoforms. *J Med Chem* **52**:6546-6557.

Burgin AB, Magnusson OT, Singh J, Witte P, Staker BL, Bjornsson JM, Thorsteinsdottir M, Hrafnsdottir S, Hagen T, Kiselyov AS, Stewart LJ and Gurney ME (2010) Design of phosphodiesterase 4D (PDE4D) allosteric modulators for enhancing cognition with improved safety. *Nat Biotechnol* **28**:63-70.

Casey DA, Antimisiaris D and O'Brien J (2010) Drugs for Alzheimer's disease: are they effective? *P & T : a peer-reviewed journal for formulary management* **35**:208-211.

Compton CH, Gubb J, Nieman R, Edelson J, Amit O, Bakst A, Ayres JG, Creemers JP, Schultze-Werninghaus G, Brambilla C and Barnes NC (2001) Cilomilast, a selective phosphodiesterase-4 inhibitor for treatment of patients with chronic obstructive pulmonary disease: a randomised, dose-ranging study. *Lancet* **358**:265-270.

Cui S-Y, Yang M-X, Zhang Y-H, Zheng V, Zhang H-T, Gurney ME, Xu Y and O'Donnell JM (2019) Protection from Amyloid β Peptide–Induced Memory, Biochemical, and Morphological Deficits by a Phosphodiesterase-4D Allosteric Inhibitor. *Journal of Pharmacology and Experimental Therapeutics* **371**:250-259.

Davis RL, Takayasu H, Eberwine M and Myres J (1989) Cloning and characterization of mammalian homologs of the Drosophila dunce+ gene. *Proceedings of the National Academy of Sciences of the United States of America* **86**:3604-3608.

Dudai Y (1988) Neurogenetic Dissection of Learning and Short-Term Memory in Drosophila. *Annual Review of Neuroscience* **11**:537-563.

Egawa T, Mishima K, Matsumoto Y, Iwasaki K, Iwasaki K and Fujiwara M (1997) Rolipram and its optical isomers, phosphodiesterase 4 inhibitors, attenuated the scopolamine-induced impairments of learning and memory in rats. *Japanese journal of pharmacology* **75**:275-281.

Gong B, Vitolo OV, Trinchese F, Liu S, Shelanski M and Arancio O (2004) Persistent improvement in synaptic and cognitive functions in an Alzheimer mouse model after rolipram treatment. *The Journal of clinical investigation* **114**:1624-1634.

Guerriero F, Sgarlata C, Francis M, Maurizi N, Faragli A, Perna S, Rondanelli M, Rollone M and Ricevuti G (2017) Neuroinflammation, immune system and Alzheimer disease: searching for the missing link. *Aging clinical and experimental research* **29**:821-831.

Guo H, Cheng Y, Wang C, Wu J, Zou Z, Niu B, Yu H, Wang H and Xu J (2017) FFPM, a PDE4 inhibitor, reverses learning and memory deficits in APP/PS1 transgenic mice via cAMP/PKA/CREB signaling and anti-inflammatory effects. *Neuropharmacology* **116**:260-269.

Gurney ME (2019) Genetic Association of Phosphodiesterases With Human Cognitive Performance. *Front Mol Neurosci* **12**:22.

Hahn B, Shoaib M and Stolerman IP (2011) Selective nicotinic receptor antagonists: effects on attention and nicotine-induced attentional enhancement. *Psychopharmacology* **217**:75.

Johnson KR, Nicodemus-Johnson J and Danziger RS (2010) An evolutionary analysis of cAMP-specific Phosphodiesterase 4 alternative splicing. *BMC evolutionary biology* **10**:247.

Kandel ER (2012) The molecular biology of memory: cAMP, PKA, CRE, CREB-1, CREB-2, and CPEB. *Molecular Brain* **5**:14.

Kelly MP (2018) Cyclic nucleotide signaling changes associated with normal aging and age-related diseases of the brain. *Cell Signal* **42**:281-291.

Kwon KJ, Kim HJ, Shin CY and Han SH (2010) Melatonin Potentiates the Neuroprotective Properties of Resveratrol Against Beta-Amyloid-Induced Neurodegeneration by Modulating AMP-Activated Protein Kinase Pathways. *Journal of clinical neurology (Seoul, Korea)* **6**:127-137.

Lee H, Graham JM, Jr., Rimoin DL, Lachman RS, Krejci P, Tompson SW, Nelson SF, Krakow D and Cohn DH (2012) Exome sequencing identifies PDE4D mutations in acrodysostosis. *Am J Hum Genet* **90**:746-751.

McDonough W, Aragon IV, Rich J, Murphy JM, Abou Saleh L, Boyd A, Koloteva A and Richter W (2020a) PAN-selective inhibition of cAMP-phosphodiesterase 4 (PDE4) induces gastroparesis in mice. *FASEB J*.

McDonough W, Rich J, Aragon IV, Abou Saleh L, Boyd A, Richter A, Koloteva A and Richter W (2020b) Inhibition of type 4 cAMP-phosphodiesterases (PDE4s) in mice induces hypothermia via effects on behavioral and central autonomous thermoregulation. *Biochem Pharmacol* **180**:114158.

McLachlan CS, Chen ML, Lynex CN, Goh DL, Brenner S and Tay SK (2007) Changes in PDE4D isoforms in the hippocampus of a patient with advanced Alzheimer disease. *Archives of neurology* **64**:456-457.

Milatovich A, Bolger G, Michaeli T and Francke U (1994) Chromosome localizations of genes for five cAMP-specific phosphodiesterases in man and mouse. *Somatic cell and molecular genetics* **20**:75-86.

Miró X, Pérez-Torres S, Artigas F, Puigdomènech P, Palacios JM and Mengod G (2002a) Regulation of cAMP phosphodiesterase mRNAs expression in rat brain by acute and chronic fluoxetine treatment. An in situ hybridization study. *Neuropharmacology* **43**:1148-1157.

Miró X, Pérez-Torres S, Puigdomènech P, Palacios JM and Mengod G (2002b) Differential distribution of PDE4D splice variant mRNAs in rat brain suggests association with specific pathways and presynaptical localization. *Synapse* **45**:259-269.

Mohammadnejad A, Li W, Lund JB, Li S, Larsen MJ, Mengel-From J, Michel TM, Christiansen L, Christensen K, Hjelmborg J, Baumbach J and Tan Q (2021) Global Gene Expression Profiling and Transcription Factor Network Analysis of Cognitive Aging in Monozygotic Twins. *Frontiers in genetics* **12**.

Paes D, Schepers M, Rombaut B, van den Hove D, Vanmierlo T and Prickaerts J (2021) The Molecular Biology of Phosphodiesterase 4 Enzymes as Pharmacological Targets: An Interplay of Isoforms, Conformational States, and Inhibitors. *Pharmacol Rev* **73**:1016-1049.

Pearse DD and Hughes ZA (2016) PDE4B as a microglia target to reduce neuroinflammation. *Glia* **64**:1698-1709.

Pérez-Torres S, Miró X, Palacios JM, Cortés R, Puigdoménech P and Mengod G (2000) Phosphodiesterase type 4 isozymes expression in human brain

examined by in situ hybridization histochemistry and [3H]rolipram binding autoradiography: Comparison with monkey and rat brain. *Journal of Chemical Neuroanatomy* **20**:349-374.

Ricciarelli R, Brullo C, Prickaerts J, Arancio O, Villa C, Rebosio C, Calcagno E, Balbi M, van Hagen BT, Argyrousi EK, Zhang H, Pronzato MA, Bruno O and Fedele E (2017) Memory-enhancing effects of GEBR-32a, a new PDE4D inhibitor holding promise for the treatment of Alzheimer's disease. *Sci Rep* **7**:46320.

Robichaud A, Savoie C, Stamatiou PB, Tattersall FD and Chan CC (2001) PDE4 inhibitors induce emesis in ferrets via a noradrenergic pathway. *Neuropharmacology* **40**:262-269.

Robichaud A, Stamatiou PB, Jin SL, Lachance N, MacDonald D, Laliberte F, Liu S, Huang Z, Conti M and Chan CC (2002) Deletion of phosphodiesterase 4D in mice shortens alpha(2)-adrenoceptor-mediated anesthesia, a behavioral correlate of emesis. *J Clin Invest* **110**:1045-1052.

Rutten K, Lieben C, Smits L and Blokland A (2007) The PDE4 inhibitor rolipram reverses object memory impairment induced by acute tryptophan depletion in the rat. *Psychopharmacology (Berl)* **192**:275-282.

Schmitz TW, Nathan Spreng R, Weiner MW, Aisen P, Petersen R, Jack CR, Jagust W, Trojanowki JQ, Toga AW, Beckett L, Green RC, Saykin AJ, Morris J, Shaw LM, Khachaturian Z, Sorensen G, Kuller L, Raichle M, Paul S, Davies P, Fillit H, Hefti F, Holtzman D, Mesulam MM, Potter W, Snyder P, Schwartz A, Montine T, Thomas RG, Donohue M, Walter S, Gessert D, Sather T, Jiminez G, Harvey D, Bernstein M, Fox N, Thompson P, Schuff N, Borowski B, Gunter J, Senjem M, Vemuri P, Jones D, Kantarci K, Ward C, Koeppe RA, Foster N, Reiman EM, Chen K, Mathis C, Landau S, Cairns NJ, Householder E, Taylor-Reinwald L, Lee V, Korecka M, Figurski M, Crawford K, Neu S, Foroud TM, Potkin S, Shen L, Faber K, Kim S, Nho K, Thal L, Buckholtz N, Albert M, Frank R, Hsiao J, Kaye J, Quinn J, Lind B, Carter R, Dolen S, Schneider LS, Pawluczyk S, Beccera M, Teodoro L, Spann BM, Brewer J, Vanderswag H, Fleisher A, Heidebrink JL, Lord JL, Mason SS, Albers CS, Knopman D, Johnson K, Doody RS, Villanueva-Meyer J, Chowdhury M, Rountree S, Dang M, Stern Y, Honig LS, Bell KL, Ances B, Carroll M, Leon S, Mintun MA, Schneider S, Oliver A, Marson D, Griffith R, Clark D, Geldmacher D, Brockington J, Roberson E, Grossman H, Mitsis E, de Toledo-Morrell L, Shah RC, Duara R, Varon D, Greig MT, Roberts P, Albert M, Onyike C, D'Agostino D, Kielb S, Galvin JE, Cerbone B, Michel CA, Rusinek H, de Leon MJ, Glodzik L, De Santi S, Doraiswamy PM, Petrella JR, Wong TZ, Arnold SE, Karlawish JH, Wolk D, Smith CD, Jicha G, Hardy P, Sinha P, Oates E, Conrad G, Lopez OL, Oakley M, Simpson DM, Porsteinsson AP, Goldstein BS, Martin K, Makino KM, Ismail MS, Brand C, Mulnard RA, Thai G, Mc-Adams-Ortiz C, Womack K, Mathews D, Quiceno M, Diaz-Arrastia R, King R, Weiner M, Martin-Cook K, DeVous M, Levey AI, Lah JJ, Cellar JS, Burns JM, Anderson HS, Swerdlow RH, Apostolova L, Tingus K, Woo E, Silverman DHS, Lu PH, Bartzokis G, Graff-Radford NR, Parfitt F, Kendall T, Johnson H, Farlow MR, Hake A, Matthews BR, Herring S, Hunt C, van Dyck CH, Carson RE, MacAvoy MG, Chertkow H, Bergman H, Hosein C, Black S, Stefanovic B, Caldwell C, Robin Hsiung G-Y, Feldman H, Mudge B, Assaly M, Kertesz A, Rogers J, Bernick C, Munic D, Kerwin D, Mesulam M-M, Lipowski K, Wu C-K, Johnson N, Sadowsky C, Martinez W, Villena T, Turner RS, Johnson K, Reynolds B, Sperling RA, Johnson KA,

Marshall G, Frey M, Lane B, Rosen A, Tinklenberg J, Sabbagh MN, Belden CM, Jacobson SA, Sirrel SA, Kowall N, Killiany R, Budson AE, Norbash A, Johnson PL, Allard J, Lerner A, Ogrocki P, Hudson L, Fletcher E, Carmichael O, Olichney J, DeCarli C, Kittur S, Borrie M, Lee TY, Bartha R, Johnson S, Asthana S, Carlsson CM, Potkin SG, Preda A, Nguyen D, Tariot P, Reeder S, Bates V, Capote H, Rainka M, Scharre DW, Kataki M, Adeli A, Zimmerman EA, Celmins D, Brown AD, Pearlson GD, Blank K, Anderson K, Santulli RB, Kitzmiller TJ, Schwartz ES, Sink KM, Williamson JD, Garg P, Watkins F, Ott BR, Querfurth H, Tremont G, Salloway S, Malloy P, Correia S, Rosen HJ, Miller BL, Mintzer J, Spicer K, Bachman D, Finger E, Pasternak S, Rachinsky I, Drost D, Pomara N, Hernando R, Sarrael A, Schultz SK, Boles Ponto LL, Shim H, Smith KE, Relkin N, Chaing G, Raudin L, Smith A, Fargher K, Raj BA, Neylan T, Grafman J, Davis M, Morrison R, Hayes J, Finley S and The Alzheimer's Disease Neuroimaging I (2016) Basal forebrain degeneration precedes and predicts the cortical spread of Alzheimer's pathology. *Nature Communications* **7**:13249.

Schwabe U, Miyake M, Ohga Y and Daly JW (1976) 4-(3-Cyclopentyloxy-4-methoxyphenyl)-2-pyrrolidone (ZK 62711): a potent inhibitor of adenosine cyclic 3',5'-monophosphate phosphodiesterases in homogenates and tissue slices from rat brain. *Mol Pharmacol* **12**:900-910.

Seibert M, Mühlbauer V, Holbrook J, Voigt-Radloff S, Brefka S, Dallmeier D, Denkinger M, Schönfeldt-Lecuona C, Klöppel S and von Arnim CAF (2021) Efficacy and safety of pharmacotherapy for Alzheimer's disease and for behavioural and psychological symptoms of dementia in older patients with moderate and severe functional impairments: a systematic review of controlled trials. *Alzheimer's Research & Therapy* **13**:131.

Sevigny J, Chiao P, Bussière T, Weinreb PH, Williams L, Maier M, Dunstan R, Salloway S, Chen T, Ling Y, O'Gorman J, Qian F, Arastu M, Li M, Chollate S, Brennan MS, Quintero-Monzon O, Scannevin RH, Arnold HM, Engber T, Rhodes K, Ferrero J, Hang Y, Mikulskis A, Grimm J, Hock C, Nitsch RM and Sandrock A (2016) The antibody aducanumab reduces Aβ plaques in Alzheimer's disease. *Nature* **537**:50-56.

Shi J, Li Y, Zhang Y, Chen J, Gao J, Zhang T, Shang X and Zhang X (2021) Baicalein Ameliorates Aβ-Induced Memory Deficits and Neuronal Atrophy via Inhibition of PDE2 and PDE4. *Front Pharmacol* **12**:794458.

Sierksma AS, van den Hove DL, Pfau F, Philippens M, Bruno O, Fedele E, Ricciarelli R, Steinbusch HW, Vanmierlo T and Prickaerts J (2014) Improvement of spatial memory function in APPswe/PS1dE9 mice after chronic inhibition of phosphodiesterase type 4D. *Neuropharmacology* **77**:120-130.

Stozická Z, Zilka N and Novák M (2007) Risk and protective factors for sporadic Alzheimer's disease. *Acta virologica* **51**:205-222.

Swinnen JV, Joseph DR and Conti M (1989a) Molecular cloning of rat homologues of the Drosophila melanogaster dunce cAMP phosphodiesterase: evidence for a family of genes. *Proc Natl Acad Sci U S A* **86**:5325-5329.

Swinnen JV, Joseph DR and Conti M (1989b) The mRNA encoding a high-affinity cAMP phosphodiesterase is regulated by hormones and cAMP. *Proc Natl Acad Sci U S A* **86**:8197-8201.

Teter B and Ashford JW (2002) Neuroplasticity in Alzheimer's disease. *Journal of Neuroscience Research* **70**:402-437.

Ugarte A, Gil-Bea F, García-Barroso C, Cedazo-Minguez Á, Ramírez MJ, Franco R, García-Osta A, Oyarzabal J and Cuadrado-Tejedor M (2015) Decreased

levels of guanosine 3', 5'-monophosphate (cGMP) in cerebrospinal fluid (CSF) are associated with cognitive decline and amyloid pathology in Alzheimer's disease. *Neuropathology and Applied Neurobiology* **41**:471-482.

Van Duinen MA, Sambeth A, Heckman PRA, Smit S, Tsai M, Lahu G, Uz T, Blokland A and Prickaerts J (2018) Acute administration of roflumilast enhances immediate recall of verbal word memory in healthy young adults. *Neuropharmacology* **131**:31-38.

van Goethem NP, Paes D, Puzzo D, Fedele E, Rebosio C, Gulisano W, Palmeri A, Wennogle LP, Peng Y, Bertrand D and Prickaerts J (2019) Antagonizing α7 nicotinic receptors with methyllycaconitine (MLA) potentiates receptor activity and memory acquisition. *Cell Signal* **62**:109338.

Vanmierlo T, Creemers P, Akkerman S, van Duinen M, Sambeth A, De Vry J, Uz T, Blokland A and Prickaerts J (2016) The PDE4 inhibitor roflumilast improves memory in rodents at non-emetic doses. *Behav Brain Res* **303**:26-33.

Vilhena ER, Bonato JM, Schepers M, Kunieda JKC, Milani H, Vanmierlo T, Prickaerts J and de Oliveira RMW (2021) Positive effects of roflumilast on behavior, neuroinflammation, and white matter injury in mice with global cerebral ischemia. *Behav Pharmacol* **32**:459-471.

Vitolo OV, Sant'Angelo A, Costanzo V, Battaglia F, Arancio O and Shelanski M (2002) Amyloid β-peptide inhibition of the PKA/CREB pathway and long-term potentiation: reversibility by drugs that enhance cAMP signaling. *Proceedings of the national academy of sciences* **99**:13217-13221.

Walaas SI and Greengard P (1991) Protein phosphorylation and neuronal function. *Pharmacol Rev* **43**:299-349.

Wang Y, Gao S, Zheng V, Chen L, Ma M, Shen S, Qu J, Zhang H, Gurney ME, O'Donnell JM and Xu Y (2020) A Novel PDE4D Inhibitor BPN14770 Reverses Scopolamine-Induced Cognitive Deficits via cAMP/SIRT1/Akt/Bcl-2 Pathway. *Front Cell Dev Biol* **8**:599389.

Xiang J, Wang X, Gao Y, Li T, Cao R, Yan T, Ma Y, Niu Y, Xue J and Wang B (2020) Phosphodiesterase 4D Gene Modifies the Functional Network of Patients With Mild Cognitive Impairment and Alzheimer's Disease. *Frontiers in genetics* **11**.

Zhang C, Xu Y, Chowdhary A, Fox D, 3rd, Gurney ME, Zhang HT, Auerbach BD, Salvi RJ, Yang M, Li G and O'Donnell JM (2018) Memory enhancing effects of BPN14770, an allosteric inhibitor of phosphodiesterase-4D, in wild-type and humanized mice. *Neuropsychopharmacology* **43**:2299-2309.

Zhang C, Xu Y, Zhang H-T, Gurney ME and O'Donnell JM (2017) Comparison of the Pharmacological Profiles of Selective PDE4B and PDE4D Inhibitors in the Central Nervous System. *Scientific Reports* **7**:40115.

Zhang H-T, Zhao Y, Huang Y, Dorairaj NR, Chandler LJ and O'Donnell JM (2004) Inhibition of the Phosphodiesterase 4 (PDE4) Enzyme Reverses Memory Deficits Produced by Infusion of the MEK Inhibitor U0126 into the CA1 Subregion of the Rat Hippocampus. *Neuropsychopharmacology* **29**:1432-1439.

Chapter 2

The molecular biology of PDE4 enzymes as pharmacological targets:

An interplay of isoforms, conformational states, and inhibitors

Published as:

Paes et al. (2021) *Pharmacol Rev.* Jul;73(3):1016-1049.
doi: 10.1124/pharmrev.120.000273

LIST OF NONSTANDARD ABBREVIATIONS:

3′UTR – 3′ untranslated region

5′UTR – 5′ untranslated region

5HT4 – 5-hydroxytryptamine 4

ADPKD – autosomal dominant polycystic kidney disease

AIP – aryl hydrocarbon receptor-interacting protein

AKA – also known as

AKAP – A-kinase anchoring protein

AMPK – AMP-activated protein kinase

AP – area postrema

ATF4 – activating transcription factor 4

CaMKII – calcium/calmodulin-dependent kinase II

cAMP – cyclic adenosine monophosphate

cat dom – catalytic domain

CDK5 – cyclin-dependent kinase 5

CK1 – casein kinase I

CREB – cAMP-response element binding protein

CRISPR – clustered regularly interspaced short palindromic repeats

DISC1 – disrupted in schizophrenia 1

ERK – extracellular signal-regulated kinase

GSK3β – glycogen synthase kinase 3β

HARBS – high-affinity rolipram binding site

HCN – hyperpolarized cyclic nucleotide-gated channel

HSP20 – heat-shock protein 20

IC50 – half-maximum inhibitory concentration

IG – intragastric

IP – intraperitoneal

IV – intravenous

JNK – c-Jun N-terminal kinase

LARBS – low-affinity rolipram binding site

LR1 – linker region 1

LR2 – linker region 2

Mdm2 – Mouse double minute 2 homolog

MITF – melanocyte inducing transcription factor

MK2 – MAPK-activated protein kinase 2

N-term – N-terminus

NTS – nucleus tractus solitaries

PDE – phosphodiesterase

PHD2 – prolyl hydroxylase domain-containing protein 2

PKA – protein kinase A

PO – per os

RACK1 – receptor of activated protein C kinase 1

RyR – ryanodine receptor

SC – subcutaneous

SH3 – SRC Homology 3 Domain

Shank2 – SH3 and multiple ankyrin repeat domains protein 2

shRNA – short-hairpin RNA

SIK1 – salt-inducible kinase 1

SQSTM1 – Sequestosome 1

UCR1 – upstream conserved region 1

UCR2 – upstream conserved region 2

XAP – HBV X-associated protein 2

CHAPTER 2: TABLE OF CONTENTS

ABSTRACT

The phosphodiesterase 4 (PDE4) enzyme family plays a pivotal role in regulating levels of the second messenger cyclic AMP (cAMP). Consequently, PDE4 inhibitors have been investigated as a therapeutic strategy to enhance cAMP signaling in a broad range of diseases, including several types of cancers, as well as in various neurological, dermatological and inflammatory diseases. Despite their widespread therapeutic potential, the progression of PDE4 inhibitors into the clinic has been hampered due to their related relatively small therapeutic window, which increases the chance of producing adverse side effects. Interestingly, the PDE4 enzyme family consists of several subtypes and isoforms, which can be modified post-translationally or can engage in specific protein-protein interactions to yield a variety of conformational states. Inhibition of specific PDE4 subtypes, isoforms, or conformational states may lead to more precise effects and hence improve the safety profile of PDE4 inhibition. In this review, we provide an overview of the variety of PDE4 isoforms and how their activity and inhibition is influenced by post-translational modifications and interactions with partner proteins. Furthermore, we describe the importance of screening potential PDE4 inhibitors in view of different PDE4 subtypes, isoforms, and conformational states rather than testing compounds directed towards a specific PDE4 catalytic domain. Lastly, potential mechanisms underlying PDE4-mediated adverse effects are outlined. In this review, we illustrate that PDE4 inhibitors retain their therapeutic potential in a myriad of diseases, but target identification should be more precise to establish selective inhibition of disease-affected PDE4 isoforms while avoiding isoforms involved in adverse effects.

SIGNIFICANCE STATEMENT

Although the PDE4 enzyme family is a therapeutic target in an extensive range of disorders, clinical use of PDE4 inhibitors has been hindered due to adverse side effects. Here, we elaborately show that safer and more effective PDE4 targeting is possible by characterizing 1) which PDE4 subtypes and isoforms exist, 2) how PDE4 isoforms can adopt specific conformations upon post-translational modifications and protein-protein interactions, and 3) which PDE4 inhibitors can selectively bind specific PDE4 subtypes, isoforms and/or conformations.

INTRODUCTION

Since the discovery of cyclic AMP (cAMP) as a second messenger by Sutherland and Rall in 1958, its role in a wide variety of cellular processes, bodily functions, and pathologies has been thoroughly studied (Rall and Sutherland, 1958; Sutherland and Rall, 1958). Upon diverse extra- and intracellular cues, the second messenger cAMP is synthesized by adenylyl cyclases to relay signaling to adaptive changes in the cell. This notion indicates that cAMP is used as a single generic signaling molecule to convey and amplify information from different sources; a notion supported by the principle that evolution promotes utilizing the same machinery for different functions (Purvis and Lahav, 2013). Through precise regulation of the localization, abundance, and dynamics of cAMP, different signaling modes can be generated using the same generic molecule. Consequently, slight disturbances in cAMP regulation could promote pathophysiology in different cell types. Levels of cAMP are predominantly controlled through exclusive breakdown by the 3',5'-cyclic nucleotide phosphodiesterase (PDE) enzyme family. This PDE enzyme family comprises 11 gene families (PDE1-11) which display different selectivity towards their substrates cAMP and cyclic GMP (cGMP). PDE4, PDE7 and PDE8 are cAMP-selective, whilst PDE5, PDE6 and PDE9 selectively degrade cGMP. The other gene families, PDE1, -2, -3, -10 and -11 can hydrolyze both cAMP and cGMP (Beavo, 1995; Bender and Beavo, 2006). PDE4 enzymes comprise a majority of cAMP-selective PDEs in different organs and cell types (Baillie et al., 2019; Lakics et al., 2010). Hence, PDE4 enzymes are interesting pharmacological targets to specifically modulate cAMP signalling. Hence, inhibition of PDE4 has been and is clinically investigated as a therapeutic strategy in a multitude of disease areas, as also recently reviewed (Peng et al., 2020), including cognitive and affective disorders (e.g. Alzheimer's disease [NCT03817684]**,** Fragile X syndrome [NCT03569631], schizophrenia [NCT02539550], depression (Hebenstreit et al., 1989), substance dependency [NCT03489850]), autoimmune disorders (e.g. multiple sclerosis

[NCT01982942] (Schepers et al., 2019), rheumatoid arthritis, atopic dermatitis, Behçet syndrome [NCT02307513]), respiratory system diseases (e.g. chronic obstructive pulmonary disease and asthma (Lipworth, 2005)), dermatological conditions (e.g. psoriasis [NCT03022617]), and cancer (e.g. glioblastoma [NCT03782415]).

Although inhibition of PDE4 shows widespread therapeutic potential in preclinical research, the progression of PDE4 inhibitors into the clinic has been held back by severe adverse effects including headaches, diarrhea, dizziness, nausea and vomiting (Spina, 2008). In fact, only three PDE4 inhibitors made it to the market due to their limited or reduced adverse effects, including roflumilast (Daliresp, Daxas), apremilast (Otezla) and crisaborole (Eucrisa), for chronic obstructive pulmonary disease, psoriasis, and moderate atopic dermatitis, respectively (Baillie et al., 2019). Interestingly, the *PDE4* gene family consists of four paralogous genes which, correspondingly, encode PDE4 subtypes (i.e. PDE4A-D). Each of these genes generates a variety of transcript variants that translate into different protein isoforms (e.g. PDE4D1-9). As these PDE4 subtypes and isoforms show tissue- and cell type-specific expression and intracellular compartmentalization patterns (Houslay, 2010)(reviewed in: (Baillie et al., 2019)), more selective inhibition could reduce the abovementioned adverse effects while maintaining treatment efficacy. An additional layer of complexity is added by the fact that PDE4 enzymes can adopt different conformational states as a result of various post-translational modifications and interactions with partner proteins. Consequently, this allows for more selective targeting as PDE4 inhibitors will likely display different affinities towards different PDE4 subtypes, isoforms, and conformational states.

This review aims to provide an overview of the variety of PDE4 subtypes and isoforms, and the mechanisms by which their cellular activity and inhibitor affinity is regulated through post-translational modifications and protein-protein interactions. Moreover, current advancements and strategies towards the development of PDE4 subtype- and/or conformation-specific compounds are discussed. Lastly, several

mechanisms that potentially contribute to adverse side effect profiles of PDE4 inhibition are outlined in order to support the development of new, more specific and safer PDE4-directed therapeutics.

I. PDE4 SUBTYPES AND ISOFORMS

Before the identification of the responsible enzymes, in 1987, rolipram was shown to inhibit cAMP-specific PDE activity (Reeves et al., 1987). As this activity was distinct from three other types of PDE activity already known at the time, it was coined PDE IV. In retrospect, earlier studies had already identified rolipram-sensitive PDE activity to be present in rat brain material and to be involved in gastric secretion (Puurunen et al., 1978; Schwabe et al., 1976). A rat orthologue of the *Drosophila* cAMP-PDE enzyme, encoded by the *dunce* gene, was found to produce an enzyme that can be inhibited by rolipram (Davis et al., 1989; Swinnen et al., 1989a; b).

In mammals, four PDE4 genes can be distinguished, all of which show similar and evolutionarily conserved exon compositions, encoding the abovementioned PDE4 subtypes PDE4A, B, C, and D (Bolger et al., 1993; Bolger, 1994; Johnson et al., 2010; Milatovich et al., 1994). Across species and among genes, there is particular sequence similarity in specific exons that encode the enzyme's catalytic domain and two regulatory domains, upstream conserved region 1 and 2 (UCR1 and UCR2). Next to their sensitivity to rolipram, PDE4 enzymes can be distinguished from other PDEs by the presence of these UCR1 and UCR2 domains. Apart from the UCR1, UCR2 and catalytic domains, the amino acid sequences of human PDE4 subtypes differ notably in the linker region 1 (LR1, between UCR1 and UCR2), LR2 (between UCR2 and catalytic domain) and the C-terminals. These differences allow for subtype-specific modulation while maintaining core PDE4 regulation and functionality as discussed in the section **PDE4 modification and interactions**.

Additional diversity is achieved at the gene level as each of the PDE4 genes contains alternative promoters that can generate distinct transcript variants by

incorporating unique exons and through recursive splicing mechanisms (Sibley et al., 2015). Different promoters may contain distinct transcription response elements that allow for transcriptional regulation associated with a diversity of signaling pathways. For example, specific promoters of the *PDE4D* gene have been identified to contain regulatory elements for the transcriptions factors cAMP-response element binding protein (CREB) (D'Sa et al., 2002; Le Jeune et al., 2002; Vicini and Conti, 1997), melanocyte inducing transcription factor (MITF) (Khaled et al., 2010) or activating transcription factor 4 (ATF4) (Soda et al., 2013). These transcriptional control mechanisms allow for intricate transcriptional feedback loops that upregulate PDE4 expression in order to terminate cAMP signaling associated with particular cascades. The activity of certain promoters is thus regulated by the presence of the various transcription factors, while the accessibility of the promoter may also be subject to epigenetic regulation. Indeed, epigenetic alterations at the level of DNA (hydroxy)methylation and histone modifications of the *PDE4D* gene have been associated with changes in expression on specific transcript variants (Paes et al., 2020a; Tilley and Maurice, 2005). Although the exact responsiveness of the different PDE4 promoters remains to be explored further, prior findings already suggest that PDE4 transcription can be regulated in an intricately regulated manner enabling organ- and cell-specific expression patterns.

Depending on the location of the promoter, PDE4 mRNA transcripts will include the exons encoding both UCR1 and UCR2, only UCR2, a truncated UCR2, or only exons that encode a part of the catalytic domain (Johnston et al., 2004; Nemoz et al., 1996). Based on the presence of these UCRs, the protein products of these transcripts can be categorized as long, short, and supershort isoforms, respectively. Transcripts encoding catalytically inactive isoforms are called dead-short (Houslay, 2001). Based on deletion mutant studies, the UCR domains were found to regulate catalytic activity showing differential enzymatic kinetics for the different isoform categories (Jacobitz et al., 1996; Saldou et al., 1998). Via alternative promoters and

alternative splicing mechanisms, more than 20 human PDE4 transcript variants have been identified, allowing for tissue- and cell-specific expression regulation.

Figure 1. Exon composition per human PDE4 transcript variant. For each of the PDE4 genes (PDE4A-D), the exon composition is shown per transcript variant. Gray boxes depict exons and their nucleotide length. The protein isoform names and associated amino acid (aa) number per transcript are shown on the left. Start and stop codons are indicated by arrows and pins, respectively. The regions translating into UCR1, UCR2 and the catalytic domain are visualized by thick horizontal bars. *: as the transcripts PDE4DN1-3 have only been identified on the mRNA level, amino acids lengths are isoform categories are predictions based on in-frame stop codons. This figure was established through analysis and cross-referencing of online databases (NCBI: https://www.ncbi.nlm.nih.gov/gene and Ensembl: http://www.ensembl.org/index.html) and original cloning studies (see references to studies per transcript variant in **Section PDE4 subtypes and isoforms**). An overview indicating which transcripts have counterparts in rodents or are only found in rodents is provided in the **Supplementary Material**.

PDE4 exon composition per transcript variant

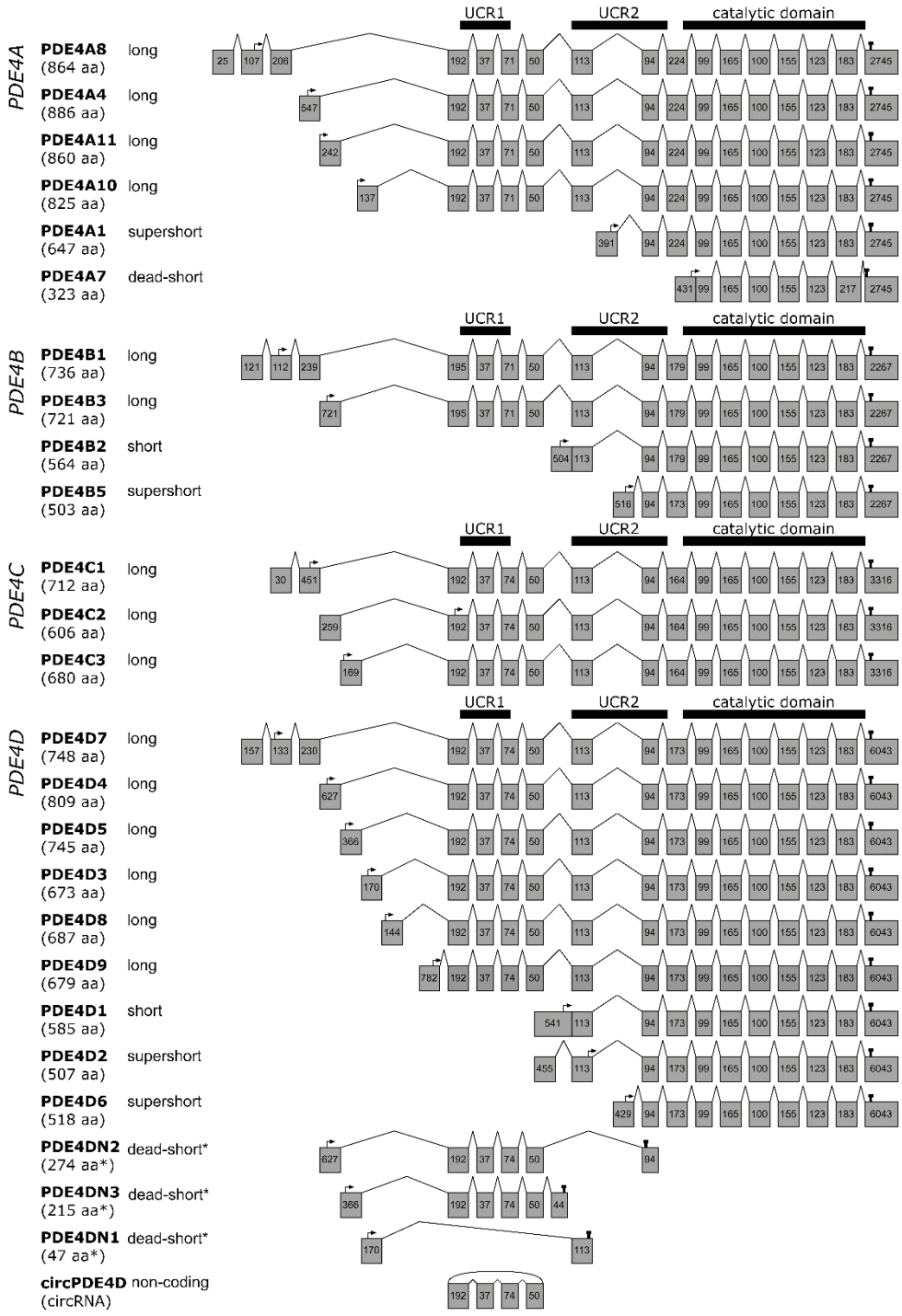

Figure 1 highlights the exon composition per human PDE4 transcript. As described below, certain PDE4 transcripts have been identified or characterized in humans or rodents only; **Supplementary Table 1** provides an overview of which PDE4 transcript has been described per species. Human *PDE4A* encodes four long isoforms (PDE4A8 (Mackenzie et al., 2008), PDE4A4 which is named PDE4A5 in rodents (Bolger et al., 1993; Naro et al., 1996), PDE4A11 (Wallace et al., 2005), and PDE4A10 (Rena et al., 2001)), one supershort isoform (PDE4A1 (Sullivan et al., 1998)) and a dead-short, catalytically inactive, isoform (PDE4A7 (Johnston et al., 2004)) (**Supplementary Table 1**),

For human PDE4B, two long (PDE4B1 (Bolger et al., 1993) and PDE4B3 (Huston et al., 1997)), one short (PDE4B2 (McLaughlin et al., 1993)) and one supershort isoform (PDE4B5 (Cheung et al., 2007)) have been identified. In rodents, in addition, a long PDE4B4 isoform has been characterized, which was suggested to have no functional equivalent in humans due to in-frame stop codons (Shepherd et al., 2003). However, PDE4B antibodies can clearly detect an 85 kDa PDE4B species in human brain tissue corresponding to rodent PDE4B4, but the exact sequence remains to be determined (Fatemi et al., 2008) (**Supplementary Table 1**).

The least well-characterized PDE4 subtype is PDE4C which comprises three long isoforms (PDE4C1 (Engels et al., 1995), PDE4C2 (Owens et al., 1997b), and PDE4C3 (Obernolte et al., 1997)), but likely generates additional variants through complex alternative splicing (Obernolte et al., 1997). Interestingly, despite relatively little insight into its function, several studies found that the DNA methylation signature of the *PDE4C* gene correlated with aging (e.g. (Marquez-Ruiz et al., 2020)).

Lastly, the human *PDE4D* gene produces the highest number of isoforms, i.e. six long isoforms (PDE4D3, PDE4D4, PDE4D5 (Bolger et al., 1997), PDE4D7, PDE4D8 (Wang et al., 2003), PDE4D9 (Gretarsdottir et al., 2003)), one short isoform (PDE4D1 (Bolger et al., 1997)) and two supershort isoforms (PDE4D2 (Bolger et al., 1997) and PDE4D6 (Wang et al., 2003)) (**Supplementary Table 1**).

Moreover, alternatively spliced transcripts have been described for PDE4D3, -D4 and -D5 that do not translate the catalytic domain due to in-frame stop codons caused by exon deletions or insertions (**Figure 1**) (Miro et al., 2000). These variations of the 'conventional' PDE4D3, -D4, and -D5 isoforms have been respectively coined PDE4DN1, PDE4DN2, and PDE4DN3 and can be categorized as dead-short forms based on the absence of the catalytic domain. For PDE4DN1, all exons encoding UCR1 are skipped, creating a transcript that encodes the unique N-terminal of PDE4D3 followed by 31 frame-shifted codons of the UCR2 (**Figure 1**). Based on this sequence, PDE4DN1 may engage in similar protein-protein interactions as PDE4D3 would using its N-terminal residues, but the exact functional role of PDE4DN1 remains undetermined (see also section **PDE4 modifications and interactions** and **Figure 2**). In contrast to PDE4DN1, PDE4DN2 and PDE4DN3 do incorporate the UCR1-encoding exons in their transcripts (**Figure 1**). Similar to PDE4DN1, the unique N-termini as also present in PDE4D4 and PDE4D5 may allow PDE4DN2 and PDE4DN3 to bind specific protein partners or putatively cause competitive binding for these binding sites with full-length PDE4D4 and PDE4D5, respectively. This competitive binding may subsequently induce altered distribution of full-length PDE4 forms causing distinct cellular cAMP dynamics. Intriguingly, the presence of UCR1 in these truncated forms may have functional consequences on full-length PDE4 forms. It has been demonstrated that a peptide fragment of the UCR1 can bind and activate full-length long PDE4 forms (Wang et al., 2015). PDE4DN2 and PDE4DN3, containing the same sequence as this peptide fragment, may exert similar actions and could biologically be relevant by providing an additional mechanism to elevate cellular PDE4 activity. The existence of these truncated forms at the protein level and their putative activating effects on full-length long PDE4D forms, however, remain to be validated.

Importantly, the existence of these truncated PDE4DN1-3 forms has a practical consequence for quantitative PCR (qPCR) measurements. Isoform-specific

PDE4D expression can be measured using qPCR primers that amplify part of the sequence of the isoform-unique exon (and the first UCR1 exon), but in case of PDE4D4 and PDE4D5 also the respective expression of PDE4DN2 and PDE4DN3 will be detected by qPCR. Hence, PCR and gel electrophoresis should be performed in parallel using appropriate primers to determine whether expression changes are found for both the full-length and truncated transcript or for only one of these transcripts.

Recently, it has been described that *PDE4D* also encodes a highly stable, mainly cytoplasmic, circular RNA, circPDE4D, which is formed through circularization of exons 2-5 of the *PDE4D* gene (**Figure 1**) (Wu et al., 2021). The expression of circPDE4D and linear PDE4D mRNA was found not to be correlated indicating that distinct mechanisms produce these transcript types. Wu et al. identified regulatory regions in the flanking introns (i.e. upstream of exon 2 and downstream of exon 5) that are crucial for circPDE4D circularization. Through specific CRISPR-Cas9 editing, the authors were able to decrease circPDE4D expression and determine that QKI response elements (QRE) are involved in circularization of the PDE4D pre-mRNA (Wu et al., 2021). QREs bind the RNA-binding protein quaking (QKI), which has previously been shown to regulate the circularization of many pre-mRNAs (Conn et al., 2015). The functional role of circPDE4D remains largely to be determined, but Wu et al. identified that circPDE4D can bind specific microRNAs and thereby indirectly modulates the translation of mRNA that otherwise would be degraded by, the now scavenged, microRNA. In the same study, circPDE4D was found to be downregulated in osteoarthritic cartilage tissue and intra-articular injection of circPDE4D could mitigate impairments in a mouse model of osteoarthritis (Wu et al., 2021).

As circPDE4D contains four exons that are also present in linear long-form PDE4D mRNA, it can be speculated that circPDE4D scavenges miRNAs that bind linear long form PDE4D mRNA and circPDE4D may therefore indirectly modulate PDE4D protein expression. Moreover, circRNAs can also directly regulate protein

function, protein scaffolding and protein localization, but these potential roles still remain to be determined for circPDE4D (Kristensen et al., 2019). These recent findings underline the complex transcriptional control of the *PDE4D* gene and warrant further investigation into non-protein-coding transcripts of the PDE4 gene family.

For murine *Pde4d*, the additional long PDE4D11 and supershort PDE4D10 isoforms have been described (Chandrasekaran et al., 2008; Lynex et al., 2008)(**Supplementary Table 1**). Furthermore, additional murine PDE4D transcripts have been identified that all encode supershort PDE4D2, but which are generated through diverse exon incorporation resulting in diverse 5'UTR sequences and lengths (Chandrasekaran et al., 2008)(**Supplementary Table 1**). Regarding 5'UTR and 3'UTR lengths, discrepancies exist regarding the reported transcript lengths when comparing NCBI Gene and Ensembl databases. 5'UTR lengths can differ depending on where the transcriptional machinery binds the DNA and initiates transcription, as exemplified for mouse PDE4D1 (McLaughlin et al., 1993). Similarly, the PDE4 transcript's 3'UTR may differ in length as it contains multiple polyadenylation sites (Sullivan et al., 1998; Wang et al., 2003). According to this variability at the 5'UTR and 3'UTR, certain gene databanks may show other lengths for the first unique and last common exons compared to those displayed in **Figure 1**. As 5'UTR and 3'UTR sequences have been found to function as 'zip-codes' for specific intracellular transcript transport, it can be speculated that variation in these PDE4 transcript sequences may contribute to specific intracellular localization patterns for the different PDE4 isoforms (Andreassi and Riccio, 2009; Chin and Lecuyer, 2017). Wang et al. identified 10 putative consensus polyadenylation signals in the 3'UTR of PDE4D mRNA, which indicates that multiple transcripts that differ in their 3'UTR length can be generated depending on which polyadenylation site is utilized (Wang et al., 2003). Subsequently, differences in 3'UTR length may give rise to mRNA transcripts that exhibit different recognition motifs for several RNA-binding proteins (Di Liegro et al., 2014). For example, self-complementary sequences in mRNA can form secondary

structure hairpin loops that can be recognized and bound by RNA-binding proteins to regulate mRNA stability and transportation (Di Liegro et al., 2014). Depending on PDE4 3'UTR length, different secondary structures may be formed and bound by different transport proteins, which localize the transcript to distinct intracellular compartments. There, the specific PDE4 mRNA may be locally translated after which the PDE4 protein isoform can be anchored to other proteins or membranes through its (isoform-specific) amino acids (see section **PDE4 modifications and interactions**). Although the role of 5'UTR and 3'UTR sequence differences in mRNA transportation has not yet been explicitly demonstrated for PDE4 transcripts, these sequence differences could provide another mechanism through which PDE4 subtypes and isoforms can display a distinct cell- and tissue-type specific intracellular distribution.

The intracellular localization of PDE4 isoforms is particularly regulated via isoform-specific N-termini at the protein level, encoded by typical unique exon incorporation. These different N-termini permit PDE4 isoforms to interact with protein partners or membranes in specific intracellular compartments (Houslay et al., 1995). In *Aplysia*, apPDE4 was found to require N-terminus residues for membrane binding, which indicates a conserved role for isoform-specific N-termini in PDE4 localization (Jang et al., 2010). Likewise, different mammalian PDE4 subtypes (e.g. PDE4B and PDE4D) locate to different intracellular compartments (Blackman et al., 2011).

In addition to the scaffolding function, interactions with partner proteins can, as mentioned above, act upon the enzyme's conformational state and hence affect its catalytic activity and inhibitor affinity. Similarly, PDE4 subtypes and isoforms are subject to post-translational modifications that differentially alter the conformation and activity of the enzyme.

To develop more efficacious and safer PDE4 inhibitors for different diseases, it is crucial to identify which PDE4 subtypes and isoforms should be targeted in

disease-relevant tissues and cell types. Similarly, insight into which PDE4 subtypes and isoforms mediate adverse effects will determine which specific targets to avoid to improve the treatment's safety profile. Additionally, understanding the conformational state of the isoform(s) involved in the compartmentalized signaling important to treat the disease at hand determines which compounds would be most potent. In the following section, an overview is provided on the different manners by which PDE4 activity and inhibitor affinity is influenced by post-translational modifications and interactions with partner proteins.

II. PDE4 MODIFICATIONS AND INTERACTIONS

As mentioned before, catalytically active PDE4 isoforms can be categorized as long, short, or supershort based on the presence of UCR1 and UCR2 domains. Depending on the PDE4 subtype, isoform category, and unique N-terminal features, different post-translational modifiers and interaction partners can influence the conformation of the enzyme. These mechanisms allow for the dynamic regulation of the amount, localization, and activity of PDE4 enzymes in order to shape and respond to spatiotemporal cAMP signaling (as also recently reviewed for all PDE gene families: (Baillie et al., 2019)). The seminal work by Houslay and collaborators has provided a detailed understanding of which PDE4 amino acid residues are crucial for several modifications and interactions (Klussmann, 2016). Those post-translational modifications and protein-protein interactions for which involved PDE4 domains or specific amino acid residues have been identified are graphically represented in **Figure 2**. These and other modifications and interactions, for which involved regions have not been determined, are discussed below in more detail. Furthermore, the known functional consequences of several modifications and interactions on PDE4 activity and inhibitor binding are elaborated upon in the following subsections and are summarized in **Table 1**.

A. UCR1-UCR2 module, dimerization, and phosphorylation

PDE4 activity is profoundly regulated by its own UCR domains as, in long isoforms, the C-terminal of UCR1 forms a module with the N-terminal of UCR2, which auto-inhibits its activity through the capping of the UCR2 alpha-helix NQVSE[F/Y]ISXTFLD across the catalytic domain (Beard et al., 2000; Houslay and Adams, 2010; Kovala et al., 1997; Lim et al., 1999) (see also **Figure 3, Table 1 and Supplementary Video**). Furthermore, the UCR1 and UCR2 domains enable long isoforms to homo- and heterodimerize, while short and supershort isoforms (lacking UCR1) exist as monomers (Xie et al., 2014). The UCR1-UCR2 module is disrupted

upon serine phosphorylation in the conserved protein kinase A (PKA) consensus motif RRES in UCR1 of all long PDE4 isoforms. The liberation of this UCR1-UCR2 module attenuates the auto-inhibitory effect causing enzyme activation (Beard et al., 2000; Hoffmann et al., 1998). As PKA is a direct downstream effector protein of cAMP, this modification serves as a negative feedback loop restoring cAMP levels through enhanced PDE4 activity. Although PKA phosphorylation can activate all long isoforms, the amplitude of PKA activation can differ among these isoforms as reported for long PDE4D isoforms (Richter et al., 2005). This indicates that additional regulatory mechanisms influence enzymatic activity. For example, the presence of additional PKA phosphorylation sites in PDE4D3 and PDE4D7, upon combined PKA phosphorylation, leads to differential effects in terms of catalytic activity (Byrne et al., 2015; Collins et al., 2008; Sette and Conti, 1996). Indeed, unique phosphorylation in the N-terminal PDE4D7, but not at the unique site in PDE4D3, induces an inhibitory effect on activity as opposed to PKA phosphorylation at the conserved UCR1 site (Byrne et al., 2015). Although PKA phosphorylation provides a negative feedback loop to restore cAMP levels, this regulation can be influenced by other protein interactors as well. For example, when PDE4D is bound by the protein CC2D1, phosphorylation by PKA is prevented (Al-Tawashi and Gehring, 2013; Al-Tawashi et al., 2012). In addition to PKA, it was found that the same serine residue in UCR1 can be phosphorylated by Akt (Fang et al., 2015). Other conserved serine residues in the UCR1 also serve as phosphorylation sites for other kinases such as MK2, SIK1, CDK5, and AMPK, which may modulate PDE4 activity by similarly affecting UCR1-UCR2 module formation/stabilization (Bolger, 2016; Houslay et al., 2019; Kim et al., 2015; MacKenzie et al., 2011; Plattner et al., 2015; Sheppard et al., 2014). Next to phosphorylation events, binding of phosphatidic acid or phosphatidylserine to the UCR1-UCR2 module increases PDE4 activity (Nemoz et al., 1997). The regulatory role of the UCR1-UCR2 module is further supported by the observation that several PDE4D mutations associated with the rare genetic disorder acrodysostosis localize

to these regions, causing either increased or decreased PDE4D activity (Briet et al., 2017; Gurney et al., 2015; Kaname et al., 2014).

Figure 2. Graphical representation of regulatory protein domains of PDE4 proteins and PDE4 amino acids or domains involved in inherent features of PDE4 enzymes, post-translational modifications and interactions with protein partners. Colored rectangles indicate regulatory domains. Inherent features of PDE4 enzymes and associated amino acids are also visualized in **Supplementary Video**. Those post-translational modifications and protein-protein interactions for which the involved PDE4 domains or specific amino acid residues have been identified are listed in this figure. If specific amino acids in involved regions have been identified to mediate the modification or interaction, these amino acids are indicated in bold and underlined. In case the specific amino acids are unidentified, the involved region is indicated by the region's first and last amino acids connected by a line. Of note, for simplicity, PDE4D amino acids are shown for non-conserved amino acids involved in modifications or interactions that can occur in multiple PDE4 subtypes. Importantly, not all proteins or mechanisms in **Figure 2** are listed in **Table 1**, and vice versa as one of both aspects (i.e. either involved amino acids or effect of activity) may not have been revealed yet. More detailed information on each of the modification or interaction can be found in the main text and the references as listed below. *Abbreviations and references: N-term, N-terminus; LR1, linker region 1; UCR1/2, upstream conserved region 1/2; LR2, linker region 2; C-term, C-terminus; UCR1-UCR2 interaction (Beard et al., 2000); dimerization (Bolger et al., 2015; Cedervall et al., 2015; Lee et al., 2002; Richter and Conti, 2002; 2004; Xie et al., 2014); Mg^{2+} binding (Alvarez et al., 1995; Laliberte et al., 2000; Liu et al., 2001; Saldou et al., 1998); PKA, protein kinase A (Alvarez et al., 1995; Beard et al., 2000; Bolger, 2016; Byrne et al., 2015; Hoffmann et al., 1998; MacKenzie et al., 2002; Sette and Conti, 1996); Akt (Fang et al., 2015); MK2, MAPK-activated protein kinase 2 (Bolger, 2016; Houslay et al., 2017; Houslay et al., 2019; MacKenzie et al., 2011); SIK1, salt-inducible kinase 1 (Kim et al., 2015); CDK5, cyclin-dependent kinase 5 (Plattner et al., 2015); AMPK, AMP-activated protein kinase (Sheppard et al., 2014); CaMKII, calcium/calmodulin-dependent kinase II (Mika et al., 2015); oxidative stress kinase (Bolger, 2016; Hill et al., 2006); ubiquitination (Li et al., 2009); ERK, extracellular signal-regulated kinase (Baillie et al., 2000; Hoffmann et al., 1999; MacKenzie et al., 2000); JNK, c-Jun N-terminal kinase (Bogoyevitch and Kobe, 2006; Sharrocks et al., 2000; Zeke et al., 2015); SUMOylation (Li et al., 2010); caspase-3 (Huston et al., 2000); β-arrestin (Baillie et al., 2007; Bolger, 2016; Bolger et al., 2006; Smith et al., 2007); RACK1, receptor of activated protein C kinase 1 (Bird et al., 2010; Bolger et al., 2006; Bolger et al., 2002; Smith et al., 2007; Yarwood et al., 1999); DISC1, disrupted in schizophrenia 1 (Cheung et al., 2007; Millar et al., 2005; Murdoch et al., 2007; Soda et al., 2013); myomegalin (Verde et al., 2001); Shank2, SH3 and multiple ankyrin repeat domains protein 2 (Lee et al., 2007); LIS1 (Murdoch et al., 2011); B55α PP2a subunit (Yun et al., 2019b); aII spectrin (Creighton et al., 2008); Src/Lyn/Fyn (Beard et al., 1999; O'Connell et al., 1996); mAKAP (Carlisle Michel et al., 2004; Dodge et al., 2001); AKAP9 (Terrenoire et al., 2009); AKAP18δ (Stefan et al., 2007); Rheb (Kim et al., 2010; Meng et al., 2017); HSP20 (Sin et al., 2011); PHD2 (Huo et al., 2012); integrin α5 (Yun et al., 2016; Yun et al., 2019b); Mdm2 (Li et al., 2009); calcineurin (Zhu et al., 2010); phosphodegron motif (Zhu et al., 2010); $p75^{NTR}$ (Houslay et al., 2019; Sachs et al., 2007); membrane binding (Baillie et al., 2002); XAP/AIP (Bolger et al., 2003); Lyn (Beard et al., 2002); Lyn + Src (McPhee et al., 1999); p62 (SQSTM1) (Christian et al., 2010).*

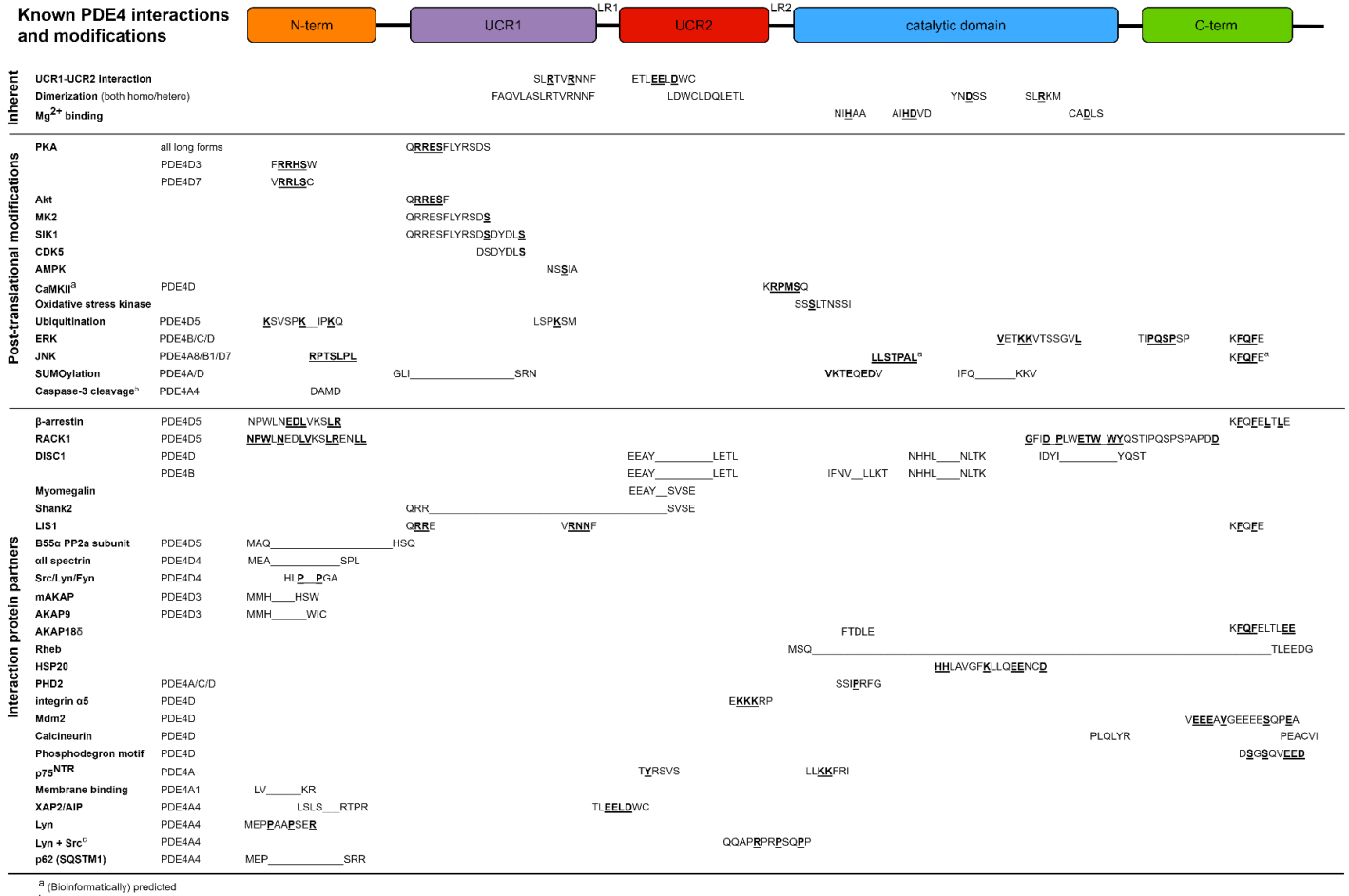

[a] (Bioinformatically) predicted
[b] Identified in rodent homolog PDE4A5 with motif DAVD
[c] Only in human PDE4A4

B. Phosphorylation at sites other than UCR1

Through the use of multiple phosphorylation sites, PDE4 functionality can be modulated in a conditional manner requiring multi-phosphorylation as has been reported for the role of PDE4D9 in mitosis (Sheppard et al., 2014). Next to the UCR1, the N-terminal of the catalytic domain comprises phosphorylation sites for CaMKII and an 'oxidative stress' or 'switch' kinase. CaMKII phosphorylation is PDE4D-specific and induces enzyme activation in a manner distinct from PKA activation (Mika et al., 2015). In response to oxidative stress, an as of yet unidentified 'oxidative stress' or 'switch' kinase can increase PDE4 enzyme activity by switching the inhibitory effect of phosphorylation by extracellular signal-regulated kinase (ERK) to an activating effect (Bolger, 2016; Hill et al., 2006). Similarly, inhibition of PDE4D by ERK is diminished upon PIASy-mediated SUMOylation, while this SUMOylation augments PKA activation of PDE4A and PDE4D **(Figure 2 and Table 1)** (Li et al., 2010).

Phosphorylation by ERK is established through the docking of ERK at the 'KIM' and 'FQF' motifs that are located in catalytic domains and C-terminus, respectively **(Figure 2)** (Houslay and Baillie, 2003). Upon docking of ERK the consensus motif PXSP can be phosphorylated, which is present at the end of the catalytic domain in PDE4B, -4C and -4D. Although PDE4A phosphorylation at this motif has been detected, this is unlikely induced by ERK, given the absence of the consensus motif, or it does not result in changed PDE4A activity (Baillie et al., 2000; Lario et al., 2001). Phosphorylation by ERK reduces the catalytic activity of long and supershort PDE4B, -4C and -4D isoforms; presumably by intramolecular stabilization of the UCR2-capped configuration (Baillie et al., 2000; Houslay and Baillie, 2003). Conversely, short isoforms are activated upon ERK phosphorylation. However, removal of the UCR2 region in the short PDE4B2 form prevents an effect by phosphorylation by ERK, which supports the notion that UCR2-capping is required for ERK-mediated effects (Rocque et al., 1997b). Moreover, when ERK phosphorylation is paired with additional PKA or 'switch' kinase phosphorylation, enzyme activity will increase in long isoforms as well (Hill et al., 2006; Hoffmann et

al., 1999). Apart from these direct effects on PDE4 activity, phosphorylation by ERK may make PDE4 less prone to proteolysis (Lenhard et al., 1996). The PDE4D5 isoform may be minimally subjected to phosphorylation by ERK as its unique N-terminus binds the protein phosphatase B55α subunit, which dephosphorylates at the ERK site reversing its inhibition (Yun et al., 2019a). Furthermore, PDE4D5 specifically interacts with the proteins β-arrestin and RACK1, which can block the docking and phosphorylation by ERK, respectively **(Table 1)** (Bolger et al., 2006). Consequently, PDE4 activity can be increased upon these interactions, as reported for RACK1 (Bird et al., 2010; Bolger et al., 2006; Bolger et al., 2002; Yarwood et al., 1999). Of note, binding of β-arrestin and RACK1 ablates dimerization, but they bind mutually exclusively due to overlapping binding residues in the PDE4D5 N-terminus (Bolger, 2016). Additional Mdm2-mediated ubiquitination primes PDE4D5 to interact with β-arrestin rather than RACK1 (Li et al., 2009). Although β-arrestin preferentially binds PDE4D5, when bound to the RXFP1 rector, it prioritizes binding PDE4D3 (Halls and Cooper, 2010). These findings indicate that, due to differential and combined interactions with partner partners, phosphorylation and binding events may be stimulated, prevented, or countered in an isoform-specific manner.

The ERK-associated KIM docking motif can also be utilized by c-Jun N-terminal kinase (JNK) (Houslay and Adams, 2003; Sharrocks et al., 2000). Intriguingly, the specific isoforms PDE4A8, PDE4B1, and PDE4D7 all contain an additional, evolutionary conserved, docking site for JNK in their unique N-terminal **(Figure 2)**. Previously, it has been demonstrated that PDE4B1 can indeed bind JNK, but it remains to be verified whether JNK effectively phosphorylates PDE4 and whether this changes PDE4 enzymatic activity (Zeke et al., 2015). A putative JNK phosphorylation site can be found in the accessible LLSTPAL motif in the catalytic domain, which corresponds with the heptapeptidic consensus sequence surrounding the JNK phosphorylation site (Bogoyevitch and Kobe, 2006).

Table 1. Overview of modifications and interactions that influence PDE4 activity and the affinity of PDE4 inhibitors

Effect on PDE4 activity	Interaction/modification	Effect on inhibitor affinity	Comments	References
Increase	Akt	-		(Fang et al., 2015)
	B55α PP2a subunit	-	dephosphorylation at ERK site on PDE4D5	(Yun et al., 2019a)
	Calcineurin	-	protects against degradation	(Zhu et al., 2010)
	CaMKII	-		(Mika et al., 2015)
	Caspase-3 cleavage	-		(Huston et al., 2000)
	CDK5	-	possible synergistic activation by PKA	(Plattner et al., 2015)
	ERK	-	short isoforms of PDE4B, -4C and -4D only	(Baillie et al., 2000; MacKenzie et al., 2000)
	mAKAP/AKAP6	-	presumably through mAKAP-sequestered PKA	(Carlisle Michel et al., 2004; Dodge et al., 2001)
	Metal binding (Mg2+)	increase (R-rolipram, S-rolipram, CDP-840, cilomilast, roflumilast, piclamilast, PMNPQ)		(Huang et al., 2007; Laliberte et al., 2000; Liu et al., 2001; Saldou et al., 1998)
	Oxidative stress 'switch' kinase	no effect (rolipram)	switches ERK inhibition to activation, phosphomimetic mutation prevents dimerization	(Bolger, 2016; Hill et al., 2006)
	Phosphatidic acid	-	dimerization necessary for activation	(Grange et al., 2000; Nemoz et al., 1997; Richter and Conti, 2004)
	Phosphatidylserine	-		(Nemoz et al., 1997)
	PI3Kγ	-		(D'Andrea et al., 2015; Ghigo et al., 2012)
	PKA	increase (rolipram, BPN14770, RS-25344, RS-33793)		(Alvarez et al., 1995; Bolger, 2016; Hoffmann et al., 1998; MacKenzie et al., 2002; Sette and Conti, 1996; Zhang et al., 2018)
	RACK1	increase (rolipram)	ablates dimerization	(Bird et al., 2010; Bolger et al., 2006; Bolger et al., 2002; Yarwood et al., 1999)
	Rheb	-	stabilizes PDE4D protein expression	(Kim et al., 2010; Meng et al., 2017)

	SIK1	-		(Kim et al., 2015; Liu et al., 2020)
Decrease	CC2D1A	-	prevents activation by PKA	(Al-Tawashi and Gehring, 2013)
	DISC1	-	PKA phosphorylation releases DISC1	(Cheung et al., 2007; Millar et al., 2005; Murdoch et al., 2007)
	ERK	-	long and supershort isoforms of PDE4B, -4C and -4D only	(Baillie et al., 2000; MacKenzie et al., 2000)
	PHD2	-	presumably induces PDE4 protein degradation	(Huo et al., 2012)
	PKA (PDE4D7 only))	-		(Byrne et al., 2015)
	Smurf2	-	ubiquitination and degradation of PDE4B	(Cai et al., 2018)
	SUMO E3 ligase PIASy	-	augments PKA phosphorylation, reduces ERK inhibition	(Li et al., 2010)
	UCR1-UCR2 interaction	no effect (IBMX, rolipram, piclamilast, RS-25344)		(Beard et al., 2000; Saldou et al., 1998)
	XAP2/AIP	increase (rolipram)		(Bolger et al., 2003)
None	dimerization	increase (R-rolipram), no effect (piclamilast) / no effect (rolipram) / increased (rolipram)	dimerization enables UCR2 to bind rolipram	(Bolger et al., 2015; Cedervall et al., 2015; Richter and Conti, 2004)
	Lyn, Src	increase for rolipram		(Beard et al., 2002; Beard et al., 1999; McPhee et al., 1999; O'Connell et al., 1996)
	MK2 phosphorylation	-	phosphomimetic mutation prevents dimerization; attenuation PKA activation and interaction with DISC1 and AIP; enhances interaction of PDE4A4 with p75NTR	(Bolger, 2016; Houslay et al., 2019; MacKenzie et al., 2011)
	p75NTR	-		(Houslay et al., 2019; Sachs et al., 2007)
	PKA (PDE4D3-only)	-	upon phosphorylation PDE4D3 is released from Ndel1	(Collins et al., 2008; Sette and Conti, 1996)
Not reported	β-arrestin2	-	ablates dimerization and preferentially binds monomeric PDE4D5	(Baillie et al., 2007; Bolger, 2016; Bolger et al., 2006)

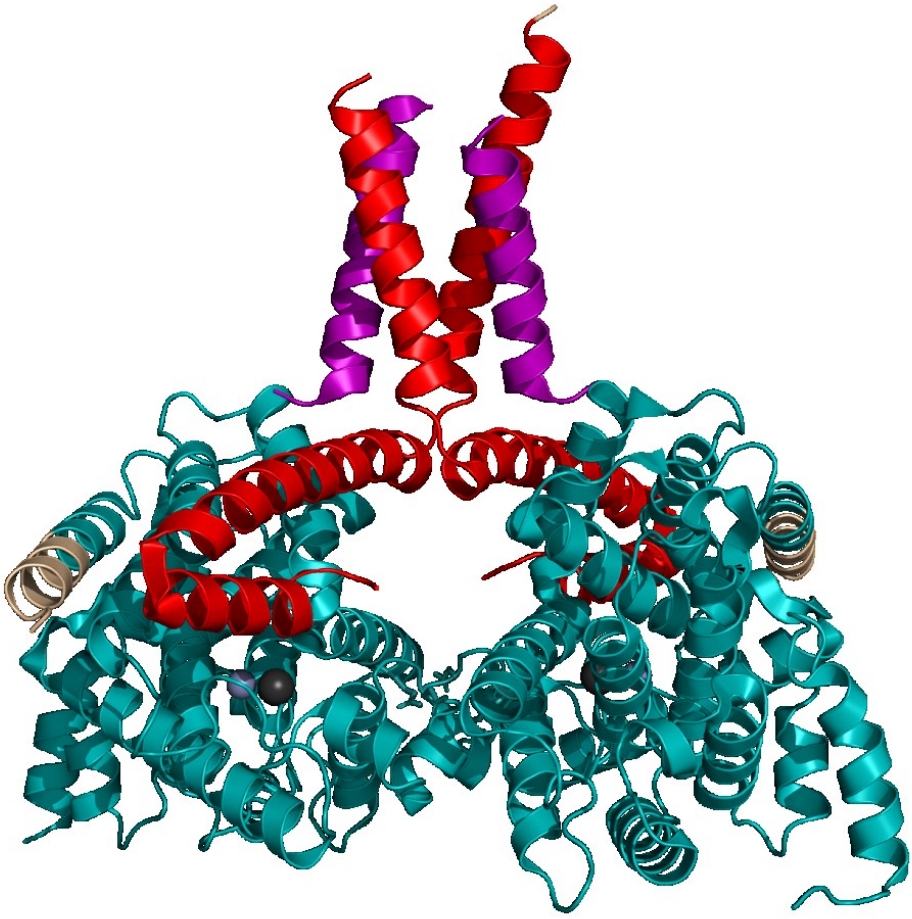

Figure 3. Tertiary structure of dimerized PDE4B demonstrating capping of UCR2 across the catalytic domain and helices 10-11. Crystal structure was derived from Protein Data Bank (PDB: 4WZI, (Cedervall et al., 2015)). UCR1 and UCR2 regions of both monomers are indicated in purple and red, respectively. Catalytic domains are colored cyan and have the catalytic metals (i.e. Mg^{2+} and Zn^{2+}) embedded as shown by the spheres. Wheat-colored helices form part of the linking region between catalytic domains and, non-modelled, C-termini. A three-dimensional representation of the image is provided in **Supplementary Video**.

C. Indirect regulation of PDE4 activity and interactions

Next to the aforementioned mechanisms, cellular PDE4 activity can be regulated through mechanisms distinct from phosphorylation. These regulatory

mechanisms may be therapeutically relevant for the disease of interest, as exemplified by the disrupted in schizophrenia 1 (DISC1) protein. DISC1 is a PDE4 interaction partner and has been found to be a risk factor for the development of psychiatric diseases when mutated (Cheung et al., 2007; Millar et al., 2005; Soda et al., 2013). DISC1 can bind and inhibit both PDE4B and PDE4D through homologous amino acids causing occlusion of the catalytic domain, while additional subtype-specific binding sites allow for a stronger interaction with PDE4B than with PDE4D **(Figure 2)**(Murdoch et al., 2007). Consequently, upon cAMP elevation, DISC1 dissociates from PDE4D while retaining its interaction with PDE4B resulting in functionally distinct roles for these PDE4 subtypes (Murdoch et al., 2007). Hence, mutations in either DISC1 or PDE4, or both, can impair or enhance this inhibitory action of DISC1 leading to aberrant PDE4 activity.

Through regulation of PDE4 mRNA and protein stability, cellular PDE4 activity can also be influenced. For example, cold-inducible RNA-binding protein (CIRP), which acts as a cellular stress regulator can stabilize PDE4B and PDE4D mRNA expression (Xie et al., 2020). Moreover, PDE4B mRNA was found to be stabilized by the common RNA modification N^6-methyladenosine, providing another mechanism to regulate PDE4 translation and subsequent activity (Huang et al., 2020). At the protein level, PDE4 expression and activity were found to be decreased upon overexpression of the oxygen-sensing protein PHD2 through hydroxylation of a specific site in the catalytic domain **(Figure 2)** (Huo et al., 2012). PDE4D contains a phosphodegron motif in its C-terminus, which upon dual phosphorylation by casein kinase I (CK1) and glycogen synthase kinase 3β (GSK3β) induces PDE4D degradation **(Figure 2)**. However, through binding of the serine/threonine protein phosphatase calcineurin, PDE4D can be protected against phosphodegron-mediated degradation, which would stabilize PDE4 activity (Zhu et al., 2010). Noteworthy, both calcineurin inhibitors and PDE4 inhibitors are used in the treatment of atopic dermatitis (Papier and Strowd, 2018). Based on the calcineurin-PDE4 interaction, these calcineurin

inhibitors may, at least in part, be effective through stimulation of PDE4 degradation. Likewise, the small GTPase Rheb stabilizes PDE4D protein expression and dissociates upon cAMP elevation to activate the mTOR pathway (Kim et al., 2010; Meng et al., 2017). Lastly, PDE4B ubiquitination can be induced upon interaction with the E3 ubiquitin ligase Smurf2 (Cai et al., 2018). Thus, PDE4 activity is indirectly regulated through control of its degradation. Conversely, when these regulatory mechanisms are affected in a disease state (e.g. in case of DISC1 mutations), PDE4 activity can consequently become dysregulated.

D. Conformational states impacting upon PDE4 activity and inhibitor binding

Upon modifications and interactions, PDE4 can exist in different conformational states. Historically, this has been recognized by PDE4 activity that could be distinguished based on different binding affinities for rolipram; a high-affinity rolipram binding site (HARBS) and low-affinity rolipram binding site (LARBS), see also **section PDE4 inhibitors** below (Jacobitz et al., 1996; Rocque et al., 1997a; Rocque et al., 1997b; Souness and Rao, 1997). Multiple studies have demonstrated several factors that contribute to the existence of distinct conformers. For example, binding Mg^{2+} in the catalytic domain dose-dependently increases enzymatic activity but also increases the affinity to bind rolipram and other inhibitors **(Table 1)**(Alvarez et al., 1995; Laliberte et al., 2000; Wilson et al., 1994). Similarly, phosphorylation by PKA and RACK1 binding both increase PDE4 activity and induce an increase in rolipram affinity (MacKenzie et al., 2002; Zhang et al., 2018). However, the effect of phosphorylation by PKA on rolipram affinity can be different per long isoform (MacKenzie et al., 2002). Interestingly, increases in enzyme activity upon phosphorylation by PKA may actually be a consequence of an increase in Mg^{2+} sensitivity, which subsequently would facilitate cAMP catalysis as well as binding of certain inhibitors through water-mediated interactions (Laliberte et al., 2000; Saldou et al., 1998). Indeed, as proposed by Houslay and Adams, modifications at the N-terminus may be relayed via conformational changes to the catalytic domain to

eventually influence enzyme activity (Houslay and Adams, 2003). For example, upon PKA phosphorylation and possibly also other PDE4-activating phosphorylation events in the UCR1 (**Figure 2**), the UCR1-UCR2 module and/or UCR2-catalytic domain interactions may be disrupted (Beard et al., 2000; Houslay and Adams, 2003). Subsequently, this altered conformation could change the orientation of helices 10 and 11 in the catalytic domain that flank the catalytic metals, thereby impacting the way these metals are held in place. More specifically, helices 10 and 11 form a tweezer-like structure (**Figure 4**, dark blue helices) and are connected by a loop (**Figure 4**, orange) which may interact with UCR2 and/or LR2 residues (**Figure 4**). As such, N-terminal modifications and interactions can, directly or through modulation of this UCR2/LR2 stretch, alter the conformation of this connecting loop, thereby changing the way helices 10 and 11 stabilize catalytic metal binding. Consequently, catalytic activity and metal-mediated inhibitor binding will be influenced. Vice versa, inhibitor binding can impact the ability of PDE4 forms to engage in protein-protein interactions via 'inside-out signaling', which supports the notion that conformational changes are relayed between the catalytic domain and N-terminal regions. (Day et al., 2011; Terry et al., 2003). Interestingly, as the LR2 region is not conserved among PDE4 subtypes, its effect on metal coordination through interaction with the helix 10-11 connecting loop may be different per PDE4 subtype. Indeed, deletion of the UCR2 and LR2 regions significantly decreases the sensitivity of PDE4D, but not PDE4A or PDE4B, to bind Mg^{2+} (Saldou et al., 1998).

PDE4 enzymes exhibiting increased activity are not analogous to increased inhibitor affinity, as also interactions that do not increase PDE4 activity influence inhibitor binding. Binding of the proteins XAP2 and Lyn enhances the sensitivity to rolipram, but has a negative or no effect on PDE4 activity, respectively **(Table 1)**(Bolger et al., 2003; McPhee et al., 1999). Furthermore, it has been postulated that the HARBS conformer constitutes of long isoforms since their dimerized state stabilizes HARBS (Richter and Conti, 2004). However, HARBS is not dependent on

dimerization or the presence of UCR1 but rather is formed by inhibitor-UCR2 interactions indicating that (super)short isoforms can also exhibit HARBS (Jacobitz et al., 1996). Indeed, truncated proteins similar to supershort forms that do possess the inhibitory UCR2 helix exhibit both HARBS and LARBS, whilst further deletion of the entire UCR2 only displays LARBS (Rocque et al., 1997a; Rocque et al., 1997b). These findings correspond to the fact that UCR2/LR2 residues may bind the connecting loop between helices 10-11 to regulate catalytic metal ion coordination. Absence of these residues would ablate the ability to change metal coordination and the consequent change in enzyme activity and metal-engaging inhibitor binding. Thus, both HARBS and LARBS comprise different states that depend on dimerization, degree of metal binding, interaction with partner proteins, and phosphorylation but which display similar affinities to inhibitors. Selective inhibition of PDE4 forms in HARBS or LARBS conformation has been shown to yield distinct biological effects although the exact PDE4 isoforms and/or conformation-mediators remain to be specified. For example, inhibition of HARBS in the brain was found to produce antidepressant-like effects in rats (Zhang et al., 2006). Moreover, using PDE4 inhibitors that selectively bind HARBS or LARBS, Boomkamp et al. identified that inhibition of HARBS, but not LARBS, mediates myelination and neurite outgrowth *in vitro* (Boomkamp et al., 2014).

The notion that inhibitors can display divergent affinities towards isoforms in different conformational states and that conformation-specific inhibition can exert different biological effects has implications for drug discovery and development. Hence, it is crucial to understand which isoforms, in what conformational state, should be targeted in the disease of interest that determine the most potent inhibitor (see also **section PDE4 inhibitors**).

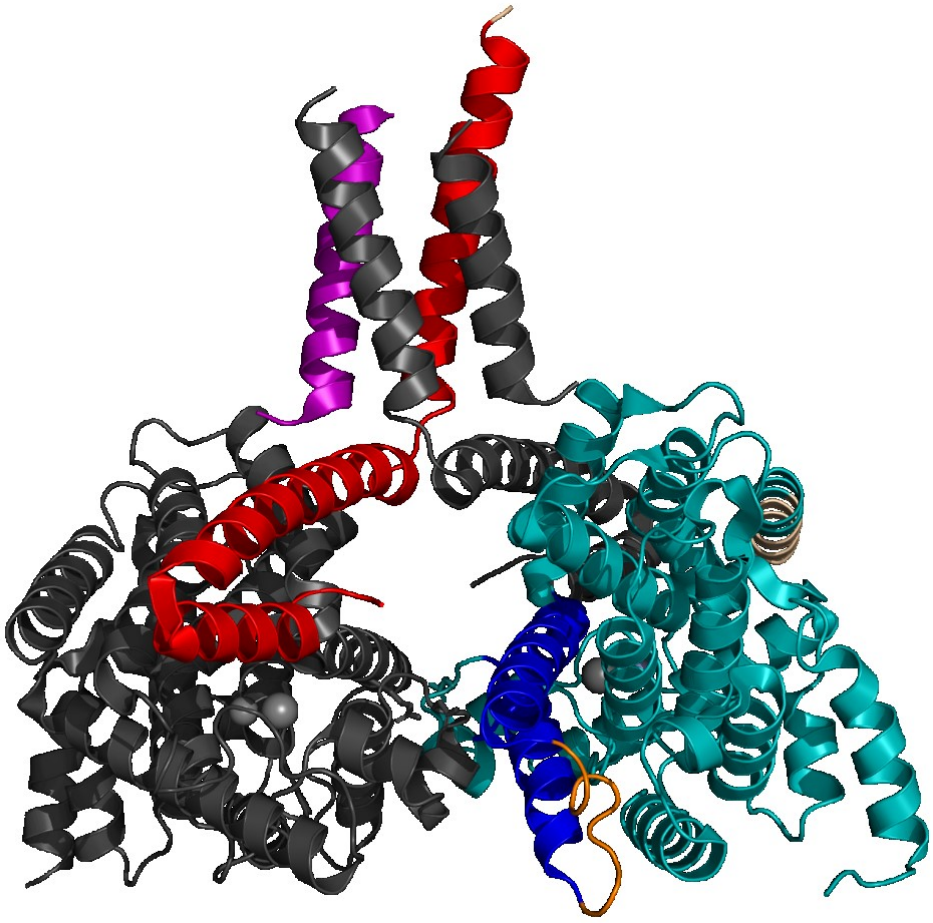

Figure 4. Tertiary structure of dimerized PDE4B demonstrating helices 10-11 and its connecting loop. One monomer is colored dark gray while helices 10-11, flanking the catalytic metals, of the other monomer are now colored dark blue. The connecting loop between helices 10-11 is indicated in orange. The C-terminal of UCR2 (red loose end in the middle) is connected to the N-terminus of the catalytic domain (loose end in cyan in right-bottom corner) via LR2 which is not modeled, but which would fold across the helix 10-11 connecting loop. Modifications and interactions in the N-terminal are hypothesized to be relayed, via UCR2/LR2-associated changes, to the connecting loop of helices 10-11 to change catalytic metal ion coordination which subsequently impacts cAMP catalysis and affinity towards certain metal-interacting inhibitors.

E. Intracellular PDE4 localization and anchoring

1. A-kinase anchoring proteins (AKAPs)

In addition to activity-altering interactions, PDE4 engages in protein-protein interactions that contribute to specific intracellular localization patterns. Accurate localization of PDE4 enzymes is crucial for the directed breakdown of compartmentalized cAMP. Many studies have indicated an essential role for A-kinase anchoring proteins (AKAP) in tethering signaling molecules regulating cAMP signaling, including PDE4 subtypes and isoforms (reviewed in e.g. (McConnachie et al., 2006; Omar and Scott, 2020; Wild and Dell'Acqua, 2018)). Through specific binding domains, the extensive collection of AKAPs allows the assembly of signaling modules consisting of PKA and PDE4 that are anchored to specific organelles, receptors (e.g. to the 5HT4b receptor (Weninger et al., 2014)), or cytoskeletal proteins (McConnachie et al., 2006)). Important to note is that phosphorylation of the PDE4D3-specific PKA site facilitates its binding to mAKAP, which localizes to the ryanodine receptor (RyR) (Carlisle Michel et al., 2004; Lehnart et al., 2005). Additionally, as PKA is bound to AKAPs as well, tethering PDE4D3 to mAKAP also promotes phosphorylation of the common PKA site causing PDE4 activation near the RyR (Dodge et al., 2001). Moreover, PDE4D3 can be brought into contact with I_K channels through selectively binding AKAP9 (Terrenoire et al., 2009; Terrin et al., 2012). Interestingly, the PDE4 residues involved in binding AKAP18δ are present in all isoforms, but tissue-specific expression causes only PDE4D3 and PDE4D9 to be associated with AKAP18δ (aka AKAP7) in the kidney, highlighting the importance of studying cellular, tissue- or disease-relevant PDE4 expression (Stefan et al., 2007). Furthermore, PDE4 has shown to associate with AKAP450 (aka AKAP350, CG-NAP, Hyperion or Yotiao) (McCahill et al., 2005; Tasken et al., 2001), AKAP95 (AKAP8) (Asirvatham et al., 2004; Clister et al., 2019), AKAP3 (does not bind PDE4D) (Bajpai et al., 2006), MTG16B (Asirvatham et al., 2004), AKAP149 (Asirvatham et al., 2004), AKAP5 (also known as AKAP79) (Choi et al., 2011; Kocer et al., 2012), and Gravin (also

called AKAP12, AKAP250 or SSeCKS; which binds PDE4D3 and PDE4D5) (Willoughby et al., 2006). Although direct effects of AKAP binding on PDE4 activity remain largely undetermined, it is known that myomegalin (PDE4DIP) utilizes the same PDE4 residues that mediate UCR1-UCR2 interaction and dimerization, and hence could influence the conformational state and activity of the bound PDE4 (Uys et al., 2011; Verde et al., 2001). Moreover, interactions between specific PDE4 forms and specific AKAPs may only occur in specific cell types or organs as more specifically described elsewhere ((Baillie et al., 2019; Zaccolo et al., 2021)).

2. Not AKAP-related

Independently of AKAPs, certain PDE4 isoforms can bind to specific structures through subtype- or isoform-specific amino acids. For example, the PDE4D4 and PDE4A4 isoforms have been found to localize to specific organelles and the plasma membrane through interactions with SH3 domains of the tyrosine kinases Lyn, Src, and Fyn via their N-terminus proline residues that possibly affect inhibitor binding **(Table 1)** (Beard et al., 2002; Beard et al., 1999; Huston et al., 2000; McPhee et al., 1999; O'Connell et al., 1996). Additionally, PDE4D4 is anchored to the cytoskeleton via interaction with αII spectrin (Creighton et al., 2008). The PDE4D-specific LR2 sequence allows interaction with integrin α5, which brings PDE4D in vicinity to a phosphatase that rectifies ERK-induced phosphorylation (**Figure 2**) (Yun et al., 2016; Yun et al., 2019a). The supershort PDE4A1 is membrane-bound via specific residues in its N-terminus (Baillie et al., 2002; Shakur et al., 1993), and similar observations have been made for the short PDE4B2 isoform (Lobban et al., 1994). Likewise, PDE4A4 is associated with the membrane, but upon cleavage by caspase-3, it is redistributed within the membrane (Huston et al., 2000). Hence, post-translational modifications can alter intracellular distribution and compartmentalization, which is also supported by the fact that phosphorylation events can translocate membrane-associated PDE4 to the cytosol (Liu and Maurice,

1999). Through interactions in UCR1 and UCR2, mainly long PDE4D forms have been found to interact with Shank2 (Lee et al., 2007). As Shank2 also binds cystic fibrosis transmembrane conductance regulator (CFTR), this may explain the association of PDE4 enzymes with CFTR (Blanchard et al., 2014; Lee et al., 2007). Lastly, PDE4 enzymes can be intracellularly recruited to the $p75^{NTR}$ and neuropilin receptors, which are involved in neuronal growth (Ge et al., 2015; Houslay et al., 2019; Sachs et al., 2007). Vice versa, PDE4 enzymes can modulate cellular signaling cascades through scaffolding other molecules away from their usual binding partners. This is exemplified by the fact that PDE4 can recruit LIS1 causing it to disassociate from dynein. Subsequently, dynein function will be impaired causing changes in microtubule transport and directed cell migration (Murdoch et al., 2011). As many interactions between PDE4 and partner proteins rely on isoform-specific amino acid stretches, these interactions can localize PDE4 isoforms to distinct subcellular compartments. Consequently, different PDE4 isoforms may regulate spatially distinct cAMP signaling cascades and isoform-specific PDE4 inhibition would enable more precise modulation of these different cAMP cascades.

III. PDE4 INHIBITORS

As an important cellular regulator of cAMP levels and associated intracellular signal transduction, PDE4 has been investigated as therapeutic target in a wide variety of disorders. Based on promising observations upon treatment with non-selective PDE inhibitors and the prototypical PDE4-selective inhibitor rolipram, PDE4 inhibitors have been developed with improved potency. Despite increased potency, clinical progression of PDE4 inhibitors has been hampered primarily due to the occurrence of severe adverse side effects (see also below in section **PDE4 side effects**). Therefore, to improve treatment efficacy and safety, PDE4 inhibitor specificity next to potency may have to be considered. As discussed above, both the diversity in PDE4 isoforms that display distinct enzymatic properties, the amino acid differences among subtypes as well as isoform-specific N-termini allow for complex activity regulation by post-translational modifications and interactions with partner proteins. Eventually, this regulatory control can influence the enzyme's activity through conformational changes. These specific interactions, non-conserved amino acids and distinct conformational states can provide the opportunity to target PDE4 activity more specifically at the subtype and isoform level.

This section will outline several aspects that should be considered when determining PDE4 inhibitor specificity towards subtypes or isoforms by providing an extensive overview of inhibitor screening literature. Furthermore, this section will summarize which PDE4 inhibitors have been developed to show more specific targeting of subtypes, isoform and/or conformations.

A. PDE4 inhibitors and HARBS and LARBS

As mentioned above, HARBS and LARBS represent different conformational states that exhibit different inhibitor affinities and that can be influenced through several mechanisms (e.g. metal binding, phosphorylation or binding of partner proteins). Based on the observation that preferential inhibition of HARBS was

correlated with adverse effects, efforts were made to develop PDE4 inhibitors with reduced HARBS binding (Barnette et al., 1995; Duplantier et al., 1996). Selective inhibition of HARBS or LARBS can produce distinct cellular effects, which provides additional support for improved therapeutic potential of conformation-specific inhibitors (Boomkamp et al., 2014; Zhang et al., 2006). However, HARBS and LARBS conformations can occur in all PDE4 subtypes and HARBS seems to require a part of the UCR2 domain, suggesting that both long and short PDE4 isoforms can exert HARBS (Souness and Rao, 1997). Thus, although HARBS and LARBS can be preferentially bound by certain inhibitors, selective binding of these conformations does not directly allow for PDE4 subtype or isoform selectivity. However, as described in **subsection II.D.**, HARBS and LARBS conformations may, in part, be a consequence of differences in the orientation of two helices that flank the catalytic domain and that coordinate the catalytic metals (Houslay and Adams, 2003). The positioning of these helices is likely impacted by LR2 residues, which are non-conserved among PDE4 subtypes. Associated with these PDE4 subtype-specific LR2 residues, changes in metal orientation between HARBS and LARBS may be different among the PDE4 subtypes, which is supported by subtype-specific sensitivities to Mg^{2+} depending on whether LR2 is present or not (Saldou et al., 1998). Hence, although highly speculative, it may be possible to alter PDE4 activity subtype-selectively by means of allosteric modulation in the LR2 region which subsequently modifies enzyme activity through changes in metal orientation. In support of this hypothesis, the kinases CaMKII and the 'oxidative stress kinase' both phosphorylate residues in the LR2 region and have been shown to modulate PDE4 activity (**Figure 2** and **Table 1**) (Hill et al., 2006; Mika et al., 2015).

As PDE4 subtypes and isoforms regulate distinct cellular and behavioral functions, PDE4 subtype-selective inhibition, rather than preferential binding of HARBS or LARBS, may show superior treatment efficacy compared to non-selective PDE4 inhibition (Blackman et al., 2011; Zhang et al., 2017).

B. Determining PDE4 inhibitor subtype- and isoform-selectivity in assays

1. The influence of PDE4 construct and assay type on PDE4 inhibitor screenings

Given the importance of subtype-, isoform- or conformation-specific inhibition for treatment efficacy and safety, it is crucial to assess these properties of PDE4 inhibitors. Initial high-throughput screenings often utilized the catalytic domain of a single PDE4 subtype only to determine the ability of a compound to inhibit PDE4 activity. Since these catalytic domain constructs may not express UCR2 domains, these enzymes do not resemble cellular PDE4 activity as UCR2-mediated auto-inhibition or capping is not possible. Furthermore, the lack of the UCR2 alters the Mg^{2+} sensitivity of the enzyme and could therefore skew screening results as both enzyme activity and Mg^{2+}-mediated inhibitor binding may be impacted (Saldou et al., 1998). Hence, compound screening for PDE4 inhibitory activity using the catalytic domain of a single PDE4 subtype only will provide limited insight into the compound's potential subtype-selectivity. Subtype-selectivity should therefore be assessed by using constructs of these different PDE4 subtypes and constituting a full-length protein rather than the catalytic domain only. Linked to this, as catalytic domains show large similarity among PDE4 subtypes, selectivity can more likely be achieved through interactions with amino acid residues outside of the catalytic domain (Wang et al., 2007a). Thus, to determine potential subtype-selectivity of PDE4 inhibitors, the use of full-length PDE4 constructs will provide a better understanding compared to using only PDE4 catalytic domains.

PDE4 inhibitors can be tested in both cellular assays and assays utilizing purified PDE4, but affinity values cannot be directly compared across studies as they are dependent on the used assay. For example, affinity values derived from assays using purified PDE4 versus overexpressed PDE4 constructs in a cellular assay can show an 80-fold difference (Wunder et al., 2013). Moreover, other studies showed that inhibitor affinity to isolated PDE4 enzymes does not reflect its potency in intact tissue

(Harris et al., 1989). Furthermore, differences exist regarding which cell lines and heterologous expression systems are used for cellular assays or purified protein assays, respectively, which prevents comparison across studies that using different methodologies. Although assays using purified protein can provide a detailed understanding on the affinity and potency of an inhibitor, these assays do not reflect dynamic changes in (subtype-specific) PDE4 conformational states and associated affinity changes that would occur in a cellular environment. Hence, when assessing potential subtype-specificity of PDE4 inhibitors, affinity values can only be compared within studies and the most accurate approximation of *in vivo* PDE4 inhibition can be assessed by using full-length enzymes that contain all regulatory elements.

Table 2 provides a comprehensive overview of studies in which affinities of PDE4 inhibitors towards different PDE4 subtypes were assessed. As mentioned, affinity values, indicated as nanomolar concentrations that cause half-maximum inhibition (IC50), cannot be compared across studies as different assays may have been used. For each subtype construct, it is indicated whether a particular isoform was used and whether the construct entailed the full-length protein or was truncated. From this overview, it becomes evident that several studies have assessed compound selectivity for PDE4 subtypes by using constructs of different isoform categories (i.e. long, short, or supershort) per subtype. Several studies indicate that inhibitors can exhibit different affinities towards PDE4 subtypes. For example, cilomilast seems to show slightly higher affinity towards PDE4D, irrespective of whether truncated supershort or long isoforms are used (Asaka et al., 2010; Huang et al., 2007). Interestingly, many compounds show notable lower affinity towards PDE4C, whilst other compounds (e.g. UFM24) preferentially bind PDE4C (Tsai et al., 2017b). As PDE4C shows the least homology with the other subtypes, PDE4C-specific residues therefore may either promote or impede inhibitor binding, yielding PDE4C-specific or PDE4C-aversive binding, respectively.

Table 2. PDE4 inhibitors tested for their selectivity against different PDE4 subtypes

Compound	Study	PDE4 form	Construct category	IC50 (nM)
A-33	(Naganuma et al., 2009)	PDE4B	cat dom + C-terminus	15
		PDE4D	cat dom + C-terminus	1700
	(Hagen et al., 2014)	PDE4B1	long	55
		PDE4D7	long	1997
CDP840	(Perry et al., 1998)	PDE4A4	long	3.5
		PDE4B3	long	3.8
		PDE4C2	long	30
		PDE4D3	long	2.6
	(Aoki et al., 2001b)	PDE4A4	long	27
		PDE4B1	long	10
		PDE4C1	long	63
		PDE4D3	long	14
Cilomilast	(Huang et al., 2007)	PDE4A	truncated (supershort)	42.9
		PDE4B	truncated (supershort)	40.7
		PDE4C	truncated (supershort)	160
		PDE4D	truncated (supershort)	6.9
	(Asaka et al., 2010)	PDE4A1	supershort	62
		PDE4B1	long	56
		PDE4C1	long	302
		PDE4D3	long	19
	(Pruniaux et al., 2010)	PDE4A4	long	34
		PDE4B2	short	70
		PDE4C2	long	238
		PDE4D3	long	7
	(Huang et al., 2006)	PDE4A	truncated (supershort)	37
		PDE4B	truncated (supershort)	34
		PDE4C	truncated (supershort)	133
		PDE4D	truncated (supershort)	7
CI-1044	(Pruniaux et al., 2010)	PDE4A4	long	290
		PDE4B2	short	80
		PDE4C2	long	560
		PDE4D3	long	90
CT-2450	(Robichaud et al., 2002b)	PDE4A	truncated (supershort)	0.9
		PDE4B	truncated (supershort)	0.7
		PDE4C	truncated (supershort)	1.6
		PDE4D	truncated (supershort)	0.5
EPPA-1	(Davis et al., 2009)	PDE4A4	long	93.0

Compound	Study	PDE4 form	Construct category	IC50 (nM)
EPPA-1 (cont.)		PDE4B2	short	45.7
		PDE4C1	long	142.2
		PDE4D3	long	35.1
GEBR4d	(Brullo et al., 2020)	PDE4B2	short	550
		PDE4D3	long	1050
GEBR5d	(Brullo et al., 2020)	PDE4B2	short	550
		PDE4D3	long	1220
GPD-1116	(Nose et al., 2016)	PDE4A4	long	100
		PDE4B2	short	500
		PDE4C2	long	100
		PDE4D3	long	50
GPD-1133	(Nose et al., 2016)	PDE4A4	long	40
		PDE4B2	short	200
		PDE4C2	long	63
		PDE4D3	long	50
Ibudilast	(Huang et al., 2006)	PDE4A	truncated (supershort)	54
		PDE4B	truncated (supershort)	65
		PDE4C	truncated (supershort)	239
		PDE4D	truncated (supershort)	166
L-454.560	(Huang et al., 2007)	PDE4A	truncated (supershort)	1.6
		PDE4B	truncated (supershort)	0.5
		PDE4C	truncated (supershort)	9.1
		PDE4D	truncated (supershort)	1.2
L-826,141	(Claveau et al., 2004)	PDE4A	truncated (supershort)	1.26
		PDE4B	truncated (supershort)	0.38
		PDE4C	truncated (supershort)	2.38
		PDE4D	truncated (supershort)	0.26
Moexipril	(Cameron et al., 2013)	PDE4A4	long	160
		PDE4B2	short	38
		PDE4D5	long	230
PMNPQ	(Bureau et al., 2006)	PDE4A	truncated (supershort)	0.1
		PDE4B	truncated (supershort)	0.1
		PDE4C	truncated (supershort)	0.1
		PDE4D	truncated (supershort)	0.1
Roflumilast	(Nose et al., 2016)	PDE4A4	long	0.17
		PDE4B2	short	0.27
		PDE4C2	long	1
		PDE4D3	long	0.15

Compound	Study	PDE4 form	Construct category	IC50 (nM)
Roflumilast (cont.)	(Claveau et al., 2004)	PDE4A	truncated (supershort)	0.16
		PDE4B	truncated (supershort)	0.11
		PDE4C	truncated (supershort)	0.61
		PDE4D	truncated (supershort)	0.11
	(Huang et al., 2007)	PDE4A	truncated (supershort)	0.16
		PDE4B	truncated (supershort)	0.11
		PDE4C	truncated (supershort)	0.61
		PDE4D	truncated (supershort)	0.11
Roflumilast N-oxide	(Claveau et al., 2004)	PDE4A	truncated (supershort)	0.58
		PDE4B	truncated (supershort)	0.37
		PDE4C	truncated (supershort)	3.2
		PDE4D	truncated (supershort)	0.31
	(Huang et al., 2007)	PDE4A	truncated (supershort)	0.58
		PDE4B	truncated (supershort)	0.37
		PDE4C	truncated (supershort)	3.2
		PDE4D	truncated (supershort)	0.31
Rolipram	(Aoki et al., 2001b)	PDE4A4	long	690
		PDE4B1	long	270
		PDE4C1	long	1900
		PDE4D3	long	260
	(Asaka et al., 2010)	PDE4A1	supershort	565
		PDE4B1	long	402
		PDE4C1	long	888
		PDE4D3	long	234
R-rolipram	(Claveau et al., 2004)	PDE4A	truncated (supershort)	4.8
		PDE4B	truncated (supershort)	5.4
		PDE4C	truncated (supershort)	40.5
		PDE4D	truncated (supershort)	3.9
	(Perry et al., 1998)	PDE4A4	long	84.4
		PDE4B3	long	69
		PDE4C2	long	612
		PDE4D3	long	84.3
RP73401	(Aoki et al., 2001b)	PDE4A4	long	0.9
		PDE4B1	long	0.32
		PDE4C1	long	4.8
		PDE4D3	long	0.42
TAS-203	(Asaka et al., 2010)	PDE4A1	supershort	47

Compound	Study	PDE4 form	Construct category	IC50 (nM)
TAS-203 (cont.)		PDE4B1	long	35
		PDE4C1	long	227
		PDE4D3	long	43
UFM24	(Tsai et al., 2017a)	PDE4A1	supershort	7510
		PDE4B2	short	8580
		PDE4C1	long	1750
		PDE4D2	supershort	3530
YM976	(Aoki et al., 2001b)	PDE4A4	long	3.5
		PDE4B1	long	1
		PDE4C1	long	13
		PDE4D3	long	1.7
9	(Hagen et al., 2014)	PDE4B1	long	770
		PDE4D7	long	5611
29	(Hagen et al., 2014)	PDE4B1	long	165
		PDE4D7	long	7
5	(Skoumbourdis et al., 2009)	PDE4A1	supershort	12.9
		PDE4B1	long	48.2
		PDE4B2	short	37.2
		PDE4C1	long	452
		PDE4D2	supershort	49.2
10	(Skoumbourdis et al., 2009)	PDE4A1	supershort	0.26
		PDE4B1	long	2.3
		PDE4B2	short	1.6
		PDE4C1	long	46
		PDE4D2	supershort	1.9
18	(Skoumbourdis et al., 2009)	PDE4A1	supershort	0.6
		PDE4B1	long	4.1
		PDE4B2	short	2.9
		PDE4C1	long	106
		PDE4D2	supershort	2.1
11r	(Tang et al., 2019)	PDE4B1	long	340
		PDE4D7	long	380
16a	(Huang et al., 2019)	PDE4B1	long	293
		PDE4D7	long	312
44	(Goto et al., 2014)	PDE4B2	short	4.6
		PDE4D2	supershort	620
5a	(Brullo et al., 2014)	PDE4B2	short	1600
		PDE4D3	long	660

Compound	Study	PDE4 form	Construct category	IC50 (nM)
10b	(Brullo et al., 2014)	PDE4B2	short	18000
		PDE4D4	long	210
1	(Purushothaman et al., 2018)	PDE4A4	long	45
		PDE4B1	long	31
		PDE4C1	long	77
		PDE4D7	long	220
2	(Purushothaman et al., 2018)	PDE4A4	long	152
		PDE4B1	long	15
		PDE4C1	long	57
		PDE4D7	long	108
A	(Manning et al., 1999)	PDE4A4	long	6.46
		PDE4B2	short	14.13
		PDE4D3	long	39.81
B	(Manning et al., 1999)	PDE4A4	long	100.00
		PDE4B2	short	77.62
		PDE4D3	long	13.49
C	(Manning et al., 1999)	PDE4A4	long	33.11
		PDE4B2	short	30.20
		PDE4D3	long	295.12
D	(Manning et al., 1999)	PDE4A4	long	1318.26
		PDE4B2	short	316.23
		PDE4D3	long	257.04
E	(Manning et al., 1999)	PDE4A4	long	208.93
		PDE4B2	short	173.78
		PDE4D3	long	36.31
F	(Manning et al., 1999)	PDE4A4	long	63.10
		PDE4B2	short	57.54
		PDE4D3	long	11.75
G	(Manning et al., 1999)	PDE4A4	long	588.84
		PDE4B2	short	389.05
		PDE4D3	long	54.95
H	(Manning et al., 1999)	PDE4A4	long	1.23
		PDE4B2	short	1.51
		PDE4D3	long	10.96
I	(Manning et al., 1999)	PDE4A4	long	0.25
		PDE4B2	short	0.69
		PDE4D3	long	4.17
J	(Manning et al., 1999)	PDE4A4	long	0.27

Compound	Study	PDE4 form	Construct category	IC50 (nM)
J		PDE4B2	short	1.35
(cont.)		PDE4D3	long	3.98

Importantly, seemingly subtype-selectivity may be a result of or biased by preferred binding to an isoform of particular length rather than specificity to the PDE4 subtype. Since isoforms of different lengths exhibit different properties due to the presence or absence of regulatory domains (e.g. long forms can dimerize via UCR1-UCR2 interactions), isoform categories of the same PDE4 subtype may be preferentially bound by certain inhibitors. To reveal potential isoform-specific binding, **Table 3** presents an overview of compounds that were tested, in the same assay, for their affinity towards PDE4 constructs of different lengths of the same PDE4 subtype. Various compounds show increased affinity towards the long isoforms compared to its catalytic domain only, in which the regulatory UCR1, UCR2, and C-terminus domains are deleted (e.g. (Wunder et al., 2013)). As these regulatory domains convey effects of post-translational modifications and interactions with partner proteins, these modifications and interactions themselves may exert an effect on inhibitor affinity within the same PDE4 isoform as explained earlier. Indeed, for example, PKA phosphorylation has been shown to profoundly impact inhibitor affinity (e.g. (Hoffmann et al., 1998)) which supports the notion that assays using purified, non-phosphorylated enzyme cannot be compared to cellular assays in which PDE4 activity is dynamically regulated (Wunder et al., 2013). As certain modifications or interactions can only occur in specific PDE4 subtypes or isoforms to induce conformational changes (**Figure 2**), these conformations provide actually other means of achieving more specific PDE4 inhibition. Therefore, it is crucial to understand how different conformational states, caused by modifications or interactions, impact inhibitor affinity.

Table 3. PDE4 inhibitors tested for their selectivity against different PDE4 isoforms or construct lengths of the same PDE4 subtype

Compound	Study	Construct	Construct category	Truncation/Modification	IC50 (nM)
CDP840	(Perry et al., 1998)	PDE4B2	short		1.9
		PDE4B3	long		3.8
		PDE4D2	supershort		2.9
		PDE4D3	long		2.6
Chlorbipram	(Zhang et al., 2013)	PDE4B2	short		99300
		PDE4B5	supershort		8320
Cilomilast	(Wunder et al., 2013)	PDE4D3		cat dom	20.5
		PDE4D3	long		10.1
Denbuylline	(Owens et al., 1997a)	PDE4A4	long		295
		PDE4A4	cat dom	UCR1-UCR2 deleted	550
D159153	(Wunder et al., 2013)	PDE4D3		cat dom	20500
		PDE4D3	long		68.3
D159404	(Wunder et al., 2013)	PDE4D3		cat dom	20000
		PDE4D3	long		380
Etazolate	(Wunder et al., 2013)	PDE4D3		cat dom	143
		PDE4D3	long		240
GEBR-32a	(Ricciarelli et al., 2017)	PDE4D1	short		4970
		PDE4D2	supershort		2890
		PDE4D3	long		2420
		PDE4D5	long		3180
		PDE4D7	long		1140
	(Prosdocimi et al., 2018)	PDE4D	cat dom	cat dom, no C-term	2300
		PDE4D3	long	PKA-mimetic, ERK-ablative	1000
(S)-(+)-GEBR-32a	(Cavalloro et al., 2020)	PDE4D	catdom	cat dom, no C-term	19500
		PDE4D3	long	PKA-mimetic, ERK-ablative	2100
(R)-(-)-GEBR-32a	(Cavalloro et al., 2020)	PDE4D	catdom	cat dom, no C-term	31800
		PDE4D3	long	PKA-mimetic, ERK-ablative	15500
GEBR-7b	(Prosdocimi et al., 2018)	PDE4D	cat dom	cat dom, no C-term	1600
		PDE4D3	long	PKA-mimetic, ERK-ablative	1100
GEBR-20b	(Prosdocimi et al., 2018)	PDE4D	cat dom	cat dom, no C-term	800
		PDE4D3	long	PKA-mimetic, ERK-ablative	600
GEBR-4a	(Prosdocimi et al., 2018)	PDE4D	cat dom	cat dom, no C-term	7000

Compound	Study	Construct	Construct category	Truncation/Modification	IC50 (nM)
GEBR-4a		PDE4D3	long	PKA-mimetic, ERK-ablative	2100
GEBR-11b	(Prosdocimi et al., 2018)	PDE4D	cat dom	cat dom, no C-term	900
		PDE4D3	long	PKA-mimetic, ERK-ablative	400
GEBR-26g	(Prosdocimi et al., 2018)	PDE4D	cat dom	cat dom, no C-term	17000
		PDE4D3	long	PKA-mimetic, ERK-ablative	3500
GEBR-54	(Prosdocimi et al., 2018)	PDE4D	cat dom	cat dom, no C-term	20000
		PDE4D3	long	PKA-mimetic, ERK-ablative	4600
GEBR-18b	(Prosdocimi et al., 2018)	PDE4D	cat dom	cat dom, no C-term	16000
		PDE4D3	long	PKA-mimetic, ERK-ablative	4800
GEBR-18a	(Prosdocimi et al., 2018)	PDE4D	cat dom	cat dom, no C-term	23000
		PDE4D3	long	PKA-mimetic, ERK-ablative	5000
Lirimilast	(Wunder et al., 2013)	PDE4D3		cat dom	3725
		PDE4D3	long		54.3
Oglemilast	(Wunder et al., 2013)	PDE4D3		cat dom	0.5
		PDE4D3	long		1.1
Piclamilast	(Wunder et al., 2013)	PDE4D3		cat dom	0.064
		PDE4D3	long		0.12
PMNPQ	(Wunder et al., 2013)	PDE4D3		cat dom	115
		PDE4D3	long		0.43
Roflumilast	(Wunder et al., 2013)	PDE4D3		cat dom	0.039
		PDE4D3	long		0.076
Roflumilast N-oxide	(Wunder et al., 2013)	PDE4D3		cat dom	0.079
		PDE4D3	long		0.26
Rolipram	(Bruno et al., 2009)	PDE4D1	short		910
		PDE4D2	supershort		1170
		PDE4D3	long		550
	(Wunder et al., 2013)	PDE4D3		cat dom	510
		PDE4D3	long		72.8
Rolipram	(Zhang et al., 2013)	PDE4D4	long		470
		PDE4D5	long		190
	(Wang et al., 2003)	PDE4D6	supershort		57
		PDE4D7	long		42
R-rolipram	(Perry et al., 1998)	PDE4B2	short		60.5
		PDE4B3	long		69
		PDE4D2	supershort		26.9
		PDE4D3	long		84.3

Compound	Study	Construct	Construct category	Truncation/Modification	IC50 (nM)
Ro20-1724	(Owens et al., 1997a)	PDE4A4	long		1450
		PDE4A4	catdom	UCR1-UCR2 deleted	4154
YM976	(Wunder et al., 2013)	PDE4D3		cat dom	0.34
		PDE4D3	long		0.73
Zardaverine	(Wunder et al., 2013)	PDE4D3		cat dom	163
		PDE4D3	long		65.3
4a	(Bruno et al., 2009)	PDE4D1	short		7090
		PDE4D2	supershort		9180
		PDE4D3	long		2860
4e	(Liang et al., 2020)	PDE4B2	short	cat dom	10
		PDE4B1	long		8
		PDE4D2	supershort	cat dom	17
		PDE4D7	long		9

Several studies have investigated these effects of conformational state on PDE4 inhibitor affinity and these findings are summarized in **Table 4**. By means of mutations that mimic phosphorylation by PKA and ablate phosphorylation by ERK, the effects of PKA phosphorylation *per se* on inhibitor affinity can be simulated (Burgin et al., 2010; Hoffmann et al., 1998). This phosphorylation-mimicking mutation profoundly increases the affinity of rolipram and BPN14770 to bind the long form PDE4D7 (Zhang et al., 2018) (see **Table 4**), indicating that inhibitors can preferentially bind PKA-phosphorylated PDE4 states. Mechanistically, increased inhibitor affinity upon phosphorylation by PKA could be due to a more favorable positioning of UCR2, increased Mg^{2+} sensitivity to aid inhibitor binding, or a combination of both. Interestingly, although PDE4 phosphorylation by PKA also increases enzymatic activity as a biological feedback loop, this feedback mechanism would actually facilitate or strengthen binding of these inhibitors. Since PKA-phosphorylated PDE4 displays higher enzymatic activity, preferential inhibition of this activated state may actually produce more potent effects on cAMP levels in an *in vitro* or *in vivo* setting. Conversely, as inhibitors may bind only the phosphorylated fraction of PDE4 forms, inhibition of non-phosphorylated PDE4 may be minimal, yielding only a partial

inhibition of total PDE4 activity. Therefore, it is essential to consider the potency of PDE4 inhibitors in addition to their affinity when determining which inhibitor, with its affinity profile against different PDE4 subtypes, isoforms and conformations, shows most therapeutic benefit in the disease of interest.

In addition to specific PDE4 phosphorylation, PDE4 isoforms can show different affinities towards inhibitors depending on whether these isoforms are located in the cytosol or have complexed with other cellular structures, as elaborately investigated by Houslay and collaborators (Bolger et al., 1997; Huston et al., 1997; Huston et al., 1996; Rena et al., 2001; Wallace et al., 2005). By subcellular fractionation, both cytosolic and particulate fractions of PDE4 forms can be separated, which can show differential affinities to inhibitors in an isoform-dependent manner (**Table 4**). Per cellular fraction, PDE4 isoforms may engage in different protein-protein interactions, which subsequently can alter their conformation leading to divergent effects on inhibitor affinity. Thus, based on its specific subcellular localization and local interactions or modifications, the same PDE4 isoform can adopt different conformations which may be preferentially bound by certain inhibitors (e.g. the different affinities of rolipram towards particulate and cytosolic PDE4A4 **Table 4**). As such, these inhibitors can modulate PDE4 activity with different potency at the subcellular level.

Table 4. PDE4 inhibitors tested for their selectivity against different PDE4 conformational states or PDE4 isoforms in different cellular fractions.

Compound	Study	Construct	Construct category	Mutation/Modification/ Cellular fraction	IC50 (nM)
A-33	(Fox et al., 2014)	PDE4B1	long	PKA-mimetic, ERK ablative	32
		PDE4B1	long	L674Q, PKA-mimetic, ERK ablative	2035
		PDE4D7	long	PKA-mimetic, ERK ablative	1569
		PDE4D7	long	Q594L, PKA-mimetic, ERK ablative	21
BPN14770	(Zhang et al., 2018)	PDE4D7	long	-	1018
		PDE4D7	long	PKA-mimetic, ERK-ablative	7.8
		PDE4D3	long	PKA-mimetic, ERK-ablative	7.4
		PDE4D2	supershort	ERK-ablative	127
		PDE4B1	long	PKA-mimetic, ERK-ablative	2013
Cilomilast	(Wallace et al., 2005)	PDE4A11	long	cytosolic	34
		PDE4A11	long	particulate P2	34
		PDE4A4	long	cytosolic	61
		PDE4A4	long	particulate P2	59
		PDE4A10	long	cytosolic	130
Denbufylline	(Wallace et al., 2005)	PDE4A11	long	cytosolic	250
		PDE4A11	long	particulate P2	310
		PDE4A4	long	cytosolic	560
		PDE4A4	long	particulate P2	460
		PDE4A10	long	cytosolic	590
PMNPQ	(Burgin et al., 2010)	PDE4D7	long	PKA-mimetic	5
		PDE4D7	long	PKA-mimetic, Phe196Ala	170
		PDE4D7	long	PKA-mimetic, Phe201Ala	310
		PDE4D7	long	PKA-mimetic, ERK ablative	0.52
		PDE4D2	supershort	ERK ablative	0.66
		PDE4B1	long	PKA-mimetic	4.4
Roflumilast	(Wallace et al., 2005)	PDE4A11	long	cytosolic	4.8
		PDE4A11	long	particulate P2	3.9
		PDE4A4	long	cytosolic	9.0
		PDE4A4	long	particulate P2	2.5
		PDE4A10	long	cytosolic	4.1
Rolipram	(Zhang et al., 2018)	PDE4D7	long	-	675
		PDE4D7	long	PKA-mimetic, ERK-ablative	32
		PDE4D3	long	PKA-mimetic, ERK-ablative	29

Compound	Study	Construct	Construct category	Mutation/Modification/ Cellular fraction	IC50 (nM)
Rolipram (cont.)		PDE4D2	supershort	ERK-ablative	142
		PDE4B1	long	PKA-mimetic, ERK-ablative	175
	(Huston et al., 1996)	PDE4A4	long	particulate	195
		PDE4A4	long	cytosolic	1600
	(Wallace et al., 2005)	PDE4A11	long	cytosolic	720
		PDE4A11	long	particulate P2	660
		PDE4A4	long	cytosolic	1310
		PDE4A4	long	particulate P2	260
		PDE4A10	long	cytosolic	64
	(Rena et al., 2001)	PDE4A10	long	particulate P1	54
		PDE4A10	long	particulate P2	52
		PDE4A10	long	cytosolic	56
	(Huston et al., 1997)	PDE4B1	long	particulate P1	100
		PDE4B1	long	particulate P2	50
		PDE4B1	long	cytosolic	80
		PDE4B3	long	particulate P1	140
		PDE4B3	long	particulate P2	100
		PDE4B3	long	cytosolic	50
		PDE4B2	short	particulate P1	180
		PDE4B2	short	particulate P2	210
		PDE4B2	short	cytosolic	20
	(Bolger et al., 1997)	PDE4D1	short	particulate P2	n/a
		PDE4D1	short	cytosolic	50
		PDE4D2	supershort	particulate P2	n/a
		PDE4D2	supershort	cytosolic	50
		PDE4D3	long	particulate P2	320
		PDE4D3	long	cytosolic	140
		PDE4D4	long	particulate P2	50
		PDE4D4	long	cytosolic	60
		PDE4D5	long	particulate P2	590
		PDE4D5	long	cytosolic	80
Ro 20-1724	(Wallace et al., 2005)	PDE4A11	long	cytosolic	990
		PDE4A11	long	particulate P2	910
		PDE4A4	long	cytosolic	2930
		PDE4A4	long	particulate P2	2900
		PDE4A10	long	cytosolic	1240
RS25344		PDE4D7	long	PKA-mimetic	19

Compound	Study	Construct	Construct category	Mutation/Modification/ Cellular fraction	IC50 (nM)
RS25344 (cont.)	(Burgin et al., 2010)	PDE4D7	long	PKA-mimetic, Phe196Ala	4.1
		PDE4D7	long	PKA-mimetic, Phe201Ala	6.2
		PDE4D7	long	PKA-mimetic, ERK ablative	0.91
		PDE4D2	supershort	ERK ablative	0.81
		PDE4B1	long	PKA-mimetic	9.4
	(Alvarez et al., 1996)	PDE4D3	long	-	3.16
		PDE4D3	long	PKA-mimetic	0.5
RS33793	(Alvarez et al., 1996)	PDE4D3	long	-	39.8
		PDE4D3	long	PKA-mimetic	0.2

2. Optimizing PDE4 inhibitor screenings

The involvement of PDE4 in various cellular processes makes these enzymes attractive pharmacological targets, but simultaneously makes non-specific PDE4 inhibition prone to modulating unwanted biological mechanisms. Hence, to optimize the efficacy and safety of PDE4 inhibitors, it is crucial to specify which PDE4 subtypes or isoforms are involved in the (disease-affected) cellular functions that are to be modified. In this subsection, we highlight how the choice of assay, target specification, and the use of 'toolbox' compounds that apply distinct binding mechanisms can guide drug development towards safe and efficacious PDE4 subtype/isoform inhibition.

Firstly, considering that PDE4 enzymes can dynamically adopt several conformational states that can show different affinities to inhibitors, screening assays using purified PDE4 constructs are limited in predicting the inhibitory potential of a compound as they assess affinities against a static, rather than a dynamic, enzyme. Hence, cell-based screening assays will more accurately indicate the PDE4 inhibitory potential of compounds when other influencing factors including phosphorylation events, interactor proteins and biological feedback mechanisms are present. When using cell-based assays, we argue it is essential to assess a PDE4-regulated phenotypical or physiological read-out that is relevant to a healthy or pathological

process of interest rather than an overall change in cAMP levels. Thus, the quality (i.e. cAMP elevation at the desired intracellular location) of PDE4 inhibition is more important than the quantity (i.e. profound cAMP elevation but not intracellularly confined) to achieve efficacious treatment while minimizing side effects. The use of cell-based assays that focus on a phenotypical or physiological read-out may also lead to discovery of efficacious PDE4 inhibitors with additional activity on other relevant targets, which would be undetectable in assays using solely purified PDE4 enzymes.

Using a cell-based, possibly disease relevant, assay, experiments can be conducted to specify which PDE4 subtypes and isoforms regulate the chosen phenotypical or physiological read-out. By means of genetic knockout (e.g. using CRISPR-Cas9) or shRNA-mediated knockdown, it can be specified which PDE4 subtypes or individual PDE4 isoforms regulate the biological read-out process. Conveniently, the typical PDE4 gene structures allow for targeting of isoforms selectively as they each contain (parts of) a unique exon that can be targeted at the DNA level (e.g. using CRISPR-Cas9) or the transcript level (e.g. using shRNAs) (**Figure 1**). Validation of the role of specific subtypes or isoforms in the chosen read-out can be performed by overexpressing the subtype/isoform in order to assess whether it induces an opposite effect on the read-out compared to subtype/isoform knockout. The involvement of specific isoforms in the process of interest can also be corroborated using a dominant-negative approach in which a catalytically inactive PDE4 form is being overexpressed. Subsequently, overexpressed inactive PDE4 isoforms will (partly) displace endogenous, active PDE4 isoforms inducing local decreases in PDE4 activity. Functional roles of specific PDE4 isoforms have already been successfully identified using this approach (e.g. (Bolger et al., 2020; Campbell et al., 2017; Perry et al., 2002)). While dominant-negative PDE4 forms can isoform-specifically displace endogenous forms, their overexpression may also cause excessive scaffolding of PDE4 interactions proteins that could alter cellular signaling.

Hence, depending of the biological mechanism of interest, validation of the role of specific PDE4 subtypes and isoforms may be best supported by a combination of the abovementioned strategies. Upon target specification and validation, drug design is suggested to be conducted in a structure-based manner. In case the functionally relevant PDE4 forms belong to a specific subtype, subtype-specific differences in PDE4 structure may be exploited to develop PDE4 subtype-selective inhibitors as described in the subsection 'Mechanisms for PDE4 subtype selectivity: interactions with regulatory domains'.

Since there already exist PDE4 inhibitors that preferentially bind certain subtypes, isoforms and/or conformations (**Tables 2-4**), these compounds can be used as 'toolbox' compounds to determine which binding mechanism induces the most prominent effect on the assay read-out. Parallel insights from the target validation approaches and use of 'toolbox' compounds would eventually provide the insight and understanding to develop PDE4 inhibitors that apply a particular binding mode to selectively bind and inhibit the most relevant PDE4 forms to subsequently efficaciously attenuate a biological dysfunction of interest.

C. Mechanisms for PDE4 subtype selectivity: interactions with regulatory domains

1. Interactions with the UCR2

Although the different subtypes possess highly similar catalytic domains, subtle amino acid differences exist in regulatory regions (i.e. UCR2 and C-terminus) that can be positioned across the catalytic pocket. When the UCR2 is capped, certain residues can interact with inhibitors as their side chains extent into the catalytic domain (**Figure 3 and Supplementary Video**). UCR2 capping is postulated to occur via intermolecular actions in long, dimerized PDE4 isoforms where the UCR2 of one monomer folds across the catalytic domain of the other monomer (Cedervall et al., 2015). As the UCR2 also is auto-inhibitory in monomeric, short PDE4D1, intramolecular UCR2-capping may also occur (Kovala et al., 1997). Irrespective of

whether UCR2 capping occurs in *trans* (intermolecularly) or in *cis* (intramolecularly), inhibitors can engage in interactions with UCR2 residues. Intriguingly, in primates, a polymorphism has occurred in PDE4D leading to the expression of a phenylalanine instead of tyrosine in the UCR2 region. This subtype-specific difference has been successfully exploited, and validated by mutation studies, to generate PDE4D-selective inhibitors (e.g. BPN14770) that interact with the PDE4D-specific phenylalanine in the UCR2 region (**Table 4**) (Burgin et al., 2010). Interestingly, Gurney et al. have shown that certain compounds that utilize UCR2 for binding, like BPN14770, behave as partial inhibitors (Gurney et al., 2019). It is hypothesized that, in dimerized PDE4, through inhibitor-UCR2 interactions at one monomer the other UCR2 cannot effectively *trans*-cap the other monomer. Since this UCR2-capping is involved in compound binding, inhibitor binding at this monomer will be reduced, resulting in overall partial inhibition. Conversely to binding the UCR2 phenylalanine, inhibitors can preferentially interact with the tyrosine residue in PDE4A-C, producing PDE4D-sparing actions, as reported for ABI-4 (PF-06266047) (Hedde et al., 2017). Notably, several classes of PDE4 inhibitors have found to stabilize a UCR2-capped state as elaborately indicated by Day and colleagues (Day et al., 2011). While PDE4 modifications and protein-protein interactions can influence inhibitor affinity by influencing UCR2-capping, stabilization of UCR2-capping by certain inhibitors can, conversely, also alter the conformation of regulatory domains that affect PDE4 modifications and interactions (Terry et al., 2003). In the case of PDE4A4, stabilization of UCR2 capping by inhibitor binding causes its intracellular redistribution, demonstrating that inhibitor binding can induce additional cellular changes next to elevation of local cAMP levels (Day et al., 2011). This use of UCR2 by certain compounds makes their affinity also dependent on post-translational modifications and interactions with partner proteins as they can influence the UCR2 capping state as explained before.

2. Interactions with the C-terminus

Similar to the use of UCR2 residues to achieve subtype selectivity, amino acid differences in the C-terminus can be employed to achieve subtype-specific inhibitor binding. Through interactions with residues unique to the PDE4B C-terminus, PDE4B-selectivity has been achieved for the compounds A33 and a tetrahydrobenzothiophene inhibitor (see **Table 4**) (Fox et al., 2014; Kranz et al., 2009; Naganuma et al., 2009). The C-terminus is capped across the catalytic domain in an intramolecular manner as the linker region between C-terminus and the catalytic domain is too short to achieve capping the other monomer in a PDE4 dimer. Inhibitors that employ C-terminus residues may therefore preferentially bind capped over uncapped states producing a degree of conformation-dependent binding. As both UCR2 and C-terminus capping are dependent on multiple cellular events including phosphorylation or interactions with partner proteins, conformation-dependent inhibitors may bind PDE4 in a selective spatial and/or temporal manner.

D. Stereoisomerism and metabolites of PDE4 inhibitors

In 1983, it had already been described that the enantiomer (R)-rolipram and racemic rolipram are more potent in increasing cerebral cAMP levels than (S)-rolipram (Schneider, 1984; Wachtel, 1983a; b). Accordingly, several studies have indicated that (R)-rolipram shows higher PDE4 affinity than (S)-rolipram (Barnette et al., 1996; Laliberte et al., 2000; Torphy et al., 1992). This suggests that stereoisomerism of PDE4 inhibitors can influence the inhibitor's affinity depending on whether a racemic mixture or purified enantiomer is tested. Both (R)-rolipram and (S)-rolipram seem to exhibit similar binding modes in PDE4D2 crystal structures, but increased affinity of (R)-rolipram may be conveyed via other isoforms and/or conformational states than those captured by the reported crystal structures (Huai et al., 2003). Indeed, rolipram can adopt a slightly different conformation in crystals that include UCR2 domains (Cedervall et al., 2015). For another set of enantiomeric

inhibitors (L-869298 and L-869299), stereochemistry does change the binding mode in a Mg^{2+}-interacting manner which is concurrent with differences in affinity (Huai et al., 2006). Next to the aforementioned enantiomeric inhibitors, also for the PDE4D-selective inhibitor GEBR32a, different affinities are reported for its enantiomers (**Table 3**) (Cavalloro et al., 2020). Hence, in case of racemic inhibitors, it has to be considered that enantiomers can exhibit different binding modes and affinities for specific PDE4 conformations. Consequently, certain enantiomers may display favorable pharmacological properties superior to its racemic mixture. Enantiomer-specific effects can provide important insights into the molecular binding modes crucial for efficacy and can subsequently facilitate pharmacophore determination and inhibitor optimization.

Similar to the use of racemic PDE4 inhibitor mixtures, metabolism of administered PDE4 inhibitors can produce multiple metabolites that each show differences in their binding mode and affinity. For example, the PDE4 inhibitor roflumilast is metabolized into roflumilast N-oxide which shows distinct subtype-selectivity compared to roflumilast itself (**Tables 2 and 3**) (Claveau et al., 2004; Huang et al., 2007; Wunder et al., 2013). The inhibitory potential of inhibitor metabolites on PDE4 activity should therefore be taken into account as combined actions of PDE4 inhibitors and its metabolites may cause certain PDE4 subtypes, isoforms or conformations to be more potently inhibited *in vivo,* resulting in a more favorable or unfavorable pharmacological profile.

E. Modulators of PDE4 activity

Next to PDE4 inhibitors, molecules have been described that influence PDE4 activity in a non-inhibiting manner. For example, atropine, a muscarinic acetylcholine receptor antagonist, has been described to allosterically inhibit PDE4 while also potentiating rolipram binding (Perera et al., 2017). These effects correspond to those of modulation by several intracellular factors as discussed above in the **section PDE4 modifications and interactions**. In contrast to allosterically inhibiting molecules,

PDE4 activity can also be stimulated through allosteric binding. For example, early studies by the Conti and coworkers showed that binding of antibodies targeting the UCR2 auto-inhibitory domain increased PDE4 activity similar to phosphorylation by PKA (Conti et al., 1995; Lim et al., 1999).

More recently, also small molecules have been described that increase PDE4 activity through allosteric binding (Omar et al., 2019). More specifically, these compounds bind and activate long, dimerized PDE4 and thereby mimic the activating actions of PKA. This mechanistic similarity of activation is further supported by the inability of these small molecules to increase activity in PKA-mimicking PDE4 mutants. Hence, these small molecule allosteric activators have therapeutic utility in disorders in which cAMP signaling is aberrantly increased. For example, in autosomal dominant polycystic kidney disease (ADPKD), elevated cAMP levels promote the formation of cysts. Omar et al. have demonstrated that the use of allosteric activators can successfully diminish cyst formation in cell models of ADPKD. It can be speculated that allosteric PDE4 activators also have therapeutic applicability in other disorders displaying elevated cAMP signaling, such as the genetic condition McCune–Albright syndrome in which gain-of-function Gs alpha subunit mutations lead to exaggerated cAMP synthesis (Innamorati et al., 2018; Levine, 1999). Hence, PDE4 enzymes have therapeutic utility as pharmacological targets both in conditions displaying reduced and heightened levels of cAMP.

Lastly, PDE4 peptide fragments have been developed which can either stimulate PDE4 activity (Wang et al., 2015), or reduce activation by 'scavenging' the PDE4-activating phosphorylation by Cdk5 (Plattner et al., 2015).

IV. ADVERSE EFFECTS OF PDE4 INHIBITION

Although PDE4 inhibition shows therapeutic potential in a variety of disease areas, clinical exploitation of PDE4 inhibitors has often been held back by dose limitations caused by adverse side effects. Side effects upon PDE4 inhibitor administration are mainly gastro-intestinal in nature (i.e. nausea, vomiting and diarrhea), but also headaches and dizziness have been reported (e.g. (Compton et al., 2001)). These side effects may be overcome by more precise targeting of PDE4 subtypes, isoforms or conformational states. Accordingly, subtype-selective PDE4 inhibitors have been developed which exploit subtle sequence differences and distinct conformational states that may result from different PDE4 lengths and specific interactions and modifications (e.g. (Burgin et al., 2010; Fox et al., 2014; Hedde et al., 2017)). While this allows for more precise targeting, insight into which PDE4 subtypes or isoforms mediate unwanted effects is therefore crucial to understand which subtypes/conformations not to target. This section will discuss PDE4 expression and functionality in brain and bodily areas, and potential molecular mechanisms related to the different PDE4-mediated side effects. In addition, an overview is provided of those PDE4 inhibitors that have been tested for possible adverse side effects.

A. Hypothermia

Several preclinical studies using mice, rats and guinea pigs have demonstrated that PDE4 inhibitors can induce hypothermia (McDonough et al., 2020b; Wachtel, 1983a; b; c). These effects seem to be regulated via PDE4-mediated dopamine signaling in the hypothalamus which is supported by the fact that PDE4 inhibitors that difficultly enter the brain have less profound effects on body temperature (McDonough et al., 2020b). Whilst not explicitly described as adverse side effect in humans, hypothermia may contribute to uncomfortable feelings during treatment with PDE4 inhibitors.

B. Dizziness

PDE4 inhibition has also been reported to cause dizziness (Blokland et al., 2019). In cochlear and vestibular nuclei in the brainstem, PDE4D was found to be highest expressed compared to other PDE4 subtypes (Iwahashi et al., 1996; Perez-Torres et al., 2000). More specifically, PDE4D1, PDE4D2, and PDE4D3 mRNA was expressed in the rat dorsal cochlear and vestibular nuclei (Miro et al., 2002b). As the cochlear and vestibular nuclei relay signaling from the inner ear, altered cAMP modulation by PDE4 inhibition in these areas may provoke feelings of dizziness and, through subsequent signaling to other brains stem areas, promote nausea and emesis. Interestingly, in the vestibular apparatus in the inner ear itself, PDE4D is expressed and rolipram induces endolymphatic hydrops in the mouse, which is associated with feelings of dizziness (Degerman et al., 2017; Nakashima et al., 2016).

C. Gastro-intestinal

1. Diarrhea

Concerning effects of PDE4 inhibition on the gastro-intestinal system, diarrhea has been reported as an adverse effect. Through PKA-dependent activation of the cystic fibrosis transmembrane conductance regulator (CFTR), PDE4 inhibition may cause diarrhea by elevating intestinal Cl^- secretion (Chao et al., 1994). Specifically, PDE4D may mediate this effect upon PDE4 inhibition as PDE4D has been found to be recruited to CFTR via binding the scaffolding protein Shank2 (Lee et al., 2007). Moreover, PDE4 inhibition can facilitate 5HT4 receptor-mediated acetylcholine release causing contraction of large intestinal circular smooth muscle (Pauwelyn et al., 2018). Specifically, the PDE4D3 and PDE4D5 isoforms have been found to associate with 5HT4(b) receptors and may, therefore, be involved in gastrointestinal effects caused by PDE4(D) inhibition (Weninger et al., 2014). Despite the fact that diarrhea has been reported as a PDE4-mediated adverse event, it is striking that roflumilast has actually been found to exhibit antidiarrheal effects in mice which may

be associated with antispasmodic actions of roflumilast in the jejenum (Rehman et al., 2020).

2. Nausea and emesis

Regarding nausea and emesis, PDE4 actions within both the central nervous and gastro-intestinal system seem to be involved. In an early study, intravenous administration of rolipram and Ro20-1724 were found to increase gastric acid and pepsin secretion in anesthetized rats (Puurunen et al., 1978). Correspondingly, Lamontagne et al. suggested that, in the stomach, pepsinogen-releasing chief cells primarily express the PDE4D subtype while acid-releasing parietal cells expressed PDE4A (Lamontagne et al., 2001). Moreover, binding of specifically HARBS configurations in gastric glands showed strong correlation with the degree of gastric acid secretion (Barnette et al., 1995). Interestingly, gastric transit was found to be more strongly inhibited by roflumilast than by a selective PDE4B inhibitor, which may suggest PDE4B inhibition contributes relatively little to gastric side effects (Suzuki et al., 2013). Recently, it was shown that non-selective PDE4 inhibition induces gastroparesis (i.e. delayed gastric transit) in mice (McDonough et al., 2020a). More importantly, this study showed that genetic ablation of any of the four PDE4 subtypes does not affect gastroparesis or protect against inhibitor-induced gastroparesis, which suggests that two or more PDE4 subtypes contribute to PDE4-mediated gastroparesis. As gastroparesis is strongly associated with nausea and emesis in humans, this physiological effect of PDE4 inhibition warrants further investigation as a possible predictive measure for the side effect profile of PDE4 inhibitors (Grover et al., 2019).

Although PDE4 inhibition causes profound local gastric effects, emesis is eventually effectuated through signaling in brainstem nuclei such as the nodose ganglion, area postrema (AP), and nucleus tractus solitarius (NTS) (du Sert et al., 2012; Miller and Leslie, 1994). In the nodose ganglion of the squirrel monkey, cell bodies

of gastric vagal nerve fibers can be found in which predominantly PDE4D is present compared to lower expression levels of PDE4C or long PDE4A forms (Lamontagne et al., 2001). Similarly, the AP and NTS were found to mainly express PDE4D and to a smaller extent PDE4B, in the mouse (Cherry and Davis, 1999), rat (Iwahashi et al., 1996; Perez-Torres et al., 2000; Takahashi et al., 1999) and human brain (Mori et al., 2010). PDE4D expression was also found in medulla oblongata neurons that are innervated by substance P, which has been reported to be involved in emetic responses upon PDE4 inhibition (Lamontagne et al., 2001; Robichaud et al., 1999). At the PDE4D transcript variant level, mRNA of PDE4D1 and PDE4D4 showed high expression in the rat AP compared to lower levels of PDE4D2 and PDE4D5, and absence of PDE4D3. Furthermore, low levels of PDE4D2, PDE4D4 and PDE4D5 were detected in the NTS (Miro et al., 2002b). Strikingly, in another study by Miró and colleagues, no PDE4D4 mRNA was detected in the rat AP (Miro et al., 2002a). Human data regarding PDE4D mRNA content in the AP also suggests that PDE4D4 is not abundantly present, while the highest expression was found for PDE4D3 and PDE4D9 (VANMIERLO, 2019).

In addition to localization studies showing high expression of PDE4D in emesis-related brainstem areas, mechanistically, PDE4D also seems to mediate emetic responses. In a study by Robichaud et al., PDE4D, but not PDE4B, knockout mice displayed reduced sleeping time under xylazine/ketamine-induced anesthesia, a measure of emetic-like behavior. Furthermore, the PDE4 inhibitor PMNPQ did reduce anesthesia duration in wild-type and PDE4B-deficient mice but not in PDE4D-deficient mice which again indicates an involvement of PDE4D in emetic-like behavior (Robichaud et al., 2002b). Xylazine/ketamine-induced anesthesia assesses emetic-like behavior in non-vomiting species through α2-adenergic receptor antagonism (Nelissen et al., 2019; Robichaud et al., 2002a; Robichaud et al., 2001). The involvement of PDE4D in this mechanism corresponds with the expression of both α2 adrenoceptor and PDE4D mRNA in the NTS (Lamontagne et al., 2001;

Scheinin et al., 1994). However, also PDE4A and PDE4B seem to mediate α2-dependent signaling, at least in retinal rod bipolar cells (Dong et al., 2014). PDE4 inhibitors may enhance neuronal firing in both the AP and NTS of rats as higher expression of the neuronal activity marker Fos was observed in these regions upon administration of rolipram or PMNPQ in rats (Bureau et al., 2006). Accordingly, AP neurons could be excited by cAMP, which would be elevated upon inhibitor administration (Carpenter et al., 1988). Noteworthy, AP neurons exhibit a hyperpolarization-activated cation current (I_h) that acts as pacemaker current and which is found to be activated through stimulation of cAMP signaling (Funahashi et al., 2003). Consequently, PDE4 inhibition may increase the frequency of this pacemaker current leading to an increased firing rate. Actually, the influence of PDE4 on pacemaker currents has already been demonstrated in the sinoatrial node of the heart (St Clair et al., 2017). The xylazine/ketamine-induced anesthesia test suggests that PDE4 inhibition alters AP activity through antagonizing α2-adenergic receptor signaling (Nelissen et al., 2019). Accordingly, α2-adrenergic receptor stimulation was shown to inhibit cAMP and close hyperpolarized cyclic nucleotide-gated (HCN) channels (Wang et al., 2007b). Vice versa, PDE4 inhibition could enhance cAMP, open HCN channels, increase I_h currents and increase the firing rate of AP neurons leading to an emetic response. Anesthesia induced by injecting an α2 adrenergic agonist into the locus coeruleus, which innervates the AP, of rats could be reversed by rolipram. However, pretreatment of a PKA inhibitor blocked the effects of rolipram, suggesting emetogenic effects by PDE4 inhibitors are mediated through actions requiring cAMP-PKA signaling (Correa-Sales et al., 1992). Moreover, phosphorylation of PKA and ERK, downstream kinases of cAMP, was found to be highest during peak emesis in AP neurons (Zhong and Darmani, 2017).

These findings support the notion that PDE4-mediated cAMP signaling and its downstream effectors contribute to emetic behavior. Still, the exact mechanism underlying these adverse side effects caused by PDE4 inhibitors remains to be

resolved. Since the AP may in part be outside of the blood-brain barrier, emetic effects can be dependent on both peripheral and central actions (Miller and Leslie, 1994). Based on the gene deletion and localization studies discussed above, PDE4D seems to be involved in central and peripheral actions leading to the induction of emesis. However, emetic(-like) effects cannot be attributed entirely to PDE4D as the PDE4D-selective inhibitors GEBR32a, V11294A and BPN14770 appear to be well-tolerated in animals and/or healthy volunteers [NCT02648672][NCT02840279] (Gale et al., 2003; Gale et al., 2002; Ricciarelli et al., 2017; Rogers and Giembycz, 1998; Sutcliffe et al., 2014). It is likely that multiple PDE4 subtypes and isoforms in different bodily tissues contribute collectively to PDE4-associated side effects, as also suggested by Richter and colleagues (McDonough et al., 2020a). Hence, subtype- or isoform-selective PDE4 inhibitor may yield less severe side effects. As PDE4 subtypes and isoforms have non-redundant roles and show specific intracellular localization, certain subtypes or isoforms may be specifically involved in mechanisms that eventually evoke unwanted effects. The potency of the inhibitor to inhibit these particular isoforms would then explain their potency to induce adverse effects. However, which exact PDE4 subtypes and isoforms mediate these processes remains to be determined. Another explanation may lay in the differential affinities of the compound to different PDE4 conformational states. Indeed, correlations have been found between the degree of binding HARBS and emetic effects (Christensen et al., 1998; Duplantier et al., 1996; Hirose et al., 2007). Inhibitors that preferentially target LARBS or show no preference would therefore be safer, which is supported by the relatively low emetogenicity of cilomilast and roflumilast (Davis et al., 2009). In contrast, the PDE4D-selective inhibitor BPN14770 preferentially binds HARBS but appears to be well-tolerated in humans [NCT02648672][NCT02840279](Tetra, 2016). Although BPN14770 can bind HARBS, its relatively low emetogenicity may be explained by its PDE4D-selective inhibition and/or the fact that it acts as a partial inhibitor (see **section PDE4 inhibitors** (Burgin et al., 2010)). Thus, the occurrence of

adverse effects may not fully attributed to preferential binding of HARBS or LARBS, or to PDE4D-selective inhibition, but rather is more complex involving inhibition of specific PDE4 subtypes and/or isoforms in different central and peripheral tissues.

Thus, it has been shown that it is possible to develop PDE4 inhibitors with safer pharmacological profile compared to the prototypical rolipram. In **Table 5**, an overview is provided of several compounds that have been tested for their ability to elicit PDE4-associated side effects compared to rolipram. Because of discrepancies among studies regarding the type of test, species and administration routes used, results can mainly be compared within studies using the same procedures. **Table 5** indicates that multiple PDE4 inhibitors induce emetic and emetic-like effects at doses more than 30-fold of those induced by rolipram (e.g. CT-2450 and D159687), whilst some compounds require lower doses than rolipram (e.g. PMNPQ and D157140). Since adverse side effects are often assessed in non-primate species (e.g. mice, rats, dogs and ferrets), it should be considered that these tests do not accurately reflect the potential emetic effects of PDE4 inhibitors that exploit the primate PDE4D-specific phenylalanine in the UCR2 region. In addition, rodents cannot vomit and therefore require an indirect emesis test like the xylazine/ketamine test or pica feeding test. Despite the fact that several compounds can be used safely at higher doses than rolipram, their therapeutic potential is also dependent on the doses required for the desired therapeutic effect. As such, the eventual therapeutic windows of these compounds, i.e. the range of doses that elicit therapeutic, yet no adverse, effects may still be similar to those of rolipram for a specific disease indication. Nevertheless, a wide variety of PDE4 inhibitors has been developed with improved affinities to specific subtypes and/or conformational states (**Tables 2-4**) and minimized emetogenicity compared to rolipram (**Table 5**). Thus, to establish safer and more efficacious PDE4 inhibition for a disease, it should be determined which PDE4 subtypes, isoforms, or conformations have to be targeted to determine which inhibitor displays the broadest therapeutic window.

D. Strategies to minimize PDE4-mediated adverse side effects

Although PDE4 inhibition can produce several adverse side effects as described above, multiple strategies can be exploited to minimize or prevent these unwanted responses while retaining efficacy. Most notably, more selective inhibition of PDE4 forms may be pursued to improve treatment efficacy and/or avoid inhibiting PDE4 forms mediating adverse side effects. Regardless, a mechanistic understanding of which PDE4 subtypes, isoforms and/or conformational states mediate adverse effects will aid in the development of new-generation PDE4 inhibitors that then should actually avoid potently inhibiting these forms. Several PDE4 inhibitors already exist that preferentially bind non-conserved amino acids and different conformational states (see **Table 4**). Moreover, partial inhibitors may provide a safer pharmacological profile compared to full inhibitors through distinct potencies for different PDE4 conformations and/or subtypes (Gurney et al., 2011). In case PDE4 inhibition is desired in peripheral organs rather than the central nervous system, PDE4 inhibitors with limited brain penetrance may minimize the occurrence of side effects that are mediated through central actions (Aoki et al., 2001a). Likewise, depending on the target organ, a particular route of administration can be chosen to minimize systemic exposure (e.g. intranasal or topical administration, or via inhalation) (Tralau-Stewart et al., 2011). More precise targeting of PDE4 inhibitors has also been achieved by using inhibitor-antibody conjugates, which are internalized specifically by cells that express the antibody's antigen (Yu et al., 2016). Systemic exposure can also be minimized by using PDE4 inhibitors that are quickly degraded, as recently reported (Larsen et al., 2020).

Finally, combination treatments may reduce the severity of PDE4-mediated side effects. For example, it has been described that diarrhea caused by high doses of roflumilast can be attenuated when paired with a cyclooxygenase inhibitor (Peter et al., 2011). Furthermore, inhibition of different PDE families (e.g. PDE4 and PDE5 or PDE2 and PDE4) can produce synergistic effects which enables to use lower doses, with reduced chances of adverse effects, to produce the same treatment effect

(Bollen et al., 2015; Gulisano et al., 2018; Paes et al., 2020b). Lastly, the treatment of certain diseases, in which cAMP elevation is desired, may benefit from dual PDE4/PDE7 inhibitors which may subsequently reduce PDE4-selective inhibition and its associated side effects (Rucilova et al., 2020; Sharma et al., 2019).

Table 5. PDE4 inhibitors tested for their potential to induce emesis-like behavior (rodents) or emesis compared to rolipram

Compound	Emetic(-like) dose (µg/kg)	Emetic(-like) dose ratio to rolipram	Adm. route	Species	Test	Study
Rolipram	300	-	IP	mouse	xylazine/ketamine/ anaesthesia test	(Vanmierlo et al., 2016)
Roflumilast	3000	10				
R-rolipram	100	-	SC	mouse	xylazine/ketamine/ anaesthesia test	(Robichaud et al., 2002b)
S-rolipram	1000	10				
PMNPQ	1	0.01				
CT-2450	>30,000	>300				
Rolipram	100	-	IV	mouse	xylazine/ketamine/ anaesthesia test	(Burgin et al., 2010)
D157140	10	0.1				
D158681	>1000	>10				
D159153	100	1				
D159382	30	0.3				
D159404	>3000	>30				
D159687	>3000	>30				
Rolipram	30	-	SC	mouse	xylazine/ketamine/ anaesthesia test	(Ricciarelli et al., 2017)
GEBR32a	>3000	>100				
Rolipram	30	-	SC	mouse	xylazine/ketamine/ anaesthesia test	(Bruno et al., 2011)
GEBR7b	300	10				
Rolipram	500	-	IG	mouse	xylazine/ketamine/ anaesthesia test	(Zhou et al., 2017)
10j	>1500	>3				
Rolipram	800	-	PO	dog	emesis incidence	(Zhou et al., 2017)
10j	>800	>1				

Compound	Emetic(-like) dose (µg/kg)	Emetic(-like) dose ratio to rolipram	Adm. route	Species	Test	Study
Rolipram	400	-	PO	rat	pica feeding	(Davis et al., 2009)
Roflumilast	1570	>3.5				
Cilomilast	6410	>16				
EPPA-1	24260	>60				
Rolipram	500	-	PO	dog	emesis incidence	(Zhang et al., 2013)
Chlorbipram	>1000	>2				
Chlorbipram HCl	>1070	>2				
Rolipram	<100	-	PO	dog	emesis incidence	(Nose et al., 2016)
Roflumilast	500	>5				
GPD-1116	1000	>10				
Rolipram	3000	-	PO	ferret	emesis incidence	(Aoki et al., 2001b)
YM976	30000	10				
RP73401	3000	1				
CPP840	30000	10				
Rolipram	10000	-	PO	ferret	emesis incidence	(Gale et al., 2003)
V11294	>30000	>3				
Rolipram	40	-	IP	mouse	acute gastric retention measurement	(McDonough et al., 2020a)
Piclamilast	200	5				
YM976	1000	25				

Abbreviations: Adm. route, administration route; IP, intraperitoneal; IV, intravenous; SC, subcutaneous; IG, intragastric; PO, per os.

V. OUTLOOK

As important regulators of cAMP signaling in the entire body, the PDE4 enzyme family presents an interesting and promising pharmacological target in a broad range of disease areas. Accordingly, PDE4 inhibition has preclinically shown therapeutic potential for many diseases, yet its non-selective inhibition is associated with severe adverse effects which has seriously hampered its translation to the clinic. To increase efficacy and avoid adverse effects more selective targeting is required. This is actually possible as PDE4 enzymes consists of multiple similar, but different, subtypes that each comprise different isoforms. In this review it is summarized how these subtypes and isoforms can, through PDE4-inherent regulation, post-translational modifications, and interactions with other proteins, adopt different conformational states to which PDE4 inhibitors can selectively bind. Since PDE4 subtypes and isoforms are expressed in specific tissue-, cell type-, and intracellular expression patterns, selective PDE4 subtype/isoform inhibition will enable a more directed modulation of cAMP signaling in the target organ of interest. To further improve PDE4 inhibitor treatment efficacy and safety, it should also be investigated which PDE4 subtypes and isoforms contribute most to the organ's disease-specific aberrant cAMP signaling. Additionally, upon PDE4 specification, the conformational state of these enzymes in their disease context would have to be determined to choose or develop the most efficacious inhibitors (**Figure 5**). Consequently, it is crucial to determine preferential binding of PDE4 inhibitors to specific subtypes, isoforms and conformations rather than testing their affinity towards PDE4 catalytic domains only. Moreover, a deeper insight into the mechanisms underlying PDE4-mediated unwanted effects in organs is also warranted to facilitate the development and use of safe PDE4 inhibitors to treat diseases. In conclusion, specification and subsequent selective inhibition of PDE4 subtypes, isoforms or conformations grants the opportunity to effectively and safely modulate aberrant cAMP signaling in a

myriad of diseases. This will increase the chance of success of more PDE4 inhibitors reaching the patient eventually.

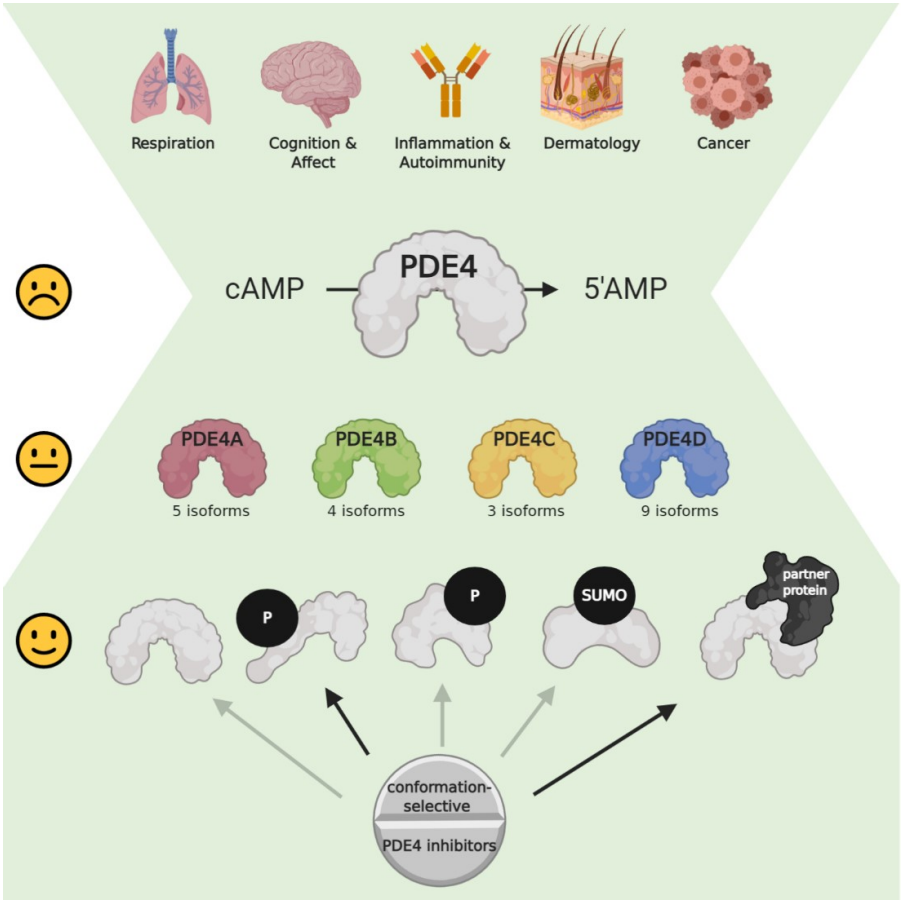

Figure 5. PDE4 as a pharmacological target in a variety of disease areas. In a broad range of diseases PDE4 inhibition shows therapeutic potential. Non-selective PDE4 inhibition is associated with adverse effects, but the existence of PDE4 subtypes (PDE4A-D) and associated isoforms allows for more specific targeting. PDE4 subtypes and isoforms can undergo conformational changes upon post-translational modifications and interactions with partner proteins. PDE4 inhibitors can display different affinities towards PDE4 subtypes, isoforms and conformations. Disease-specific determination of which PDE4 isoform(s) should be inhibited will facilitate the development of safe and efficacious PDE4 inhibitors. *Abbreviations: P, phosphorylation; SUMO, SUMOylation.* This figure was created with BioRender.com.

REFERENCES

Al-Tawashi A and Gehring C (2013) Phosphodiesterase activity is regulated by CC2D1A that is implicated in non-syndromic intellectual disability. *Cell Commun Signal* **11**:47.

Al-Tawashi A, Jung SY, Liu D, Su B and Qin J (2012) Protein implicated in nonsyndromic mental retardation regulates protein kinase A (PKA) activity. *J Biol Chem* **287**:14644-14658.

Alvarez R, Daniels DV, Shelton ER, Baecker PA, Annie T, Fong T, Devens B, Wilhelm R, Eglen RM and Conti M (1996) 11 - An Isoform-selective Inhibitor of Cyclic AMP-Specific Phosphodiesterase (PDE4) with Anti-inflammatory Properties, in *Phosphodiesterase Inhibitors* (Schudt C, Dent G and Rabe KF eds) pp 161-171, Academic Press, San Diego.

Alvarez R, Sette C, Yang D, Eglen RM, Wilhelm R, Shelton ER and Conti M (1995) Activation and selective inhibition of a cyclic AMP-specific phosphodiesterase, PDE-4D3. *Mol Pharmacol* **48**:616-622.

Andreassi C and Riccio A (2009) To localize or not to localize: mRNA fate is in 3'UTR ends. *Trends Cell Biol* **19**:465-474.

Aoki M, Fukunaga M, Sugimoto T, Hirano Y, Kobayashi M, Honda K and Yamada T (2001a) Studies on mechanisms of low emetogenicity of YM976, a novel phosphodiesterase type 4 inhibitor. *J Pharmacol Exp Ther* **298**:1142-1149.

Aoki M, Yamamoto S, Kobayashi M, Ohga K, Kanoh H, Miyata K, Honda K and Yamada T (2001b) Antiasthmatic effect of YM976, a novel PDE4 inhibitor, in guinea pigs. *J Pharmacol Exp Ther* **297**:165-173.

Asaka N, Kakuo H, Ohmori K, Sasaki E, Togawa M, Yamada S, Oka T and Kiniwa M (2010) Effects of the new benzimidazole derivative TAS-203, an orally active phosphodiesterase 4 inhibitor, on airway inflammation in rats and emetic responses in ferrets. *Arzneimittelforschung* **60**:564-570.

Asirvatham AL, Galligan SG, Schillace RV, Davey MP, Vasta V, Beavo JA and Carr DW (2004) A-kinase anchoring proteins interact with phosphodiesterases in T lymphocyte cell lines. *J Immunol* **173**:4806-4814.

Baillie GS, Adams DR, Bhari N, Houslay TM, Vadrevu S, Meng D, Li X, Dunlop A, Milligan G, Bolger GB, Klussmann E and Houslay MD (2007) Mapping binding sites for the PDE4D5 cAMP-specific phosphodiesterase to the N- and C-domains of beta-arrestin using spot-immobilized peptide arrays. *Biochem J* **404**:71-80.

Baillie GS, Huston E, Scotland G, Hodgkin M, Gall I, Peden AH, MacKenzie C, Houslay ES, Currie R, Pettitt TR, Walmsley AR, Wakelam MJ, Warwicker J and Houslay MD (2002) TAPAS-1, a novel microdomain within the unique N-terminal region of the PDE4A1 cAMP-specific phosphodiesterase that allows rapid, Ca2+-triggered membrane association with selectivity for interaction with phosphatidic acid. *J Biol Chem* **277**:28298-28309.

Baillie GS, MacKenzie SJ, McPhee I and Houslay MD (2000) Sub-family selective actions in the ability of Erk2 MAP kinase to phosphorylate and regulate the activity of PDE4 cyclic AMP-specific phosphodiesterases. *Br J Pharmacol* **131**:811-819.

Baillie GS, Tejeda GS and Kelly MP (2019) Therapeutic targeting of 3',5'-cyclic nucleotide phosphodiesterases: inhibition and beyond. *Nat Rev Drug Discov* **18**:770-796.

Bajpai M, Fiedler SE, Huang Z, Vijayaraghavan S, Olson GE, Livera G, Conti M and Carr DW (2006) AKAP3 selectively binds PDE4A isoforms in bovine spermatozoa. *Biol Reprod* **74**:109-118.

Barnette MS, Bartus JO, Burman M, Christensen SB, Cieslinski LB, Esser KM, Prabhakar US, Rush JA and Torphy TJ (1996) Association of the anti-inflammatory activity of phosphodiesterase 4 (PDE4) inhibitors with either inhibition of PDE4 catalytic activity or competition for [3H]rolipram binding. *Biochem Pharmacol* **51**:949-956.

Barnette MS, Grous M, Cieslinski LB, Burman M, Christensen SB and Torphy TJ (1995) Inhibitors of phosphodiesterase IV (PDE IV) increase acid secretion in rabbit isolated gastric glands: correlation between function and interaction with a high-affinity rolipram binding site. *J Pharmacol Exp Ther* **273**:1396-1402.

Beard MB, Huston E, Campbell L, Gall I, McPhee I, Yarwood S, Scotland G and Houslay MD (2002) In addition to the SH3 binding region, multiple regions within the N-terminal noncatalytic portion of the cAMP-specific phosphodiesterase, PDE4A5, contribute to its intracellular targeting. *Cell Signal* **14**:453-465.

Beard MB, O'Connell JC, Bolger GB and Houslay MD (1999) The unique N-terminal domain of the cAMP phosphodiesterase PDE4D4 allows for interaction with specific SH3 domains. *FEBS Lett* **460**:173-177.

Beard MB, Olsen AE, Jones RE, Erdogan S, Houslay MD and Bolger GB (2000) UCR1 and UCR2 domains unique to the cAMP-specific phosphodiesterase family form a discrete module via electrostatic interactions. *J Biol Chem* **275**:10349-10358.

Beavo JA (1995) Cyclic nucleotide phosphodiesterases: functional implications of multiple isoforms. *Physiol Rev* **75**:725-748.

Bender AT and Beavo JA (2006) Cyclic nucleotide phosphodiesterases: molecular regulation to clinical use. *Pharmacol Rev* **58**:488-520.

Bird RJ, Baillie GS and Yarwood SJ (2010) Interaction with receptor for activated C-kinase 1 (RACK1) sensitizes the phosphodiesterase PDE4D5 towards hydrolysis of cAMP and activation by protein kinase C. *Biochem J* **432**:207-216.

Blackman BE, Horner K, Heidmann J, Wang D, Richter W, Rich TC and Conti M (2011) PDE4D and PDE4B function in distinct subcellular compartments in mouse embryonic fibroblasts. *J Biol Chem* **286**:12590-12601.

Blanchard E, Zlock L, Lao A, Mika D, Namkung W, Xie M, Scheitrum C, Gruenert DC, Verkman AS, Finkbeiner WE, Conti M and Richter W (2014) Anchored PDE4 regulates chloride conductance in wild-type and DeltaF508-CFTR human airway epithelia. *FASEB J* **28**:791-801.

Blokland A, Van Duinen MA, Sambeth A, Heckman PRA, Tsai M, Lahu G, Uz T and Prickaerts J (2019) Acute treatment with the PDE4 inhibitor roflumilast improves verbal word memory in healthy old individuals: a double-blind placebo-controlled study. *Neurobiol Aging* **77**:37-43.

Bogoyevitch MA and Kobe B (2006) Uses for JNK: the many and varied substrates of the c-Jun N-terminal kinases. *Microbiol Mol Biol Rev* **70**:1061-1095.

Bolger G, Michaeli T, Martins T, St John T, Steiner B, Rodgers L, Riggs M, Wigler M and Ferguson K (1993) A family of human phosphodiesterases homologous to the dunce learning and memory gene product of Drosophila melanogaster are potential targets for antidepressant drugs. *Mol Cell Biol* **13**:6558-6571.

Bolger GB (1994) Molecular biology of the cyclic AMP-specific cyclic nucleotide phosphodiesterases: a diverse family of regulatory enzymes. *Cell Signal* **6**:851-859.

Bolger GB (2016) RACK1 and beta-arrestin2 attenuate dimerization of PDE4 cAMP phosphodiesterase PDE4D5. *Cell Signal* **28**:706-712.

Bolger GB, Baillie GS, Li X, Lynch MJ, Herzyk P, Mohamed A, Mitchell LH, McCahill A, Hundsrucker C, Klussmann E, Adams DR and Houslay MD (2006) Scanning peptide array analyses identify overlapping binding sites for the signalling scaffold proteins, beta-arrestin and RACK1, in cAMP-specific phosphodiesterase PDE4D5. *Biochem J* **398**:23-36.

Bolger GB, Dunlop AJ, Meng D, Day JP, Klussmann E, Baillie GS, Adams DR and Houslay MD (2015) Dimerization of cAMP phosphodiesterase-4 (PDE4) in living cells requires interfaces located in both the UCR1 and catalytic unit domains. *Cell Signal* **27**:756-769.

Bolger GB, Erdogan S, Jones RE, Loughney K, Scotland G, Hoffmann R, Wilkinson I, Farrell C and Houslay MD (1997) Characterization of five different proteins produced by alternatively spliced mRNAs from the human cAMP-specific phosphodiesterase PDE4D gene. *Biochem J* **328 (Pt 2)**:539-548.

Bolger GB, McCahill A, Yarwood SJ, Steele MR, Warwicker J and Houslay MD (2002) Delineation of RAID1, the RACK1 interaction domain located within the unique N-terminal region of the cAMP-specific phosphodiesterase, PDE4D5. *BMC Biochem* **3**:24.

Bolger GB, Peden AH, Steele MR, MacKenzie C, McEwan DG, Wallace DA, Huston E, Baillie GS and Houslay MD (2003) Attenuation of the activity of the cAMP-specific phosphodiesterase PDE4A5 by interaction with the immunophilin XAP2. *J Biol Chem* **278**:33351-33363.

Bolger GB, Smoot LHM and van Groen T (2020) Dominant-Negative Attenuation of cAMP-Selective Phosphodiesterase PDE4D Action Affects Learning and Behavior. *Int J Mol Sci* **21**:5704.

Bollen E, Akkerman S, Puzzo D, Gulisano W, Palmeri A, D'Hooge R, Balschun D, Steinbusch HW, Blokland A and Prickaerts J (2015) Object memory enhancement by combining sub-efficacious doses of specific phosphodiesterase inhibitors. *Neuropharmacology* **95**:361-366.

Boomkamp SD, McGrath MA, Houslay MD and Barnett SC (2014) Epac and the high affinity rolipram binding conformer of PDE4 modulate neurite outgrowth and myelination using an in vitro spinal cord injury model. *Br J Pharmacol* **171**:2385-2398.

Briet C, Pereda A, Le Stunff C, Motte E, de Dios Garcia-Diaz J, de Nanclares GP, Dumaz N and Silve C (2017) Mutations causing acrodysostosis-2 facilitate activation of phosphodiesterase 4D3. *Hum Mol Genet* **26**:3883-3894.

Brullo C, Massa M, Rapetti F, Alfei S, Bertolotto MB, Montecucco F, Signorello MG and Bruno O (2020) New Hybrid Pyrazole and Imidazopyrazole Antinflammatory Agents Able to Reduce ROS Production in Different Biological Targets. *Molecules* **25**.

Brullo C, Massa M, Rocca M, Rotolo C, Guariento S, Rivera D, Ricciarelli R, Fedele E, Fossa P and Bruno O (2014) Synthesis, biological evaluation, and molecular modeling of new 3-(cyclopentyloxy)-4-methoxybenzaldehyde O-(2-(2,6-dimethylmorpholino)-2-oxoethyl) Oxime (GEBR-7b) related phosphodiesterase 4D (PDE4D) inhibitors. *J Med Chem* **57**:7061-7072.

Bruno O, Fedele E, Prickaerts J, Parker LA, Canepa E, Brullo C, Cavallero A, Gardella E, Balbi A, Domenicotti C, Bollen E, Gijselaers HJ, Vanmierlo T,

Erb K, Limebeer CL, Argellati F, Marinari UM, Pronzato MA and Ricciarelli R (2011) GEBR-7b, a novel PDE4D selective inhibitor that improves memory in rodents at non-emetic doses. *Br J Pharmacol* **164**:2054-2063.

Bruno O, Romussi A, Spallarossa A, Brullo C, Schenone S, Bondavalli F, Vanthuyne N and Roussel C (2009) New selective phosphodiesterase 4D inhibitors differently acting on long, short, and supershort isoforms. *J Med Chem* **52**:6546-6557.

Bureau Y, Handa M, Zhu Y, Laliberte F, Moore CS, Liu S, Huang Z, MacDonald D, Xu DG and Robertson GS (2006) Neuroanatomical and pharmacological assessment of Fos expression induced in the rat brain by the phosphodiesterase-4 inhibitor 6-(4-pyridylmethyl)-8-(3-nitrophenyl) quinoline. *Neuropharmacology* **51**:974-985.

Burgin AB, Magnusson OT, Singh J, Witte P, Staker BL, Bjornsson JM, Thorsteinsdottir M, Hrafnsdottir S, Hagen T, Kiselyov AS, Stewart LJ and Gurney ME (2010) Design of phosphodiesterase 4D (PDE4D) allosteric modulators for enhancing cognition with improved safety. *Nat Biotechnol* **28**:63-70.

Byrne AM, Elliott C, Hoffmann R and Baillie GS (2015) The activity of cAMP-phosphodiesterase 4D7 (PDE4D7) is regulated by protein kinase A-dependent phosphorylation within its unique N-terminus. *FEBS Lett* **589**:750-755.

Cai Y, Huang G, Ma L, Dong L, Chen S, Shen X, Zhang S, Xue R, Sun D and Zhang S (2018) Smurf2, an E3 ubiquitin ligase, interacts with PDE4B and attenuates liver fibrosis through miR-132 mediated CTGF inhibition. *Biochim Biophys Acta Mol Cell Res* **1865**:297-308.

Cameron RT, Coleman RG, Day JP, Yalla KC, Houslay MD, Adams DR, Shoichet BK and Baillie GS (2013) Chemical informatics uncovers a new role for moexipril as a novel inhibitor of cAMP phosphodiesterase-4 (PDE4). *Biochem Pharmacol* **85**:1297-1305.

Campbell SL, van Groen T, Kadish I, Smoot LHM and Bolger GB (2017) Altered phosphorylation, electrophysiology, and behavior on attenuation of PDE4B action in hippocampus. *BMC neuroscience* **18**:77.

Carlisle Michel JJ, Dodge KL, Wong W, Mayer NC, Langeberg LK and Scott JD (2004) PKA-phosphorylation of PDE4D3 facilitates recruitment of the mAKAP signalling complex. *Biochem J* **381**:587-592.

Carpenter DO, Briggs DB, Knox AP and Strominger N (1988) Excitation of area postrema neurons by transmitters, peptides, and cyclic nucleotides. *J Neurophysiol* **59**:358-369.

Cavalloro V, Russo K, Vasile F, Pignataro L, Torretta A, Donini S, Semrau MS, Storici P, Rossi D, Rapetti F, Brullo C, Parisini E, Bruno O and Collina S (2020) Insight into GEBR-32a: Chiral Resolution, Absolute Configuration and Enantiopreference in PDE4D Inhibition. *Molecules* **25**.

Cedervall P, Aulabaugh A, Geoghegan KF, McLellan TJ and Pandit J (2015) Engineered stabilization and structural analysis of the autoinhibited conformation of PDE4. *Proc Natl Acad Sci U S A* **112**:E1414-1422.

Chandrasekaran A, Toh KY, Low SH, Tay SK, Brenner S and Goh DL (2008) Identification and characterization of novel mouse PDE4D isoforms: molecular cloning, subcellular distribution and detection of isoform-specific intracellular localization signals. *Cell Signal* **20**:139-153.

Chao AC, de Sauvage FJ, Dong YJ, Wagner JA, Goeddel DV and Gardner P (1994) Activation of intestinal CFTR Cl- channel by heat-stable enterotoxin and guanylin via cAMP-dependent protein kinase. *EMBO J* **13**:1065-1072.

Cherry JA and Davis RL (1999) Cyclic AMP phosphodiesterases are localized in regions of the mouse brain associated with reinforcement, movement, and affect. *J Comp Neurol* **407**:287-301.

Cheung YF, Kan Z, Garrett-Engele P, Gall I, Murdoch H, Baillie GS, Camargo LM, Johnson JM, Houslay MD and Castle JC (2007) PDE4B5, a novel, super-short, brain-specific cAMP phosphodiesterase-4 variant whose isoform-specifying N-terminal region is identical to that of cAMP phosphodiesterase-4D6 (PDE4D6). *J Pharmacol Exp Ther* **322**:600-609.

Chin A and Lecuyer E (2017) RNA localization: Making its way to the center stage. *Biochim Biophys Acta Gen Subj* **1861**:2956-2970.

Choi YH, Suzuki A, Hajarnis S, Ma Z, Chapin HC, Caplan MJ, Pontoglio M, Somlo S and Igarashi P (2011) Polycystin-2 and phosphodiesterase 4C are components of a ciliary A-kinase anchoring protein complex that is disrupted in cystic kidney diseases. *Proc Natl Acad Sci U S A* **108**:10679-10684.

Christensen SB, Guider A, Forster CJ, Gleason JG, Bender PE, Karpinski JM, DeWolf WE, Jr., Barnette MS, Underwood DC, Griswold DE, Cieslinski LB, Burman M, Bochnowicz S, Osborn RR, Manning CD, Grous M, Hillegas LM, Bartus JO, Ryan MD, Eggleston DS, Haltiwanger RC and Torphy TJ (1998) 1,4-Cyclohexanecarboxylates: potent and selective inhibitors of phosophodiesterase 4 for the treatment of asthma. *J Med Chem* **41**:821-835.

Christian F, Anthony DF, Vadrevu S, Riddell T, Day JP, McLeod R, Adams DR, Baillie GS and Houslay MD (2010) p62 (SQSTM1) and cyclic AMP phosphodiesterase-4A4 (PDE4A4) locate to a novel, reversible protein aggregate with links to autophagy and proteasome degradation pathways. *Cell Signal* **22**:1576-1596.

Claveau D, Chen SL, O'Keefe S, Zaller DM, Styhler A, Liu S, Huang Z, Nicholson DW and Mancini JA (2004) Preferential inhibition of T helper 1, but not T helper 2, cytokines in vitro by L-826,141 [4-[2-(3,4-Bisdifluromethoxyphenyl)-2-[4-(1,1,1,3,3,3-hexafluoro-2-hydroxypropan- 2-yl)-phenyl]-ethyl]3-methylpyridine-1-oxide], a potent and selective phosphodiesterase 4 inhibitor. *J Pharmacol Exp Ther* **310**:752-760.

Clister T, Greenwald EC, Baillie GS and Zhang J (2019) AKAP95 Organizes a Nuclear Microdomain to Control Local cAMP for Regulating Nuclear PKA. *Cell Chem Biol* **26**:885-891 e884.

Collins DM, Murdoch H, Dunlop AJ, Charych E, Baillie GS, Wang Q, Herberg FW, Brandon N, Prinz A and Houslay MD (2008) Ndel1 alters its conformation by sequestering cAMP-specific phosphodiesterase-4D3 (PDE4D3) in a manner that is dynamically regulated through Protein Kinase A (PKA). *Cell Signal* **20**:2356-2369.

Compton CH, Gubb J, Nieman R, Edelson J, Amit O, Bakst A, Ayres JG, Creemers JP, Schultze-Werninghaus G, Brambilla C, Barnes NC and International Study G (2001) Cilomilast, a selective phosphodiesterase-4 inhibitor for treatment of patients with chronic obstructive pulmonary disease: a randomised, dose-ranging study. *Lancet* **358**:265-270.

Conn SJ, Pillman KA, Toubia J, Conn VM, Salmanidis M, Phillips CA, Roslan S, Schreiber AW, Gregory PA and Goodall GJ (2015) The RNA binding protein quaking regulates formation of circRNAs. *Cell* **160**:1125-1134.

Conti M, Iona S, Cuomo M, Swinnen JV, Odeh J and Svoboda ME (1995) Characterization of a hormone-inducible, high affinity adenosine 3'-5'-cyclic monophosphate phosphodiesterase from the rat Sertoli cell. *Biochemistry* **34**:7979-7987.

Correa-Sales C, Nacif-Coelho C, Reid K and Maze M (1992) Inhibition of adenylate cyclase in the locus coeruleus mediates the hypnotic response to an alpha 2 agonist in the rat. *J Pharmacol Exp Ther* **263**:1046-1049.

Creighton J, Zhu B, Alexeyev M and Stevens T (2008) Spectrin-anchored phosphodiesterase 4D4 restricts cAMP from disrupting microtubules and inducing endothelial cell gap formation. *J Cell Sci* **121**:110-119.

D'Andrea I, Fardella V, Fardella S, Pallante F, Ghigo A, Iacobucci R, Maffei A, Hirsch E, Lembo G and Carnevale D (2015) Lack of kinase-independent activity of PI3Kgamma in locus coeruleus induces ADHD symptoms through increased CREB signaling. *EMBO Mol Med* **7**:904-917.

D'Sa C, Tolbert LM, Conti M and Duman RS (2002) Regulation of cAMP-specific phosphodiesterases type 4B and 4D (PDE4) splice variants by cAMP signaling in primary cortical neurons. *Journal of neurochemistry* **81**:745-757.

Davis RL, Takayasu H, Eberwine M and Myres J (1989) Cloning and characterization of mammalian homologs of the Drosophila dunce+ gene. *Proc Natl Acad Sci U S A* **86**:3604-3608.

Davis TG, Peterson JJ, Kou JP, Capper-Spudich EA, Ball D, Nials AT, Wiseman J, Solanke YE, Lucas FS, Williamson RA, Ferrari L, Wren P, Knowles RG, Barnette MS and Podolin PL (2009) The identification of a novel phosphodiesterase 4 inhibitor, 1-ethyl-5-{5-[(4-methyl-1-piperazinyl)methyl]-1,3,4-oxadiazol-2-yl}-N-(tetrahydro -2H-pyran-4-yl)-1H-pyrazolo[3,4-b]pyridin-4-amine (EPPA-1), with improved therapeutic index using pica feeding in rats as a measure of emetogenicity. *J Pharmacol Exp Ther* **330**:922-931.

Day JP, Lindsay B, Riddell T, Jiang Z, Allcock RW, Abraham A, Sookup S, Christian F, Bogum J, Martin EK, Rae RL, Anthony D, Rosair GM, Houslay DM, Huston E, Baillie GS, Klussmann E, Houslay MD and Adams DR (2011) Elucidation of a structural basis for the inhibitor-driven, p62 (SQSTM1)-dependent intracellular redistribution of cAMP phosphodiesterase-4A4 (PDE4A4). *J Med Chem* **54**:3331-3347.

Degerman E, In 't Zandt R, Palbrink A, Eliasson L, Caye-Thomasen P and Magnusson M (2017) Inhibition of phosphodiesterase 3, 4, and 5 induces endolymphatic hydrops in mouse inner ear, as evaluated with repeated 9.4T MRI. *Acta Otolaryngol* **137**:8-15.

Di Liegro CM, Schiera G and Di Liegro I (2014) Regulation of mRNA transport, localization and translation in the nervous system of mammals (Review). *International journal of molecular medicine* **33**:747-762.

Dodge KL, Khouangsathiene S, Kapiloff MS, Mouton R, Hill EV, Houslay MD, Langeberg LK and Scott JD (2001) mAKAP assembles a protein kinase A/PDE4 phosphodiesterase cAMP signaling module. *The EMBO journal* **20**:1921-1930.

Dong CJ, Guo Y, Ye Y and Hare WA (2014) Presynaptic inhibition by alpha2 receptor/adenylate cyclase/PDE4 complex at retinal rod bipolar synapse. *J Neurosci* **34**:9432-9440.

du Sert NP, Holmes AM, Wallis R and Andrews PL (2012) Predicting the emetic liability of novel chemical entities: a comparative study. *Br J Pharmacol* **165**:1848-1867.

Duplantier AJ, Biggers MS, Chambers RJ, Cheng JB, Cooper K, Damon DB, Eggler JF, Kraus KG, Marfat A, Masamune H, Pillar JS, Shirley JT, Umland JP and Watson JW (1996) Biarylcarboxylic acids and -amides: inhibition of phosphodiesterase type IV versus [3H]rolipram binding activity and their relationship to emetic behavior in the ferret. *J Med Chem* **39**:120-125.

Engels P, Sullivan M, Muller T and Lubbert H (1995) Molecular cloning and functional expression in yeast of a human cAMP-specific phosphodiesterase subtype (PDE IV-C). *FEBS Lett* **358**:305-310.

Fang R, Cui Q, Sun J, Duan X, Ma X, Wang W, Cheng B, Liu Y, Hou Y and Bai G (2015) PDK1/Akt/PDE4D axis identified as a target for asthma remedy synergistic with beta2 AR agonists by a natural agent arctigenin. *Allergy* **70**:1622-1632.

Fatemi SH, King DP, Reutiman TJ, Folsom TD, Laurence JA, Lee S, Fan YT, Paciga SA, Conti M and Menniti FS (2008) PDE4B polymorphisms and decreased PDE4B expression are associated with schizophrenia. *Schizophr Res* **101**:36-49.

Fox D, 3rd, Burgin AB and Gurney ME (2014) Structural basis for the design of selective phosphodiesterase 4B inhibitors. *Cell Signal* **26**:657-663.

Funahashi M, Mitoh Y, Kohjitani A and Matsuo R (2003) Role of the hyperpolarization-activated cation current (Ih) in pacemaker activity in area postrema neurons of rat brain slices. *J Physiol* **552**:135-148.

Gale DD, Hofer P, Spina D, Seeds EA, Banner KH, Harrison S, Douglas G, Matsumoto T, Page CP, Wong RH, Jordan S, Smith F, Banik N, Halushka PV, Cavalla D, Rotshteyn Y, Kyle DJ, Burch RM and Chasin M (2003) Pharmacology of a new cyclic nucleotide phosphodiesterase type 4 inhibitor, V11294. *Pulm Pharmacol Ther* **16**:97-104.

Gale DD, Landells LJ, Spina D, Miller AJ, Smith K, Nichols T, Rotshteyn Y, Tonelli A, Lacouture P, Burch RM, Page CP and O'Connor BJ (2002) Pharmacokinetic and pharmacodynamic profile following oral administration of the phosphodiesterase (PDE)4 inhibitor V11294A in healthy volunteers. *Br J Clin Pharmacol* **54**:478-484.

Ge X, Milenkovic L, Suyama K, Hartl T, Purzner T, Winans A, Meyer T and Scott MP (2015) Phosphodiesterase 4D acts downstream of Neuropilin to control Hedgehog signal transduction and the growth of medulloblastoma. *Elife* **4**.

Ghigo A, Perino A, Mehel H, Zahradnikova A, Jr., Morello F, Leroy J, Nikolaev VO, Damilano F, Cimino J, De Luca E, Richter W, Westenbroek R, Catterall WA, Zhang J, Yan C, Conti M, Gomez AM, Vandecasteele G, Hirsch E and Fischmeister R (2012) Phosphoinositide 3-kinase gamma protects against catecholamine-induced ventricular arrhythmia through protein kinase A-mediated regulation of distinct phosphodiesterases. *Circulation* **126**:2073-2083.

Goto T, Shiina A, Murata T, Tomii M, Yamazaki T, Yoshida K, Yoshino T, Suzuki O, Sogawa Y, Mizukami K, Takagi N, Yoshitomi T, Etori M, Tsuchida H, Mikkaichi T, Nakao N, Takahashi M, Takahashi H and Sasaki S (2014)

Identification of the 5,5-dioxo-7,8-dihydro-6H-thiopyrano[3,2-d]pyrimidine derivatives as highly selective PDE4B inhibitors. *Bioorg Med Chem Lett* **24**:893-899.

Grange M, Sette C, Cuomo M, Conti M, Lagarde M, Prigent AF and Nemoz G (2000) The cAMP-specific phosphodiesterase PDE4D3 is regulated by phosphatidic acid binding. Consequences for cAMP signaling pathway and characterization of a phosphatidic acid binding site. *J Biol Chem* **275**:33379-33387.

Gretarsdottir S, Thorleifsson G, Reynisdottir ST, Manolescu A, Jonsdottir S, Jonsdottir T, Gudmundsdottir T, Bjarnadottir SM, Einarsson OB, Gudjonsdottir HM, Hawkins M, Gudmundsson G, Gudmundsdottir H, Andrason H, Gudmundsdottir AS, Sigurdardottir M, Chou TT, Nahmias J, Goss S, Sveinbjornsdottir S, Valdimarsson EM, Jakobsson F, Agnarsson U, Gudnason V, Thorgeirsson G, Fingerle J, Gurney M, Gudbjartsson D, Frigge ML, Kong A, Stefansson K and Gulcher JR (2003) The gene encoding phosphodiesterase 4D confers risk of ischemic stroke. *Nat Genet* **35**:131-138.

Grover M, Farrugia G and Stanghellini V (2019) Gastroparesis: a turning point in understanding and treatment. *Gut* **68**:2238-2250.

Gulisano W, Tropea MR, Arancio O, Palmeri A and Puzzo D (2018) Sub-efficacious doses of phosphodiesterase 4 and 5 inhibitors improve memory in a mouse model of Alzheimer's disease. *Neuropharmacology* **138**:151-159.

Gurney ME, Burgin AB, Magnusson OT and Stewart LJ (2011) Small molecule allosteric modulators of phosphodiesterase 4. *Handb Exp Pharmacol*:167-192.

Gurney ME, D'Amato EC and Burgin AB (2015) Phosphodiesterase-4 (PDE4) molecular pharmacology and Alzheimer's disease. *Neurotherapeutics* **12**:49-56.

Gurney ME, Nugent RA, Mo X, Sindac JA, Hagen TJ, Fox D, 3rd, O'Donnell JM, Zhang C, Xu Y, Zhang HT, Groppi VE, Bailie M, White RE, Romero DL, Vellekoop AS, Walker JR, Surman MD, Zhu L and Campbell RF (2019) Design and Synthesis of Selective Phosphodiesterase 4D (PDE4D) Allosteric Inhibitors for the Treatment of Fragile X Syndrome and Other Brain Disorders. *J Med Chem* **62**:4884-4901.

Hagen TJ, Mo X, Burgin AB, Fox D, 3rd, Zhang Z and Gurney ME (2014) Discovery of triazines as selective PDE4B versus PDE4D inhibitors. *Bioorganic & medicinal chemistry letters* **24**:4031-4034.

Halls ML and Cooper DM (2010) Sub-picomolar relaxin signalling by a pre-assembled RXFP1, AKAP79, AC2, beta-arrestin 2, PDE4D3 complex. *EMBO J* **29**:2772-2787.

Harris AL, Connell MJ, Ferguson EW, Wallace AM, Gordon RJ, Pagani ED and Silver PJ (1989) Role of low Km cyclic AMP phosphodiesterase inhibition in tracheal relaxation and bronchodilation in the guinea pig. *J Pharmacol Exp Ther* **251**:199-206.

Hebenstreit GF, Fellerer K, Fichte K, Fischer G, Geyer N, Meya U, Sastre-y-Hernandez M, Schony W, Schratzer M, Soukop W and et al. (1989) Rolipram in major depressive disorder: results of a double-blind comparative study with imipramine. *Pharmacopsychiatry* **22**:156-160.

Hedde JR, Hanks AN, Schmidt CJ and Hughes ZA (2017) The isozyme selective phosphodiesterase-4 inhibitor, ABI-4, attenuates the effects of

lipopolysaccharide in human cells and rodent models of peripheral and CNS inflammation. *Brain Behav Immun* **64**:285-295.

Hill EV, Sheppard CL, Cheung YF, Gall I, Krause E and Houslay MD (2006) Oxidative stress employs phosphatidyl inositol 3-kinase and ERK signalling pathways to activate cAMP phosphodiesterase-4D3 (PDE4D3) through multi-site phosphorylation at Ser239 and Ser579. *Cell Signal* **18**:2056-2069.

Hirose R, Manabe H, Nonaka H, Yanagawa K, Akuta K, Sato S, Ohshima E and Ichimura M (2007) Correlation between emetic effect of phosphodiesterase 4 inhibitors and their occupation of the high-affinity rolipram binding site in Suncus murinus brain. *Eur J Pharmacol* **573**:93-99.

Hoffmann R, Baillie GS, MacKenzie SJ, Yarwood SJ and Houslay MD (1999) The MAP kinase ERK2 inhibits the cyclic AMP-specific phosphodiesterase HSPDE4D3 by phosphorylating it at Ser579. *The EMBO journal* **18**:893-903.

Hoffmann R, Wilkinson IR, McCallum JF, Engels P and Houslay MD (1998) cAMP-specific phosphodiesterase HSPDE4D3 mutants which mimic activation and changes in rolipram inhibition triggered by protein kinase A phosphorylation of Ser-54: generation of a molecular model. *Biochem J* **333 (Pt 1)**:139-149.

Houslay KF, Christian F, MacLeod R, Adams DR, Houslay MD and Baillie GS (2017) Identification of a multifunctional docking site on the catalytic unit of phosphodiesterase-4 (PDE4) that is utilised by multiple interaction partners. *Biochem J* **474**:597-609.

Houslay KF, Fertig BA, Christian F, Tibbo AJ, Ling J, Findlay JE, Houslay MD and Baillie GS (2019) Phosphorylation of PDE4A5 by MAPKAPK2 attenuates fibrin degradation via p75 signalling. *J Biochem* **166**:97-106.

Houslay MD (2001) PDE4 cAMP-specific phosphodiesterases. *Prog Nucleic Acid Res Mol Biol* **69**:249-315.

Houslay MD (2010) Underpinning compartmentalised cAMP signalling through targeted cAMP breakdown. *Trends Biochem Sci* **35**:91-100.

Houslay MD and Adams DR (2003) PDE4 cAMP phosphodiesterases: modular enzymes that orchestrate signalling cross-talk, desensitization and compartmentalization. *Biochem J* **370**:1-18.

Houslay MD and Adams DR (2010) Putting the lid on phosphodiesterase 4. *Nat Biotechnol* **28**:38-40.

Houslay MD and Baillie GS (2003) The role of ERK2 docking and phosphorylation of PDE4 cAMP phosphodiesterase isoforms in mediating cross-talk between the cAMP and ERK signalling pathways. *Biochemical Society transactions* **31**:1186-1190.

Houslay MD, Scotland G, Pooley L, Spence S, Wilkinson I, McCallum F, Julien P, Rena NG, Michie AM, Erdogan S and et al. (1995) Alternative splicing of the type-IVA cyclic AMP phosphodiesterase gene provides isoform variants with distinct N-terminal domains fused to a common, soluble catalytic unit: 'designer' changes in Vmax, stability and membrane association. *Biochem Soc Trans* **23**:393-398.

Huai Q, Sun Y, Wang H, Macdonald D, Aspiotis R, Robinson H, Huang Z and Ke H (2006) Enantiomer discrimination illustrated by the high resolution crystal structures of type 4 phosphodiesterase. *J Med Chem* **49**:1867-1873.

Huai Q, Wang H, Sun Y, Kim HY, Liu Y and Ke H (2003) Three-dimensional structures of PDE4D in complex with roliprams and implication on inhibitor selectivity. *Structure* **11**:865-873.

Huang C, Zhong QP, Tang L, Wang HT, Xu JP and Zhou ZZ (2019) Discovery of 2-(3,4-dialkoxyphenyl)-2-(substituted pyridazin-3-yl)acetonitriles as phosphodiesterase 4 inhibitors with anti-neuroinflammation potential based on three-dimensional quantitative structure-activity relationship study. *Chem Biol Drug Des* **93**:484-502.

Huang H, Wang Y, Kandpal M, Zhao G, Cardenas H, Ji Y, Chaparala A, Tanner EJ, Chen J, Davuluri RV and Matei D (2020) FTO-Dependent N (6)-Methyladenosine Modifications Inhibit Ovarian Cancer Stem Cell Self-Renewal by Blocking cAMP Signaling. *Cancer research* **80**:3200-3214.

Huang Z, Dias R, Jones T, Liu S, Styhler A, Claveau D, Otu F, Ng K, Laliberte F, Zhang L, Goetghebeur P, Abraham WM, Macdonald D, Dube D, Gallant M, Lacombe P, Girard Y, Young RN, Turner MJ, Nicholson DW and Mancini JA (2007) L-454,560, a potent and selective PDE4 inhibitor with in vivo efficacy in animal models of asthma and cognition. *Biochem Pharmacol* **73**:1971-1981.

Huang Z, Liu S, Zhang L, Salem M, Greig GM, Chi Chung C, Natsumeda Y and Noguchi K (2006) Preferential inhibition of human phosphodiesterase 4 by ibudilast. *Life Sciences* **78**:2663-2668.

Huo Z, Ye JC, Chen J, Lin X, Zhou ZN, Xu XR, Li CM, Qi M, Liang D, Liu Y and Li J (2012) Prolyl hydroxylase domain protein 2 regulates the intracellular cyclic AMP level in cardiomyocytes through its interaction with phosphodiesterase 4D. *Biochem Biophys Res Commun* **427**:73-79.

Huston E, Beard M, McCallum F, Pyne NJ, Vandenabeele P, Scotland G and Houslay MD (2000) The cAMP-specific phosphodiesterase PDE4A5 is cleaved downstream of its SH3 interaction domain by caspase-3. Consequences for altered intracellular distribution. *J Biol Chem* **275**:28063-28074.

Huston E, Lumb S, Russell A, Catterall C, Ross AH, Steele MR, Bolger GB, Perry MJ, Owens RJ and Houslay MD (1997) Molecular cloning and transient expression in COS7 cells of a novel human PDE4B cAMP-specific phosphodiesterase, HSPDE4B3. *Biochem J* **328 (Pt 2)**:549-558.

Huston E, Pooley L, Julien P, Scotland G, McPhee I, Sullivan M, Bolger G and Houslay MD (1996) The human cyclic AMP-specific phosphodiesterase PDE-46 (HSPDE4A4B) expressed in transfected COS7 cells occurs as both particulate and cytosolic species that exhibit distinct kinetics of inhibition by the antidepressant rolipram. *J Biol Chem* **271**:31334-31344.

Innamorati G, Wilkie TM, Kantheti HS, Valenti MT, Dalle Carbonare L, Giacomello L, Parenti M, Melisi D and Bassi C (2018) The curious case of Galphas gain-of-function in neoplasia. *BMC Cancer* **18**:293.

Iwahashi Y, Furuyama T, Tano Y, Ishimoto I, Shimomura Y and Inagaki S (1996) Differential distribution of mRNA encoding cAMP-specific phosphodiesterase isoforms in the rat brain. *Brain Res Mol Brain Res* **38**:14-24.

Jacobitz S, McLaughlin MM, Livi GP, Burman M and Torphy TJ (1996) Mapping the functional domains of human recombinant phosphodiesterase 4A: structural requirements for catalytic activity and rolipram binding. *Mol Pharmacol* **50**:891-899.

Jang DJ, Park SW, Lee JA, Lee C, Chae YS, Park H, Kim MJ, Choi SL, Lee N, Kim H and Kaang BK (2010) N termini of apPDE4 isoforms are responsible for

targeting the isoforms to different cellular membranes. *Learn Mem* **17**:469-479.
Johnson KR, Nicodemus-Johnson J and Danziger RS (2010) An evolutionary analysis of cAMP-specific Phosphodiesterase 4 alternative splicing. *BMC Evol Biol* **10**:247.
Johnston LA, Erdogan S, Cheung YF, Sullivan M, Barber R, Lynch MJ, Baillie GS, Van Heeke G, Adams DR, Huston E and Houslay MD (2004) Expression, intracellular distribution and basis for lack of catalytic activity of the PDE4A7 isoform encoded by the human PDE4A cAMP-specific phosphodiesterase gene. *Biochem J* **380**:371-384.
Kaname T, Ki CS, Niikawa N, Baillie GS, Day JP, Yamamura K, Ohta T, Nishimura G, Mastuura N, Kim OH, Sohn YB, Kim HW, Cho SY, Ko AR, Lee JY, Kim HW, Ryu SH, Rhee H, Yang KS, Joo K, Lee J, Kim CH, Cho KH, Kim D, Yanagi K, Naritomi K, Yoshiura K, Kondoh T, Nii E, Tonoki H, Houslay MD and Jin DK (2014) Heterozygous mutations in cyclic AMP phosphodiesterase-4D (PDE4D) and protein kinase A (PKA) provide new insights into the molecular pathology of acrodysostosis. *Cell Signal* **26**:2446-2459.
Khaled M, Levy C and Fisher DE (2010) Control of melanocyte differentiation by a MITF-PDE4D3 homeostatic circuit. *Genes & development* **24**:2276-2281.
Kim HW, Ha SH, Lee MN, Huston E, Kim DH, Jang SK, Suh PG, Houslay MD and Ryu SH (2010) Cyclic AMP controls mTOR through regulation of the dynamic interaction between Rheb and phosphodiesterase 4D. *Mol Cell Biol* **30**:5406-5420.
Kim MJ, Park SK, Lee JH, Jung CY, Sung DJ, Park JH, Yoon YS, Park J, Park KG, Song DK, Cho H, Kim ST and Koo SH (2015) Salt-Inducible Kinase 1 Terminates cAMP Signaling by an Evolutionarily Conserved Negative-Feedback Loop in beta-Cells. *Diabetes* **64**:3189-3202.
Klussmann E (2016) Protein-protein interactions of PDE4 family members - Functions, interactions and therapeutic value. *Cell Signal* **28**:713-718.
Kocer SS, Wang HY and Malbon CC (2012) "Shaping" of cell signaling via AKAP-tethered PDE4D: Probing with AKAR2-AKAP5 biosensor. *J Mol Signal* **7**:4.
Kovala T, Sanwal BD and Ball EH (1997) Recombinant expression of a type IV, cAMP-specific phosphodiesterase: characterization and structure-function studies of deletion mutants. *Biochemistry* **36**:2968-2976.
Kranz M, Wall M, Evans B, Miah A, Ballantine S, Delves C, Dombroski B, Gross J, Schneck J, Villa JP, Neu M and Somers DO (2009) Identification of PDE4B Over 4D subtype-selective inhibitors revealing an unprecedented binding mode. *Bioorg Med Chem* **17**:5336-5341.
Kristensen LS, Andersen MS, Stagsted LVW, Ebbesen KK, Hansen TB and Kjems J (2019) The biogenesis, biology and characterization of circular RNAs. *Nature reviews Genetics* **20**:675-691.
Lakics V, Karran EH and Boess FG (2010) Quantitative comparison of phosphodiesterase mRNA distribution in human brain and peripheral tissues. *Neuropharmacology* **59**:367-374.
Laliberte F, Han Y, Govindarajan A, Giroux A, Liu S, Bobechko B, Lario P, Bartlett A, Gorseth E, Gresser M and Huang Z (2000) Conformational difference between PDE4 apoenzyme and holoenzyme. *Biochemistry* **39**:6449-6458.
Lamontagne S, Meadows E, Luk P, Normandin D, Muise E, Boulet L, Pon DJ, Robichaud A, Robertson GS, Metters KM and Nantel F (2001) Localization

of phosphodiesterase-4 isoforms in the medulla and nodose ganglion of the squirrel monkey. *Brain Res* **920**:84-96.

Lario PI, Bobechko B, Bateman K, Kelly J, Vrielink A and Huang Z (2001) Purification and characterization of the human PDE4A catalytic domain (PDE4A330-723) expressed in Sf9 cells. *Arch Biochem Biophys* **394**:54-60.

Larsen J, Lambert M, Pettersson H, Vifian T, Larsen M, Ollerstam A, Hegardt P, Eskilsson C, Laursen S, Soehoel A, Skak-Nielsen T, Hansen LM, Knudsen NO, Eirefelt S, Sorensen MD, Stilou TG and Nielsen SF (2020) Discovery and Early Clinical Development of Isobutyl 1-[8-Methoxy-5-(1-oxo-3H-isobenzofuran-5-yl)-[1,2,4]triazolo[1,5-a]pyridin-2-yl]c yclopropanecarboxylate (LEO 39652), a Novel "Dual-Soft" PDE4 Inhibitor for Topical Treatment of Atopic Dermatitis. *J Med Chem*.

Le Jeune IR, Shepherd M, Van Heeke G, Houslay MD and Hall IP (2002) Cyclic AMP-dependent transcriptional up-regulation of phosphodiesterase 4D5 in human airway smooth muscle cells. Identification and characterization of a novel PDE4D5 promoter. *J Biol Chem* **277**:35980-35989.

Lee JH, Richter W, Namkung W, Kim KH, Kim E, Conti M and Lee MG (2007) Dynamic regulation of cystic fibrosis transmembrane conductance regulator by competitive interactions of molecular adaptors. *J Biol Chem* **282**:10414-10422.

Lee ME, Markowitz J, Lee JO and Lee H (2002) Crystal structure of phosphodiesterase 4D and inhibitor complex(1). *FEBS Lett* **530**:53-58.

Lehnart SE, Wehrens XH, Reiken S, Warrier S, Belevych AE, Harvey RD, Richter W, Jin SL, Conti M and Marks AR (2005) Phosphodiesterase 4D deficiency in the ryanodine-receptor complex promotes heart failure and arrhythmias. *Cell* **123**:25-35.

Lenhard JM, Kassel DB, Rocque WJ, Hamacher L, Holmes WD, Patel I, Hoffman C and Luther M (1996) Phosphorylation of a cAMP-specific phosphodiesterase (HSPDE4B2B) by mitogen-activated protein kinase. *Biochem J* **316 (Pt 3)**:751-758.

Levine MA (1999) Clinical implications of genetic defects in G proteins: oncogenic mutations in G alpha s as the molecular basis for the McCune-Albright syndrome. *Arch Med Res* **30**:522-531.

Li X, Baillie GS and Houslay MD (2009) Mdm2 directs the ubiquitination of beta-arrestin-sequestered cAMP phosphodiesterase-4D5. *J Biol Chem* **284**:16170-16182.

Li X, Vadrevu S, Dunlop A, Day J, Advant N, Troeger J, Klussmann E, Jaffrey E, Hay RT, Adams DR, Houslay MD and Baillie GS (2010) Selective SUMO modification of cAMP-specific phosphodiesterase-4D5 (PDE4D5) regulates the functional consequences of phosphorylation by PKA and ERK. *Biochem J* **428**:55-65.

Liang J, Huang YY, Zhou Q, Gao Y, Li Z, Wu D, Yu S, Guo L, Chen Z, Huang L, Liang SH, He X, Wu R and Luo HB (2020) Discovery and Optimization of alpha-Mangostin Derivatives as Novel PDE4 Inhibitors for the Treatment of Vascular Dementia. *J Med Chem* **63**:3370-3380.

Lim J, Pahlke G and Conti M (1999) Activation of the cAMP-specific phosphodiesterase PDE4D3 by phosphorylation. Identification and function of an inhibitory domain. *J Biol Chem* **274**:19677-19685.

Lipworth BJ (2005) Phosphodiesterase-4 inhibitors for asthma and chronic obstructive pulmonary disease. *Lancet* **365**:167-175.

Liu H and Maurice DH (1999) Phosphorylation-mediated activation and translocation of the cyclic AMP-specific phosphodiesterase PDE4D3 by cyclic AMP-dependent protein kinase and mitogen-activated protein kinases. A potential mechanism allowing for the coordinated regulation of PDE4D activity and targeting. *J Biol Chem* **274**:10557-10565.

Liu S, Huang S, Wu X, Feng Y, Shen Y, Zhao QS and Leng Y (2020) Activation of SIK1 by phanginin A inhibits hepatic gluconeogenesis by increasing PDE4 activity and suppressing cAMP signaling pathway. *Mol Metab*:101045.

Liu S, Laliberte F, Bobechko B, Bartlett A, Lario P, Gorseth E, Van Hamme J, Gresser MJ and Huang Z (2001) Dissecting the cofactor-dependent and independent bindings of PDE4 inhibitors. *Biochemistry* **40**:10179-10186.

Lobban M, Shakur Y, Beattie J and Houslay MD (1994) Identification of two splice variant forms of type-IVB cyclic AMP phosphodiesterase, DPD (rPDE-IVB1) and PDE-4 (rPDE-IVB2) in brain: selective localization in membrane and cytosolic compartments and differential expression in various brain regions. *Biochem J* **304 (Pt 2)**:399-406.

Lynex CN, Li Z, Chen ML, Toh KY, Low RW, Goh DL and Tay SK (2008) Identification and molecular characterization of a novel PDE4D11 cAMP-specific phosphodiesterase isoform. *Cell Signal* **20**:2247-2255.

Mackenzie KF, Topping EC, Bugaj-Gaweda B, Deng C, Cheung YF, Olsen AE, Stockard CR, High Mitchell L, Baillie GS, Grizzle WE, De Vivo M, Houslay MD, Wang D and Bolger GB (2008) Human PDE4A8, a novel brain-expressed PDE4 cAMP-specific phosphodiesterase that has undergone rapid evolutionary change. *Biochem J* **411**:361-369.

MacKenzie KF, Wallace DA, Hill EV, Anthony DF, Henderson DJ, Houslay DM, Arthur JS, Baillie GS and Houslay MD (2011) Phosphorylation of cAMP-specific PDE4A5 (phosphodiesterase-4A5) by MK2 (MAPKAPK2) attenuates its activation through protein kinase A phosphorylation. *Biochem J* **435**:755-769.

MacKenzie SJ, Baillie GS, McPhee I, Bolger GB and Houslay MD (2000) ERK2 mitogen-activated protein kinase binding, phosphorylation, and regulation of the PDE4D cAMP-specific phosphodiesterases. The involvement of COOH-terminal docking sites and NH2-terminal UCR regions. *J Biol Chem* **275**:16609-16617.

MacKenzie SJ, Baillie GS, McPhee I, MacKenzie C, Seamons R, McSorley T, Millen J, Beard MB, van Heeke G and Houslay MD (2002) Long PDE4 cAMP specific phosphodiesterases are activated by protein kinase A-mediated phosphorylation of a single serine residue in Upstream Conserved Region 1 (UCR1). *Br J Pharmacol* **136**:421-433.

Manning CD, Burman M, Christensen SB, Cieslinski LB, Essayan DM, Grous M, Torphy TJ and Barnette MS (1999) Suppression of human inflammatory cell function by subtype-selective PDE4 inhibitors correlates with inhibition of PDE4A and PDE4B. *Br J Pharmacol* **128**:1393-1398.

Marquez-Ruiz AB, Gonzalez-Herrera L, Luna JD and Valenzuela A (2020) DNA methylation levels and telomere length in human teeth: usefulness for age estimation. *Int J Legal Med* **134**:451-459.

McCahill A, McSorley T, Huston E, Hill EV, Lynch MJ, Gall I, Keryer G, Lygren B, Tasken K, van Heeke G and Houslay MD (2005) In resting COS1 cells a dominant negative approach shows that specific, anchored PDE4 cAMP phosphodiesterase isoforms gate the activation, by basal cyclic AMP

production, of AKAP-tethered protein kinase A type II located in the centrosomal region. *Cell Signal* **17**:1158-1173.
McConnachie G, Langeberg LK and Scott JD (2006) AKAP signaling complexes: getting to the heart of the matter. *Trends Mol Med* **12**:317-323.
McDonough W, Aragon IV, Rich J, Murphy JM, Abou Saleh L, Boyd A, Koloteva A and Richter W (2020a) PAN-selective inhibition of cAMP-phosphodiesterase 4 (PDE4) induces gastroparesis in mice. *FASEB J*.
McDonough W, Rich J, Aragon IV, Abou Saleh L, Boyd A, Richter A, Koloteva A and Richter W (2020b) Inhibition of type 4 cAMP-phosphodiesterases (PDE4s) in mice induces hypothermia via effects on behavioral and central autonomous thermoregulation. *Biochem Pharmacol* **180**:114158.
McLaughlin MM, Cieslinski LB, Burman M, Torphy TJ and Livi GP (1993) A low-Km, rolipram-sensitive, cAMP-specific phosphodiesterase from human brain. Cloning and expression of cDNA, biochemical characterization of recombinant protein, and tissue distribution of mRNA. *J Biol Chem* **268**:6470-6476.
McPhee I, Yarwood SJ, Scotland G, Huston E, Beard MB, Ross AH, Houslay ES and Houslay MD (1999) Association with the SRC family tyrosyl kinase LYN triggers a conformational change in the catalytic region of human cAMP-specific phosphodiesterase HSPDE4A4B. Consequences for rolipram inhibition. *J Biol Chem* **274**:11796-11810.
Meng W, Liang X, Chen H, Luo H, Bai J, Li G, Zhang Q, Xiao T, He S, Zhang Y, Xu Z, Xiao B, Liu M, Hu F and Liu F (2017) Rheb Inhibits Beiging of White Adipose Tissue via PDE4D5-Dependent Downregulation of the cAMP-PKA Signaling Pathway. *Diabetes* **66**:1198-1213.
Mika D, Richter W and Conti M (2015) A CaMKII/PDE4D negative feedback regulates cAMP signaling. *Proc Natl Acad Sci U S A* **112**:2023-2028.
Milatovich A, Bolger G, Michaeli T and Francke U (1994) Chromosome localizations of genes for five cAMP-specific phosphodiesterases in man and mouse. *Somat Cell Mol Genet* **20**:75-86.
Millar JK, Pickard BS, Mackie S, James R, Christie S, Buchanan SR, Malloy MP, Chubb JE, Huston E, Baillie GS, Thomson PA, Hill EV, Brandon NJ, Rain JC, Camargo LM, Whiting PJ, Houslay MD, Blackwood DH, Muir WJ and Porteous DJ (2005) DISC1 and PDE4B are interacting genetic factors in schizophrenia that regulate cAMP signaling. *Science* **310**:1187-1191.
Miller AD and Leslie RA (1994) The area postrema and vomiting. *Front Neuroendocrinol* **15**:301-320.
Miro X, Casacuberta JM, Gutierrez-Lopez MD, de Landazuri MO and Puigdomenech P (2000) Phosphodiesterases 4D and 7A splice variants in the response of HUVEC cells to TNF-alpha(1). *Biochem Biophys Res Commun* **274**:415-421.
Miro X, Perez-Torres S, Artigas F, Puigdomenech P, Palacios JM and Mengod G (2002a) Regulation of cAMP phosphodiesterase mRNAs expression in rat brain by acute and chronic fluoxetine treatment. An in situ hybridization study. *Neuropharmacology* **43**:1148-1157.
Miro X, Perez-Torres S, Puigdomenech P, Palacios JM and Mengod G (2002b) Differential distribution of PDE4D splice variant mRNAs in rat brain suggests association with specific pathways and presynaptical localization. *Synapse* **45**:259-269.
Mori F, Perez-Torres S, De Caro R, Porzionato A, Macchi V, Beleta J, Gavalda A, Palacios JM and Mengod G (2010) The human area postrema and other

nuclei related to the emetic reflex express cAMP phosphodiesterases 4B and 4D. *J Chem Neuroanat* **40**:36-42.
Murdoch H, Mackie S, Collins DM, Hill EV, Bolger GB, Klussmann E, Porteous DJ, Millar JK and Houslay MD (2007) Isoform-selective susceptibility of DISC1/phosphodiesterase-4 complexes to dissociation by elevated intracellular cAMP levels. *J Neurosci* **27**:9513-9524.
Murdoch H, Vadrevu S, Prinz A, Dunlop AJ, Klussmann E, Bolger GB, Norman JC and Houslay MD (2011) Interaction between LIS1 and PDE4, and its role in cytoplasmic dynein function. *J Cell Sci* **124**:2253-2266.
Naganuma K, Omura A, Maekawara N, Saitoh M, Ohkawa N, Kubota T, Nagumo H, Kodama T, Takemura M, Ohtsuka Y, Nakamura J, Tsujita R, Kawasaki K, Yokoi H and Kawanishi M (2009) Discovery of selective PDE4B inhibitors. *Bioorg Med Chem Lett* **19**:3174-3176.
Nakashima T, Pyykko I, Arroll MA, Casselbrant ML, Foster CA, Manzoor NF, Megerian CA, Naganawa S and Young YH (2016) Meniere's disease. *Nat Rev Dis Primers* **2**:16028.
Naro F, Zhang R and Conti M (1996) Developmental regulation of unique adenosine 3',5'-monophosphate-specific phosphodiesterase variants during rat spermatogenesis. *Endocrinology* **137**:2464-2472.
Nelissen E, van Goethem NP, Bonassoli VT, Heckman PRA, van Hagen BTJ, Suay D, Wouters C and Prickaerts J (2019) Validation of the xylazine/ketamine anesthesia test as a predictor of the emetic potential of pharmacological compounds in rats. *Neurosci Lett* **699**:41-46.
Nemoz G, Sette C and Conti M (1997) Selective activation of rolipram-sensitive, cAMP-specific phosphodiesterase isoforms by phosphatidic acid. *Mol Pharmacol* **51**:242-249.
Nemoz G, Zhang R, Sette C and Conti M (1996) Identification of cyclic AMP-phosphodiesterase variants from the PDE4D gene expressed in human peripheral mononuclear cells. *FEBS Lett* **384**:97-102.
Nose T, Kondo M, Shimizu M, Hamura H, Yamaguchi Y, Sekine T and Ishitani K (2016) Pharmacological Profile of GPD-1116, an Inhibitor of Phosphodiesterase 4. *Biol Pharm Bull* **39**:689-698.
O'Connell JC, McCallum JF, McPhee I, Wakefield J, Houslay ES, Wishart W, Bolger G, Frame M and Houslay MD (1996) The SH3 domain of Src tyrosyl protein kinase interacts with the N-terminal splice region of the PDE4A cAMP-specific phosphodiesterase RPDE-6 (RNPDE4A5). *Biochem J* **318 (Pt 1)**:255-261.
Obernolte R, Ratzliff J, Baecker PA, Daniels DV, Zuppan P, Jarnagin K and Shelton ER (1997) Multiple splice variants of phosphodiesterase PDE4C cloned from human lung and testis. *Biochim Biophys Acta* **1353**:287-297.
Omar F, Findlay JE, Carfray G, Allcock RW, Jiang Z, Moore C, Muir AL, Lannoy M, Fertig BA, Mai D, Day JP, Bolger G, Baillie GS, Schwiebert E, Klussmann E, Pyne NJ, Ong ACM, Bowers K, Adam JM, Adams DR, Houslay MD and Henderson DJP (2019) Small-molecule allosteric activators of PDE4 long form cyclic AMP phosphodiesterases. *Proc Natl Acad Sci U S A* **116**:13320-13329.
Omar MH and Scott JD (2020) AKAP Signaling Islands: Venues for Precision Pharmacology. *Trends in Pharmacological Sciences*.
Owens RJ, Catterall C, Batty D, Jappy J, Russell A, Smith B, O'Connell J and Perry MJ (1997a) Human phosphodiesterase 4A: characterization of full-length

and truncated enzymes expressed in COS cells. *Biochem J* **326 (Pt 1)**:53-60.
Owens RJ, Lumb S, Rees-Milton K, Russell A, Baldock D, Lang V, Crabbe T, Ballesteros M and Perry MJ (1997b) Molecular cloning and expression of a human phosphodiesterase 4C. *Cell Signal* **9**:575-585.
Paes D, Lardenoije R, Carollo RM, Roubroeks JAY, Schepers M, Coleman P, Mastroeni D, Delvaux E, Pishva E, Lunnon K, Vanmierlo T, van den Hove D and Prickaerts J (2020a) Increased isoform-specific phosphodiesterase 4D expression is associated with pathology and cognitive impairment in Alzheimer's disease. *Neurobiol Aging* **97**:56-64.
Paes D, Xie K, Wheeler DG, Zook D, Prickaerts J and Peters M (2020b) Inhibition of PDE2 and PDE4 synergistically improves memory consolidation processes. *Neuropharmacology* **184**:108414.
Papier A and Strowd LC (2018) Atopic dermatitis: a review of topical nonsteroid therapy. *Drugs Context* **7**:212521.
Pauwelyn V, Ceelen W and Lefebvre RA (2018) Synergy between 5-HT4 receptor stimulation and phosphodiesterase 4 inhibition in facilitating acetylcholine release in human large intestinal circular muscle. *Neurogastroenterol Motil* **30**.
Peng T, Qi B, He J, Ke H and Shi J (2020) Advances in the Development of Phosphodiesterase-4 Inhibitors. *J Med Chem* **63**:10594-10617.
Perera RK, Fischer TH, Wagner M, Dewenter M, Vettel C, Bork NI, Maier LS, Conti M, Wess J, El-Armouche A, Hasenfuss G and Nikolaev VO (2017) Atropine augments cardiac contractility by inhibiting cAMP-specific phosphodiesterase type 4. *Sci Rep* **7**:15222.
Perez-Torres S, Miro X, Palacios JM, Cortes R, Puigdomenech P and Mengod G (2000) Phosphodiesterase type 4 isozymes expression in human brain examined by in situ hybridization histochemistry and[3H]rolipram binding autoradiography. Comparison with monkey and rat brain. *J Chem Neuroanat* **20**:349-374.
Perry MJ, O'Connell J, Walker C, Crabbe T, Baldock D, Russell A, Lumb S, Huang Z, Howat D, Allen R, Merriman M, Walls J, Daniel T, Hughes B, Laliberte F, Higgs GA and Owens RJ (1998) CDP840: a novel inhibitor of PDE-4. *Cell Biochem Biophys* **29**:113-132.
Perry SJ, Baillie GS, Kohout TA, McPhee I, Magiera MM, Ang KL, Miller WE, McLean AJ, Conti M, Houslay MD and Lefkowitz RJ (2002) Targeting of cyclic AMP degradation to beta 2-adrenergic receptors by beta-arrestins. *Science* **298**:834-836.
Peter D, Goggel R, Colbatzky F and Nickolaus P (2011) Inhibition of cyclooxygenase-2 prevents adverse effects induced by phosphodiesterase type 4 inhibitors in rats. *Br J Pharmacol* **162**:415-427.
Plattner F, Hayashi K, Hernandez A, Benavides DR, Tassin TC, Tan C, Day J, Fina MW, Yuen EY, Yan Z, Goldberg MS, Nairn AC, Greengard P, Nestler EJ, Taussig R, Nishi A, Houslay MD and Bibb JA (2015) The role of ventral striatal cAMP signaling in stress-induced behaviors. *Nat Neurosci* **18**:1094-1100.
Prosdocimi T, Mollica L, Donini S, Semrau MS, Lucarelli AP, Aiolfi E, Cavalli A, Storici P, Alfei S, Brullo C, Bruno O and Parisini E (2018) Molecular Bases of PDE4D Inhibition by Memory-Enhancing GEBR Library Compounds. *Biochemistry* **57**:2876-2888.

Pruniaux MP, Lagente V, Ouaged M, Bertin B, Moreau F, Julien-Larose C, Rocher MN, Leportier C, Martin B, Bouget A, Dubuit JP, Burnouf C, Doherty AM and Bertrand CP (2010) Relationship between phosphodiesterase type 4 inhibition and anti-inflammatory activity of CI-1044 in rat airways. *Fundam Clin Pharmacol* **24**:73-82.

Purushothaman B, Arumugam P and Song JM (2018) A Novel Catecholopyrimidine Based Small Molecule PDE4B Inhibitor Suppresses Inflammatory Cytokines in Atopic Mice. *Front Pharmacol* **9**:485.

Purvis JE and Lahav G (2013) Encoding and decoding cellular information through signaling dynamics. *Cell* **152**:945-956.

Puurunen J, Lucke C and Schwabe U (1978) Effect of the phosphodiesterase inhibitor 4-(3-cyclopentyloxy-4-methoxyphenyl)-2-pyrrolidone (ZK 62711) on gastric secretion and gastric mucosal cyclic AMP. *Naunyn Schmiedebergs Arch Pharmacol* **304**:69-75.

Rall TW and Sutherland EW (1958) Formation of a cyclic adenine ribonucleotide by tissue particles. *J Biol Chem* **232**:1065-1076.

Reeves ML, Leigh BK and England PJ (1987) The identification of a new cyclic nucleotide phosphodiesterase activity in human and guinea-pig cardiac ventricle. Implications for the mechanism of action of selective phosphodiesterase inhibitors. *Biochem J* **241**:535-541.

Rehman NU, Ansari MN and Samad A (2020) In Silico, Ex Vivo and In Vivo Studies of Roflumilast as a Potential Antidiarrheal and Antispasmodic agent: Inhibition of the PDE-4 Enzyme and Voltage-gated Ca++ ion Channels. *Molecules* **25**.

Rena G, Begg F, Ross A, MacKenzie C, McPhee I, Campbell L, Huston E, Sullivan M and Houslay MD (2001) Molecular cloning, genomic positioning, promoter identification, and characterization of the novel cyclic amp-specific phosphodiesterase PDE4A10. *Mol Pharmacol* **59**:996-1011.

Ricciarelli R, Brullo C, Prickaerts J, Arancio O, Villa C, Rebosio C, Calcagno E, Balbi M, van Hagen BT, Argyrousi EK, Zhang H, Pronzato MA, Bruno O and Fedele E (2017) Memory-enhancing effects of GEBR-32a, a new PDE4D inhibitor holding promise for the treatment of Alzheimer's disease. *Sci Rep* **7**:46320.

Richter W and Conti M (2002) Dimerization of the type 4 cAMP-specific phosphodiesterases is mediated by the upstream conserved regions (UCRs). *J Biol Chem* **277**:40212-40221.

Richter W and Conti M (2004) The oligomerization state determines regulatory properties and inhibitor sensitivity of type 4 cAMP-specific phosphodiesterases. *J Biol Chem* **279**:30338-30348.

Richter W, Jin SL and Conti M (2005) Splice variants of the cyclic nucleotide phosphodiesterase PDE4D are differentially expressed and regulated in rat tissue. *Biochem J* **388**:803-811.

Robichaud A, Savoie C, Stamatiou PB, Lachance N, Jolicoeur P, Rasori R and Chan CC (2002a) Assessing the emetic potential of PDE4 inhibitors in rats. *Br J Pharmacol* **135**:113-118.

Robichaud A, Savoie C, Stamatiou PB, Tattersall FD and Chan CC (2001) PDE4 inhibitors induce emesis in ferrets via a noradrenergic pathway. *Neuropharmacology* **40**:262-269.

Robichaud A, Stamatiou PB, Jin SL, Lachance N, MacDonald D, Laliberte F, Liu S, Huang Z, Conti M and Chan CC (2002b) Deletion of phosphodiesterase 4D

in mice shortens alpha(2)-adrenoceptor-mediated anesthesia, a behavioral correlate of emesis. *J Clin Invest* **110**:1045-1052.
Robichaud A, Tattersall FD, Choudhury I and Rodger IW (1999) Emesis induced by inhibitors of type IV cyclic nucleotide phosphodiesterase (PDE IV) in the ferret. *Neuropharmacology* **38**:289-297.
Rocque WJ, Holmes WD, Patel IR, Dougherty RW, Ittoop O, Overton L, Hoffman CR, Wisely GB, Willard DH and Luther MA (1997a) Detailed characterization of a purified type 4 phosphodiesterase, HSPDE4B2B: differentiation of high- and low-affinity (R)-rolipram binding. *Protein Expr Purif* **9**:191-202.
Rocque WJ, Tian G, Wiseman JS, Holmes WD, Zajac-Thompson I, Willard DH, Patel IR, Wisely GB, Clay WC, Kadwell SH, Hoffman CR and Luther MA (1997b) Human recombinant phosphodiesterase 4B2B binds (R)-rolipram at a single site with two affinities. *Biochemistry* **36**:14250-14261.
Rogers DF and Giembycz MA (1998) Asthma therapy for the 21st century. *Trends Pharmacol Sci* **19**:160-164.
Rucilova V, Swierczek A, Vanda D, Funk P, Lemrova B, Gawalska A, Bucki A, Nowak B, Zadrozna M, Pociecha K, Soural M, Wyska E, Pawlowski M, Chlon-Rzepa G and Zajdel P (2020) New imidazopyridines with phosphodiesterase 4 and 7 inhibitory activity and their efficacy in animal models of inflammatory and autoimmune diseases. *Eur J Med Chem* **209**:112854.
Sachs BD, Baillie GS, McCall JR, Passino MA, Schachtrup C, Wallace DA, Dunlop AJ, MacKenzie KF, Klussmann E, Lynch MJ, Sikorski SL, Nuriel T, Tsigelny I, Zhang J, Houslay MD, Chao MV and Akassoglou K (2007) p75 neurotrophin receptor regulates tissue fibrosis through inhibition of plasminogen activation via a PDE4/cAMP/PKA pathway. *J Cell Biol* **177**:1119-1132.
Saldou N, Obernolte R, Huber A, Baecker PA, Wilhelm R, Alvarez R, Li B, Xia L, Callan O, Su C, Jarnagin K and Shelton ER (1998) Comparison of recombinant human PDE4 isoforms: interaction with substrate and inhibitors. *Cell Signal* **10**:427-440.
Scheinin M, Lomasney JW, Hayden-Hixson DM, Schambra UB, Caron MG, Lefkowitz RJ and Fremeau RT, Jr. (1994) Distribution of alpha 2-adrenergic receptor subtype gene expression in rat brain. *Brain Res Mol Brain Res* **21**:133-149.
Schepers M, Tiane A, Paes D, Sanchez S, Rombaut B, Piccart E, Rutten BPF, Brone B, Hellings N, Prickaerts J and Vanmierlo T (2019) Targeting Phosphodiesterases-Towards a Tailor-Made Approach in Multiple Sclerosis Treatment. *Front Immunol* **10**:1727.
Schneider HH (1984) Brain cAMP response to phosphodiesterase inhibitors in rats killed by microwave irradiation or decapitation. *Biochem Pharmacol* **33**:1690-1693.
Schwabe U, Miyake M, Ohga Y and Daly JW (1976) 4-(3-Cyclopentyloxy-4-methoxyphenyl)-2-pyrrolidone (ZK 62711): a potent inhibitor of adenosine cyclic 3',5'-monophosphate phosphodiesterases in homogenates and tissue slices from rat brain. *Mol Pharmacol* **12**:900-910.
Sette C and Conti M (1996) Phosphorylation and activation of a cAMP-specific phosphodiesterase by the cAMP-dependent protein kinase. Involvement of serine 54 in the enzyme activation. *J Biol Chem* **271**:16526-16534.

Shakur Y, Pryde JG and Houslay MD (1993) Engineered deletion of the unique N-terminal domain of the cyclic AMP-specific phosphodiesterase RD1 prevents plasma membrane association and the attainment of enhanced thermostability without altering its sensitivity to inhibition by rolipram. *Biochem J* **292 (Pt 3)**:677-686.

Sharma H, Lather V, Grewal AS and Pandita D (2019) Synthesis, Anti-inflammatory Activity and Docking Studies of Some Newer 1,3-Thiazolidine-2,4-dione Derivatives as Dual Inhibitors of PDE4 and PDE7. *Curr Comput Aided Drug Des* **15**:225-234.

Sharrocks AD, Yang SH and Galanis A (2000) Docking domains and substrate-specificity determination for MAP kinases. *Trends Biochem Sci* **25**:448-453.

Shepherd M, McSorley T, Olsen AE, Johnston LA, Thomson NC, Baillie GS, Houslay MD and Bolger GB (2003) Molecular cloning and subcellular distribution of the novel PDE4B4 cAMP-specific phosphodiesterase isoform. *Biochem J* **370**:429-438.

Sheppard CL, Lee LC, Hill EV, Henderson DJ, Anthony DF, Houslay DM, Yalla KC, Cairns LS, Dunlop AJ, Baillie GS, Huston E and Houslay MD (2014) Mitotic activation of the DISC1-inducible cyclic AMP phosphodiesterase-4D9 (PDE4D9), through multi-site phosphorylation, influences cell cycle progression. *Cell Signal* **26**:1958-1974.

Sibley CR, Emmett W, Blazquez L, Faro A, Haberman N, Briese M, Trabzuni D, Ryten M, Weale ME, Hardy J, Modic M, Curk T, Wilson SW, Plagnol V and Ule J (2015) Recursive splicing in long vertebrate genes. *Nature* **521**:371-375.

Sin YY, Edwards HV, Li X, Day JP, Christian F, Dunlop AJ, Adams DR, Zaccolo M, Houslay MD and Baillie GS (2011) Disruption of the cyclic AMP phosphodiesterase-4 (PDE4)-HSP20 complex attenuates the beta-agonist induced hypertrophic response in cardiac myocytes. *J Mol Cell Cardiol* **50**:872-883.

Skoumbourdis AP, Leclair CA, Stefan E, Turjanski AG, Maguire W, Titus SA, Huang R, Auld DS, Inglese J, Austin CP, Michnick SW, Xia M and Thomas CJ (2009) Exploration and optimization of substituted triazolothiadiazines and triazolopyridazines as PDE4 inhibitors. *Bioorg Med Chem Lett* **19**:3686-3692.

Smith KJ, Baillie GS, Hyde EI, Li X, Houslay TM, McCahill A, Dunlop AJ, Bolger GB, Klussmann E, Adams DR and Houslay MD (2007) 1H NMR structural and functional characterisation of a cAMP-specific phosphodiesterase-4D5 (PDE4D5) N-terminal region peptide that disrupts PDE4D5 interaction with the signalling scaffold proteins, beta-arrestin and RACK1. *Cell Signal* **19**:2612-2624.

Soda T, Frank C, Ishizuka K, Baccarella A, Park YU, Flood Z, Park SK, Sawa A and Tsai LH (2013) DISC1-ATF4 transcriptional repression complex: dual regulation of the cAMP-PDE4 cascade by DISC1. *Mol Psychiatry* **18**:898-908.

Souness JE and Rao S (1997) Proposal for pharmacologically distinct conformers of PDE4 cyclic AMP phosphodiesterases. *Cell Signal* **9**:227-236.

Spina D (2008) PDE4 inhibitors: current status. *Br J Pharmacol* **155**:308-315.

St Clair JR, Larson ED, Sharpe EJ, Liao Z and Proenza C (2017) Phosphodiesterases 3 and 4 Differentially Regulate the Funny Current, If, in Mouse Sinoatrial Node Myocytes. *J Cardiovasc Dev Dis* **4**.

Stefan E, Wiesner B, Baillie GS, Mollajew R, Henn V, Lorenz D, Furkert J, Santamaria K, Nedvetsky P, Hundsrucker C, Beyermann M, Krause E, Pohl P, Gall I, MacIntyre AN, Bachmann S, Houslay MD, Rosenthal W and Klussmann E (2007) Compartmentalization of cAMP-dependent signaling by phosphodiesterase-4D is involved in the regulation of vasopressin-mediated water reabsorption in renal principal cells. *J Am Soc Nephrol* **18**:199-212.

Sullivan M, Rena G, Begg F, Gordon L, Olsen AS and Houslay MD (1998) Identification and characterization of the human homologue of the short PDE4A cAMP-specific phosphodiesterase RD1 (PDE4A1) by analysis of the human HSPDE4A gene locus located at chromosome 19p13.2. *Biochem J* **333 (Pt 3)**:693-703.

Sutcliffe JS, Beaumont V, Watson JM, Chew CS, Beconi M, Hutcheson DM, Dominguez C and Munoz-Sanjuan I (2014) Efficacy of selective PDE4D negative allosteric modulators in the object retrieval task in female cynomolgus monkeys (Macaca fascicularis). *PLoS One* **9**:e102449.

Sutherland EW and Rall TW (1958) Fractionation and characterization of a cyclic adenine ribonucleotide formed by tissue particles. *J Biol Chem* **232**:1077-1091.

Suzuki O, Mizukami K, Etori M, Sogawa Y, Takagi N, Tsuchida H, Morimoto K, Goto T, Yoshino T, Mikkaichi T, Hirahara K, Nakamura S and Maeda H (2013) Evaluation of the therapeutic index of a novel phosphodiesterase 4B-selective inhibitor over phosphodiesterase 4D in mice. *J Pharmacol Sci* **123**:219-226.

Swinnen JV, Joseph DR and Conti M (1989a) Molecular cloning of rat homologues of the Drosophila melanogaster dunce cAMP phosphodiesterase: evidence for a family of genes. *Proc Natl Acad Sci U S A* **86**:5325-5329.

Swinnen JV, Joseph DR and Conti M (1989b) The mRNA encoding a high-affinity cAMP phosphodiesterase is regulated by hormones and cAMP. *Proc Natl Acad Sci U S A* **86**:8197-8201.

Takahashi M, Terwilliger R, Lane C, Mezes PS, Conti M and Duman RS (1999) Chronic antidepressant administration increases the expression of cAMP-specific phosphodiesterase 4A and 4B isoforms. *J Neurosci* **19**:610-618.

Tang L, Huang C, Zhong J, He J, Guo J, Liu M, Xu JP, Wang HT and Zhou ZZ (2019) Discovery of arylbenzylamines as PDE4 inhibitors with potential neuroprotective effect. *Eur J Med Chem* **168**:221-231.

Tasken KA, Collas P, Kemmner WA, Witczak O, Conti M and Tasken K (2001) Phosphodiesterase 4D and protein kinase a type II constitute a signaling unit in the centrosomal area. *J Biol Chem* **276**:21999-22002.

Terrenoire C, Houslay MD, Baillie GS and Kass RS (2009) The cardiac IKs potassium channel macromolecular complex includes the phosphodiesterase PDE4D3. *J Biol Chem* **284**:9140-9146.

Terrin A, Monterisi S, Stangherlin A, Zoccarato A, Koschinski A, Surdo NC, Mongillo M, Sawa A, Jordanides NE, Mountford JC and Zaccolo M (2012) PKA and PDE4D3 anchoring to AKAP9 provides distinct regulation of cAMP signals at the centrosome. *J Cell Biol* **198**:607-621.

Terry R, Cheung YF, Praestegaard M, Baillie GS, Huston E, Gall I, Adams DR and Houslay MD (2003) Occupancy of the catalytic site of the PDE4A4 cyclic AMP phosphodiesterase by rolipram triggers the dynamic redistribution of this specific isoform in living cells through a cyclic AMP independent process. *Cell Signal* **15**:955-971.

Tetra (2016) https://tetratherapeutics.com/wp-content/uploads/2016/11/FINAL-Tetra-Phase-1-121616-FINAL.pdf].

Tilley DG and Maurice DH (2005) Vascular smooth muscle cell phenotype-dependent phosphodiesterase 4D short form expression: role of differential histone acetylation on cAMP-regulated function. *Mol Pharmacol* **68**:596-605.

Torphy TJ, Stadel JM, Burman M, Cieslinski LB, McLaughlin MM, White JR and Livi GP (1992) Coexpression of human cAMP-specific phosphodiesterase activity and high affinity rolipram binding in yeast. *J Biol Chem* **267**:1798-1804.

Tralau-Stewart CJ, Williamson RA, Nials AT, Gascoigne M, Dawson J, Hart GJ, Angell AD, Solanke YE, Lucas FS, Wiseman J, Ward P, Ranshaw LE and Knowles RG (2011) GSK256066, an exceptionally high-affinity and selective inhibitor of phosphodiesterase 4 suitable for administration by inhalation: in vitro, kinetic, and in vivo characterization. *J Pharmacol Exp Ther* **337**:145-154.

Tsai Y-F, Chu T-C, Chang W-Y, Wu Y-C, Chang F-R, Yang S-C, Wu T-Y, Hsu Y-M, Chen C-Y, Chang S-H and Hwang T-L (2017a) 6-Hydroxy-5,7-dimethoxy-flavone suppresses the neutrophil respiratory burst via selective PDE4 inhibition to ameliorate acute lung injury. *Free Radical Biology and Medicine* **106**:379-392.

Tsai YF, Chu TC, Chang WY, Wu YC, Chang FR, Yang SC, Wu TY, Hsu YM, Chen CY, Chang SH and Hwang TL (2017b) 6-Hydroxy-5,7-dimethoxy-flavone suppresses the neutrophil respiratory burst via selective PDE4 inhibition to ameliorate acute lung injury. *Free Radic Biol Med* **106**:379-392.

Uys GM, Ramburan A, Loos B, Kinnear CJ, Korkie LJ, Mouton J, Riedemann J and Moolman-Smook JC (2011) Myomegalin is a novel A-kinase anchoring protein involved in the phosphorylation of cardiac myosin binding protein C. *BMC Cell Biol* **12**:18.

Vanmierlo T, Creemers P, Akkerman S, van Duinen M, Sambeth A, De Vry J, Uz T, Blokland A and Prickaerts J (2016) The PDE4 inhibitor roflumilast improves memory in rodents at non-emetic doses. *Behav Brain Res* **303**:26-33.

VANMIERLO T, PRICKAERTS, J., WIERINGA, P. (2019) SELECTIVE PDE4D INHIBITORS AGAINST DEMYELINATING DISEASES, (UNIVERSITEIT HASSELT UM, ACADEMISCH ZIEKENHUIS MAASTRICHT ed).

Verde I, Pahlke G, Salanova M, Zhang G, Wang S, Coletti D, Onuffer J, Jin SL and Conti M (2001) Myomegalin is a novel protein of the golgi/centrosome that interacts with a cyclic nucleotide phosphodiesterase. *J Biol Chem* **276**:11189-11198.

Vicini E and Conti M (1997) Characterization of an intronic promoter of a cyclic adenosine 3',5'-monophosphate (cAMP)-specific phosphodiesterase gene that confers hormone and cAMP inducibility. *Molecular endocrinology (Baltimore, Md)* **11**:839-850.

Wachtel H (1983a) Neurotropic effects of the optical isomers of the selective adenosine cyclic 3',5'-monophosphate phosphodiesterase inhibitor rolipram in rats in-vivo. *J Pharm Pharmacol* **35**:440-444.

Wachtel H (1983b) Potential antidepressant activity of rolipram and other selective cyclic adenosine 3',5'-monophosphate phosphodiesterase inhibitors. *Neuropharmacology* **22**:267-272.

Wachtel H (1983c) Species differences in behavioural effects of rolipram and other adenosine cyclic 3H, 5H-monophosphate phosphodiesterase inhibitors. *J Neural Transm* **56**:139-152.

Wallace DA, Johnston LA, Huston E, MacMaster D, Houslay TM, Cheung YF, Campbell L, Millen JE, Smith RA, Gall I, Knowles RG, Sullivan M and Houslay MD (2005) Identification and characterization of PDE4A11, a novel, widely expressed long isoform encoded by the human PDE4A cAMP phosphodiesterase gene. *Mol Pharmacol* **67**:1920-1934.

Wang D, Deng C, Bugaj-Gaweda B, Kwan M, Gunwaldsen C, Leonard C, Xin X, Hu Y, Unterbeck A and De Vivo M (2003) Cloning and characterization of novel PDE4D isoforms PDE4D6 and PDE4D7. *Cell Signal* **15**:883-891.

Wang H, Peng MS, Chen Y, Geng J, Robinson H, Houslay MD, Cai J and Ke H (2007a) Structures of the four subfamilies of phosphodiesterase-4 provide insight into the selectivity of their inhibitors. *Biochem J* **408**:193-201.

Wang L, Burmeister BT, Johnson KR, Baillie GS, Karginov AV, Skidgel RA, O'Bryan JP and Carnegie GK (2015) UCR1C is a novel activator of phosphodiesterase 4 (PDE4) long isoforms and attenuates cardiomyocyte hypertrophy. *Cell Signal* **27**:908-922.

Wang M, Ramos BP, Paspalas CD, Shu Y, Simen A, Duque A, Vijayraghavan S, Brennan A, Dudley A, Nou E, Mazer JA, McCormick DA and Arnsten AF (2007b) Alpha2A-adrenoceptors strengthen working memory networks by inhibiting cAMP-HCN channel signaling in prefrontal cortex. *Cell* **129**:397-410.

Weninger S, Van Craenenbroeck K, Cameron RT, Vandeput F, Movsesian MA, Baillie GS and Lefebvre RA (2014) Phosphodiesterase 4 interacts with the 5-HT4(b) receptor to regulate cAMP signaling. *Cell Signal* **26**:2573-2582.

Wild AR and Dell'Acqua ML (2018) Potential for therapeutic targeting of AKAP signaling complexes in nervous system disorders. *Pharmacol Ther* **185**:99-121.

Willoughby D, Wong W, Schaack J, Scott JD and Cooper DM (2006) An anchored PKA and PDE4 complex regulates subplasmalemmal cAMP dynamics. *EMBO J* **25**:2051-2061.

Wilson M, Sullivan M, Brown N and Houslay MD (1994) Purification, characterization and analysis of rolipram inhibition of a human type-IVA cyclic AMP-specific phosphodiesterase expressed in yeast. *Biochem J* **304 (Pt 2)**:407-415.

Wu Y, Hong Z, Xu W, Chen J, Wang Q, Chen J, Ni W, Mei Z, Xie Z, Ma Y, Wang J, Lu J, Chen C, Fan S and Shen S (2021) Circular RNA circPDE4D Protects against Osteoarthritis by Binding to miR-103a-3p and Regulating FGF18. *Mol Ther* **29**:308-323.

Wunder F, Quednau R, Geerts A, Barg M and Tersteegen A (2013) Characterization of the cellular activity of PDE 4 inhibitors using two novel PDE 4 reporter cell lines. *Mol Pharm* **10**:3697-3705.

Xie D, Geng L, Xiong K, Zhao T, Wang S, Xue J, Wang C, Wang G, Feng Z, Zhou H, Li Y, Li L, Liu Y, Xue Z, Yang J, Ma H, Liang D and Chen YH (2020) Cold-Inducible RNA-Binding Protein Prevents an Excessive Heart Rate Response to Stress by Targeting Phosphodiesterase. *Circ Res* **126**:1706-1720.

Xie M, Blackman B, Scheitrum C, Mika D, Blanchard E, Lei T, Conti M and Richter W (2014) The upstream conserved regions (UCRs) mediate homo- and hetero-oligomerization of type 4 cyclic nucleotide phosphodiesterases (PDE4s). *Biochem J* **459**:539-550.

Yarwood SJ, Steele MR, Scotland G, Houslay MD and Bolger GB (1999) The RACK1 signaling scaffold protein selectively interacts with the cAMP-specific phosphodiesterase PDE4D5 isoform. *J Biol Chem* **274**:14909-14917.

Yu S, Pearson AD, Lim RK, Rodgers DT, Li S, Parker HB, Weglarz M, Hampton EN, Bollong MJ, Shen J, Zambaldo C, Wang D, Woods AK, Wright TM, Schultz PG, Kazane SA, Young TS and Tremblay MS (2016) Targeted Delivery of an Anti-inflammatory PDE4 Inhibitor to Immune Cells via an Antibody-drug Conjugate. *Mol Ther* **24**:2078-2089.

Yun S, Budatha M, Dahlman JE, Coon BG, Cameron RT, Langer R, Anderson DG, Baillie G and Schwartz MA (2016) Interaction between integrin alpha5 and PDE4D regulates endothelial inflammatory signalling. *Nat Cell Biol* **18**:1043-1053.

Yun S, Hu R, Schwaemmle ME, Scherer AN, Zhuang Z, Koleske AJ, Pallas DC and Schwartz MA (2019a) Integrin alpha5beta1 regulates PP2A complex assembly through PDE4D in atherosclerosis. *J Clin Invest* **130**:4863-4874.

Yun S, Hu R, Schwaemmle ME, Scherer AN, Zhuang Z, Koleske AJ, Pallas DC and Schwartz MA (2019b) Integrin alpha5beta1 regulates PP2A complex assembly through PDE4D in atherosclerosis. *J Clin Invest* **129**:4863-4874.

Zaccolo M, Zerio A and Lobo MJ (2021) Subcellular Organization of the cAMP Signaling Pathway. *Pharmacol Rev* **73**:278-309.

Zeke A, Bastys T, Alexa A, Garai A, Meszaros B, Kirsch K, Dosztanyi Z, Kalinina OV and Remenyi A (2015) Systematic discovery of linear binding motifs targeting an ancient protein interaction surface on MAP kinases. *Mol Syst Biol* **11**:837.

Zhang C, Xu Y, Chowdhary A, Fox D, 3rd, Gurney ME, Zhang HT, Auerbach BD, Salvi RJ, Yang M, Li G and O'Donnell JM (2018) Memory enhancing effects of BPN14770, an allosteric inhibitor of phosphodiesterase-4D, in wild-type and humanized mice. *Neuropsychopharmacology* **43**:2299-2309.

Zhang C, Xu Y, Zhang HT, Gurney ME and O'Donnell JM (2017) Comparison of the Pharmacological Profiles of Selective PDE4B and PDE4D Inhibitors in the Central Nervous System. *Sci Rep* **7**:40115.

Zhang HT, Zhao Y, Huang Y, Deng C, Hopper AT, De Vivo M, Rose GM and O'Donnell JM (2006) Antidepressant-like effects of PDE4 inhibitors mediated by the high-affinity rolipram binding state (HARBS) of the phosphodiesterase-4 enzyme (PDE4) in rats. *Psychopharmacology (Berl)* **186**:209-217.

Zhang MZ, Zhou ZZ, Yuan X, Cheng YF, Bi BT, Gong MF, Chen YP and Xu JP (2013) Chlorbipram: a novel PDE4 inhibitor with improved safety as a potential antidepressant and cognitive enhancer. *Eur J Pharmacol* **721**:56-63.

Zhong W and Darmani NA (2017) Intracellular vomit signals and cascades downstream of emetic receptors: Evidence from the least shrew (Cryptotis parva) model of vomiting. *Rem Open Access* **2**.

Zhou ZZ, Cheng YF, Zou ZQ, Ge BC, Yu H, Huang C, Wang HT, Yang XM and Xu JP (2017) Discovery of N-Alkyl Catecholamides as Selective Phosphodiesterase-4 Inhibitors with Anti-neuroinflammation Potential Exhibiting Antidepressant-like Effects at Non-emetic Doses. *ACS Chem Neurosci* **8**:135-146.

Zhu H, Suk HY, Yu RY, Brancho D, Olabisi O, Yang TT, Yang X, Zhang J, Moussaif M, Durand JL, Jelicks LA, Kim JY, Scherer PE, Frank PG, Lisanti MP, Calvert JW, Duranski MR, Lefer DJ, Huston E, Baillie GS, Houslay MD, Molkentin JD, Jin J and Chow CW (2010) Evolutionarily conserved role of calcineurin

in phosphodegron-dependent degradation of phosphodiesterase 4D. *Mol Cell Biol* **30**:4379-4390.

Supplementary Table 1

Human isoform	Reference	Rodent isoform	Reference	Comments
PDE4A8	(Mackenzie et al., 2008)	**Pde4a8**	(Bolger et al., 1996)	homology at the nucleotide level, but encoding proteins with different N-termini
PDE4A4	(Mackenzie et al., 2008)	**Pde4a5**	(Naro et al., 1996)	human isoform is named PDE4A4 whilst rodent equivalent is named PDE4A5
PDE4A11	(Wallace et al., 2005)	**Pde4a11**	(Wallace et al., 2005)	
PDE4A10	(Rena et al., 2001)	**Pde4a10**	(Rena et al., 2001)	
PDE4A1	(Sullivan et al., 1998)	**Pde4a1**	(Olsen and Bolger, 2000)	
PDE4A7	(Johnston et al., 2004)	**x**	x	dead-short isoform, not (yet) identified in rodents
x	x	**Pde4a7**	(Naro et al., 1996)	long form found in rat testis, not (yet) characterized in human
PDE4B1	(Bolger et al., 1993)	**Pde4b1**	(Huston et al., 1997)	
PDE4B3	(Huston et al., 1997)	**Pde4b3**	(Huston et al., 1997)	
x	x	**Pde4b4**	(Shepherd et al., 2003)	not (yet) identified in humans, but a protein of similar weight as rodent PDE4D4 has been detected in immunoblots of human brain tissue (Fatemi et al., 2008)
PDE4B2	(McLaughlin et al., 1993)	**Pde4b2**	(Swinnen et al., 1991)	
PDE4B5	(Cheung et al., 2007)	**Pde4b5**	(Cheung et al., 2007)	
PDE4C1	(Engels et al., 1995)	x	x	only partial clones have been obtained of rat PDE4C (Owens et al., 1997)
PDE4C2	(Owens et al., 1997)	x	x	only partial clones have been obtained of rat PDE4C (Owens et al., 1997)
PDE4C3	(Obernolte et al., 1997)	x	x	only partial clones have been obtained of rat PDE4C (Owens et al., 1997)
PDE4D7	(Wang et al., 2003)	**Pde4d7**	(Richter et al., 2005)	
PDE4D4	(Bolger et al., 1997)	**Pde4d4**	(Richter et al., 2005)	
PDE4D5	(Bolger et al., 1997)	**Pde4d5**	(Richter et al., 2005)	
PDE4D3	(Bolger et al., 1997)	**Pde4d3**	(Richter et al., 2005)	
PDE4D8	(Wang et al., 2003)	**Pde4d8**	(Richter et al., 2005)	
PDE4D9	(Gretarsdottir et al., 2003)	**Pde4d9**	(Richter et al., 2005)	
x	x	**Pde4d11**	(Lynex et al., 2008)	identical human genomic sequence identified *in silico* but not validated *in vitro* on the mRNA or protein level
PDE4D1	(Bolger et al., 1997)	**Pde4d1**	(Richter et al., 2005)	
PDE4D2	(Bolger et al., 1997)	**Pde4d2v2**	(Chandrasekaran et al., 2008)	
x	x	**Pde4d2v1**	(Chandrasekaran et al., 2008)	different 5'UTR sequence to PDE4D2v2, but same coding sequence as PDE4D2; not (yet) identified in humans
x	x	**Pde4d2v3**	(Chandrasekaran et al., 2008)	different 5'UTR sequence to PDE4D2v2, but same coding sequence as PDE4D2; not (yet) identified in humans
x	x	**Pde4d10**	(Chandrasekaran et al., 2008)	probably non-existing in humans
PDE4D6	(Wang et al., 2003)	**Pde4d6**	(Richter et al., 2005)	

SUPPLEMENTARY REFERENCES

Bolger G, Michaeli T, Martins T, St John T, Steiner B, Rodgers L, Riggs M, Wigler M and Ferguson K (1993) A family of human phosphodiesterases homologous to the dunce learning and memory gene product of Drosophila melanogaster are potential targets for antidepressant drugs. *Mol Cell Biol* **13**:6558-6571.

Bolger GB, Erdogan S, Jones RE, Loughney K, Scotland G, Hoffmann R, Wilkinson I, Farrell C and Houslay MD (1997) Characterization of five different proteins produced by alternatively spliced mRNAs from the human cAMP-specific phosphodiesterase PDE4D gene. *Biochem J* **328 (Pt 2)**:539-548.

Bolger GB, McPhee I and Houslay MD (1996) Alternative splicing of cAMP-specific phosphodiesterase mRNA transcripts. Characterization of a novel tissue-specific isoform, RNPDE4A8. *J Biol Chem* **271**:1065-1071.

Chandrasekaran A, Toh KY, Low SH, Tay SK, Brenner S and Goh DL (2008) Identification and characterization of novel mouse PDE4D isoforms: molecular cloning, subcellular distribution and detection of isoform-specific intracellular localization signals. *Cell Signal* **20**:139-153.

Cheung YF, Kan Z, Garrett-Engele P, Gall I, Murdoch H, Baillie GS, Camargo LM, Johnson JM, Houslay MD and Castle JC (2007) PDE4B5, a novel, super-short, brain-specific cAMP phosphodiesterase-4 variant whose isoform-specifying N-terminal region is identical to that of cAMP phosphodiesterase-4D6 (PDE4D6). *J Pharmacol Exp Ther* **322**:600-609.

Engels P, Sullivan M, Muller T and Lubbert H (1995) Molecular cloning and functional expression in yeast of a human cAMP-specific phosphodiesterase subtype (PDE IV-C). *FEBS Lett* **358**:305-310.

Fatemi SH, King DP, Reutiman TJ, Folsom TD, Laurence JA, Lee S, Fan YT, Paciga SA, Conti M and Menniti FS (2008) PDE4B polymorphisms and decreased PDE4B expression are associated with schizophrenia. *Schizophr Res* **101**:36-49.

Gretarsdottir S, Thorleifsson G, Reynisdottir ST, Manolescu A, Jonsdottir S, Jonsdottir T, Gudmundsdottir T, Bjarnadottir SM, Einarsson OB, Gudjonsdottir HM, Hawkins M, Gudmundsson G, Gudmundsdottir H, Andrason H, Gudmundsdottir AS, Sigurdardottir M, Chou TT, Nahmias J, Goss S, Sveinbjornsdottir S, Valdimarsson EM, Jakobsson F, Agnarsson U, Gudnason V, Thorgeirsson G, Fingerle J, Gurney M, Gudbjartsson D, Frigge ML, Kong A, Stefansson K and Gulcher JR (2003) The gene encoding phosphodiesterase 4D confers risk of ischemic stroke. *Nat Genet* **35**:131-138.

Huston E, Lumb S, Russell A, Catterall C, Ross AH, Steele MR, Bolger GB, Perry MJ, Owens RJ and Houslay MD (1997) Molecular cloning and transient expression in COS7 cells of a novel human PDE4B cAMP-specific phosphodiesterase, HSPDE4B3. *Biochem J* **328 (Pt 2)**:549-558.

Johnston LA, Erdogan S, Cheung YF, Sullivan M, Barber R, Lynch MJ, Baillie GS, Van Heeke G, Adams DR, Huston E and Houslay MD (2004) Expression, intracellular distribution and basis for lack of catalytic activity of the PDE4A7 isoform encoded by the human PDE4A cAMP-specific phosphodiesterase gene. *Biochem J* **380**:371-384.

Lynex CN, Li Z, Chen ML, Toh KY, Low RW, Goh DL and Tay SK (2008) Identification and molecular characterization of a novel PDE4D11 cAMP-specific phosphodiesterase isoform. *Cell Signal* **20**:2247-2255.

Mackenzie KF, Topping EC, Bugaj-Gaweda B, Deng C, Cheung YF, Olsen AE, Stockard CR, High Mitchell L, Baillie GS, Grizzle WE, De Vivo M, Houslay MD, Wang D and Bolger GB (2008) Human PDE4A8, a novel brain-expressed PDE4 cAMP-specific phosphodiesterase that has undergone rapid evolutionary change. *Biochem J* **411**:361-369.

McLaughlin MM, Cieslinski LB, Burman M, Torphy TJ and Livi GP (1993) A low-Km, rolipram-sensitive, cAMP-specific phosphodiesterase from human brain. Cloning and expression of cDNA, biochemical characterization of recombinant protein, and tissue distribution of mRNA. *J Biol Chem* **268**:6470-6476.

Chapter 3

Increased isoform-specific phosphodiesterase 4D (PDE4D) expression is associated with pathology and cognitive impairment in Alzheimer's disease

Published as:

Paes et al. (2020) *Neurobiol Aging.* Jan;97:56-64.
doi: 10.1016/j.neurobiolaging.2020.10.004

ABSTRACT

Pharmacological phosphodiesterase 4D (PDE4D) inhibition shows therapeutic potential to restore memory function in Alzheimer's disease (AD), but will likely evoke adverse side effects. *PDE4D* encodes multiple isoforms and therefore targeting of specific PDE4D isoforms may improve treatment efficacy and safety. Here, we investigated whether PDE4D isoform expression and *PDE4D* DNA methylation is differentially affected in AD and whether expression changes are associated with severity of pathology and cognitive impairment. In post-mortem temporal lobe brain material from AD patients (n=42) and age-matched controls (n=40), we measured PDE4D isoform expression and *PDE4D* DNA (hydroxy)methylation using qPCR and Illumina 450k Beadarrays, respectively. Linear regression revealed increased expression of PDE4D1, -D3, -D5 and -D8 in AD cases with concurrent (hydroxy)methylation changes in associated promoter regions. Moreover, increased PDE4D1 and -D3 expression was associated with higher levels of tau and plaque pathology, higher Braak stages and more severe cognitive impairment. Future studies should indicate functional roles of specific PDE4D isoforms and the efficacy and safety of their selective inhibition to restore memory function in AD.

INTRODUCTION

Impaired memory function in Alzheimer's disease (AD) patients has a debilitating effect on daily activities and, consequently, negatively affects the quality of life of patients, their caretakers, and family (Schneider et al., 1999). The second messenger cyclic adenosine monophosphate (cAMP) is crucial in the molecular signaling cascades underlying memory function (Kandel, 2012). Intracellular cAMP levels are mainly controlled through degradation by the phosphodiesterase 4 (PDE4) enzyme family (Houslay, 2010). Accordingly, previous studies have shown that PDE4 inhibition can improve memory consolidation processes in rodents (Vanmierlo et al., 2016). In humans, the PDE4 inhibitor roflumilast was found to enhance verbal learning in young adults and old healthy volunteers (Blokland et al., 2019; Van Duinen et al., 2018). Thus, PDE4 inhibition seems to hold clinical potential as a treatment to enhance memory functioning. The therapeutic potential in AD is supported by the finding that PDE4 inhibition can restore memory impairments induced by intra-hippocampal injections with amyloid β in rats (Cheng et al., 2010). Moreover, in a mouse model of tauopathy, the number of tau aggregates was reduced after administration of the non-selective PDE4 inhibitor rolipram (Myeku et al., 2016). Despite these promising results, progression of new PDE4 inhibitors into the clinic is hampered by the occurrence of dose-limiting side effects; mainly nausea and emesis. More selective inhibition of PDE4 subtypes or isoforms may circumvent these adverse effects. In the present study, we investigated whether expression regulation of PDE4D isoforms is altered in AD brain material to identify potential targets for more selective PDE4 inhibition. The PDE4 family consists of four genes (PDE4A-D) of which *PDE4D* seems to be mostly involved in the modulation of cognitive functions (Zhang et al., 2017). Hence, inhibitors selective for PDE4D have been developed to investigate their cognition-enhancing potential. These new selective PDE4D inhibitors have been found to enhance memory performance in rodents, including models of AD (Ricciarelli et al., 2017; Zhang et al., 2018). The procognitive effects of

PDE4D-specific inhibition are supported by *PDE4D* knock-down studies (Baumgartel et al., 2018). The memory-enhancing potential of PDE4D inhibition has also been tested in Phase I clinical trials (ClinicalTrials.gov Identifier: NCT02648672 and NCT02840279) and currently, preparations are under way to initiate a Phase II trial in patients with early-stage AD (ClinicalTrials.gov Identifier: NCT03817684). Notably, PDE4D inhibition is also hypothesized to induce emetic side effects given its expression in brain areas involved in emesis, i.e. the area postrema, and based on gene deletion studies (Mori et al., 2010; Robichaud et al., 2002). The human *PDE4D* gene gives rise to multiple protein isoforms, i.e. PDE4D1-9, through alternative promoters and alternative splicing. These isoforms regulate a multitude of different processes and are localized to specific compartments within the cell owing to specific amino acids in the N-terminal domain (Houslay, 2010; Houslay et al., 2007). Hence, by inhibiting specific PDE4D isoforms, it can be argued that memory-enhancing effects could be retained without evoking side effects (Schepers et al., 2019). Despite the potential of PDE4D isoform-specific inhibition as a safe and efficacious treatment strategy in AD, the role of PDE4D isoforms in the context of specific brain functions or AD has only sporadically been described (McLachlan et al., 2007; Perez-Torres et al., 2000; Ugarte et al., 2015).

PDE4D isoforms showing high or increased expression in AD could be interesting targets, as these isoforms may contribute largely to cAMP hydrolysis and consequently impede memory functioning. PDE4D isoform expression is likely controlled by epigenetic mechanisms to regulate e.g. isoform-specific promoter accessibility. Previous research indicated that epigenetic modifications at the histone level influence promoter accessibility in the *PDE4D* gene and consequently affect isoform-specific expression in vascular smooth muscle cells (VSMCs) (Tilley and Maurice, 2005). At the nucleotide level, epigenetic processes can reversibly influence transcription through conversion of unmethylated cytosines (UC) into methylated (5mC) or hydroxymethylated (5hmC) cytosines. Specific changes in DNA methylation

and hydroxymethylation have previously been associated with AD (Smith et al., 2019). Recently, *PDE4D* was found those genes displaying differentially methylated in AD in an epigenome-wide association study (Lardenoije et al., 2019).

To investigate whether PDE4D isoform expression is altered in AD and whether this is associated with epigenetic changes at specific positions in the *PDE4D* gene, we established PDE4D expression and epigenetic profiles of human post-mortem brain material of AD patients and age-matched controls. Since AD is a progressive disease, we also explored whether changes in expression were associated with region-specific plaque and tau load, Braak stage and the degree of cognitive impairment.

METHODS

Brain material and study cohort

Informed consent was obtained from all individual participants included in the study. Human post-mortem brain material from the middle temporal gyrus (MTG) of AD patients and neurologically healthy controls was obtained from the Banner Sun Health Research Institute (BSHRI) in Sun City, AZ, USA. For every sample information on Mini-Mental State Examination (MMSE) score (Folstein et al., 1975), gender, age, post-mortem interval (PMI), *APOE* ε4 possession, amyloid-β plaque load, tau tangle load, Braak stage and diagnosis was documented and tissue was prepared by standardized procedures (Beach et al., 2015). Braak staging was evaluated as previously described (Braak and Braak, 1991). AD diagnostic criteria followed guidelines for the National Institute on Aging (NIA)-Reagan Institute criteria (The National Institute on Aging, and Reagan Institute Working Group on Diagnostic Criteria for the Neuropathological Assessment of Alzheimer's Disease, 1997) combined with clinical diagnosis reports. Samples collected after a PMI of more than 5 hours and samples from patients with comorbidities were excluded. A total of 82

samples were included from AD patients (n=42) and age- and gender-matched neurologically healthy controls (n=40) with an average PMI of 2.8 hours. For subsequent analysis investigating associations between expression and MMSE score, cases for which cognitive performance in the MMSE was assessed longer than 36 months before death were excluded, leaving a subset of 41 cases. A detailed description of the cohort demographics can be found in Table 1.

Table 1. Demographic characteristics of the cohort

Characteristic	Non-demented controls	AD patients
Gender (male/female)	20/20	19/23
***APOE* ε4** (present/absent)	9/31	27/15
Braak stage (I-II/III-IV/V-VI)	16/24/0	0/14/28
Age mean (SD)	84.3 (5.81)	85.1 (6.49)
PMI mean (SD)	2.77 (0.75)	2.75 (0.73)

RNA isolation, cDNA synthesis and qPCR

Total RNA was isolated from frozen MTG tissue using the TRIzol® Plus RNA Purification Kit (Life Technologies, Carlsbad, CA) following the manufacturer's protocol. Isolated RNA pellets were dissolved in RNAse-free water and assessed for quantity and quality (average RIN: 9.1) using a Nanodrop ND-1000 spectrophotometer (Thermo Scientific, DE, USA) and Bioanalyzer (Agilent). Then, cDNA was synthesized using the Revert Aid First Strand Synthesis Kit (Thermo Scientific, Landsmeer, Netherlands) according to the manufacturer's protocol.

TaqMan based qPCR primers were used for the following PDE4D isoforms: PDE4D2, PDE4D4, PDE4D5, PDE4D6, PDE4D8 and PDE4D9 (Applied Biosystems, Foster City, California, USA). PDE4D2 could not be detected. Primers were designed for PDE4D1, PDE4D3 and PDE4D7 as no TaqMan-based qPCR primers were available for these isoforms (SIGMA Life Science). Housekeeping gene expression of *EIF4A2* and *TOP1* showed the most stable expression based on geNorm criteria and was

used for normalization (Vandesompele et al., 2002). TaqMan probe and primer sequences are listed in Table 2. TaqMan based qPCR was performed using TaqMan Assay 20x and TaqMan Universal Master Mix II, with UNG 2x (Applied Biosystems, Foster City, California, USA) following the manufacturer's protocol. For qPCR using primers, SensiMix 2X (Bioline), was used according to the manufacturer's protocol. All reactions were performed using 6 ng cDNA on a LightCycler 480 (Roche).

Table 2. TaqMan probe and primer sequences.

Isoform	**Forward primer (5'-3')**	**Reverse primer (5'-3')**
PDE4D1	AGAACTGAGTCCCCCTTTCC	TGAGCTCCCGATTAAGCATC
PDE4D3	CCACGATAGCTGCTCAAACA	GTGCCATTGTCCACATCAAA
PDE4D7	GAACATTCAACGACCAACCA	TTCCGGGACATAGACTTTGG
EIF4A2	GGTCAGGGTCAAGTCGTGTT	CCCCTCTGCCAATTCTGTGA
TOP1	CCCTGTACTTCATCGACAAGC	CCACAGTGTCCGCTGTTTC
Isoform	**TaqMan probe sequence (5'-3')**	**TaqMan Assay ID**
PDE4D2	TCCGAGCATGGCGGGAGGAGGCCTA	Rn01494075_g1
PDE4D4	TTCCAGGGACTCAGGCGTTTTGATG	Hs01588302_m1
PDE4D5	CACATACATGTTTTGATGTGGACAA	Hs01588303_m1
PDE4D6	ATAAAGTTTAAAAGGATGCTTAATC	Hs01572151_m1
PDE4D8	GTTTCTCAAAGTCCTACAGTTTTGA	Hs00938323_m1
PDE4D9	GCAGTTTGTTTTGATGTGGACAATG	Hs01572149_m1

Tissue preparation for (hydroxy)methylomic profiling

DNA was isolated from the MTG at the BSHRI. From 81 of the 82 subjects, a total of 76 mg of frozen tissue was obtained(Beach et al., 2015). Tissue was digested at 55°C in lysis buffer (100 mM Tris HCl pH 8.5, 200 mM NaCl, 5 mM EDTA, 100 µg/ml Proteinase K [Sigma-Aldrich, St. Louis, Missouri, USA], and 0.2% SDS) and homogenized in a pellet mixer (Kontes). After addition of RNase (Qiagen, Valencia,

California, USA), DNA was isolated by means of phenol/chloroform (Sigma) extraction followed by ethanol precipitation and resuspension in TE buffer (pH 8.0). Ultimately, DNA samples were quantified and checked for purity by means of spectrophotometry.

Oxidative bisulfite conversion and DNA (hydroxy)methylation assay

The (oxidative) bisulfite conversion procedures and HumanMethylation450 BeadChip array were carried out at ServiceXS (ServiceXS B.V., Leiden, the Netherlands), in accordance to the manufacturer's protocols and as described previously (Lardenoije et al., 2019). Briefly, A TrueMethylTM 24 kit version 2.0 by CEGXTM (Cambridge Epigenetix Limited, Cambridge, UK) was used to convert the isolated genomic DNA (gDNA) by bisulfite (BS) or oxidative bisulfite (oxBS) treatments to detect and localize 5mC and 5hmC marks at single-base resolution. Before conversion, gDNA quality was assessed using a PicoGreen assay (Invitrogen, Carlsbad, California, USA) and high molecular weight gDNA (HMW-gDNA) was quantified by gel-electrophoresis. Upon purification and denaturation, HMW-gDNA (0.5 µg per treatment) was used for DNA oxidation or mock DNA oxidation treatments followed by bisulfite conversion. DNA yield was assessed by Qubit ssDNA assay (Invitrogen) and qualitative assessment of 5hmC oxidation and bisulfite conversion was performed using a restriction quality control. Then, 8 µl of each DNA sample was used for amplification and hybridization on the HumanMethylation450 BeadChip (Illumina, Inc., San Diego, CA, U.S.A.) according to the Illumina 'Infinium II Methylation Assay Manual' protocol. Eventually, the Illumina iScan was used to scan the samples.

Processing of DNA (hydroxy)methylation assay data

For (hydroxy)methylomic profiling, data was processed and analyzed using R statistical programming language (version 3.5.3)(R Development Core Team, 2019) and RStudio (version 1.2.1335)(RStudio Team, 2019). The minfi package (version

1.28.4) was used to load raw IDAT files from the Illumina iScan(Aryee et al., 2014). Probes that cross-hybridize, locate to X and Y chromosomes and probes binding within 10 bp of a common SNP location were removed (Chen et al., 2013). Remaining probes were filtered using the 'pfilter' function of the wateRmelon package (version 1.26.0) (6,414 probes were removed)(Pidsley et al., 2013). Data from 397,160 remaining probes were split into two sets of beta values according to the oxBS and BS arrays, representing 5mC and 5mC+5hmC, respectively. These data were *dasen* normalized using the wateRmelon package (Pidsley et al., 2013). The maximum likelihood methylation levels (MLML) method was used, by means of the 'MLML' function within the MLML2R package (version 0.3.2), to calculate the proportions of 5mC, 5hmC and UC by combining the signal from the BS and oxBS arrays as input(Kiihl et al., 2019; Qu et al., 2013). Subsequently, probes showing either a 5hmC value of zero in at least half of the cases or BS beta value lower than 0.1 were filtered out (112,697 5hmC values were excluded). Data distributions of raw and normalized beta values per sample were visualized in boxplots and density plots to identify outliers (3 samples were excluded due to clear deviation from the other samples; data not shown). Data were processed again upon removal of these outliers.

After data processing, 78 samples remained, with 397,160 remaining probes for 5mC and UC, and 284,463 5hmC probes. Data were split into two sets of beta values according to the oxBS and BS arrays, representing 5mC and 5mC+5hmC, respectively.

Statistical Analysis

Raw expression data from the LightCycler 480 were analyzed using LinRegPCR to determine logarithmic fluorescence values at cycle zero (Ruijter et al., 2009). qPCR reactions that did not show fluorescent signal amplification were excluded from further analysis. Logarithmic fluorescence values were normalized

against the average expression of reference genes *TOP1* and *EIF4A2*. Normalized data followed a Gaussian distribution and were used for statistical analysis.

For expression data, linear regression analyses were performed using IBM SPSS Statistics for Windows, Version 25.0 (IBM Corp., Armonk, United States) with normalized starting fluorescence values per isoform as dependent variable and diagnosis (control = 0, AD = 1, respectively), plaque load in the temporal lobe (0-3), tangle load in the temporal lobe (0-3), Braak stage level (Braak I-II =0, Braak III-IV = 1, and Braak V-VI = 2) or MMSE score (0-30) as independent variable. Age, gender, PMI, *APOE* ε4 possession and qPCR plate were included as covariates. Unstandardized regression coefficients were exponentially transformed to calculate the fold expression change in AD. P values were Bonferroni-corrected by multiplying P values by the number of dependent variables (i.e. expression of isoforms) tested per model, and values smaller than 0.05 were considered statistically significant.

For (hydroxy)methylomic data, a surrogate variable (SV) analysis was done with the sva package (version 3.30.1)(Leek et al., 2012) on an initial linear regression model with beta values as dependent variable, diagnosis as independent variable, and age, gender, PMI and *APOE* ε4 possession as covariates. To adjust for unobserved confounders, the first five SVs of the SV analysis were included in the regression model. Linear regression was performed using the limma package (version 3.38.3)(Ritchie et al., 2015). Adjustment for bias and inflation of test statistics was done with the bacon package (version 1.10.1)(van Iterson et al., 2017). To explore whether isoform-specific expression changes could be mechanistically explained by specific epigenetic changes, only probes that locate closest to PDE4D isoform promoters showing significant expression changes (i.e. PDE4D1, -D3, -D5 and -D8) were selected (24 probes). Nominal significance for DNA methylation changes between AD cases and controls was set at *P*-value < 0.05. Diagnosis-associated methylation changes were investigated further by follow-up linear regression analyses using the same model, but instead of diagnosis, using plaque load in the

temporal lobe (0-3), tangle load in the temporal lobe (0-3), Braak stage level (Braak I-II =0, Braak III-IV = 1, and Braak V-VI = 2) or MMSE score (0-30) as predictor variable. False discovery rates (FDR) for these predictors' P values were determined by the Benjamini-Hochberg procedure.

RESULTS

Increased PDE4D isoform expression in Alzheimer's disease

Linear regression analyses revealed that AD diagnosis was significantly associated with increased expression levels of PDE4D1, -D3, -D5, and -D8, in the range of 2.56-3.85 fold increased expression ($P < 0.05$; Table 3).

Table 3. PDE4D isoform expression in MTG tissue from AD patients compared to controls.

Isoform expression	**N**	**Diagnosis** standardized coefficient	***P*-value** Bonferroni-corrected	**Fold change in AD**
PDE4D1	82	0.383	0.013	2.99
PDE4D3	82	0.435	0.002	3.85
PDE4D4	67	0.259	0.487	2.14
PDE4D5	67	0.356	0.040	2.56
PDE4D6	77	0.267	0.257	2.90
PDE4D7	82	0.309	0.091	2.82
PDE4D8	62	0.394	0.045	3.85
PDE4D9	77	0.249	0.212	2.24

Linear regression analyses were performed according to the following formula: Expression = Intercept + Diagnosis + Gender + Age + *APOE* ε4 possession + PMI + qPCR plate. Significance levels are Bonferroni-corrected for the number of dependent variables tested. P values and fold changes are rounded to three and two decimals, respectively.

Differential epigenetic signatures in *PDE4D* promoter regions in Alzheimer's disease

As *PDE4D* was found to be differentially methylated in AD in an epigenome-wide association study using the same tissue (Lardenoije et al., 2019), as an exploratory approach, we investigated whether CpG sites within the promoter regions of differentially expressed PDE4D1, -D3, -D5, -D8 were subject to methylation differences. Twenty-four of the EWAS assay probes located to these promoters and allowed the assessment of the methylation status (5mC, 5hmC or UC) of specific CpG sites. Linear regression analyses revealed diagnosis-dependent methylation status differences in each of the promoters. The CpG sites for which methylation status was associated with diagnosis are shown in Table 4. AD-associated effects on methylation status appear to be different per promoter region. For example, in the PDE4D3 promoter, at position cg13112511, AD diagnosis was associated with decreased 5mC (fold change [FC] = .9818, $P < 0.05$) and increased 5hmC (FC = 1.0197, $P < 0.05$) levels. Contrastingly, increased 5mC (FC = 1.0144, $P < 0.01$) and decreased 5hmC (FC = .9812, $P < 0.05$) levels were found in the PDE4D8 promoter at cg23987137 in AD cases. Within the PDE4D5 promoter, effects with opposite directionality were found; increased 5mC and decreased UC levels were detected in AD cases at position cg03653541 (5mC: FC = 1.0023, $P < 0.05$ and UC: FC = .9972, $P < 0.05$), while position cg14784398 indicated decreased 5mC (FC = .9958, $P < 0.05$) and increased UC (FC = 1.0035, $P < 0.05$) levels. These findings suggest that AD is associated with *PDE4D* DNA (hydroxy)methylation changes that are promoter- and site-specific, concomitant with expression changes of the corresponding isoforms.

Table 4. CpG sites in PDE4D promoter regions showing altered methylation status in AD.

Promoter	N	CpG probe	Status	Fold change in AD	Mean	t	df	*P*-value
PDE4D1	78	cg19539826	UC	0.9871	0.5871	-2.363	67	0.018
PDE4D3	78	cg13112511	5mC	0.9818	0.3211	-2.571	67	0.010
	78	cg13112511	5hmC	1.0197	0.0537	2.299	67	0.022
PDE4D5	78	cg03653541	5mC	1.0023	0.0729	2.402	67	0.016
	78	cg14784398	5mC	0.9958	0.1267	-2.330	67	0.020
	78	cg12519013	5mC	0.9965	0.0849	-1.970	67	0.049
	78	cg14784398	UC	1.0035	0.8722	2.098	67	0.036
	78	cg03653541	UC	0.9972	0.9178	-2.010	67	0.044
PDE4D8	78	cg23987137	5mC	1.0144	0.3957	2.833	67	0.006
	78	cg23987137	5hmC	0.9812	0.1765	-2.391	67	0.017
	78	cg17584009	5hmC	1.0162	0.2300	1.961	67	0.050

Linear regressions were performed according to the following formula: Methylation status = Intercept + Diagnosis + Gender + Age + *APOE* ε4 possession + PMI + five surrogate variables.

Abbreviations: df, degrees of freedom; UC, unmethylated cytosine; 5mC, 5-methylcytosine; 5hmC, 5-hydroxymethylcytosine.

PDE4D isoform expression is associated with AD pathology and cognitive impairment

For isoforms showing different expression between AD and controls (i.e. PDE4D1, -D3, -D5 and -D8), linear regression analyses were performed to investigate whether expression was associated with the degree of pathology or cognitive impairment. Higher levels of plaque pathology in the temporal lobe were associated with increased PDE4D1 and -D3 expression ($P < 0.05$), while tangle pathology in the temporal lobe was associated with increased expression of PDE4D1 ($P < 0.05$), PDE4D3 ($P < 0.01$) and PDE4D5 ($P < 0.05$; Table 5 and Figure 1). In addition, Braak staging associated significantly with increased expression of PDE4D1 ($P < 0.05$) and PDE4D3 ($P < 0.001$). Additionally, we examined the association between isoform expression and the level of cognitive impairment as assessed by the MMSE. Lower MMSE scores were significantly associated with increased expression of PDE4D1 ($P < 0.01$), PDE4D3 ($P < 0.01$) and PDE4D5 ($P < 0.05$; Table 5 and Figure 1). These results indicate that increased expression, of mainly the PDE4D1 and PDE4D3 isoforms, correlates with higher pathology levels and more severe cognitive impairment.

Table 5. Association of pathology and cognitive impairment level with PDE4D isoform expression.

Dependent variable		Standardized coefficient per pathology variable			Standardized coefficient for MMSE	
Isoform	**N**	**Plaque load**	**Tangle load**	**Braak stage**	**N**	**MMSE**
PDE4D1	82	0.313*	0.352*	0.445*	41	-0.577**
PDE4D3	82	0.332*	0.374**	0.508***	41	-0.610**
PDE4D5	67	0.207	0.344*	0.315	33	-0.475*
PDE4D8	62	0.211	0.203	0.178	32	-0.448

Linear regressions were performed according to the following formula: Expression = Intercept + Pathology variable (i.e. plaque load, tangle load, Braak) or MMSE + Gender + Age + ApoE allele ε4 possession + PMI + qPCR plate. Cases for which MMSE scores were assessed more than 36 months before death were excluded. Significance levels Bonferroni-corrected for the amount of dependent variables tested; *: $p < 0.05$, **: $p < 0.01$, ***: $p < 0.001$.

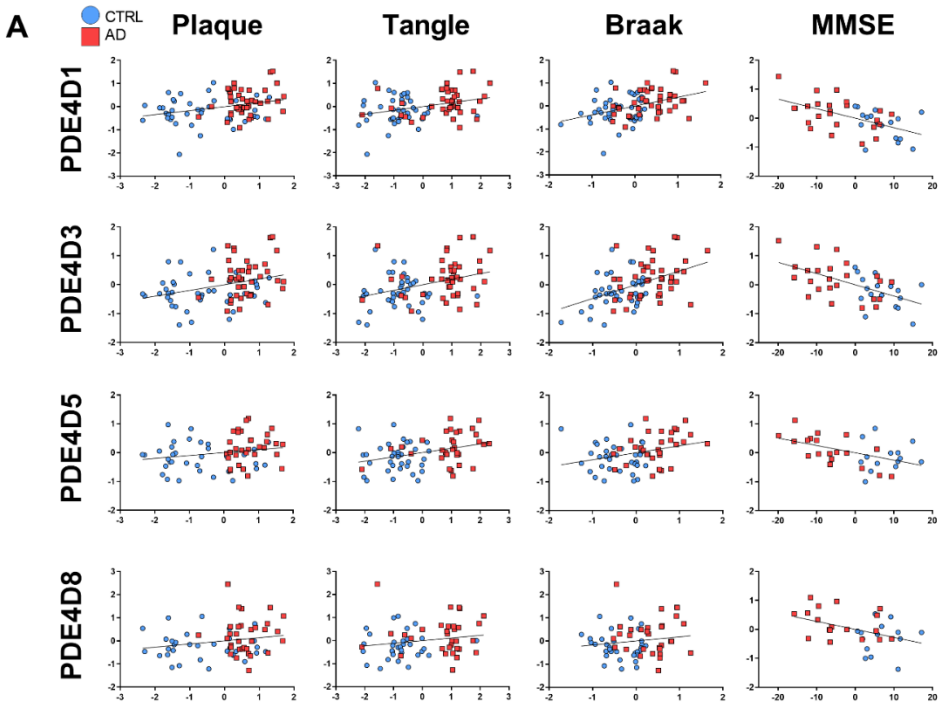

B

	Plaque		Tangle		Braak		MMSE	
	β	R^2	β	R^2	β	R^2	β	R^2
D1	0.173*	0.09	0.168*	0.11	0.385*	0.17	-0.033**	0.30
D3	0.199*	0.10	0.194**	0.13	0.476***	0.22	-0.039**	0.32
D5	0.100	0.04	0.151*	0.12	0.242	0.10	-0.026*	0.24
D8	0.138	0.04	0.117	0.03	0.186	0.02	-0.030	0.17

Figure 1. Association of pathology and cognitive impairment level with PDE4D isoform expression.

A) Partial regression plots visualizing the associations between PDE4D isoform expression and the degree of pathology (plaque and tangle load in the temporal lobe, and Braak stage level) or cognitive impairment (MMSE score), corrected for gender, age, ApoE allele ε4 possession, PMI and qPCR plate. Marker types reflect the diagnosis status of the cases (blue circles: controls, red squares: AD cases). B) Overview of slope values (β) and squared correlation coefficients of the regression lines in the partial regression plots in panel A. β values correspond to the unstandardized coefficients of pathology and MMSE variables in the regressions according to the formula described in Table 5. Significance levels Bonferroni-corrected for the amount of dependent variables tested; *: $p < 0.05$, **: $p < 0.01$, ***: $p < 0.001$.

PDE4D promoter methylation is associated with AD pathology and cognitive impairment

The diagnosis-dependent methylation changes as determined in Table 4 were investigated further for their potential association with the degree of pathology or cognitive impairment by means of linear regression analyses. These analyses revealed significant associations between methylation status changes and pathology or cognitive impairment in accordance to the directionality of changes observed between AD cases and controls. In the PDE4D3 promoter, both decreased 5mC (hypomethylation) and increased 5hmC (hyperhydroxymethylation) at CpG site cg13112511 were found to associate with an increased plaque load and a higher Braak stage (Table 6). Contrarily, in the PDE4D8 promoter, increased 5mC and decreased 5hmC at position cg23987137 was associated with increased pathology levels. Methylation status in the PDE4D5 promoter also associated with levels of pathology but the directionality of methylation status change was different per CpG site (e.g. cg03653541 shows increased 5mC, whilst cg12519013 shows decreased 5mC with higher levels of pathology; Table 6). Lastly, lower MMSE scores were associated with increased 5mC levels in the PDE4D5 promoter (cg03653541) and PDE4D8 promoter (cg23987137).

Table 6. Significant associations of PDE4D promoter methylation status with pathology and cognitive impairment.

Promoter	CpG probe	Status	N	Variable	Fold change	Mean	t	df	*P*-value	FDR
PDE4D3	cg13112511	5mC	78	Plaque	0.9917	0.3211	-2.561	67	0.010	0.017
			78	Braak	0.9858	0.3211	-2.929	67	0.003	0.008
		5hmC	78	Plaque	1.0095	0.0537	2.456	67	0.014	0.042
			78	Braak	1.0167	0.0537	2.674	67	0.007	0.011
PDE4D5	cg03653541	5mC	78	Tangle	1.0010	0.0729	2.805	67	0.005	0.025
			78	Braak	1.0014	0.0729	2.104	67	0.035	0.035
			39	MMSE	0.9997	0.0732	-3.533	28	<0.001	0.001
		UC	78	Plaque	0.9984	0.9178	-2.533	67	0.011	0.034
	cg14784398	5mC	78	Tangle	0.9983	0.1267	-2.363	67	0.018	0.030
			78	Braak	0.9972	0.1267	-2.200	67	0.028	0.035
		UC	78	Plaque	1.0015	0.8722	2.175	67	0.030	0.044
	cg12519013	5mC	78	Plaque	0.9980	0.0849	-2.612	67	0.009	0.022
			78	Tangle	0.9985	0.0849	-2.157	67	0.031	0.039
			78	Braak	0.9973	0.0849	-2.202	67	0.027	0.046
PDE4D8	cg23987137	5mC	78	Plaque	1.0063	0.3957	2.791	67	0.005	0.026
			78	Tangle	1.0047	0.3957	2.384	67	0.017	0.043
			78	Braak	1.0108	0.3957	3.034	67	0.002	0.012
			39	MMSE	0.9987	0.4035	-4.126	28	<0.001	<0.001
		5hmC	78	Plaque	0.9922	0.1765	-2.178	67	0.029	0.044
			78	Braak	0.9851	0.1765	-2.735	67	0.006	0.019

Linear regressions were performed according to the following formula: Methylation status = Intercept + Pathology variable (i.e. plaque load, tangle load, Braak) or MMSE + Gender + Age + *APOE* ε4 possession + PMI + five surrogate variables. Cases for which MMSE scores were assessed more than 36 months before death were excluded. Abbreviations: df, degrees of freedom; FDR, false discovery rate (Benjamini–Hochberg); UC, unmethylated cytosine; 5mC, 5-methylcytosine; 5hmC, 5-hydroxymethylcytosine.

DISCUSSION

Inhibition of PDE4D has been shown to hold promise as an effective strategy to enhance memory in humans (clinical trials NCT02648672 and NCT02840279), but is also assumed to contribute to possible emetic side effects upon non-selective PDE4 inhibition (Giembycz, 2002; Mori et al., 2010). The *PDE4D* gene encodes multiple isoforms that, e.g. by specific intracellular localization, can regulate different compartmentalized pools of cAMP (Houslay et al., 2007). Hence, targeting specific PDE4D isoforms may provide a safer and more efficacious treatment strategy to alleviate memory deficits in AD without evoking side effects (Schepers et al., 2019). To investigate which specific PDE4D isoform(s) is/are altered in terms of expression in AD, we established PDE4D isoform expression profiles in post-mortem MTG tissue derived from AD patients and healthy non-demented controls by means of isoform-specific qPCR.

Regression analyses revealed that AD was associated with increased expression of PDE4D1, -D3, -D5 and –D8. Expression of these isoforms was increased in the range of 2.56-3.85 fold. Previous studies have indicated that 3-4 fold increased PDE4D (isoform) mRNA expression results into similar increases in both PDE4D protein expression and PDE4 activity (Levallet et al., 2007; Peter et al., 2007). Therefore, the 2.59-3.85 fold expression increases likely increase PDE4 activity. To our knowledge, the number of studies investigating PDE4D expression in light of AD is limited. Ugarte et al. did not find a difference in overall PDE4D expression in temporal lobe material from AD patients (n=7) and controls (n=8) (Ugarte et al., 2015). McLachlan et al. investigated hippocampal PDE4D isoform expression in material from a single patient with advanced AD and three control cases and found a 2.62-fold increase in PDE4D1 expression, while the expression of other isoforms was reduced or unaffected (McLachlan et al., 2007). Our study, making use of a much larger sample size, shows, in addition to a similar increase in PDE4D1 expression,

increased expression of PDE4D3, -D5 and –D8. The current findings imply that PDE4D expression is affected in AD in an isoform-specific manner.

Since AD is a progressive disease, we also inspected whether PDE4D isoform expression increases with higher degrees of pathology or more severe cognitive impairment. Expression of PDE4D1 and PDE4D3 was associated with temporal plaque load, temporal tangle load, Braak staging as well as cognitive impairment. PDE4D5 expression was found to be only associated with temporal tangle load and cognitive impairment, while PDE4D8 expression was not associated with any pathology measure or cognitive impairment. These findings suggest that mainly PDE4D1 and PDE4D3 expression changes as the disease progresses and cognitive impairment worsens. The observation that PDE4D3 transcription is increased in presence of higher amyloid-β plaque load corresponds to earlier findings. Hippocampal injections of $A\beta_{1\text{-}42}$ in mice caused memory deficits and increased protein expression of PDE4D3, which was reversed upon non-selective PDE4 inhibition by resveratrol (Wang et al., 2016). Interestingly, Oláh et al. found a direct interaction between oligomeric Aβ and PDE4D (Olah et al., 2011). Whether this interaction occurs *in vivo* and how this interaction affects PDE4D enzymatic activity remains to be determined. From a potentially therapeutic perspective, it would be interesting to identify whether inhibition of PDE4D1 and/or PDE4D3 specifically can delay disease progression and improve cognitive functioning.

As the *PDE4D* gene, with its various isoforms embedded, contains multiple promoter regions, epigenetic mechanisms are likely involved in its isoform-specific expression regulation, e.g. by influencing promoter accessibility (Maunakea et al., 2010; Tilley and Maurice, 2005). Here, we found that DNA (hydroxy)methylation signatures in the promoter regions of PDE4D1, -D3, -D5 and –D8 were altered in the same tissue as used for the expression profiling. Results showed differentially methylated CpG sites in these promoters that were associated with AD diagnosis. Moreover, methylation status was also associated with the degree of pathology and

cognitive impairment for several CpG sites. Various effects were observed, i.e. both increased and decreased 5mC, 5hmC and UC levels. Differences in methylation and hydroxymethylation can be linked to altered gene expression by affecting the binding of transcription factors and chromatin proteins to the DNA (Suzuki and Bird, 2008; Yin et al., 2017). As such, decreased methylation and increased hydroxymethylation in AD in the PDE4D3 promoter might explain, at least in part, the observed pathology- and AD-associated increased expression of PDE4D3. In contrast, in the PDE4D8 promoter, cg23987137 displayed AD-associated hypermethylation and hypohydroxymethylation. However, cytosine methylation can have differential effects on transcription factor binding and subsequent gene expression. Interestingly, cg23987137 is located 14 nucleotides downstream of an AP-1 binding site (Farre et al., 2003). The transcription factor AP-1 is usually described as a transcriptional activator, but can also act as transcriptional repressor (Brellier et al., 2004). Moreover, it has been shown that methylation adjacent to, but not within, the AP-1 binding site can hamper AP-1 binding and consequently induce transcription (Fujimoto et al., 2005). Although purely speculative, a similar mechanism might affect transcription near the PDE4D8 promoter resulting in increased expression upon CpG site hypermethylation. Similarly, epigenetic changes observed in the other promoters can, by influencing binding of transcriptional activators and repressors, induce increased expression of the associated isoforms. Interestingly, increased methylation at cg23987137 PDE4D8 promoter was associated with worse cognitive performance whilst PDE4D8 expression did not associate with cognitive performance. This discrepancy may suggest that DNA methylation may not solely influence expression via its closest located promoter but may also regulate expression of other isoforms which do show associations with cognitive performance (i.e. PDE4D1, -D3 and –D5).

The current findings show that in AD, expression of specific PDE4D isoforms is altered with concurrent changes (hydroxy)methylation changes in associated

promoters of the *PDE4D* gene. Although PDE4D isoforms locate to specific cellular compartments, the role of individual PDE4D isoforms in specific cellular processes is still largely unknown. The mouse orthologue of PDE4D1 is reported to localize to the nucleus (Chandrasekaran et al., 2008). With 95.6% homology in the N-terminal, human PDE4D1 may share a similar localization signal and hence could be involved in the regulation of nuclear cAMP levels which may directly affect PKA-CREB mediated transcription crucial for memory consolidation(Kandel, 2012). Transgenic overexpression of PDE4D1 in specific neurons was found to decrease Ca^{2+} oscillations, which may imply a specific role for this isoform in neuronal firing (Yoshida et al., 2003). Increased PDE4D1 expression in AD may therefore decrease neuronal firing rates that subsequently impacts neuronal plasticity and memory formation processes.

Specific interactions have been reported between PDE4D3 and A-kinase anchoring proteins (AKAPs), e.g., AKAP9 and mAKAPα, through which PDE4D3 can locally degrade cAMP pools(Boczek et al., 2019; Terrenoire et al., 2009). Disrupting the perinuclear PDE4D3- mAKAPα signaling complex promoted survival and axon growth in neurons (Boczek et al., 2019). Vice versa, increased PDE4D3 expression as observed in the current study could hamper these effects, thereby likely impairing neuronal plasticity and memory processes in AD.

Similar to PDE4D3-AKAP interactions, the scaffolding protein β-arrestin was found to preferentially interact with PDE4D5 (Baillie et al., 2007). β-arrestin is recruited to G-protein coupled receptors (GPCRs) upon activation, which places PDE4D5 in close proximity to sites where cAMP is produced, i.e. close to GPCRs and activated adenylyl cyclases that produce cAMP (Baillie et al., 2003; Houslay and Baillie, 2005). Increased PDE4D5 levels may therefore excessively degrade cAMP at the site of synthesis. Vice versa, downregulation of PDE4D5 may stimulate cAMP signaling, which is supported by the interesting finding that knockdown of PDE4D4 or PDE4D5 can improve memory performance in mice (MacKenzie et al., 2011; Wang et al., 2013). In addition

to cytosolic interactions, it was found that PDE4D5 also regulates cAMP levels in nuclear signaling complexes, indicating that a specific isoform can regulate cAMP levels in spatially distinct compartments (Clister et al., 2019).

Regarding PDE4D8, most insights have been gathered through cardiovascular research. In cardiomyocytes, PDE4D8 is located near the β1-adrenergic receptor through a SAP97-mediated interaction and dissociates upon receptor stimulation (Fu et al., 2014; Richter et al., 2008). As SAP97 is a synapse-associated protein that scaffolds multiple receptors, including AMPA receptors crucial for memory processes, similar interactions may occur in the brain (Zhang et al., 2015). Moreover, PDE4D8 is found to localize in leading-edge structures of migrating vascular smooth muscle cells and affects actin organization upon overexpression (Raymond et al., 2009). Actin-rich leading edges in neuronal or glial cells may also be affected by increased PDE4D8 levels and consequently induce dysfunctional migration and growth, possibly contributing to impaired cognitive functioning eventually.

Through their specific localizations, the isoforms PDE4D3, -D5 and -D8 have all been reported to modulate downstream signaling of β-adrenergic receptors(Baillie et al., 2003; De Arcangelis et al., 2009; Richter et al., 2008). As adrenergic signaling is involved in cognitive functioning and can be affected in AD (Gannon et al., 2015), changes in expression of PDE4D isoforms may disrupt downstream β-adrenergic signaling leading to cognitive dysfunction. In sum, upcoming studies will have to indicate isoform-specific roles in memory processes, so local cAMP compartments can be targeted and treatment efficacy can be increased.

Lastly, the current findings represent PDE4D isoform expression and DNA (hydroxy)methylation in homogenized brain tissue, meaning no conclusions can be drawn yet on potential cell type-specific effects. Hence, follow-up studies will have to indicate whether the current findings can be linked to changes in specific cell types

(e.g., neurons, microglia, astrocytes, oligodendrocytes, endothelial cells). Also, whether increased PDE4D expression is causal to or a consequence of worsening pathology remains to be specified. Nevertheless, these findings highlight isoform-specific PDE4D inhibition as a potential strategy to aid in delaying disease progression with associated procognitive effects.

CONCLUSION

Taken together, regulation of PDE4D transcription is affected in AD as indicated by differences in gene (hydroxy)methylation and expression levels. Moreover, the specific isoforms PDE4D1 and PDE4D3 show a significant association with the degree of pathology and cognitive impairment. In line with the fact that PDE4D isoforms regulate specific intracellular processes, this implies that targeting specific PDE4D isoforms may provide a more efficacious treatment strategy with less adverse effects in different stages of the disease. For this purpose, future studies will have to reveal which PDE4D isoforms regulate mechanisms underlying memory enhancement and do not show adverse effects upon inhibition in the context of brain function in both health and AD.

ACKNOWLEDGEMENTS

This work was financially supported by grants from ISAO/Alzheimer Nederland WE.03-2016-07, Young European Research Universities Network (YERUN) and the Baeter Laeve foundation. Additional funds have been provided by the Internationale Stichting Alzheimer Onderzoek (ISAO) / Alzheimer Netherlands (Award #11532; Funded by the Dorpmans-Wigmans Foundation) (DvdH), and by the Joint Programme—Neurodegenerative Disease Research (JPND) for the EPI-AD consortium (http://www.neurodegenerationresearch.eu/wp-content/uploads/2015/10/Factsheet_EPI-AD.pdf). The project is supported through the following funding organizations under the aegis of JPND; The Netherlands, The Netherlands Organisation for Health Research and Development (ZonMw); United Kingdom, Medical Research Council; Germany, German Federal Ministry of Education and Research (BMBF); Luxembourg, National Research Fund (FNR). This project has received funding from the European Union's Horizon 2020 research and innovation programme under Grant Agreement No. 643417.

We thank Dr. Ir. Jochen De Vry for primer and qPCR experiment design.

DISCLOSURE STATEMENT

TV and JP have a proprietary interest in selective PDE4D inhibitors for the treatment of neurodegenerative disorders. The other authors declare that they have no competing interests.

REFERENCES

(1997) Consensus recommendations for the postmortem diagnosis of Alzheimer's disease. The National Institute on Aging, and Reagan Institute Working Group on Diagnostic Criteria for the Neuropathological Assessment of Alzheimer's Disease. *Neurobiol Aging* **18**:S1-2.

Aryee MJ, Jaffe AE, Corrada-Bravo H, Ladd-Acosta C, Feinberg AP, Hansen KD and Irizarry RA (2014) Minfi: a flexible and comprehensive Bioconductor package for the analysis of Infinium DNA methylation microarrays. *Bioinformatics (Oxford, England)* **30**:1363-1369.

Baillie GS, Adams DR, Bhari N, Houslay TM, Vadrevu S, Meng D, Li X, Dunlop A, Milligan G, Bolger GB, Klussmann E and Houslay MD (2007) Mapping binding sites for the PDE4D5 cAMP-specific phosphodiesterase to the N- and C-domains of beta-arrestin using spot-immobilized peptide arrays. *Biochem J* **404**:71-80.

Baillie GS, Sood A, McPhee I, Gall I, Perry SJ, Lefkowitz RJ and Houslay MD (2003) beta-Arrestin-mediated PDE4 cAMP phosphodiesterase recruitment regulates beta-adrenoceptor switching from Gs to Gi. *Proc Natl Acad Sci U S A* **100**:940-945.

Baumgartel K, Green A, Hornberger D, Lapira J, Rex C, Wheeler DG and Peters M (2018) PDE4D regulates Spine Plasticity and Memory in the Retrosplenial Cortex. *Scientific reports* **8**:3895.

Beach TG, Adler CH, Sue LI, Serrano G, Shill HA, Walker DG, Lue L, Roher AE, Dugger BN, Maarouf C, Birdsill AC, Intorcia A, Saxon-Labelle M, Pullen J, Scroggins A, Filon J, Scott S, Hoffman B, Garcia A, Caviness JN, Hentz JG, Driver-Dunckley E, Jacobson SA, Davis KJ, Belden CM, Long KE, Malek-Ahmadi M, Powell JJ, Gale LD, Nicholson LR, Caselli RJ, Woodruff BK, Rapscak SZ, Ahern GL, Shi J, Burke AD, Reiman EM and Sabbagh MN (2015) Arizona Study of Aging and Neurodegenerative Disorders and Brain and Body Donation Program. *Neuropathology : official journal of the Japanese Society of Neuropathology* **35**:354-389.

Blokland A, Van Duinen MA, Sambeth A, Heckman PRA, Tsai M, Lahu G, Uz T and Prickaerts J (2019) Acute treatment with the PDE4 inhibitor roflumilast improves verbal word memory in healthy old individuals: a double-blind placebo-controlled study. *Neurobiol Aging* **77**:37-43.

Boczek T, Cameron EG, Yu W, Xia X, Shah SH, Castillo Chabeco B, Galvao J, Nahmou M, Li J, Thakur H, Goldberg JL and Kapiloff MS (2019) Regulation of Neuronal Survival and Axon Growth by a Perinuclear cAMP Compartment. *J Neurosci* **39**:5466-5480.

Braak H and Braak E (1991) Demonstration of amyloid deposits and neurofibrillary changes in whole brain sections. *Brain Pathol* **1**:213-216.

Brellier F, Marionnet C, Chevallier-Lagente O, Toftgard R, Mauviel A, Sarasin A and Magnaldo T (2004) Ultraviolet irradiation represses PATCHED gene transcription in human epidermal keratinocytes through an activator protein-1-dependent process. *Cancer research* **64**:2699-2704.

Chandrasekaran A, Toh KY, Low SH, Tay SK, Brenner S and Goh DL (2008) Identification and characterization of novel mouse PDE4D isoforms: molecular cloning, subcellular distribution and detection of isoform-specific intracellular localization signals. *Cell Signal* **20**:139-153.

Chen YA, Lemire M, Choufani S, Butcher DT, Grafodatskaya D, Zanke BW, Gallinger S, Hudson TJ and Weksberg R (2013) Discovery of cross-reactive

probes and polymorphic CpGs in the Illumina Infinium HumanMethylation450 microarray. *Epigenetics* **8**:203-209.
Cheng YF, Wang C, Lin HB, Li YF, Huang Y, Xu JP and Zhang HT (2010) Inhibition of phosphodiesterase-4 reverses memory deficits produced by Abeta25-35 or Abeta1-40 peptide in rats. *Psychopharmacology* **212**:181-191.
Clister T, Greenwald EC, Baillie GS and Zhang J (2019) AKAP95 Organizes a Nuclear Microdomain to Control Local cAMP for Regulating Nuclear PKA. *Cell Chem Biol* **26**:885-891 e884.
De Arcangelis V, Liu R, Soto D and Xiang Y (2009) Differential association of phosphodiesterase 4D isoforms with beta2-adrenoceptor in cardiac myocytes. *J Biol Chem* **284**:33824-33832.
Farre D, Roset R, Huerta M, Adsuara JE, Rosello L, Alba MM and Messeguer X (2003) Identification of patterns in biological sequences at the ALGGEN server: PROMO and MALGEN. *Nucleic Acids Res* **31**:3651-3653.
Folstein MF, Folstein SE and McHugh PR (1975) "Mini-mental state". A practical method for grading the cognitive state of patients for the clinician. *J Psychiatr Res* **12**:189-198.
Fu Q, Kim S, Soto D, De Arcangelis V, DiPilato L, Liu S, Xu B, Shi Q, Zhang J and Xiang YK (2014) A long lasting beta1 adrenergic receptor stimulation of cAMP/protein kinase A (PKA) signal in cardiac myocytes. *J Biol Chem* **289**:14771-14781.
Fujimoto M, Kitazawa R, Maeda S and Kitazawa S (2005) Methylation adjacent to negatively regulating AP-1 site reactivates TrkA gene expression during cancer progression. *Oncogene* **24**:5108-5118.
Gannon M, Che P, Chen Y, Jiao K, Roberson ED and Wang Q (2015) Noradrenergic dysfunction in Alzheimer's disease. *Front Neurosci* **9**:220-220.
Giembycz MA (2002) 4D or not 4D - the emetogenic basis of PDE4 inhibitors uncovered? *Trends Pharmacol Sci* **23**:548.
Houslay MD (2010) Underpinning compartmentalised cAMP signalling through targeted cAMP breakdown. *Trends Biochem Sci* **35**:91-100.
Houslay MD and Baillie GS (2005) Beta-arrestin-recruited phosphodiesterase-4 desensitizes the AKAP79/PKA-mediated switching of beta2-adrenoceptor signalling to activation of ERK. *Biochemical Society transactions* **33**:1333-1336.
Houslay MD, Baillie GS and Maurice DH (2007) cAMP-Specific phosphodiesterase-4 enzymes in the cardiovascular system: a molecular toolbox for generating compartmentalized cAMP signaling. *Circ Res* **100**:950-966.
Kandel ER (2012) The molecular biology of memory: cAMP, PKA, CRE, CREB-1, CREB-2, and CPEB. *Mol Brain* **5**:14.
Kiihl SF, Martinez-Garrido MJ, Domingo-Relloso A, Bermudez J and Tellez-Plaza M (2019) MLML2R: an R package for maximum likelihood estimation of DNA methylation and hydroxymethylation proportions. *Stat Appl Genet Mol Biol* **18**.
Lardenoije R, Roubroeks JAY, Pishva E, Leber M, Wagner H, Iatrou A, Smith AR, Smith RG, Eijssen LMT, Kleineidam L, Kawalia A, Hoffmann P, Luck T, Riedel-Heller S, Jessen F, Maier W, Wagner M, Hurlemann R, Kenis G, Ali M, Del Sol A, Mastroeni D, Delvaux E, Coleman PD, Mill J, Rutten BPF, Lunnon K, Ramirez A and van den Hove DLA (2019) Alzheimer's disease-associated (hydroxy)methylomic changes in the brain and blood. *Clin Epigenetics* **11**:164.

Leek JT, Johnson WE, Parker HS, Jaffe AE and Storey JD (2012) The sva package for removing batch effects and other unwanted variation in high-throughput experiments. *Bioinformatics (Oxford, England)* **28**:882-883.

Levallet G, Levallet J, Bouraima-Lelong H and Bonnamy PJ (2007) Expression of the cAMP-phosphodiesterase PDE4D isoforms and age-related changes in follicle-stimulating hormone-stimulated PDE4 activities in immature rat sertoli cells. *Biol Reprod* **76**:794-803.

MacKenzie KF, Wallace DA, Hill EV, Anthony DF, Henderson DJ, Houslay DM, Arthur JS, Baillie GS and Houslay MD (2011) Phosphorylation of cAMP-specific PDE4A5 (phosphodiesterase-4A5) by MK2 (MAPKAPK2) attenuates its activation through protein kinase A phosphorylation. *Biochem J* **435**:755-769.

Maunakea AK, Nagarajan RP, Bilenky M, Ballinger TJ, D'Souza C, Fouse SD, Johnson BE, Hong C, Nielsen C, Zhao Y, Turecki G, Delaney A, Varhol R, Thiessen N, Shchors K, Heine VM, Rowitch DH, Xing X, Fiore C, Schillebeeckx M, Jones SJ, Haussler D, Marra MA, Hirst M, Wang T and Costello JF (2010) Conserved role of intragenic DNA methylation in regulating alternative promoters. *Nature* **466**:253-257.

McLachlan CS, Chen ML, Lynex CN, Goh DL, Brenner S and Tay SK (2007) Changes in PDE4D isoforms in the hippocampus of a patient with advanced Alzheimer disease. *Archives of neurology* **64**:456-457.

Mori F, Perez-Torres S, De Caro R, Porzionato A, Macchi V, Beleta J, Gavalda A, Palacios JM and Mengod G (2010) The human area postrema and other nuclei related to the emetic reflex express cAMP phosphodiesterases 4B and 4D. *J Chem Neuroanat* **40**:36-42.

Myeku N, Clelland CL, Emrani S, Kukushkin NV, Yu WH, Goldberg AL and Duff KE (2016) Tau-driven 26S proteasome impairment and cognitive dysfunction can be prevented early in disease by activating cAMP-PKA signaling. *Nature medicine* **22**:46-53.

Olah J, Vincze O, Virok D, Simon D, Bozso Z, Tokesi N, Horvath I, Hlavanda E, Kovacs J, Magyar A, Szucs M, Orosz F, Penke B and Ovadi J (2011) Interactions of pathological hallmark proteins: tubulin polymerization promoting protein/p25, beta-amyloid, and alpha-synuclein. *J Biol Chem* **286**:34088-34100.

Perez-Torres S, Miro X, Palacios JM, Cortes R, Puigdomenech P and Mengod G (2000) Phosphodiesterase type 4 isozymes expression in human brain examined by in situ hybridization histochemistry and[3H]rolipram binding autoradiography. Comparison with monkey and rat brain. *J Chem Neuroanat* **20**:349-374.

Peter D, Jin SL, Conti M, Hatzelmann A and Zitt C (2007) Differential expression and function of phosphodiesterase 4 (PDE4) subtypes in human primary CD4+ T cells: predominant role of PDE4D. *J Immunol* **178**:4820-4831.

Pidsley R, CC YW, Volta M, Lunnon K, Mill J and Schalkwyk LC (2013) A data-driven approach to preprocessing Illumina 450K methylation array data. *BMC genomics* **14**:293.

Qu J, Zhou M, Song Q, Hong EE and Smith AD (2013) MLML: consistent simultaneous estimates of DNA methylation and hydroxymethylation. *Bioinformatics (Oxford, England)* **29**:2645-2646.

R Development Core Team (2019) R: A language and environment for statistical computing., pp Available from: https://www.r-project.org/, R Foundation for Statistical Computing, Vienna, Austria.

Raymond DR, Carter RL, Ward CA and Maurice DH (2009) Distinct phosphodiesterase-4D variants integrate into protein kinase A-based signaling complexes in cardiac and vascular myocytes. *American journal of physiology Heart and circulatory physiology* **296**:H263-271.

Ricciarelli R, Brullo C, Prickaerts J, Arancio O, Villa C, Rebosio C, Calcagno E, Balbi M, van Hagen BT, Argyrousi EK, Zhang H, Pronzato MA, Bruno O and Fedele E (2017) Memory-enhancing effects of GEBR-32a, a new PDE4D inhibitor holding promise for the treatment of Alzheimer's disease. *Scientific reports* **7**:46320.

Richter W, Day P, Agrawal R, Bruss MD, Granier S, Wang YL, Rasmussen SG, Horner K, Wang P, Lei T, Patterson AJ, Kobilka B and Conti M (2008) Signaling from beta1- and beta2-adrenergic receptors is defined by differential interactions with PDE4. *The EMBO journal* **27**:384-393.

Ritchie ME, Phipson B, Wu D, Hu Y, Law CW, Shi W and Smyth GK (2015) limma powers differential expression analyses for RNA-sequencing and microarray studies. *Nucleic Acids Res* **43**:e47.

Robichaud A, Stamatiou PB, Jin SL, Lachance N, MacDonald D, Laliberte F, Liu S, Huang Z, Conti M and Chan CC (2002) Deletion of phosphodiesterase 4D in mice shortens alpha(2)-adrenoceptor-mediated anesthesia, a behavioral correlate of emesis. *J Clin Invest* **110**:1045-1052.

RStudio Team (2019) RStudio: Integrated Development for R p Available from: htttp://www.rstudio.com/, RStudio, Inc., Boston, MA.

Ruijter JM, Ramakers C, Hoogaars WM, Karlen Y, Bakker O, van den Hoff MJ and Moorman AF (2009) Amplification efficiency: linking baseline and bias in the analysis of quantitative PCR data. *Nucleic acids research* **37**:e45.

Schepers M, Tiane A, Paes D, Sanchez S, Rombaut B, Piccart E, Rutten BPF, Brône B, Hellings N, Prickaerts J and Vanmierlo T (2019) Targeting Phosphodiesterases—Towards a Tailor-Made Approach in Multiple Sclerosis Treatment. *Frontiers in Immunology* **10**.

Schneider J, Murray J, Banerjee S and Mann A (1999) EUROCARE: a cross-national study of co-resident spouse carers for people with Alzheimer's disease: I--Factors associated with carer burden. *International journal of geriatric psychiatry* **14**:651-661.

Smith AR, Smith RG, Pishva E, Hannon E, Roubroeks JAY, Burrage J, Troakes C, Al-Sarraj S, Sloan C, Mill J, van den Hove DL and Lunnon K (2019) Parallel profiling of DNA methylation and hydroxymethylation highlights neuropathology-associated epigenetic variation in Alzheimer's disease. *Clin Epigenetics* **11**:52.

Suzuki MM and Bird A (2008) DNA methylation landscapes: provocative insights from epigenomics. *Nature Reviews Genetics* **9**:465-476.

Terrenoire C, Houslay MD, Baillie GS and Kass RS (2009) The cardiac IKs potassium channel macromolecular complex includes the phosphodiesterase PDE4D3. *J Biol Chem* **284**:9140-9146.

Tilley DG and Maurice DH (2005) Vascular smooth muscle cell phenotype-dependent phosphodiesterase 4D short form expression: role of differential histone acetylation on cAMP-regulated function. *Mol Pharmacol* **68**:596-605.

Ugarte A, Gil-Bea F, Garcia-Barroso C, Cedazo-Minguez A, Ramirez MJ, Franco R, Garcia-Osta A, Oyarzabal J and Cuadrado-Tejedor M (2015) Decreased levels of guanosine 3', 5'-monophosphate (cGMP) in cerebrospinal fluid

(CSF) are associated with cognitive decline and amyloid pathology in Alzheimer's disease. *Neuropathol Appl Neurobiol* **41**:471-482.
Van Duinen MA, Sambeth A, Heckman PRA, Smit S, Tsai M, Lahu G, Uz T, Blokland A and Prickaerts J (2018) Acute administration of roflumilast enhances immediate recall of verbal word memory in healthy young adults. *Neuropharmacology* **131**:31-38.
van Iterson M, van Zwet EW, Consortium B and Heijmans BT (2017) Controlling bias and inflation in epigenome- and transcriptome-wide association studies using the empirical null distribution. *Genome Biol* **18**:19.
Vandesompele J, De Preter K, Pattyn F, Poppe B, Van Roy N, De Paepe A and Speleman F (2002) Accurate normalization of real-time quantitative RT-PCR data by geometric averaging of multiple internal control genes. *Genome biology* **3**:Research0034.
Vanmierlo T, Creemers P, Akkerman S, van Duinen M, Sambeth A, De Vry J, Uz T, Blokland A and Prickaerts J (2016) The PDE4 inhibitor roflumilast improves memory in rodents at non-emetic doses. *Behav Brain Res* **303**:26-33.
Wang G, Chen L, Pan X, Chen J, Wang L, Wang W, Cheng R, Wu F, Feng X, Yu Y, Zhang HT, O'Donnell JM and Xu Y (2016) The effect of resveratrol on beta amyloid-induced memory impairment involves inhibition of phosphodiesterase-4 related signaling. *Oncotarget* **7**:17380-17392.
Wang ZZ, Zhang Y, Liu YQ, Zhao N, Zhang YZ, Yuan L, An L, Li J, Wang XY, Qin JJ, Wilson SP, O'Donnell JM, Zhang HT and Li YF (2013) RNA interference-mediated phosphodiesterase 4D splice variants knock-down in the prefrontal cortex produces antidepressant-like and cognition-enhancing effects. *Br J Pharmacol* **168**:1001-1014.
Yin Y, Morgunova E, Jolma A, Kaasinen E, Sahu B, Khund-Sayeed S, Das PK, Kivioja T, Dave K, Zhong F, Nitta KR, Taipale M, Popov A, Ginno PA, Domcke S, Yan J, Schubeler D, Vinson C and Taipale J (2017) Impact of cytosine methylation on DNA binding specificities of human transcription factors. *Science* **356**.
Yoshida H, Beltran-Parrazal L, Butler P, Conti M, Charles AC and Weiner RI (2003) Lowering cyclic adenosine-3',5'-monophosphate (cAMP) levels by expression of a cAMP-specific phosphodiesterase decreases intrinsic pulsatile gonadotropin-releasing hormone secretion from GT1 cells. *Mol Endocrinol* **17**:1982-1990.
Zhang C, Xu Y, Chowdhary A, Fox D, 3rd, Gurney ME, Zhang HT, Auerbach BD, Salvi RJ, Yang M, Li G and O'Donnell JM (2018) Memory enhancing effects of BPN14770, an allosteric inhibitor of phosphodiesterase-4D, in wild-type and humanized mice. *Neuropsychopharmacology* **43**:2299-2309.
Zhang C, Xu Y, Zhang HT, Gurney ME and O'Donnell JM (2017) Comparison of the Pharmacological Profiles of Selective PDE4B and PDE4D Inhibitors in the Central Nervous System. *Scientific reports* **7**:40115.
Zhang L, Hsu FC, Mojsilovic-Petrovic J, Jablonski AM, Zhai J, Coulter DA and Kalb RG (2015) Structure-function analysis of SAP97, a modular scaffolding protein that drives dendrite growth. *Mol Cell Neurosci* **65**:31-44.

Chapter 4

Ablation of specific long PDE4D isoforms increases neurite elongation and conveys protection against amyloid-β pathology

Published as:

Paes et al. (2023) *Cell Mol Life Sci.* Jun 12;80(7):178.

doi: 10.1007/s00018-023-04804-w

ABSTRACT

Inhibition of phosphodiesterase 4D (PDE4D) enzymes has been investigated as a therapeutic strategy to treat memory problems in Alzheimer's disease (AD). Although PDE4D inhibitors are effective in enhancing memory processes in rodents and humans, severe side effects may hamper their clinical use. PDE4D enzymes comprise different isoforms, which, when targeted specifically, can increase treatment efficacy and safety. The role of PDE4D isoforms in AD and in molecular memory processes per se has remained unresolved. Hippocampus and prefrontal cortex were harvested from APPswe/PS1dE9 transgenic mice. Differences in PDE4D, PKA and pCREB protein levels and PDE4 activity were assessed by means of Western blot and activity assays, respectively (two-tailed t-test). The effect of amyloid-β exposure on PDE4D isoform expression was evaluated using qPCR in the *ex vivo* mouse brain material and in mouse hippocampal neurons. Moreover, using these neurons, the effects of the PDE4D-selective inhibitor GEBR32a and PDE4D isoform knockdown using CRISPR-Cas9 on neurite outgrowth were assessed, both with and without exposure to amyloid-β (Dunnett's post hoc t-test). We report the upregulation of specific PDE4D isoforms in transgenic AD mice and hippocampal neurons exposed to amyloid-β. Furthermore, by means of pharmacological inhibition and CRISPR-Cas9 knockdown, we demonstrate that inhibition of the long-form PDE4D3, -D5, -D7, and -D9 isoforms enhances neuronal plasticity and conveys resilience against amyloid-β induced decreases in neuroplasticity *in vitro*. These results indicate that isoform-specific ablation, next to non-selective PDE4D inhibition is efficient in promoting neuroplasticity in an AD context. Therapeutic effects of non-selective PDE4D inhibitors are likely achieved through actions on long isoforms. Future research should identify which long PDE4D isoforms should be specifically targeted *in vivo* to improve treatment efficacy and reduce side effects.

INTRODUCTION

Memory consolidation deficits associated with Alzheimer's disease (AD) cause severe impairment in AD patients, and place a tremendous burden on their caretakers and family members. Hence, pharmacological interventions that stimulate the molecular machinery underlying memory consolidation would improve the quality of life of AD patients and people close to them. Cyclic adenosine monophosphate (cAMP) plays a pivotal role as second messenger in signaling cascades that regulate memory consolidation (Kandel, 2012). Enzymatic degradation of cAMP predominantly occurs by phosphodiesterase 4 (PDE4) enzymes (Houslay, 2010). Consequently, inhibition of PDE4 would promote cAMP signaling and associated memory consolidation processes (Blokland et al., 2019a). Accordingly, PDE4 inhibition has been found to enhance memory functioning in both rodents and healthy humans (Blokland et al., 2019b; Van Duinen et al., 2018; Vanmierlo et al., 2016). In addition, PDE4 inhibition has shown pro-cognitive effects in AD animal models (Ashour et al., 2021; Cheng et al., 2010; Feng et al., 2019; Myeku et al., 2016; Schepers et al., 2019; Wang et al., 2020).

Despite the therapeutic potential of PDE4 inhibitors to restore memory functioning in AD, clinical use is hindered due to severe side effects such as nausea and emesis (Paes et al., 2021). Interestingly, the PDE4 enzyme family is encoded by four genes (*PDE4A-D*), each producing a sub-family comprising of several isoforms (e.g. PDE4D1-9). By specific inhibition of PDE4 sub-families or isoforms rather than non-selective PDE4 inhibition, adverse effects may be minimized or prevented (Bhat et al., 2020; Blokland et al., 2019a; Paes et al., 2021). The PDE4D subtype has shown to be a promising target for memory enhancement. In a recent exploratory study, PDE4D expression in blood was found to negatively correlate with cognitive function in monozygotic twins (Mohammadnejad et al., 2021). Moreover, *PDE4D* gene variants affect functional brain networks in patients with mild cognitive impairment and AD (Xiang et al., 2020). In rodents, inhibition of PDE4D, rather than PDE4B, was

found to enhance memory functioning (Zhang et al., 2017). Moreover, in AD mouse models, pharmacological inhibition or shRNA-mediated knockdown of PDE4D has been reported to restore amyloid-β (Aβ) induced memory deficits (Cui et al., 2019; Shi et al., 2021b; Sierksma et al., 2014; Zhang et al., 2014).

While PDE4D is a promising target to restore AD-associated memory deficits, inhibition of the PDE4D sub-family has been associated with the onset of side effects similar to those caused by non-specific PDE4 inhibitors when compared to non-specific PDE4 inhibition (Mori et al., 2010; Paes et al., 2021; Robichaud et al., 2002). Hence, even more specific targeting, i.e. of individual PDE4D isoforms, may be needed for an efficacious and clinically safe treatment strategy. Previously, we reported that PDE4D expression is isoform-specifically altered in post-mortem brains of AD patients and that this expression correlates with the degree of pathology and cognitive decline (Paes et al., 2020a). Specific PDE4D isoforms may therefore contribute more to AD-associated memory deficits and thus be more promising pharmacological targets. Strikingly, the different isoforms encoded by the *PDE4D* gene localize to different intracellular compartments and regulate distinct cAMP signaling domains (Baillie, 2009; Baillie et al., 2019; Houslay, 2010; Paes et al., 2021). Neuronal plasticity, which is modulated by cAMP and involves dynamic neurite growth, is crucial for proper memory consolidation (Batty et al., 2017; Mingorance-Le Meur and O'Connor, 2009). In AD, neuronal plasticity is found to be heavily impaired (Mesulam, 1999). Non-selective PDE4 inhibition promotes neuronal plasticity and can restore Aβ-induced plasticity impairments (Shrestha et al., 2006). Moreover, genetic ablation of PDE4D appears to specifically increase the number of neurites *in vivo* (Shelly et al., 2010). These findings indicate that PDE4D regulates cAMP signaling domains involved in neuronal plasticity. Therefore, it is crucial to understand which specific PDE4D isoforms control these processes to identify safe pharmacological targets for memory enhancement in AD.

Here, we investigated how PDE4D isoform expression levels and downstream cAMP-PKA-CREB signaling are affected in transgenic AD mouse brains and in Aβ-exposed mouse hippocampal neurons. Furthermore, by means of pharmacological inhibition and CRISPR-Cas9-mediated knockdown, we determined which individual PDE4D isoforms regulate neuronal plasticity *in vitro* and whether ablation of specific isoforms can convey resilience against Aβ toxicity.

METHODS

Animals and behavioral testing

All experimental procedures were approved by the local ethical committee of Hasselt University for animal experiments and met governmental guidelines. Eighteen female wild-type (C57bl/6 OlaHsd) and twenty-two female transgenic Alzheimer mice (APPswe/PS1dE9) were used. Mice were genotyped by PCR analysis of ear biopsies. At the age of 7 months, animals were housed individually in standard cages on sawdust bedding in an air-conditioned room (about 20°C). They were kept under a reversed 12/12 h light/dark cycle (lights on from 20.00 to 08.00) and had free access to food and water. Mice were housed and tested in the same room. A radio, which was playing softly, provided background noise in the room. The object location task and Y-maze spontaneous alterations were performed as previously described (Sierksma et al., 2014; Sierksma et al., 2013).

Brain and stomach tissue processing

Mice were sacrificed by intracardial perfusion using PBS and heparin solution for 10 minutes under deep pentobarbital anesthesia (200 mg/kg). Stomachs (n=8 of wild-type mice) and brains (n=14/genotype) were removed and hippocampus and prefrontal cortex were dissected, snap-frozen in liquid nitrogen and stored at −80 °C until further processing.

Cell culture

Neuro2a (N2a) mouse neuroblastoma (CCL-131™, ATCC, Wesel, Germany) and HT22 mouse hippocampal cell lines (kind gift from Dr. Amalia Dolga, Rijksuniversiteit Groningen) (Davis and Maher, 1994; Morimoto and Koshland, 1990) were cultured in DMEM/F-12 supplemented with GlutaMAX™ (Gibco), 10% fetal bovine serum and penicillin/streptomycin. For treatment with GEBR32a (European patent EP2907806A1) and/or amyloid-β_{1-42} ($A\beta_{1-42}$; AS-24224, Eurogentec),

compounds were dissolved in 100% dimethyl sulfoxide (DMSO) and diluted into culture medium at a final concentration of 0.1% DMSO.

Brain PDE4 activity

PDE activity was measured using a radioactive cAMP hydrolysis assay as described previously (Marchmont and Houslay, 1980). Specific PDE4 activity was determined as pmol cAMP hydrolyzed/min/mg protein as the activity that was ablated by inclusion of 10 μM rolipram (PDE4 inhibitor). Background readings were determined in control tubes where no protein was added. Background values were subtracted before values were normalized to pmol cAMP hydrolyzed/min/mg protein.

Quantitative PCR

RNA was extracted from hippocampal and prefrontal cortical tissue, HT22 cells (treated with 0.1% DMSO or 1 μM $A\beta_{1-42}$ for 24h) and mouse stomach tissue using standard TRIzol-chloroform procedure (TRIzol, Invitrogen). Subsequently, complementary DNA (cDNA) was synthesized using qScript™ cDNA SuperMix (QuantaBio) according to the manufacturer's protocol. Quantitative PCR (qPCR) was performed using the primers listed in Table 1 in combination with SensiMix 2X (Bioline) according to the manufacturer's protocol. All qPCR reactions were performed in duplicate using 12.5 ng sample cDNA and the LightCycler 480 (Roche). The reaction protocol consisted of a polymerase activation cycle (95 °C for 10 min), 40 amplification cycles (95°C for 15 s, primer-specific annealing temperature (T_a; Table 1) for 15 s and 72°C for 15 s), followed by a melting curve cycle (95°C for 5 s and 70°C for 1 min) and cooling cycle (40°C for 30 s). Raw expression data from the LightCycler 480 were analyzed using LinRegPCR to determine logarithmic fluorescence values at cycle zero (Log10 start fluorescence) (Ruijter et al., 2009). qPCR reactions that did not show fluorescent signal amplification were excluded from further analysis. Logarithmic fluorescence values were normalized against the

average expression of the reference genes that showed most stable expression based on geNorm criteria (i.e. Ywhaz and Ppia for hippocampus; Ywhaz and 18s for frontal cortex; Ppia for HT22; Gapdh and Ppia for stomach) (Vandesompele et al., 2002). Normalized data were used for statistical analysis.

Table 1. Primer sequences and annealing temperatures used for qPCR.

Transcript	Forward primer (5'-3')	Reverse primer (5'-3')	T_a (°C)
Pde4d1	GTCAAGCTGGAGCATCTCAGCC	TTCGTAAGCGCTTCACGGG	63
Pde4d3	GCTCAAACCAGAGTGTTGGG	TTCGCAGCTCTTCCGTCATT	58
Pde4d4	GAGCGCTACCTGTACTGCCG	ATGGGATCCAAGGGACTCCG	58
Pde4d5	AATGGCTCAGCAGACGACAA	GGGGAGAGCTTGGGAGAAAC	58
Pde4d6	AGCTGCTGAATTCCGTTCCA	GCCATTCAGGGTGTGGGAAT	58
Pde4d7	CTCACCACCTGCCCTCAAAT	AGGCTCTCCTCACTCTCTCC	58
Pde4d8	CCAGGACCATCTCCAAGAACTA	GCTGTCAGATCGGTACAGGAA	58
Pde4d9	GTTCCCTGAGGACAACGGAG	TGCTTGGAGAATCAGCCCAG	58
18s	ACGGACCAGAGCGAAAGCAT	TGTCAATCCTGTCCGTGTCC	55
Ppia	GCGTCTCCTTCGAGCTGTT	AAGTCACCACCCTGGCA	55
Ywhaz	GCAACGATGTACTGTCTCTTTTGG	GTACACAATTCCTTTCTTGTCATC	49
Gapdh	ACCACAGTCCATGCCATCAC	TCCACCACCCTGTTGCTGTA	58

Genetic knockdown of PDE4D isoforms

Single guide RNAs (gRNA) targeted against murine *Pde4d* isoform-specific DNA sequences (Table 2) were designed with the Zhang-lab online webtool (http://crispr.mit.edu) and cloned as annealed oligos into the pSpCas9(BB)-2A-GFP (PX458) vector (kindly provided by Feng Zhang; Addgene plasmid #48138 ; http://n2t.net/addgene:48138; RRID:Addgene_48138) as described previously (Ran et al., 2013). Briefly, purchased E. coli (Stabl) expressing the PX458 vectors were cultured in LBwith 100 ng/µl ampicillin. PX458 vectors were isolated and purified using a NucleoSpin Plasmid EasyPure kit (Macherey-Nagel). Purified DNA was quantified using a NanoDrop™ 2000 Spectrophotometer (ThermoFisher) and used for restriction using the FastDigest BpiI (IIs class) restriction enzyme (FD1014, Thermo Scientific). Digestion was validated by means of agarose gel electrophoresis and cut vector was excised from the agarose gel using a NucleoSpin Gel and PCR Clean-up kit (Macherey-Nagel). Annealed gRNA oligos were ligated into the restricted and

purified PX458 vector using T4 DNA Ligase (EL0014, Thermo Scientific). Correct incorporation of the gRNA and vector integrity were validated by means of Sanger sequencing and restriction analysis. One Shot Stbl3 chemically competent E. coli (Invitrogen) were transformed with the ligated vectors by means of heatshock and then cultured in ampicillin-containing LB agar plates for subsequent colony selection. Colonies were picked and cultured, followed by vector isolation and purification using a NucleoBond Xtra Midi EF kit (Macherey-Nagel, Düren, Germany). Purified PX458 containing the gRNAs complementary to PDE4D isoform-specific sequences were used to transfect HT22 cells using NeuroMag reagent (Oz Biosciences). Unrestricted vector with a short scrambled gRNA sequence was used as a negative control vector. The expected frameshift frequencies upon CRISPR-induced DNA cuts (Table 2) were calculated using the inDelphi machine-learning algorithm established by David K. Gifford, Jonathan Yee-Ting Hsu and Max Walt Shen (Shen et al., 2018).

Table 2. Oligonucleotide sequences to be annealed and ligated in the PX458 vector as gRNA against PDE4D isoforms.

Isoform	Forward gRNA (5'-3')	Reverse gRNA (5'-3')	Frameshift frequency
Pde4d1	CACCGCATCCGAGCATGGCGGGGTA	AAACTACCCCGCCATGCTCGGATG	67,7%
Pde4d3	CACCGTACATGCAACATAGGAGACG	AAACCGTCTCCTATGTTGCATGTAC	89,4%
Pde4d4	CACCGCCCGGGCGGTCAGCGAAGA	AAACTCTTCGCTGACCGCCCGGGC	61,6%
Pde4d5	CACCGAAGTGGATAATCCGCATGT	AAACACATGCGGATTATCCACTTC	61,5%
Pde4d6	CACCGTATTTATTGTCAGTGTCTTG	AAACCAAGACACTGACAATAAATA	80,5%
Pde4d7	CACCGATCTCGTACGGCGACTTTCT	AAACAGAAAGTCGCCGTACGAGAT	85.9%
Pde4d8	CACCGAGAACTAGAACAAGATTGCG	AAACCGCAATCTTGTTCTAGTTCTC	73,7%
Pde4d9	CACCGGTCTACAAGTTCCCTGAGG	AAACCCTCAGGGAACTTGTAGACC	57,5%

Following the functional experiments, a selection of sgRNAs were validated for their effective targeting of the predicted site. DNA from HT22 cells was isolated with the DNeasy Blood & Tissue kit (Qiagen) according to manufacturer's

instructions. A cell-free cleavage assay was performed using the Guide-It sgRNA In Vitro Transcription and Screening System (Takara Bio) according to manufacturer's instructions. Primer sequences and results are described in Supplementary Table 1, Supplementary Table 2, and Supplementary Figure 1.

Western blotting

Mouse hippocampal (HIP) and prefrontal cortex (PFC) tissues were homogenised and reconstituted in lysis buffer (25 mM Tris–HCl, 150 mM NaCl, 0.5% sodium deoxycholate, 1% NP-40, 1 mM DTT, 0.1% SDS; pH 7.5), supplemented with complete protease inhibitor and PhosSTOP phosphatase inhibitor (Roche). Protein extracts were diluted in SDS sample buffer (10% SDS, 300mM Tris-HCl, 0.05% bromothymol blue, 10% β-mercaptoethanol) and combined to create three replicates of 12.5 µg total protein per condition per tissue type. Cell extracts were resolved in 4-12% gradient SDS-PAGE and transferred onto nitrocellulose membranes (Bio-Rad Laboratories). Membranes were blocked in TBS-based Intercept Blocking Buffer (Li-Cor) for 1h at room temperature, followed by incubation in Total Protein stain (Li-Cor, 926-11011) to confirm appropriate transfer. Membranes were then destained as per manufacturer's instructions (Li-Cor) and incubated overnight in rabbit anti-phosphoCREB (Ser133) (1:1000, #9191, Cell Signaling Technology), rabbit anti-CREB (1:1000, #9192, Cell Signaling Technology), rabbit anti-PKA phospho-substrate (1:1000, # 9621, Cell Signaling Technology), rabbit anti-Pan PDE4D (1:3000, Abcam, ab171749) and mouse anti-GAPHD (1:3000, Abcam, ab8245) at 4°C, and subsequently incubated with donkey anti-rabbit IRDye 800nm (1:10.000, Li-Cor, 926-33213) and donkey anti-mouse IRDye 700nm (1:10.000, Li-Cor, 926-68072) for 1h at room temperature.

For western blots of N2a cell extracts, cells were lysed using 3T3 lysis buffer (25 mM HEPES, 25 mM EDTA, 50 mM NaCl, 50 mM NAF, 30 mM sodium pyrophosphate, 10% glycerol, 1% Triton-X; pH 7.5) supplemented with protease inhibitor mix and PhosSTOP phosphatase inhibitor (Roche). Cell extracts (12.5 µg

total protein) were resolved in 10% SDS polyacrylamide gel electrophoresis and then transferred onto nitrocellulose membranes (Bio-Rad Laboratories). The membranes were blocked (50% Odyssey blocking buffer in PBS; Li-Cor, Lincoln, NE) for 1h at room temperature, followed by overnight incubation rabbit anti-phosphoCREB (Ser133) (1:1000, #9198, Cell Signaling Technology), mouse anti-CREB (1:1000, #9104, Cell Signaling Technology) and mouse anti-GAPDH (1:1,000,000, #10R-G109A; Fitzgerald Industries, Acton, MA) at 4°C. Membranes were subsequently incubated with goat anti-rabbit IRDye 800 (1:10.000, Li-Cor, 926-32211) and donkey anti-mouse IRDye 680 (1:10.000, Li-Cor, 926-68072) for 1h at room temperature. All immunoblots were visualized using the Odyssey CLx scanner, and protein bands were quantified using ImageJ by means of densitometry (Schneider et al., 2012).

Neuronal morphology assessment

To assess neuronal morphology of N2a and HT22 cells, cells were seeded in 24- or 48-wells plates to be treated with GEBR32a and/or $A\beta_{1-42}$ or to be transfected. N2a cells were treated with DMSO or 0.1-1.0 µM GEBR32a for 48h (n=6/condition). HT22 cells were incubated with DMSO (n=12/condition) or 0.01-1.0 µM GEBR32a (n=6/condition). In another set of experiments, HT22 cells were treated with 0.5-1.0 µM $A\beta_{1-42}$ alone and GEBR32a (1 µM) and $A\beta_{1-42}$ (1 µM) and incubated for 24h (n=6/condition). For transfection experiments, HT22 cells were cultivated for 48h upon transfection or exposed to 1 µM $A\beta_{1-42}$ for 24h, one day post-transfection (n=9-12/condition). To visualize and quantify neuronal morphology, the Neurite Outgrowth Staining Kit (A15001, Invitrogen) was used to fix and membrane-stain the cells according to the manufacturer's protocol. Pictures (20x magnification) were taken with an Olympus IX81 inverted microscope connected to an ORCA-fusion digital CMOS camera (C14440-20UP, Hamamatsu) using the MicroManager open source software (Edelstein et al., 2010; Edelstein et al., 2014). Per well, three images were captured and used for neurite outgrowth analysis by the NeuronJ plugin for ImageJ (Meijering et al., 2004; Schneider et al., 2012). Average neurite length per

condition was normalized against the control conditions (i.e. DMSO-treated or control-transfected cells).

cAMP determination in cultured cells

To evaluate the effect of PDE4D-inhibition by GEBR32a on global intracellular cAMP levels, N2a and HT22 cells were seeded in 12 well plates at 10^6 cells per well. Cells were treated with DMSO or GEBR32a 0.01-3 µM (n≥4/condition) and 1 µM of the adenylyl cyclase activator forskolin (MedChemExpress, HY-15371) for 1h and subsequently lysated in 0.1M HCl. Concentrations of cAMP were measured using the Cyclic AMP ELISA Kit (Cayman Chemical Company, 581001) according to manufacturer's instructions. Results are depicted as fold change over DMSO control.

Immunocytochemisty

To investigate PDE4D protein localization, HT22 cells were seeded on 12mm glass coverslips (VWR, 631-1577) coated with 100 µg/mL Poly-L-Ornithine (Sigma, P4957) and 1 µg/mL laminin (Sigma, L2020) and grown for 24h. After fixation in 4% paraformaldehyde, cells were permeabilized using 0.1% TritonX-100. After blocking with 10% BSA for 1h, cells were incubated with rabbit anti-PDE4D (1:250; ab14613, Abcam) overnight at 4°C. Then, cells were incubated with goat anti-rabbit Alexa647 (1:250; Invitrogen) for 1h at room temperature. Finally, nuclei were counterstained with Hoechst (1:500; Sigma).

For immunocytochemistry following transfection experiments in HT22, the same protocol was used except for the antibodies used. Mouse anti-FLAG primary antibodies (1:1000; M2 clone, Sigma-Aldrich) and donkey anti-mouse Alexa488-conjugated secondary antibody (1:250; Invitrogen) were used to determine which cells were successfully transfected and expressed the FLAG-encoding PX458 plasmid. PDE4D localization was imaged after mounting the coverslips on microscope glasses

using a disc spinning unit (DSU) microscope (Olympus). Morphology assessment of transfected, FLAG-positive HT22 cells was performed as described above.

Gene ontology (GO) term enrichment analysis

Determining the involvement of PDE4D in specific biological processes was approached by examining whether known PDE4D interaction proteins are enriched in these processes. The list of known PDE4D interactors was retrieved from BioGRID (https://thebiogrid.org/)(Stark et al., 2006) and used for gene ontology (GO) term enrichment analysis using ToppGene Suite with default settings (https://toppgene.cchmc.org/)(Chen et al., 2009). The complete GO analysis output of significantly enriched Biological Process GO terms can be found in Table 3.

Statistical analysis

For the OLT and Y-maze behavioral tasks, memory performance of WT and APPswe/PS1dE9 was assessed statistically by performing two-tailed paired t-tests between genotypes and comparing performance of each genotype against chance performance (i.e. 0 for OLT and 50% for Y-maze). Likewise, normalized qPCR, PDE4 activity, and WB values were used to compare expression/activity differences between genotypes by means of two-tailed t-tests. For *in vitro* studies on neurite length, CREB phosphorylation, and cAMP concentration, one-way ANOVAs were performed with Dunnett's post-hoc t-tests using the DMSO condition as control. Differences in PDE4D isoform mRNA expression between DMSO- and Aβ-treated HT22 cells were investigated by means of two-tailed t-tests. The effect of genetic knockdown of PDE4D isoforms on neuronal morphology was analyzed by means of one-way ANOVA of normalized neurite lengths followed by Dunnett's post-hoc t-tests. The effect of genetic knockdown of PDE4D isoforms in combination with Aβ exposure was compared to control-transfected conditions with and without exposure to Aβ by means of one-way ANOVA followed by Dunnett's post-hoc t-tests.

Table 3. GO analysis output of significantly enriched terms of PDE4D interactors.

ID	Name	q-value Bonferroni	Hit # Query	Hit # Genome
GO:0031175	neuron projection development	4,46E-07	19	1151
GO:0090087	regulation of peptide transport	8,55E-07	17	867
GO:0120036	plasma membrane bounded cell projection organization	8,91E-07	22	1790
GO:0030030	cell projection organization	1,37E-06	22	1828
GO:1904951	positive regulation of establishment of protein localization	2,73E-06	14	521
GO:0048666	neuron development	3,79E-06	19	1298
GO:0051223	regulation of protein transport	6,25E-06	16	825
GO:0048667	cell morphogenesis involved in neuron differentiation	7,15E-06	15	689
GO:0070201	regulation of establishment of protein localization	1,49E-05	16	874
GO:0051222	positive regulation of protein transport	2,06E-05	13	483
GO:0048812	neuron projection morphogenesis	2,10E-05	15	743
GO:0120039	plasma membrane bounded cell projection morphogenesis	2,78E-05	15	758
GO:0048858	cell projection morphogenesis	3,06E-05	15	763
GO:0032990	cell part morphogenesis	4,41E-05	15	783
GO:0007409	axonogenesis	7,72E-05	13	537
GO:0051050	positive regulation of transport	8,53E-05	17	1157
GO:0030182	neuron differentiation	1,18E-04	19	1579
GO:0038093	Fc receptor signaling pathway	1,23E-04	10	242
GO:0009967	positive regulation of signal transduction	1,49E-04	20	1823
GO:0000904	cell morphogenesis involved in differentiation	2,04E-04	15	873
GO:0061564	axon development	2,19E-04	13	584
GO:0022008	neurogenesis	2,30E-04	20	1867
GO:0007267	cell-cell signaling	3,13E-04	20	1899
GO:1901701	cellular response to oxygen-containing compound	5,35E-04	17	1301
GO:1902533	positive regulation of intracellular signal transduction	5,95E-04	16	1119
GO:0048699	generation of neurons	7,06E-04	19	1752
GO:0002768	immune response-regulating cell surface receptor signaling pathway	8,80E-04	12	519
GO:0001775	cell activation	9,48E-04	18	1559
GO:0000902	cell morphogenesis	1,28E-03	16	1179
GO:0032880	regulation of protein localization	1,43E-03	16	1188
GO:1901700	response to oxygen-containing compound	1,62E-03	19	1839
GO:0002764	immune response-regulating signaling pathway	1,99E-03	13	699
GO:0030100	regulation of endocytosis	3,17E-03	9	241
GO:0090316	positive regulation of intracellular protein transport	5,02E-03	8	171

ID	Name	q-value Bonferroni	Hit # Query	Hit # Genome
GO:0032989	cellular component morphogenesis	5,15E-03	16	1297
GO:0035690	cellular response to drug	6,76E-03	11	485
GO:1903829	positive regulation of cellular protein localization	6,87E-03	10	366
GO:0002682	regulation of immune system process	7,78E-03	18	1776
GO:0060627	regulation of vesicle-mediated transport	8,07E-03	12	631
GO:0042325	regulation of phosphorylation	8,13E-03	18	1781
GO:0043549	regulation of kinase activity	1,11E-02	14	978
GO:0032386	regulation of intracellular transport	1,30E-02	10	391
GO:0120035	regulation of plasma membrane bounded cell projection organization	1,41E-02	13	822
GO:0031344	regulation of cell projection organization	1,63E-02	13	832
GO:0046824	positive regulation of nucleocytoplasmic transport	1,84E-02	6	71
GO:0042110	T cell activation	1,95E-02	11	537
GO:0050804	modulation of chemical synaptic transmission	2,03E-02	11	539
GO:0099177	regulation of trans-synaptic signaling	2,07E-02	11	540
GO:0034504	protein localization to nucleus	2,15E-02	9	300
GO:0071417	cellular response to organonitrogen compound	2,62E-02	12	701
GO:0060341	regulation of cellular localization	3,10E-02	14	1060
GO:0038096	Fc-gamma receptor signaling pathway involved in phagocytosis	3,45E-02	7	139
GO:0002433	immune response-regulating cell surface receptor signaling pathway involved in phagocytosis	3,45E-02	7	139
GO:0051098	regulation of binding	3,74E-02	10	437
GO:0010941	regulation of cell death	4,00E-02	18	1969
GO:0051057	positive regulation of small GTPase mediated signal transduction	4,11E-02	6	81
GO:0038094	Fc-gamma receptor signaling pathway	4,20E-02	7	143
GO:0051960	regulation of nervous system development	4,31E-02	14	1088
GO:0051338	regulation of transferase activity	4,36E-02	14	1089
GO:0002431	Fc receptor mediated stimulatory signaling pathway	4,63E-02	7	145
GO:0019220	regulation of phosphate metabolic process	4,88E-02	18	1994
GO:0051174	regulation of phosphorus metabolic process	4,92E-02	18	1995

RESULTS

Impaired spatial memory and altered PDE4D-mediated cAMP-PKA-CREB signaling in female APP/PS1 mice

Spatial memory assessment in the OLT and Y-maze spontaneous alterations task demonstrated that APP/PS1 mice were cognitively impaired compared to WT mice. More specifically, in the OLT, both genotypes showed intact memory performance using a 1-hour inter-trial interval (Fig 1A; ###: $P<0.001$ two-tailed t-test against 0). Using a 4-hour interval, WT mice showed intact spatial memory, whilst APP/PS1 did not (###: $P<0.001$ paired two-tailed t-test against 0). In addition, APP/PS1 mice performed significantly worse than WT mice (Fig 1A; ***: $P<0.001$ two-tailed t-test). Similarly, whilst both genotypes performed significantly better than chance level in the Y-maze spontaneous alterations task (Fig 1B; ##: $P<0.01$, ###: $P<0.001$, paired two-tailed t-test against 50%), APP/PS1 mice performed worse than WT mice (*: $P<0.05$, two-tailed t-test).

After observing the memory deficits in APP/PS1 mice, hippocampal and frontal cortical tissue of these animals was used for biochemical assessments to investigate potentially associated alterations in PDE4D-mediated cAMP-PKA-CREB signaling. PDE4D mRNA expression of specific isoforms was found to be higher in APP/PS1 in both brain regions. In the hippocampus, PDE4D1, -D3, and -D8 expression was 1.6 to 4.6-fold higher, whilst PDE4D3 and -D5 were 2.1 to 3.7-fold upregulated in the frontal cortex (Fig 1C-D; *: $P<0.05$, two-tailed t-test). At the protein level, general PDE4D expression showed a non-significant increase in the APP/PS1 hippocampus, which was not observed in the frontal cortex (Fig 2A). PDE4 activity was found to be 3-fold higher in the hippocampus, but not in the frontal cortex, of APP/PS1 compared to WT mice (Fig 2B; ***: $P<0.001$, two-tailed t-test). Moreover, assessment of protein expression of phosphorylated PKA substrates and phosphorylated CREB were found to be significantly lower in the hippocampus and

frontal cortex of APP/PS1 mice (Fig 2C-D; *: P<0.05, **: P<0.01; ***: P<0.001, ****: P<0.0001).

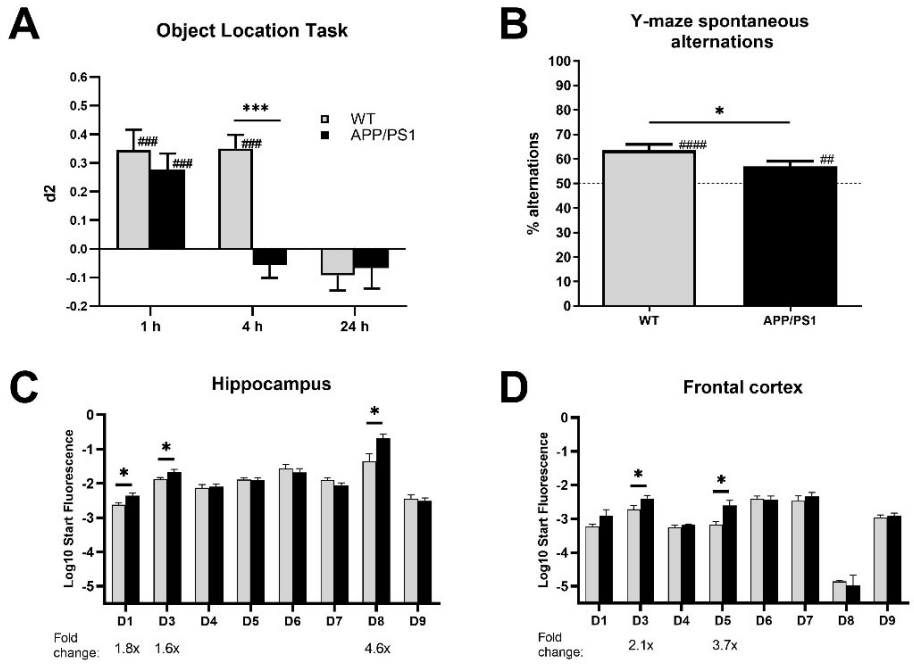

Figure 1. Changes in memory performance and PDE4D-mediated cAMP-PKA-CREB signaling in female APP/PS1 mice compared to wild-type mice. A) Spatial memory performance of WT and APP/PS1 mice in the object location task. Using a 4-hour inter-trial interval revealed impaired memory performance in APP/PS1, but not wild-type (WT) mice (***: P<0.001, two-tailed t-test comparing genotypes; ###: P<0.001, paired two-tailed t-test against 0; n=18-22/genotype). B) Spatial memory performance in the Y-maze spontaneous alterations task. Intact memory, i.e. higher than chance (50%), was found for both genotypes and significantly higher memory performance in WT versus APP/PS1 mice (*: P<0.05, two-tailed t-test; ##: P<0.01, ###: P<0.001, paired two-tailed t-test against 50%; n=18-22/genotype). C-D) PDE4D isoform mRNA expression in hippocampus and frontal cortex of WT and APP/PS1 mice (n=7-8/genotype). Significantly increased expression of specific isoforms was measured in APP/PS1 versus WT mice (*:P<0.05, two-tailed t-test).

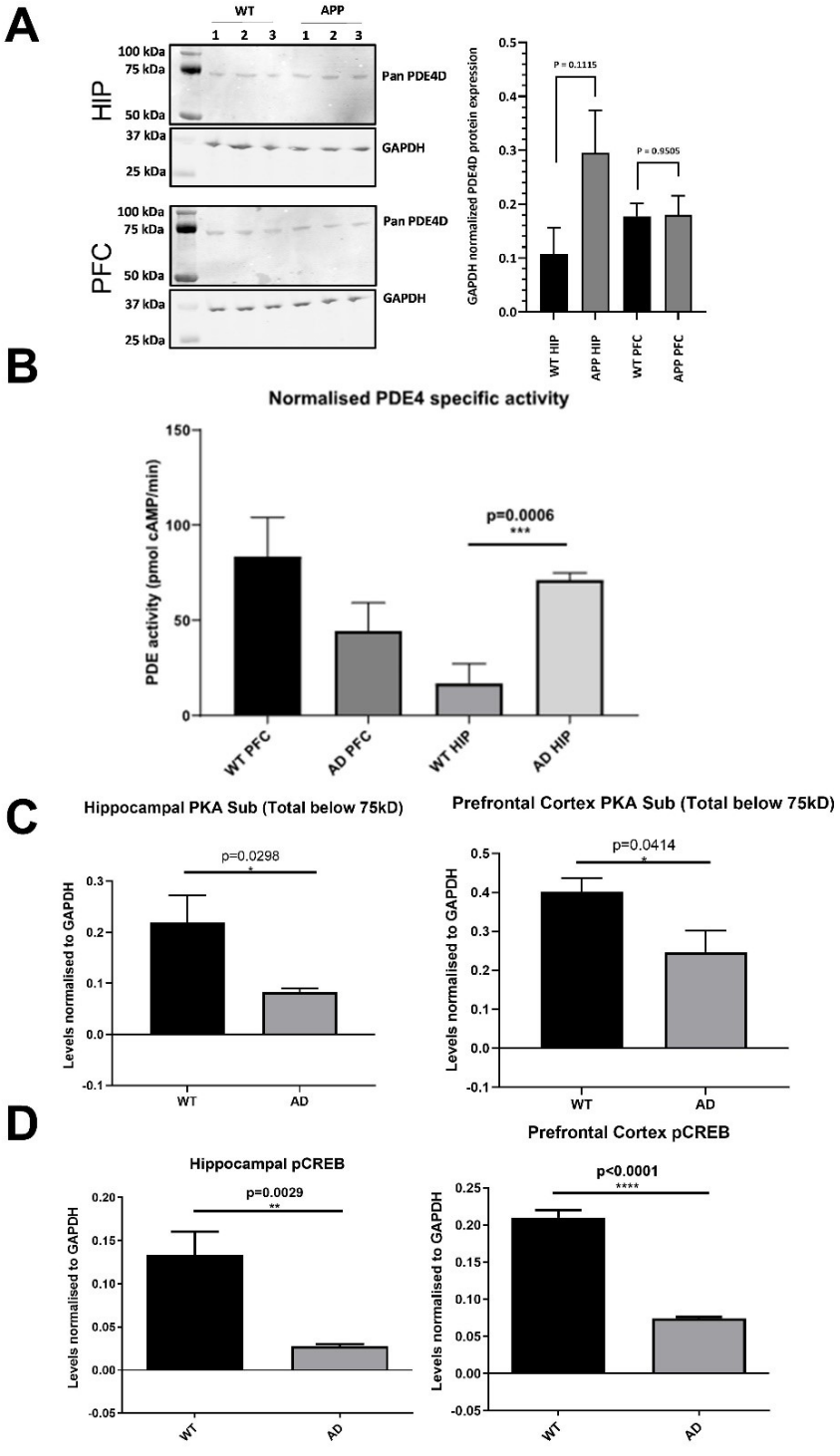
A
WT
APP
1 2 3 1 2 3
HIP
100 kDa
75 kDa
50 kDa
37 kDa
25 kDa
Pan PDE4D
GAPDH
PFC
GAPDH normalized PDE4D protein expression
P = 0.1115
P = 0.9505
WT HIP
APP HIP
WT PFC
APP PFC
B
Normalised PDE4 specific activity
PDE activity (pmol cAMP/min)
p=0.0006
***
WT PFC
AD PFC
WT HIP
AD HIP
C
Hippocampal PKA Sub (Total below 75kD)
p=0.0298
*
Levels normalised to GAPDH
WT
AD
Prefrontal Cortex PKA Sub (Total below 75kD)
p=0.0414
*
D
Hippocampal pCREB
p=0.0029
**
Prefrontal Cortex pCREB
p<0.0001
****

Figure 2. PDE4D protein expression, PDE4 activity and cAMP-PKA-CREB signaling changes in hippocampus and cortex of WT and APP/PS1 mice. A) PDE4D protein expression in hippocampus and cortex of WT and APP/PS1 mice (n=3/genotype). B) Specific PDE4 activity in homogenates of PFC and hippocampal tissue excised from APP/PS1 and WT mice normalized for amount of protein (n=3/genotype). C) Densitometric quantification of western blots measuring phospho-PKA substrates normalized to GAPDH in WT versus APP/PS1 mice (n=6/genotype). D) Densitometric quantification of western blots measuring phosphorylated CREB normalized to GAPDH in WT versus APP/PS1 mice (n=6/genotype, *: $P<0.05$, **: $P<0.01$, ****: $P< 0.0001$, two-tailed t-test). Data are presented as mean + SEM. Western blot scans are provided in the Supplementary Material.

Pharmacological PDE4D inhibition increases CREB phosphorylation and neurite length in N2a cells

To validate the involvement of PDE4D in cAMP-PKA-CREB signaling and neuronal plasticity, N2a cells were treated with the PDE4D-selective inhibitor GEBR32a. After 1h incubation with GEBR32a (0.03-1.0 μM), phosphorylated CREB (pCREB) and total CREB levels were measured by means of western blotting. One-way ANOVA revealed significant differences in normalized pCREB/CREB ratio between conditions ($F(5,30) = 17.83$, $P<0.0001$). Compared to the DMSO condition, significant increases in pCREB/CREB ratio were found for 0.3 and 1.0 μM GEBR32a (*:$P < 0.05$, **:$P < 0.05$, Dunnett's post-hoc t-tests; Fig 3A). Moreover, upon 1h treatment with 3 μM GEBR32a, cAMP levels in N2a cells can increase up to 5-fold compared to the DMSO control (Dunnett's post-hoc t-tests; Supplementary Fig 1).

Similarly, N2a cells were treated with GEBR32a to assess the effects of PDE4D inhibition on neuronal morphology by measuring neurite lengths. After 48h incubation with GEBR32a (0.1-1.0 μM) neurite lengths were measured. One-way ANOVA revealed significant differences in the average neurite length between conditions ($F(3,20) = 6.886$, $P<0.01$). Compared to the DMSO condition, significant increases in average neurite length were found for 0.3 and 1.0 μM GEBR32a (**:$P < 0.01$, Dunnett's post-hoc t-tests; Fig 3B-C). These findings indicate that, in the N2a

cell line, CREB phosphorylation and neurite elongation are stimulated by GEBR32a-induced PDE4D inhibition at 1h and 48h, respectively.

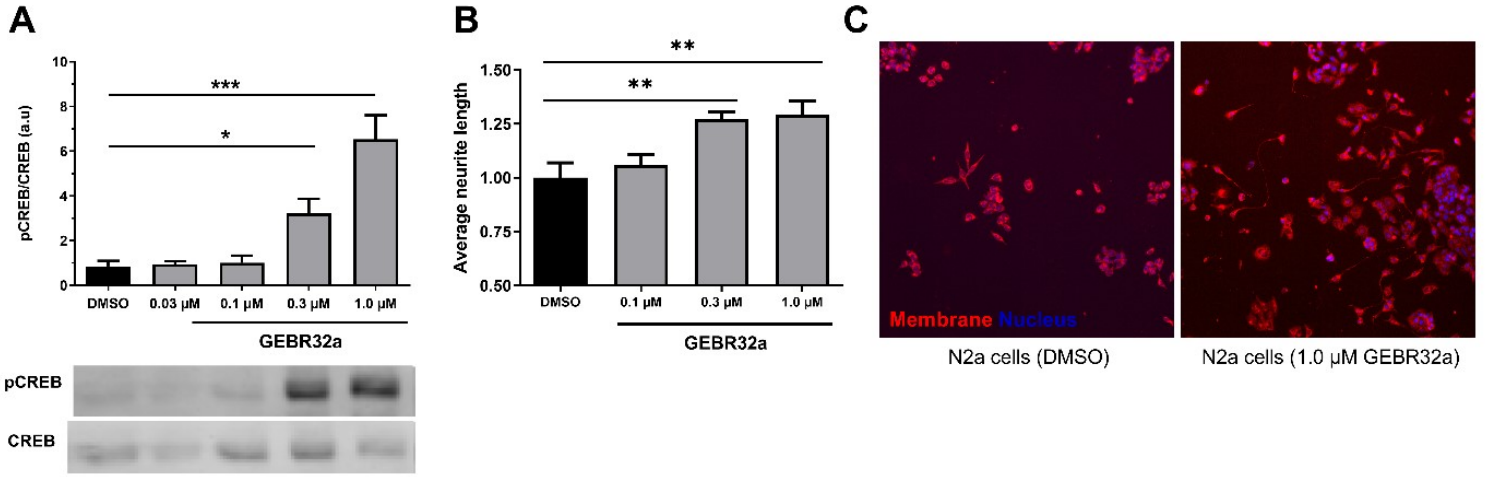

Figure 3. PDE4D inhibition dose-dependently increased CREB phosphorylation and neurite length in N2a cells. A) Phosphorylated CREB (pCREB) to total CREB ratios in N2a cells upon treatment with 0.03-1.0 µM GEBR32a for 1h (Dunnett's post-hoc: *P<0.05, ***P<0.001; n=6/condition). Representative blot scans are shown under the graph. B) Average neurite after incubation with 0.1-1.0 µM GEBR32a for 48h in N2a cells (Dunnett's post-hoc: **P<0.01; n=6/condition). C) Exemplary microscope images indicating N2a neurites in the DMSO (left) and 1.0 µM GEBR32a (right) conditions that were visualized for subsequent tracing. Data is presented as mean + SEM.

Pharmacological PDE4D inhibition induces longer neurites in mouse hippocampal cells

Next, complementing the findings in the mouse neuroblastoma N2a cells, we sought to identify the role of PDE4D in regulating neuronal morphology in the mouse hippocampal HT22 cell line to better approximate the *in vivo* context in which we found changes in hippocampal PDE4D-mediated cAMP-PKA-CREB signaling (Fig 1 and 2). Specifically, HT22 cells were incubated with 0.01-1.0 μM GEBR32a for 48h to assess the effects of pharmacological PDE4D inhibition on neuronal morphology. One-way ANOVA revealed significant differences in the average neurite length between conditions ($F(5,36) = 14.60$, $P<0.001$). Compared to control samples, significant increases in average neurite length were found in cells treated with 0.03-1.0 μM GEBR32a (Fig 4A-B; ***:$P < 0.001$, ****:$P<0.0001$, Dunnett's post-hoc t-tests). Incubation with 3 μM GEBR32a increased cAMP levels 5-fold (Supplementary Fig 2).

As inhibition of PDE4D significantly increased neurite length, we investigated whether PDE4D is localized in or near neurite growth cones to locally regulate cAMP signaling. Based on immunocytochemistry, it was found that PDE4D is expressed in the neurite growth cones of HT22 cells (Fig 4C). Additional support for a role of PDE4D in regulating neuronal morphology was found by investigating the shared biological processes of known PDE4D interaction proteins. The list of known PDE4D interaction proteins was retrieved from BioGRID (Stark et al., 2006) and subjected to gene ontology (GO) enrichment analysis using ToppGene Suite (Chen et al., 2009). PDE4D interacting proteins were found to be significantly enriched in biological processes regulating (neuronal) morphology (Fig 4D). More specifically, 'neuron project development' (GO:0031175) was found to be most significantly enriched. Through interaction with the proteins enriched in these processes, PDE4D is likely to be optimally localized to regulate neuronal morphology. The complete GO analysis including interaction proteins per biological process can be found in Supplementary Table 3.

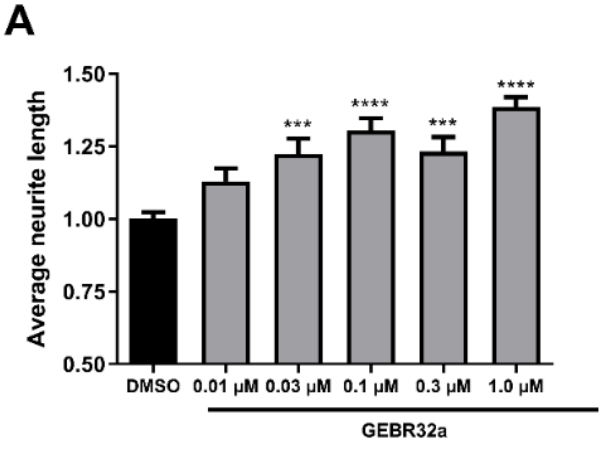

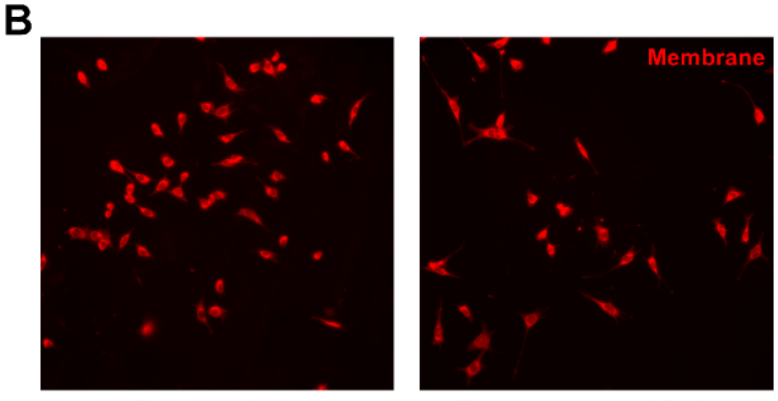

HT22 cells (DMSO)

HT22 cells (0.1 µM GEBR32a)

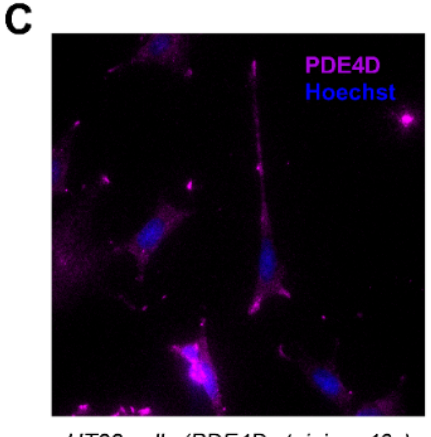

HT22 cells (PDE4D staining, 40x)

D

ID	Name	p-value	q-value Bonferroni	Hit Count (Query)	Hit Count (Genome)
GO:0031175	**neuron projection development**	1,53E-10	4,46E-07	19	1151
GO:0090087	regulation of peptide transport	2,93E-10	8,55E-07	17	867
GO:0120036	**plasma membrane bounded cell projection organization**	3,05E-10	8,91E-07	22	1790
GO:0030030	**cell projection organization**	4,68E-10	1,37E-06	22	1828
GO:1904951	positive regulation of establishment of protein localization	9,35E-10	2,73E-06	14	521
GO:0048666	**neuron development**	1,30E-09	3,79E-06	19	1298
GO:0051223	regulation of protein transport	2,14E-09	6,25E-06	16	825
GO:0048667	**cell morphogenesis involved in neuron differentiation**	2,45E-09	7,15E-06	15	689
GO:0070201	regulation of establishment of protein localization	5,12E-09	1,49E-05	16	874
GO:0051222	positive regulation of protein transport	7,04E-09	2,06E-05	13	483
GO:0048812	**neuron projection morphogenesis**	7,18E-09	2,10E-05	15	743
GO:0120039	**plasma membrane bounded cell projection morphogenesis**	9,53E-09	2,78E-05	15	758
GO:0048858	**cell projection morphogenesis**	1,05E-08	3,06E-05	15	763
GO:0032990	**cell part morphogenesis**	1,51E-08	4,41E-05	15	783
GO:0007409	**axonogenesis**	2,64E-08	7,72E-05	13	537
GO:0051050	positive regulation of transport	2,92E-08	8,53E-05	17	1157
GO:0030182	**neuron differentiation**	4,03E-08	1,18E-04	19	1579
GO:0038093	Fc receptor signaling pathway	4,20E-08	1,23E-04	10	242
GO:0009967	positive regulation of signal transduction	5,11E-08	1,49E-04	20	1823
GO:0000904	**cell morphogenesis involved in differentiation**	6,99E-08	2,04E-04	15	873

Figure 4. PDE4D regulates neuronal morphology based on HT22 neurite assessment, PDE4D localization and gene ontology term enrichment of PDE4D interaction proteins. A) Average neurite length after incubation of HT22 cells with 0.01-1.0 µM GEBR32a for 48h (Dunnett's post-hoc: ***P<0.001, ****P<0.0001; n=6-12/condition). B) Representative microscope images indicating HT22 neurites in the DMSO (left) and 0.1 µM GEBR32a (right) conditions that were visualized for subsequent tracing. C) Representative HT22 immunofluorescence image showing the predominant localization of PDE4D in neurites and their growth cones. D) Gene ontology (GO) term enrichment analysis of biological processes of PDE4D interaction proteins (retrieved from BioGRID (Stark et al., 2006)) showing enrichment for processes related to (neuronal) morphology regulation (in bold). Top twenty terms are shown, the entire list is provided in Supplementary Table 3. Data is presented as mean + SEM.

Pharmacological PDE4D inhibition protects against $A\beta_{1-42}$-induced reductions in neurite length

Since APP/PS1 mice showed impaired spatial memory performance and altered cAMP-PKA-CREB signaling as a result of excessive Aβ production, we subsequently examined whether $A\beta_{1-42}$ exposure negatively impacts neurite growth in HT22 cells and whether PDE4D inhibition can protect against these effects. HT22 cells were incubated for 24h with 0.5-1.0 µM $A\beta_{1-42}$ or a combination of $A\beta_{1-42}$ and GEBR32a (both 1 µM). One-way ANOVA revealed significant differences in the average neurite length between conditions ($F(3,20) = 6.932$, $P<0.01$). Compared to the DMSO condition, a significantly decreased average neurite length was found for 1.0 µM $A\beta_{1-42}$ (Fig 5A ; *:$P < 0.05$, Dunnett's post-hoc t-tests). Combined incubation with $A\beta_{1-42}$ and GEBR32a was able to prevent this $A\beta_{1-42}$-induced neurite length reduction (Fig 5A; ##:$P<0.01$, two-tailed t-test). PDE4D expression measurement indicated that, concurrent with reducing the HT22 average neurite length, 1 µM $A\beta_{1-42}$ increases mRNA expression of the specific isoforms PDE4D3 and -D5 (Fig 5B; *:$P<0.05$, **:$P<0.01$, two-tailed t-test). It should be noted that PDE4D4 and PDE4D8 mRNA could not be detected in HT22 cells.

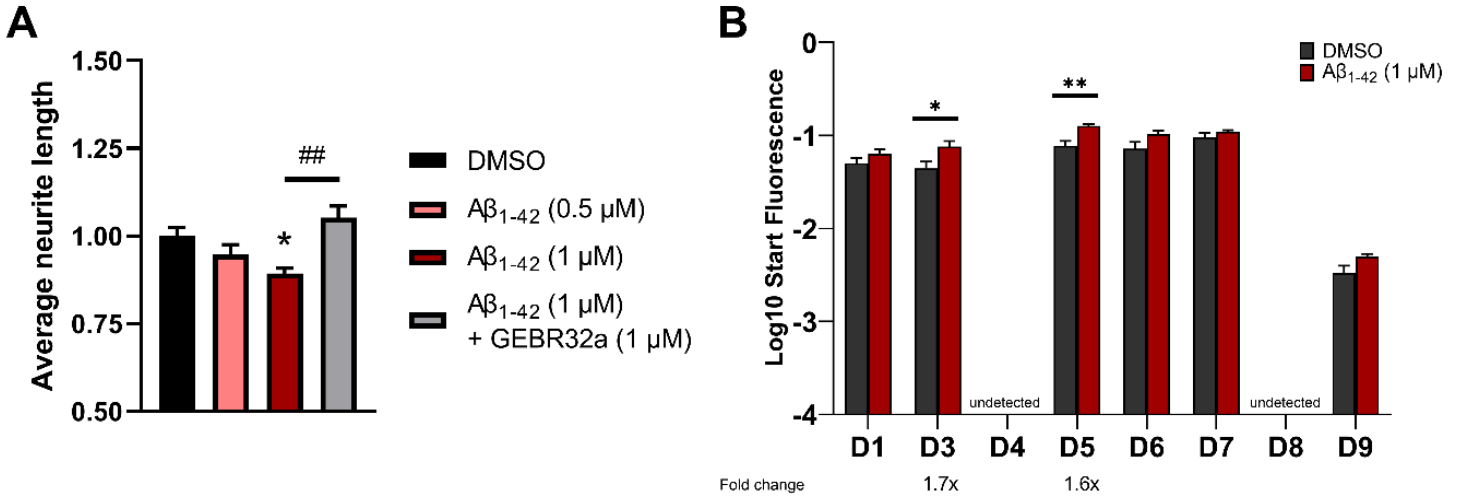

Figure 5. $A\beta_{1-42}$ exposure reduced the average neurite length in HT22 cells and increased isoform-specific PDE4D expression. A) Average neurite length after incubation of HT22 cells with 0.5-1.0 μM $A\beta_{1-42}$ or GEBR32a and $A\beta_{1-42}$ (both 1 μM) for 24h (Dunnett's post-hoc: *P<0.05; two-tailed t-test: ##:P<0.01; n=6/condition). B) PDE4D isoform mRNA expression after 1 μM $A\beta_{1-42}$ exposure for 24h in HT22 (*:P<0.05, **:P<0.01, two-tailed t-test; n=6/condition). Data is presented as mean + SEM.

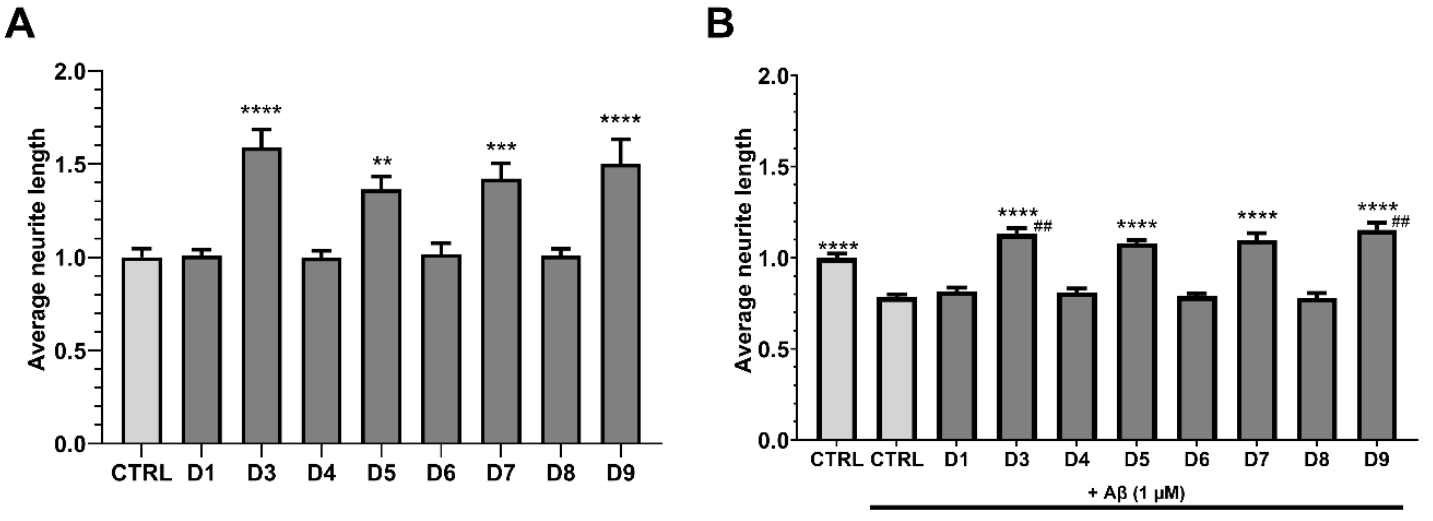

Figure 6. Genetic knockdown of specific PDE4D isoforms caused increased HT22 neurite length and protected against $A\beta_{1-42}$-induced neurite length reduction. HT22 cells were transfected with CRISPR-Cas9 vectors to genetically knock down specific PDE4D isoforms. A) Average neurite lengths upon PDE4D isoform knockdown 48h after transfection (**:P<0.01, ***:P<0.001, ****:P<0.0001, Dunnett's post-hoc t-tests; n=9-12/condition). B) Average neurite lengths upon PDE4D isoform knockdown 48h after transfection with 1 μM $A\beta_{1-42}$ exposure during the last 24h (****:P<0.0001, Dunnett's post-hoc t-tests compared to control with $A\beta_{1-42}$ exposure; n=9/condition). Comparisons against control transfection without $A\beta_{1-42}$ exposure with higher average neurite lengths are shown by hashes (##: P<0.01, Dunnett's post-hoc t-tests). For clarity, significantly lower neurite lengths than control without $A\beta_{1-42}$ (i.e. CTRL+ $A\beta_{1-42}$, D1, D4, D6, and D8 based on Dunnett's post-hoc t-tests) are not indicated in the graph. Data is presented as mean + SEM.

Neurite growth is regulated by long PDE4D isoforms both in absence and presence of $A\beta_{1-42}$

PDE4D isoforms seem to be differentially expressed upon $A\beta_{1-42}$ exposure both *in vivo* (Fig 1C-D) and *in vitro* (Fig 5B), and isoforms are known to localize to distinct cellular compartments to regulate specific processes (Houslay, 2010). As non-specific inhibition of all PDE4D isoforms may cause severe adverse effects, we investigated whether specific PDE4D isoforms regulate neurite growth in HT22 cells and could serve as a more specific therapeutic target for AD treatment. Individual PDE4D isoforms were genetically knocked down in HT22 cells by transfection with CRISPR-Cas9 vectors, after which average neurite length was measured. 48h after transfection, one-way ANOVA revealed significant differences in the average neurite length between conditions ($F(8,75) = 12.36$, $P<0.0001$). Compared to the control condition, 1.36 to 1.59-fold increased average neurite lengths were found for knockdown of PDE4D3, -D5, -D7, and -D9 (Fig 6A; **:P<0.01, ***:P<0.001, ****:P<0.0001, Dunnett's post-hoc t-tests).

Next, it was examined whether PDE4D isoform knockdown could prevent $A\beta_{1-42}$-induced reductions in average neurite length. To this purpose, PDE4D isoforms were knocked down and cells were exposed to 1 µM $A\beta_{1-42}$ for 24h one day post-transfection after which average neurite lengths were measured. One-way ANOVA revealed significant differences in the average neurite length between conditions ($F(8,68) = 36.34$, $P<0.0001$). In the presence of $A\beta_{1-42}$, knockdown of PDE4D3, -D5, -D7, and -D9 increased average neurite length by 1.38 to 1.46-fold increased average neurite lengths were found for when compared to the control condition with $A\beta_{1-42}$ (****:P<0.0001, Dunnett's post-hoc t-tests; Fig 6B). Moreover, in the absence of $A\beta_{1-42}$, average neurite length upon control transfection was significantly higher than upon control transfection with $A\beta_{1-42}$ (****:P<0.0001, Dunnett's post-hoc t-tests; Fig 6B). Compared to the control condition without $A\beta_{1-42}$, PDE4D3 and -D9 knockdown countered the effect of $A\beta_{1-42}$ and was associated

with significantly increased average neurite length (##:P<0.01, Dunnett's post-hoc t-tests, Fig 6B). Knockdown of PDE4D1, -D4, -D6, and -D8 with exposure to $A\beta_{1-42}$ led to significantly lower average neurite lengths compared to the control condition without $A\beta_{1-42}$ exposure (P<0.0001, Dunnett's post-hoc t-test, not shown in the graph).

Not all neurite growth-controlling PDE4D isoforms are expressed in the mouse stomach

Upon determining PDE4D isoforms mediating neurite growth processes, PDE4D isoform expression was measured in the mouse stomach to assess which PDE4D isoforms would likely mediate gastrointestinal side effects in the stomach upon PDE4(D) inhibition. As shown in Figure 7, the expression profile of PDE4D in the mouse stomach differs from the expression in the mouse hippocampus (Fig 1C), prefrontal cortex (Fig 1D), and HT22 cells (Fig 5B). Interestingly, of the neurite growth-controlling PDE4D isoforms (i.e. PDE4D3, -D5, -D7, and -D9), PDE4D3 and PDE4D5 show a similarly high level of expression in the mouse stomach, whilst PDE4D7 and PDE4D9 are 6.6-fold and >1700-fold lower expressed than PDE4D3 and PDE4D5.

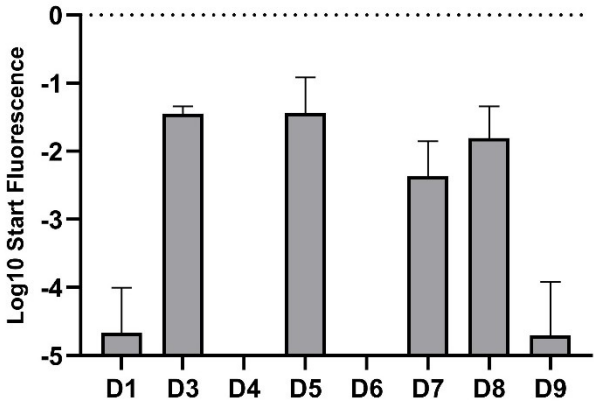

Figure 7. Isoform-specific PDE4D expression in the stomach of wild-type mice. mRNA expression of PDE4D isoforms was measured in stomach tissue of wild-type mice by means of qPCR (n=8) indicating highest expression of PDE4D3 and PDE4D5.

DISCUSSION

cAMP-PKA-CREB signaling has been well-established as a pathway that is crucial for synaptic plasticity and memory consolidation (Kandel, 2012). Moreover, impaired memory consolidation and cognitive deficits in AD have been associated with deficient cAMP-PKA-CREB signaling (Saura and Valero, 2011). Inhibition of the cAMP-degrading PDE4D enzymes has been found to restore memory functioning in transgenic AD mice (Cui et al., 2019; Sierksma et al., 2014). Despite this therapeutic potential, non-specific PDE4D inhibition has been associated with severe adverse effects (e.g. nausea and vomiting), which has hampered clinical progression of PDE4(D) inhibitors (Blokland et al., 2019a; Paes et al., 2021). Remarkably, PDE4D enzymes comprise multiple protein isoforms that show tissue- and cell type-specific expression and regulate distinct intracellular processes (Baillie et al., 2019; Houslay, 2010; Paes et al., 2021). Hence, treatment efficacy may be enhanced or maintained, while side effects are reduced, by specifically targeting those PDE4D isoforms that are involved in synaptic plasticity. Therefore, we investigated whether PDE4D isoforms are differentially expressed in transgenic AD mice and whether specific PDE4D isoforms control neurite growth as a measure of plasticity. Additionally, we examined whether PDE4D inhibition or individual PDE4D isoform knockdown could protect against Aβ-induced toxicity.

Cognitive phenotyping revealed spatial memory deficits in female APP/PS1 mice at 7 months of age. These findings replicate a prior study using the same genotypes and behavioral tasks (Sierksma et al., 2014). In our follow-up biochemical assessment, it was demonstrated that CREB phosphorylation was reduced in the hippocampus and frontal cortex of APP/PS1 mice. Moreover, we measured mRNA expression increases for PDE4D1, -D3, and -D8 in the hippocampus and for PDE4D3 and -D5 in the frontal cortex of APP/PS1 mice. Recently, we also found the same PDE4D isoforms to show pathology-associated, increased expression in post-mortem human middle temporal gyrus tissue of AD patients (Paes et al., 2020a). In

addition, the observation of increased PDE4D3 mRNA expression in the hippocampus of APP/PS1 mice corresponds to the fact that hippocampal injections of $A\beta_{1-42}$ in wild type mice caused elevated PDE4D(3) protein expression (Wang et al., 2016). Here, we also show that PDE4 activity was increased in the hippocampus of APP/PS1 mice, which may be a result of increases in PDE4D3 expression. While we report changes in PDE4D isoform mRNA expression, a non-significant trend of increase was found for PDE4D protein expression in the hippocampus of APP/PS1 mice using an antibody that is not isoform-specific. Multiple isoforms (e.g. PDE4D3 and PDE4D8) would migrate identically on SDS-PAGE and could therefore not be distinguished (Houslay and Conti, 2010). However, our observations are in accordance with previous reports showing increases in hippocampal PDE4D protein expression in transgenic Alzheimer mice and mice exposed to exogenous Aβ (Shi et al., 2021a; Wang et al., 2020). Whether protein levels of specific PDE4D isoforms are upregulated whilst others are unaffected or are downregulated remains to be determined. Most importantly, we conducted the *in vivo* experiment to provide proof-of-concept of the change in PDE4D isoform signature associated with AD-related cognitive decline. Results are similar to the results from our previously reported and abovementioned human AD post-mortem study in which we included both females and males, yielding comparable results (Paes et al., 2020a). Hence, the finding in these female mice provided a step towards the *in vitro* pharmacological inhibition and genetic editing in murine cells.

When examining whether PDE4D inhibition can stimulate cAMP-PKA-CREB signaling, we found that the PDE4D-selective inhibitor GEBR32a significantly increased CREB phosphorylation *in vitro*, which is in accordance with previous studies using PDE4 and PDE4D inhibitors (MacKenzie and Houslay, 2000; Zhang et al., 2017). Moreover, GEBR32a at a concentration of 3 μM substantially increased global intracellular cAMP levels in both N2a and HT22 cells. This is in line with the IC_{50} of the compound, 2.43 μM (Prosdocimi et al., 2018). Furthermore, pharmacological

PDE4D inhibition induced a dose-dependent increase in neurite length in both N2a and HT22 cells. The role of PDE4D in regulating neurite outgrowth was supported by the localization of PDE4D protein in growth cones and the fact that many of known PDE4D-interacting proteins are involved in neuron projection development. As PDE4D was also found to localize to microtubules in neurons of the macaque prefrontal cortex (Datta et al., 2020), there is evidence that PDE4D also regulates neuronal morphology *in vivo*. Pharmacological PDE4D inhibition by GEBR32a enhances neurite outgrowth in N2a and HT22 cells starting at a concentration of 0.03 µM. Considering that global cellular cAMP levels only rise detectably with an ELISA upon 3 µM GEBR32a exposure, lower-dose initiated cAMP changes on a nanoscale level, which would require new high-end detection techniques, are likely sufficient to stimulate neurite growth, providing additional support for PDE4D-associated low-cAMP compartments near growth cones (Bock et al., 2020). Early studies already showed that Aβ exposure can cause neurite degeneration in hippocampal neurons (Ivins et al., 1998). The HT22 mouse hippocampal neuronal cell line we used here also showed reduced neurite length when exposed to 1 µM $A\beta_{1-42}$, which corresponds to the concentrations that were neurotoxic to HT22 cells in prior studies (Kwon et al., 2010). Pharmacological PDE4D inhibition protected against this $A\beta_{1-42}$-induced neurite length reduction.

However, as PDE4D inhibition has been associated with severe adverse effects, which may be due to central and/or peripheral actions, targeting of specific PDE4D isoforms could be therapeutically more effective or enable maintenance of efficacy while improving safety. The PDE4D isoforms (PDE4D1-9) are categorized into long, short, and supershort isoforms, which is based on the inclusion of specific exons and the isoform's eventual protein sequence. The differences in sequence enable for isoform-specific activity modulation by post-translational modifications and for specific intracellular targeting to regulate specific processes (Paes et al., 2021). Hence, we sought to investigate which PDE4D isoforms regulate neurite growth and

convey the protective effect of PDE4D inhibition against $A\beta_{1-42}$ exposure. We found that genetic ablation of the long PDE4D isoforms PDE4D3, -D5, -D7, and -D9 increased average neurite length both in absence and in presence of the neurotoxic $A\beta_{1-42}$ concentration. Genetic knockdown of the other long isoforms, PDE4D4 and PDE4D8, had no effect on neurite length, which can be explained by the observation that these forms are not expressed in HT22 cells. Since PDE4D8 was expressed more in APP/PS1 hippocampus, this may be linked to expression in non-neuronal cell types (e.g. microglia, astrocytes and/or oligodendrocytes). Remarkably, the short PDE4D1 and supershort PDE4D6 isoform did not affect neurite growth upon genetic knockdown, which implies that neurite outgrowth is specifically regulated by long PDE4D isoforms. The question remains whether these long isoforms regulate the same cellular process or modulate different processes that eventually influence neurite outgrowth. For example, non-specific PDE4 inhibition was found to increase phosphorylation of vasodilator-stimulated phosphoprotein (VASP), a protein that is associated with the cytoskeleton (Fleming et al., 2004), which is likely caused by PKA activation and will promote neurite elongation (Batty et al., 2017; Drees and Gertler, 2008; Mingorance-Le Meur and O'Connor, 2009). Since PDE4D localizes in HT22 neurite growth cones and long PDE4D isoforms appear to regulate neurite outgrowth, these long isoforms may control neuronal morphology by controlling PKA activity, and subsequent phosphorylation of specific targets, in neurite growth cones.

PDE4 subtypes and isoforms are known to localize to specific intracellular compartments (Baillie, 2009; Baillie et al., 2019; Blackman et al., 2011; Houslay, 2010; Terrin et al., 2006; Yougbare et al., 2021). Previous studies may provide insight into how PDE4D3, -D5, -D7, and -D9 influence cAMP signaling in regulating neurite growth. Most notably, PDE4D3 has been reported to bind perinuclear mAKAP, and the PDE4D3/mAKAP complex was found to support survival of and axon growth in neurons (Boczek et al., 2019; Boczek and Kapiloff, 2020). Moreover, PDE4D3 can bind

to the centrosome via AKAP9, thereby regulating cell cycle progression (Terrin et al., 2012). Thus, genetic knockdown of PDE4D3 likely promoted cAMP-PKA signaling in both the perinuclear and centrosomal regions, which may have halted cell cycle progression and promoted neurite growth. In addition, the increased perinuclear cAMP-PKA signaling may have stimulated PKA-mediated CREB phosphorylation, which subsequently could have promoted neuronal plasticity processes (e.g. neurite outgrowth).

By preferentially binding the scaffolding β-arrestin, PDE4D5 can be located in close vicinity of G-protein coupled receptors (GPCRs) to regulate cAMP levels at the site of synthesis near GPCR-stimulated adenylyl cyclase (Baillie, 2009; Baillie et al., 2003; Houslay and Baillie, 2005). Additionally, PDE4D5 is located in the nucleus through interaction with AKAP95 and may therefore also be the specific isoform found in nuclei of cortical neurons in the macaque brain (Clister et al., 2019; Datta et al., 2020). Upon PDE4D5 knockdown, nuclear cAMP-PKA-CREB-mediated signaling and subsequent transcription may be stimulated while also cAMP levels are elevated near GPCRs to induce PKA-mediated phosphorylation of, for example, cytoskeletal proteins to promote neurite outgrowth. Cytoskeletal remodeling and neuronal motility are likely regulated by PDE4D5 species that are complexed with focal adhesion kinase (FAK) through interactions with the scaffold protein RACK1 (Navarro and Rico, 2014; Serrels et al., 2010). Recently, it has been described that GPCR activation can actually recruit PDE4D5 out of the nucleus to allow for nuclear cAMP signaling that promotes memory consolidation (Martinez et al., 2023); PDE4D5 knockdown would have a similar effect.

Similar to PDE4D5, PDE4D7 has been found to locate to the plasma membrane in a prostate cancer cell line and has been linked to regulation of cell proliferation (Henderson et al., 2014). Furthermore, in different cell types, i.e. human arterial endothelial cells, PDE4D7 was found to specifically regulate transcriptional responses to extracellular cues (Burke-Kleinman and Maurice, 2021). Based on these

studies, neuronal PDE4D7 may also locate near the membrane to regulate cAMP-mediated relaying of extracellular signaling to an adaptive transcriptional response. Intriguingly, several single-nucleotide polymorphisms (SNPs) in the PDE4D7 and PDE4D5 promoter regions of the *PDE4D* gene showed significant associations with cognitive performance in humans (Gurney, 2019). Based on our data, it could be suggested that these SNPs, by influencing PDE4D isoform expression, may cause changes in neuronal plasticity (e.g. growing neurites) and thereby cause differences in cognition.

Regarding PDE4D9, a similar intracellular distribution as PDE4D3, i.e. perinuclear and under the plasma membrane, has been reported (Sheppard et al., 2014). In the submembrane compartment, PDE4D9 can bind to and regulate the function of β_2-adrenergic receptors (De Arcangelis et al., 2009). As these receptors regulate neurite outgrowth and are also expressed in HT22 cells, PDE4D9 knockdown may contribute to a stronger or longer sustained signaling downstream of these receptors to facilitate neurite outgrowth (Day et al., 2014; Schmidt et al., 2001). Functionally, PDE4D9 was also found to be phosphorylated by a multitude of kinases to regulate cAMP levels during mitosis (Sheppard et al., 2014) and could, therefore, halt cell cycle progression and induce neurite outgrowth upon knockdown. Moreover, PDE4D9 transcription is repressed by the scaffolding protein disrupted in schizophrenia 1 (DISC1), suggesting that DISC1 loss-of-function can induce increased PDE4D9 expression (Soda et al., 2013). At the protein level, DISC1 directly binds and inhibits PDE4B and PDE4D, providing an additional manner to regulate PDE4D activity (Murdoch et al., 2007). Interestingly, DISC1 loss-of-function mutations have been associated with psychiatric disorders associated with altered neuronal morphology (Tropea et al., 2018). These morphological changes may be partly explained by aberrant cAMP signaling caused by the impaired PDE4D9 transcription regulation and deficient PDE4(D) scaffolding by DISC1.

Thus, the long isoforms PDE4D3, -D5, -D7, and -D9 are well positioned in several cellular compartments to regulate (downstream) GPCR signaling, cAMP-PKA-CREB-mediated transcription, proliferation, cytoskeletal modulation and local PKA-mediated phosphorylation events (Fig 8). By genetic knockdown of separate PDE4D isoforms, local cAMP signaling is enhanced, which translates into a more complex morphology. Moreover, as PDE4D isoform knockdown also provided resilience against $A\beta_{1-42}$-induced neurotoxicity, additional cellular mechanisms may be stimulated. The current findings indicate that genetic knockdown of a single PDE4D isoform is sufficient to induce these effects. This may imply that PDE4D isoform knockdown is not directly compensated for by other PDE4D isoforms, at least in the acute setting used here. Based on this rationale, follow-up studies would have to investigate potential synergistic actions of knockdown of multiple PDE4D isoforms. Previous studies have shown that inhibition of different PDE families, that would localize to different intracellular locations, can have synergistic effects (Gulisano et al., 2018; Paes et al., 2020b). Possible additive effects of knockdown of multiple PDE4D isoforms would have to be revealed in such studies. However, pharmacological PDE4D inhibition, which would target multiple PDE4D isoforms, showed effects of similar potency as those observed for single isoform knockdown, making additive effects unlikely. Future studies should determine which (combinations of these) PDE4D isoforms, bound to which interactor proteins, regulate which local signaling module in the context of neuronal plasticity processes like neurite growth. Previously, the use of dominant-negative approaches has proven to be successful in elucidating the localization and function of specific PDE4 isoforms, and may therefore provide a useful tool for follow-up research (McCahill et al., 2005; Ong et al., 2009).

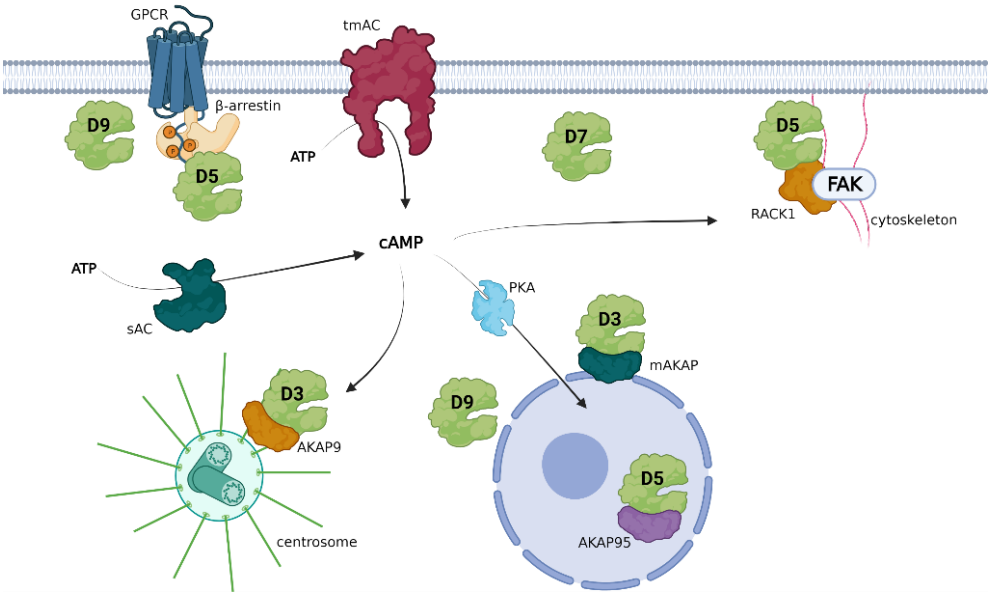

Figure 8. Intracellular positioning of specific PDE4D isoforms allows control of cAMP signaling involved in processes regulating neuronal plasticity. PDE4D isoforms can regulate cAMP signaling at the site of synthesis (PDE4D9 near β-adrenergic receptors, PDE4D5 binding GPCR-recruited β-arrestin, and submembranous PDE4D7). Upon synthesis by transmembrane (tmAC) or soluble (sAC) adenylyl cyclases, cAMP signals can be relayed to centrosomal areas where PDE4D3 is sequestered by AKAP9 or to cytoskeletal areas where PDE4D5 is complexed to FAK by RACK1. This localization allows for PDE4D-mediated control of cell cycle progression and morphology changes. Moreover, cAMP-PKA-CREB signaling can be influenced by PDE4D isoforms in peri- and intranuclear locations (i.e. PDE4D3, PDE4D5, and PDE4D9) to control cAMP-mediated transcriptional responses. This image was created using Biorender.

In general, long PDE4(D) isoforms share the ability to be phosphorylated by PKA which subsequently induces conformational changes leading to activation of these PDE4D isoforms (Hoffmann et al., 1998; Richter et al., 2005). By adopting different conformational states, PDE4 enzymes can also exhibit different affinities towards inhibitors (Paes et al., 2021). Historically, a high-affinity rolipram-binding state (HARBS) and low-affinity rolipram-binding state (LARBS) have been described, which can be bound specifically by different PDE4 types of PDE4 inhibitors (Rocque et al., 1997; Souness and Rao, 1997). Long PDE4(D) can dimerize and thereby stabilize the HARBS conformation (Richter and Conti, 2004). Interestingly, as inhibition of HARBS was found to stimulate neurite outgrowth whilst inhibition of LARBS did not (Boomkamp et al., 2014), these functional effects may also be contributing to inhibition of long PDE4D isoforms. Additional support for the role of long PDE4D isoforms in regulating neuronal plasticity and protection against $A\beta_{1-42}$-induced neurotoxicity was found by *in vivo* preclinical studies using shRNA-mediated knockdown of long PDE4D isoforms (Li et al., 2011; Shi et al., 2021b; Wang et al., 2013). Reassuringly, these studies found dendritic complexity, CREB signaling, and cognitive performance to be enhanced upon PDE4D long-form knockdown. These effects were ascribed to knockdown of PDE4D4 and PDE4D5 as qPCR indicated decreased expression of these forms. However, expression effects on other long PDE4D isoforms (i.e. PDE4D7, -D8 and -D9) were not reported although the shRNA sequence used would be expected to also cause degradation of these other isoforms (Li et al., 2011; Wang et al., 2013). Thus, knockdown of PDE4D7 and/or PDE4D9 might have contributed to the enhanced morphology complexity, CREB signaling and cognitive performance. The seemingly predominant role of long PDE4D isoforms in regulating neuroplasticity and cognition is further underlined by the association of mutations in *PDE4D* exons specific to long isoforms and the rare genetic disorder acrodysostosis, which is characterized by intellectual disability (Michot et al., 2018).

Strikingly, many of these mutations occur in protein domains that are unique to long PDE4D isoforms (Bolger, 2021).

The current findings also imply that the effects of pharmacological PDE4D inhibition on neurite growth are mediated by inhibition of long PDE4D forms specifically, which consequently has implications for PDE4D inhibitor drug development. The PDE4D inhibitor used in this study, GEBR32a, has been reported to show higher affinity for long, PKA-phosphorylated PDE4D forms, which may explain its efficacy (Cavalloro et al., 2020; Paes et al., 2021; Prosdocimi et al., 2018). Moreover, another example of a PDE4D long form-specific inhibitor is zatolmilast (formerly BPN14770) which binds a PDE4D-specific residue in a conformation that is adopted by long forms only (Burgin et al., 2010; Cedervall et al., 2015). Zatolmilast has shown efficacy in stimulating cAMP-PKA-CREB signalling and neuroplasticity in preclinical studies using wild-type animals and transgenic AD mice and enhances cognition in non-human primates (Cui et al., 2019; Sutcliffe et al., 2014). In fact, BPN14770/zatolmilast is under study in a Phase II clinical trial to assess its effects in early AD patients [NCT03817684].

While the results presented here show robustly that silencing of long PDE4D isoforms specifically enhances neuronal plasticity, the question remains whether these specific long PDE4D isoforms also mediate processes contributing to the adverse side effects associated with PDE4D inhibition. The molecular mechanisms underlying these side effects remain to be defined but seem to be induced by PDE4(D) inhibition in both the emetic brainstem regions as well as the gastrointestinal system (McDonough et al., 2020; Paes et al., 2021; Robichaud et al., 2002). Emesis-inducing cAMP signaling in the area postrema in the brainstem may rely on signaling downstream of the glucagon-like peptide 1 receptor (GLP1R) (Han and de Araujo, 2021; Zhang et al., 2021). Thus, it can be argued that the PDE4D isoforms that mediate cAMP signaling induced by GLP1Rs should not be inhibited to prevent these emetic brainstem regions from being activated. Remarkably, PDE4D5

has been linked to GLP1 release, but a possible link between PDE4D and GLP1-induced signal transduction upon GLP1R activation remains to be elucidated (Ong et al., 2009). Regarding peripherally-regulated side effects, it has recently been described that non-selective PDE4 inhibition induces gastroparesis (i.e. delayed gastric transit), which could subsequently trigger nausea and emesis (McDonough et al., 2020). However, it remains to be elucidated whether long isoforms of the different PDE4 subtypes predominantly mediate these processes. Encouragingly, we found here that not all (long) PDE4D isoforms are (equally high) expressed in the mouse stomach. Specifically, PDE4D3 and PDE4D5 exhibited high expression, whilst expression of PDE4D7 and PDE4D9 was substantially lower. Future studies could therefore investigate whether targeting of PDE4D7 and/or PDE4D9 as expressed in the brain would increase neuronal plasticity without contributing to stomach-mediated side effects that are associated with non-specific PDE4(D) inhibition.

CONCLUSION

In summary, this study shows that inhibition of individual long PDE4D isoforms specifically enhances neuronal plasticity, and that inhibition of these isoforms can yield resilience against Aβ-induced pathology in neurons. Hence, this target specification provides insights for the development of efficacious PDE4D inhibitors and supports the potential of PDE4D as a pharmacological target for the treatment of memory deficits in AD.

ABBREVIATIONS

Aβ	Amyloid-β
AC	Adenylyl cyclase
AD	Alzheimer's disease
cAMP	Cyclic adenosine monophosphate
DISC1	Disrupted in schizophrenia 1
DMSO	Dimethyl sulfoxide
FAK	Focal adhesion kinase
GLP1R	Glucagon-like peptide 1 receptor
GPCR	G protein-coupled receptor
HARBS	High-affinity rolipram-binding state
HIP	Hippocampus
LARBS	Low-affinity rolipram-binding state
PDE	Phosphodiesterase
PFC	Prefrontal cortex
SNP	Single-nucleotide polymorphism
sAC	Soluble adenlylyl cyclase
tmAC	Transmembrane adenylyl cyclase
VASP	Vasodilator-stimulated phosphoprotein

ACKNOWLEDGMENTS

TV and JP have a proprietary interest in selective PDE4D inhibitors for the treatment of demyelinating disorders and neurodegenerative disorders. JP has a proprietary interest in the PDE4 inhibitor roflumilast for the treatment of cognitive impairment as well as PDE4D inhibitors for the treatment of Alzheimer’s disease. OB, CB, EF, RR, JP have a proprietary interest in GEBR32a compound.

REFERENCES

Ashour NH, El-Tanbouly DM, El Sayed NS and Khattab MM (2021) Roflumilast ameliorates cognitive deficits in a mouse model of amyloidogenesis and tauopathy: Involvement of nitric oxide status, Aβ extrusion transporter ABCB1, and reversal by PKA inhibitor H89. *Progress in neuro-psychopharmacology & biological psychiatry* **111**:110366.

Baillie GS (2009) Compartmentalized signalling: spatial regulation of cAMP by the action of compartmentalized phosphodiesterases. *FEBS J* **276**:1790-1799.

Baillie GS, Sood A, McPhee I, Gall I, Perry SJ, Lefkowitz RJ and Houslay MD (2003) beta-Arrestin-mediated PDE4 cAMP phosphodiesterase recruitment regulates beta-adrenoceptor switching from Gs to Gi. *Proc Natl Acad Sci U S A* **100**:940-945.

Baillie GS, Tejeda GS and Kelly MP (2019) Therapeutic targeting of 3',5'-cyclic nucleotide phosphodiesterases: inhibition and beyond. *Nat Rev Drug Discov* **18**:770-796.

Batty NJ, Fenrich KK and Fouad K (2017) The role of cAMP and its downstream targets in neurite growth in the adult nervous system. *Neuroscience Letters* **652**:56-63.

Bhat A, Ray B, Mahalakshmi AM, Tuladhar S, Nandakumar DN, Srinivasan M, Essa MM, Chidambaram SB, Guillemin GJ and Sakharkar MK (2020) Phosphodiesterase-4 enzyme as a therapeutic target in neurological disorders. *Pharmacological Research* **160**:105078.

Blackman BE, Horner K, Heidmann J, Wang D, Richter W, Rich TC and Conti M (2011) PDE4D and PDE4B function in distinct subcellular compartments in mouse embryonic fibroblasts. *The Journal of biological chemistry* **286**:12590-12601.

Blokland A, Heckman P, Vanmierlo T, Schreiber R, Paes D and Prickaerts J (2019a) Phosphodiesterase Type 4 Inhibition in CNS Diseases. *Trends Pharmacol Sci* **40**:971-985.

Blokland A, Van Duinen MA, Sambeth A, Heckman PRA, Tsai M, Lahu G, Uz T and Prickaerts J (2019b) Acute treatment with the PDE4 inhibitor roflumilast improves verbal word memory in healthy old individuals: a double-blind placebo-controlled study. *Neurobiol Aging* **77**:37-43.

Bock A, Annibale P, Konrad C, Hannawacker A, Anton SE, Maiellaro I, Zabel U, Sivaramakrishnan S, Falcke M and Lohse MJ (2020) Optical Mapping of cAMP Signaling at the Nanometer Scale. *Cell* **182**:1519-1530.e1517.

Boczek T, Cameron EG, Yu W, Xia X, Shah SH, Castillo Chabeco B, Galvao J, Nahmou M, Li J, Thakur H, Goldberg JL and Kapiloff MS (2019) Regulation of Neuronal Survival and Axon Growth by a Perinuclear cAMP Compartment. *The Journal of neuroscience : the official journal of the Society for Neuroscience* **39**:5466-5480.

Boczek T and Kapiloff MS (2020) Compartmentalization of local cAMP signaling in neuronal growth and survival. *Neural Regen Res* **15**:453-454.

Bolger GB (2021) The PDE-opathies: diverse phenotypes produced by a functionally related multigene family. *Trends in Genetics*.

Boomkamp SD, McGrath MA, Houslay MD and Barnett SC (2014) Epac and the high affinity rolipram binding conformer of PDE4 modulate neurite outgrowth and myelination using an in vitro spinal cord injury model. *Br J Pharmacol* **171**:2385-2398.

Burgin AB, Magnusson OT, Singh J, Witte P, Staker BL, Bjornsson JM, Thorsteinsdottir M, Hrafnsdottir S, Hagen T, Kiselyov AS, Stewart LJ and Gurney ME (2010) Design of phosphodiesterase 4D (PDE4D) allosteric modulators for enhancing cognition with improved safety. *Nat Biotechnol* **28**:63-70.

Burke-Kleinman J and Maurice DH (2021) Phosphodiesterase 4D7 selectively regulates cAMP-mediated control of human arterial endothelial cell transcriptomic responses to fluid shear stress. *Canadian journal of physiology and pharmacology* **99**:179-184.

Cavalloro V, Russo K, Vasile F, Pignataro L, Torretta A, Donini S, Semrau MS, Storici P, Rossi D, Rapetti F, Brullo C, Parisini E, Bruno O and Collina S (2020) Insight into GEBR-32a: Chiral Resolution, Absolute Configuration and Enantiopreference in PDE4D Inhibition. *Molecules* **25**.

Cedervall P, Aulabaugh A, Geoghegan KF, McLellan TJ and Pandit J (2015) Engineered stabilization and structural analysis of the autoinhibited conformation of PDE4. *Proc Natl Acad Sci U S A* **112**:E1414-1422.

Chen J, Bardes EE, Aronow BJ and Jegga AG (2009) ToppGene Suite for gene list enrichment analysis and candidate gene prioritization. *Nucleic Acids Research* **37**:W305-W311.

Cheng Y-F, Wang C, Lin H-B, Li Y-F, Huang Y, Xu J-P and Zhang H-T (2010) Inhibition of phosphodiesterase-4 reverses memory deficits produced by Aβ25–35 or Aβ1–40 peptide in rats. *Psychopharmacology* **212**:181-191.

Clister T, Greenwald EC, Baillie GS and Zhang J (2019) AKAP95 Organizes a Nuclear Microdomain to Control Local cAMP for Regulating Nuclear PKA. *Cell chemical biology* **26**:885-891.e884.

Cui S-Y, Yang M-X, Zhang Y-H, Zheng V, Zhang H-T, Gurney ME, Xu Y and O'Donnell JM (2019) Protection from amyloid β peptide-induced memory, biochemical and morphological deficits by a phosphodiesterase-4D (PDE4D) allosteric inhibitor. *Journal of Pharmacology and Experimental Therapeutics*:jpet.119.259986.

Datta D, Enwright JF, Arion D, Paspalas CD, Morozov YM, Lewis DA and Arnsten AFT (2020) Mapping Phosphodiesterase 4D (PDE4D) in Macaque Dorsolateral Prefrontal Cortex: Postsynaptic Compartmentalization in Layer III Pyramidal Cell Circuits. *Front Neuroanat* **14**:578483-578483.

Davis JB and Maher P (1994) Protein kinase C activation inhibits glutamate-induced cytotoxicity in a neuronal cell line. *Brain Res* **652**:169-173.

Day JS, O'Neill E, Cawley C, Aretz NK, Kilroy D, Gibney SM, Harkin A and Connor TJ (2014) Noradrenaline acting on astrocytic β_2-adrenoceptors induces neurite outgrowth in primary cortical neurons. *Neuropharmacology* **77**:234-248.

De Arcangelis V, Liu R, Soto D and Xiang Y (2009) Differential association of phosphodiesterase 4D isoforms with beta2-adrenoceptor in cardiac myocytes. *The Journal of biological chemistry* **284**:33824-33832.

Drees F and Gertler FB (2008) Ena/VASP: proteins at the tip of the nervous system. *Current Opinion in Neurobiology* **18**:53-59.

Edelstein A, Amodaj N, Hoover K, Vale R and Stuurman N (2010) Computer control of microscopes using μManager. *Current protocols in molecular biology* **Chapter 14**:Unit14.20.

Edelstein AD, Tsuchida MA, Amodaj N, Pinkard H, Vale RD and Stuurman N (2014) Advanced methods of microscope control using μManager software. *Journal of biological methods* **1**.

Feng H, Wang C, He W, Wu X, Li S, Zeng Z, Wei M and He B (2019) Roflumilast ameliorates cognitive impairment in APP/PS1 mice via cAMP/CREB/BDNF signaling and anti-neuroinflammatory effects. *Metabolic Brain Disease* **34**:583-591.

Fleming YM, Frame MC and Houslay MD (2004) PDE4-regulated cAMP degradation controls the assembly of integrin-dependent actin adhesion structures and REF52 cell migration. *Journal of Cell Science* **117**:2377-2388.

Gulisano W, Tropea MR, Arancio O, Palmeri A and Puzzo D (2018) Sub-efficacious doses of phosphodiesterase 4 and 5 inhibitors improve memory in a mouse model of Alzheimer's disease. *Neuropharmacology* **138**:151-159.

Gurney ME (2019) Genetic Association of Phosphodiesterases With Human Cognitive Performance. *Front Mol Neurosci* **12**:22.

Han W and de Araujo IE (2021) Nausea and the Brain: The Chemoreceptor Trigger Zone Enters the Molecular Age. *Neuron* **109**:391-393.

Henderson DJP, Byrne A, Dulla K, Jenster G, Hoffmann R, Baillie GS and Houslay MD (2014) The cAMP phosphodiesterase-4D7 (PDE4D7) is downregulated in androgen-independent prostate cancer cells and mediates proliferation by compartmentalising cAMP at the plasma membrane of VCaP prostate cancer cells. *British Journal of Cancer* **110**:1278-1287.

Hoffmann R, Wilkinson IR, McCallum JF, Engels P and Houslay MD (1998) cAMP-specific phosphodiesterase HSPDE4D3 mutants which mimic activation and changes in rolipram inhibition triggered by protein kinase A phosphorylation of Ser-54: generation of a molecular model. *Biochem J* **333 (Pt 1)**:139-149.

Houslay M and Conti M (2010) Phosphodiesterase 4D, cAMP specific. UCSD-Nature Molecule Pages, UCSD-Nature Signaling Gateway (www signaling-gateway org).

Houslay MD (2010) Underpinning compartmentalised cAMP signalling through targeted cAMP breakdown. *Trends Biochem Sci* **35**:91-100.

Houslay MD and Baillie GS (2005) Beta-arrestin-recruited phosphodiesterase-4 desensitizes the AKAP79/PKA-mediated switching of beta2-adrenoceptor signalling to activation of ERK. *Biochemical Society transactions* **33**:1333-1336.

Ivins KJ, Bui ET and Cotman CW (1998) Beta-amyloid induces local neurite degeneration in cultured hippocampal neurons: evidence for neuritic apoptosis. *Neurobiol Dis* **5**:365-378.

Kandel ER (2012) The molecular biology of memory: cAMP, PKA, CRE, CREB-1, CREB-2, and CPEB. *Mol Brain* **5**:14.

Kwon KJ, Kim HJ, Shin CY and Han SH (2010) Melatonin Potentiates the Neuroprotective Properties of Resveratrol Against Beta-Amyloid-Induced Neurodegeneration by Modulating AMP-Activated Protein Kinase Pathways. *Journal of clinical neurology (Seoul, Korea)* **6**:127-137.

Li YF, Cheng YF, Huang Y, Conti M, Wilson SP, O'Donnell JM and Zhang HT (2011) Phosphodiesterase-4D knock-out and RNA interference-mediated knock-down enhance memory and increase hippocampal neurogenesis via increased cAMP signaling. *J Neurosci* **31**:172-183.

MacKenzie SJ and Houslay MD (2000) Action of rolipram on specific PDE4 cAMP phosphodiesterase isoforms and on the phosphorylation of cAMP-response-element-binding protein (CREB) and p38 mitogen-activated protein (MAP) kinase in U937 monocytic cells. *Biochem J* **347**:571-578.

Marchmont RJ and Houslay MD (1980) A peripheral and an intrinsic enzyme constitute the cyclic AMP phosphodiesterase activity of rat liver plasma membranes. *Biochem J* **187**:381-392.

Martinez JM, Shen A, Xu B, Jovanovic A, de Chabot J, Zhang J and Xiang YK (2023) Arrestin-dependent nuclear export of phosphodiesterase 4D promotes GPCR-induced nuclear cAMP signaling required for learning and memory. *Sci Signal* **16**:eade3380.

McCahill A, McSorley T, Huston E, Hill EV, Lynch MJ, Gall I, Keryer G, Lygren B, Tasken K, van Heeke G and Houslay MD (2005) In resting COS1 cells a dominant negative approach shows that specific, anchored PDE4 cAMP phosphodiesterase isoforms gate the activation, by basal cyclic AMP production, of AKAP-tethered protein kinase A type II located in the centrosomal region. *Cell Signal* **17**:1158-1173.

McDonough W, Aragon IV, Rich J, Murphy JM, Abou Saleh L, Boyd A, Koloteva A and Richter W (2020) PAN-selective inhibition of cAMP-phosphodiesterase 4 (PDE4) induces gastroparesis in mice. *FASEB J*.

Meijering E, Jacob M, Sarria JC, Steiner P, Hirling H and Unser M (2004) Design and validation of a tool for neurite tracing and analysis in fluorescence microscopy images. *Cytometry Part A : the journal of the International Society for Analytical Cytology* **58**:167-176.

Mesulam MM (1999) Neuroplasticity failure in Alzheimer's disease: bridging the gap between plaques and tangles. *Neuron* **24**:521-529.

Michot C, Le Goff C, Blair E, Blanchet P, Capri Y, Gilbert-Dussardier B, Goldenberg A, Henderson A, Isidor B, Kayserili H, Kinning E, Le Merrer M, Lyonnet S, Odent S, Simsek-Kiper PO, Quelin C, Savarirayan R, Simon M, Splitt M, Verhagen JMA, Verloes A, Munnich A, Baujat G and Cormier-Daire V (2018) Expanding the phenotypic spectrum of variants in PDE4D/PRKAR1A: from acrodysostosis to acroscyphodysplasia. *European Journal of Human Genetics* **26**:1611-1622.

Mingorance-Le Meur A and O'Connor TP (2009) Neurite consolidation is an active process requiring constant repression of protrusive activity. *The EMBO journal* **28**:248-260.

Mohammadnejad A, Li W, Lund JB, Li S, Larsen MJ, Mengel-From J, Michel TM, Christiansen L, Christensen K, Hjelmborg J, Baumbach J and Tan Q (2021) Global Gene Expression Profiling and Transcription Factor Network Analysis of Cognitive Aging in Monozygotic Twins. *Frontiers in genetics* **12**:675587.

Mori F, Perez-Torres S, De Caro R, Porzionato A, Macchi V, Beleta J, Gavalda A, Palacios JM and Mengod G (2010) The human area postrema and other nuclei related to the emetic reflex express cAMP phosphodiesterases 4B and 4D. *J Chem Neuroanat* **40**:36-42.

Morimoto BH and Koshland DE, Jr. (1990) Induction and expression of long- and short-term neurosecretory potentiation in a neural cell line. *Neuron* **5**:875-880.

Murdoch H, Mackie S, Collins DM, Hill EV, Bolger GB, Klussmann E, Porteous DJ, Millar JK and Houslay MD (2007) Isoform-selective susceptibility of DISC1/phosphodiesterase-4 complexes to dissociation by elevated intracellular cAMP levels. *The Journal of neuroscience : the official journal of the Society for Neuroscience* **27**:9513-9524.

Myeku N, Clelland CL, Emrani S, Kukushkin NV, Yu WH, Goldberg AL and Duff KE (2016) Tau-driven 26S proteasome impairment and cognitive dysfunction

can be prevented early in disease by activating cAMP-PKA signaling. *Nature medicine* **22**:46-53.
Navarro AI and Rico B (2014) Focal adhesion kinase function in neuronal development. *Current Opinion in Neurobiology* **27**:89-95.
Ong WK, Gribble FM, Reimann F, Lynch MJ, Houslay MD, Baillie GS, Furman BL and Pyne NJ (2009) The role of the PDE4D cAMP phosphodiesterase in the regulation of glucagon-like peptide-1 release. *Br J Pharmacol* **157**:633-644.
Paes D, Lardenoije R, Carollo RM, Roubroeks JAY, Schepers M, Coleman P, Mastroeni D, Delvaux E, Pishva E, Lunnon K, Vanmierlo T, van den Hove D and Prickaerts J (2020a) Increased isoform-specific phosphodiesterase 4D expression is associated with pathology and cognitive impairment in Alzheimer's disease. *Neurobiol Aging* **97**:56-64.
Paes D, Schepers M, Rombaut B, van den Hove D, Vanmierlo T and Prickaerts J (2021) The Molecular Biology of Phosphodiesterase 4 Enzymes as Pharmacological Targets: An Interplay of Isoforms, Conformational States, and Inhibitors. *Pharmacol Rev* **73**:1016-1049.
Paes D, Xie K, Wheeler DG, Zook D, Prickaerts J and Peters M (2020b) Inhibition of PDE2 and PDE4 synergistically improves memory consolidation processes. *Neuropharmacology* **184**:108414.
Prosdocimi T, Mollica L, Donini S, Semrau MS, Lucarelli AP, Aiolfi E, Cavalli A, Storici P, Alfei S, Brullo C, Bruno O and Parisini E (2018) Molecular Bases of PDE4D Inhibition by Memory-Enhancing GEBR Library Compounds. *Biochemistry* **57**:2876-2888.
Ran FA, Hsu PD, Wright J, Agarwala V, Scott DA and Zhang F (2013) Genome engineering using the CRISPR-Cas9 system. *Nat Protoc* **8**:2281-2308.
Richter W and Conti M (2004) The oligomerization state determines regulatory properties and inhibitor sensitivity of type 4 cAMP-specific phosphodiesterases. *J Biol Chem* **279**:30338-30348.
Richter W, Jin SL and Conti M (2005) Splice variants of the cyclic nucleotide phosphodiesterase PDE4D are differentially expressed and regulated in rat tissue. *Biochem J* **388**:803-811.
Robichaud A, Stamatiou PB, Jin SL, Lachance N, MacDonald D, Laliberte F, Liu S, Huang Z, Conti M and Chan CC (2002) Deletion of phosphodiesterase 4D in mice shortens alpha(2)-adrenoceptor-mediated anesthesia, a behavioral correlate of emesis. *J Clin Invest* **110**:1045-1052.
Rocque WJ, Tian G, Wiseman JS, Holmes WD, Zajac-Thompson I, Willard DH, Patel IR, Wisely GB, Clay WC, Kadwell SH, Hoffman CR and Luther MA (1997) Human recombinant phosphodiesterase 4B2B binds (R)-rolipram at a single site with two affinities. *Biochemistry* **36**:14250-14261.
Ruijter JM, Ramakers C, Hoogaars WMH, Karlen Y, Bakker O, van den Hoff MJB and Moorman AFM (2009) Amplification efficiency: linking baseline and bias in the analysis of quantitative PCR data. *Nucleic Acids Research* **37**:e45-e45.
Saura CA and Valero J (2011) The role of CREB signaling in Alzheimer's disease and other cognitive disorders. *Reviews in the neurosciences* **22**:153-169.
Schepers M, Tiane A, Paes D, Sanchez S, Rombaut B, Piccart E, Rutten BPF, Brone B, Hellings N, Prickaerts J and Vanmierlo T (2019) Targeting Phosphodiesterases-Towards a Tailor-Made Approach in Multiple Sclerosis Treatment. *Front Immunol* **10**:1727.

Schmidt P, Holsboer F and Spengler D (2001) β2-Adrenergic Receptors Potentiate Glucocorticoid Receptor Transactivation via G Proteinβγ -Subunits and the Phosphoinositide 3-Kinase Pathway. *Molecular Endocrinology* **15**:553-564.

Schneider CA, Rasband WS and Eliceiri KW (2012) NIH Image to ImageJ: 25 years of image analysis. *Nature methods* **9**:671-675.

Serrels B, Sandilands E, Serrels A, Baillie G, Houslay MD, Brunton VG, Canel M, Machesky LM, Anderson KI and Frame MC (2010) A Complex between FAK, RACK1, and PDE4D5 Controls Spreading Initiation and Cancer Cell Polarity. *Current Biology* **20**:1086-1092.

Shelly M, Lim BK, Cancedda L, Heilshorn SC, Gao H and Poo MM (2010) Local and long-range reciprocal regulation of cAMP and cGMP in axon/dendrite formation. *Science* **327**:547-552.

Shen MW, Arbab M, Hsu JY, Worstell D, Culbertson SJ, Krabbe O, Cassa CA, Liu DR, Gifford DK and Sherwood RI (2018) Predictable and precise template-free CRISPR editing of pathogenic variants. *Nature* **563**:646-651.

Sheppard CL, Lee LCY, Hill EV, Henderson DJP, Anthony DF, Houslay DM, Yalla KC, Cairns LS, Dunlop AJ, Baillie GS, Huston E and Houslay MD (2014) Mitotic activation of the DISC1-inducible cyclic AMP phosphodiesterase-4D9 (PDE4D9), through multi-site phosphorylation, influences cell cycle progression. *Cellular Signalling* **26**:1958-1974.

Shi J, Li Y, Zhang Y, Chen J, Gao J, Zhang T, Shang X and Zhang X (2021a) Baicalein Ameliorates Aβ-Induced Memory Deficits and Neuronal Atrophy via Inhibition of PDE2 and PDE4. *Front Pharmacol* **12**:794458.

Shi Y, Lv J, Chen L, Luo G, Tao M, Pan J, Hu X, Sheng J, Zhang S, Zhou M and Fan H (2021b) Phosphodiesterase-4D Knockdown in the Prefrontal Cortex Alleviates Memory Deficits and Synaptic Failure in Mouse Model of Alzheimer's Disease. *Front Aging Neurosci* **13**:722580-722580.

Shrestha BR, Vitolo OV, Joshi P, Lordkipanidze T, Shelanski M and Dunaevsky A (2006) Amyloid β peptide adversely affects spine number and motility in hippocampal neurons. *Molecular and Cellular Neuroscience* **33**:274-282.

Sierksma AS, van den Hove DL, Pfau F, Philippens M, Bruno O, Fedele E, Ricciarelli R, Steinbusch HW, Vanmierlo T and Prickaerts J (2014) Improvement of spatial memory function in APPswe/PS1dE9 mice after chronic inhibition of phosphodiesterase type 4D. *Neuropharmacology* **77**:120-130.

Sierksma ASR, Prickaerts J, Chouliaras L, Rostamian S, Delbroek L, Rutten BPF, Steinbusch HWM and van den Hove DLA (2013) Behavioral and neurobiological effects of prenatal stress exposure in male and female APPswe/PS1dE9 mice. *Neurobiology of Aging* **34**:319-337.

Soda T, Frank C, Ishizuka K, Baccarella A, Park YU, Flood Z, Park SK, Sawa A and Tsai LH (2013) DISC1-ATF4 transcriptional repression complex: dual regulation of the cAMP-PDE4 cascade by DISC1. *Mol Psychiatry* **18**:898-908.

Souness JE and Rao S (1997) Proposal for pharmacologically distinct conformers of PDE4 cyclic AMP phosphodiesterases. *Cell Signal* **9**:227-236.

Stark C, Breitkreutz BJ, Reguly T, Boucher L, Breitkreutz A and Tyers M (2006) BioGRID: a general repository for interaction datasets. *Nucleic Acids Res* **34**:D535-539.

Sutcliffe JS, Beaumont V, Watson JM, Chew CS, Beconi M, Hutcheson DM, Dominguez C and Munoz-Sanjuan I (2014) Efficacy of selective PDE4D

negative allosteric modulators in the object retrieval task in female cynomolgus monkeys (Macaca fascicularis). *PLoS One* **9**:e102449.

Terrin A, Di Benedetto G, Pertegato V, Cheung Y-F, Baillie G, Lynch MJ, Elvassore N, Prinz A, Herberg FW, Houslay MD and Zaccolo M (2006) PGE(1) stimulation of HEK293 cells generates multiple contiguous domains with different [cAMP]: role of compartmentalized phosphodiesterases. *The Journal of cell biology* **175**:441-451.

Terrin A, Monterisi S, Stangherlin A, Zoccarato A, Koschinski A, Surdo NC, Mongillo M, Sawa A, Jordanides NE, Mountford JC and Zaccolo M (2012) PKA and PDE4D3 anchoring to AKAP9 provides distinct regulation of cAMP signals at the centrosome. *Journal of Cell Biology* **198**:607-621.

Tropea D, Hardingham N, Millar K and Fox K (2018) Mechanisms underlying the role of DISC1 in synaptic plasticity. *The Journal of Physiology* **596**:2747-2771.

Van Duinen MA, Sambeth A, Heckman PRA, Smit S, Tsai M, Lahu G, Uz T, Blokland A and Prickaerts J (2018) Acute administration of roflumilast enhances immediate recall of verbal word memory in healthy young adults. *Neuropharmacology* **131**:31-38.

Vandesompele J, De Preter K, Pattyn F, Poppe B, Van Roy N, De Paepe A and Speleman F (2002) Accurate normalization of real-time quantitative RT-PCR data by geometric averaging of multiple internal control genes. *Genome Biology* **3**:research0034.0031.

Vanmierlo T, Creemers P, Akkerman S, van Duinen M, Sambeth A, De Vry J, Uz T, Blokland A and Prickaerts J (2016) The PDE4 inhibitor roflumilast improves memory in rodents at non-emetic doses. *Behav Brain Res* **303**:26-33.

Wang G, Chen L, Pan X, Chen J, Wang L, Wang W, Cheng R, Wu F, Feng X, Yu Y, Zhang H-T, O'Donnell JM and Xu Y (2016) The effect of resveratrol on beta amyloid-induced memory impairment involves inhibition of phosphodiesterase-4 related signaling. *Oncotarget* **7**.

Wang H, Zhang FF, Xu Y, Fu HR, Wang XD, Wang L, Chen W, Xu XY, Gao YF, Zhang JG and Zhang HT (2020) The Phosphodiesterase-4 Inhibitor Roflumilast, a Potential Treatment for the Comorbidity of Memory Loss and Depression in Alzheimer's Disease: A Preclinical Study in APP/PS1 Transgenic Mice. *Int J Neuropsychopharmacol* **23**:700-711.

Wang Z-Z, Zhang Y, Liu Y-Q, Zhao N, Zhang Y-Z, Yuan L, An L, Li J, Wang X-Y, Qin J-J, Wilson SP, O'Donnell JM, Zhang H-T and Li Y-F (2013) RNA interference-mediated phosphodiesterase 4D splice variants knock-down in the prefrontal cortex produces antidepressant-like and cognition-enhancing effects. *British Journal of Pharmacology* **168**:1001-1014.

Xiang J, Wang X, Gao Y, Li T, Cao R, Yan T, Ma Y, Niu Y, Xue J and Wang B (2020) Phosphodiesterase 4D Gene Modifies the Functional Network of Patients With Mild Cognitive Impairment and Alzheimer's Disease. *Frontiers in genetics* **11**.

Yougbare I, Keravis T and Lugnier C (2021) NCS 613, a PDE4 inhibitor, by increasing cAMP level suppresses systemic inflammation and immune complexes deposition in kidney of MRL/lpr lupus- prone mice. *Biochimica et Biophysica Acta (BBA) - Molecular Basis of Disease* **1867**:166019.

Zhang C, Cheng Y, Wang H, Wang C, Wilson SP, Xu J and Zhang HT (2014) RNA interference-mediated knockdown of long-form phosphodiesterase-4D

(PDE4D) enzyme reverses amyloid-β42-induced memory deficits in mice. *J Alzheimers Dis* **38**:269-280.

Zhang C, Kaye JA, Cai Z, Wang Y, Prescott SL and Liberles SD (2021) Area Postrema Cell Types that Mediate Nausea-Associated Behaviors. *Neuron* **109**:461-472.e465.

Zhang C, Xu Y, Zhang H-T, Gurney ME and O'Donnell JM (2017) Comparison of the Pharmacological Profiles of Selective PDE4B and PDE4D Inhibitors in the Central Nervous System. *Scientific Reports* **7**:40115.

SUPPLEMENTARY MATERIAL

Supplementary Table 1. Primers for HT22 genomic amplicon generation for the in vitro cell-free cleavage assay.

Isoform	Forward primer (5'-3')	Reverse primer (5'-3')	Amplicon size (bp)	Fragment sizes (bp)
Pde4d1	AGCTGATTCATTCGCTTCGC	AGGTCACAGGGATCGGTGAT	681	283 + 398
Pde4d3	TCACCAGGACAATACTCGCC	CTTCTATGGAAATGCAGGCCA	739	286 + 453
Pde4d6	TGCTGAATTCCGTTCCATTTTGG	AGCTTTAAAGACGAAGGTGGGAA	720	261 + 459
Pde4d9	GAACTCCCTTCGGAAGAGCC	ATGCTCGTGTTTAGCCTCGT	753	239 + 514

Supplementary Table 2. sgRNA 58bp forward templates including T7 promoter sequence for the in vitro cell-free cleavage assay. sgRNA sequence in bold.

Isoform	Forward sequence (5'-3')
Pde4d1	CCTCTAATACGACTCACTATAGG**CATCCGAGCATGGCGGGGTA**GTTTAAGAGCTATGC
Pde4d3	CCTCTAATACGACTCACTATAGG**TACATGCAACATAGGAGACG**GTTTAAGAGCTATGC
Pde4d6	CCTCTAATACGACTCACTATAGG**TATTTATTGTCAGTGTCTTG**GTTTAAGAGCTATGC
Pde4d9	CCTCTAATACGACTCACTATAGG**CCTCAGGGAACTTGTAGACC**GTTTAAGAGCTATGC

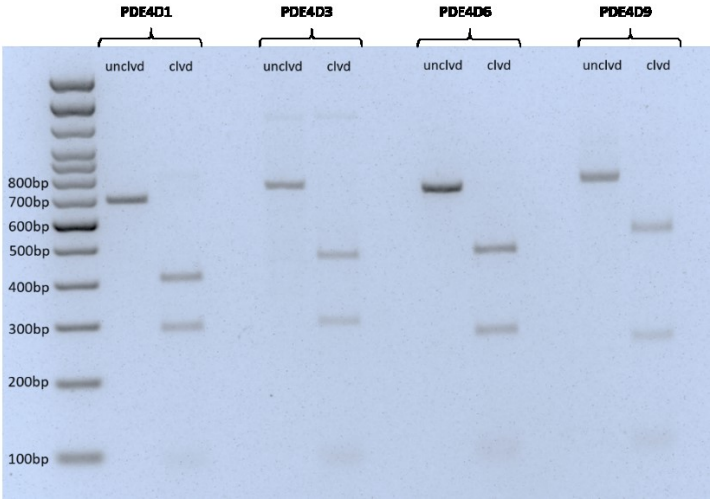

Supplementary Figure 1. A cell-free in vitro cleavage assay indicates that the sgRNA designed for PDE4D1, PDE4D3, PDE4D6, and PDE4D9 induces a double stranded break at the predicted site. sgRNAs for PDE4D1 and PDE4D6 were evaluated in this assay as these target (super)short PDE4D isoforms

that did not show a biological effect in the neurite outgrowth assay. sgRNAs for PDE4D3 and PDE4D9 were evaluated as knocking down these long isoforms showed the largest effect in the neurite outgrowth assay. For each sgRNA, the figure shows an uncleaved (unclvd) fragment in lane 1, and two cleaved (clvd) fragments in lane 2. Fragment size is based on primer design as shown in supplementary table 3. The sgRNA itself appears slightly near the 130bp position.

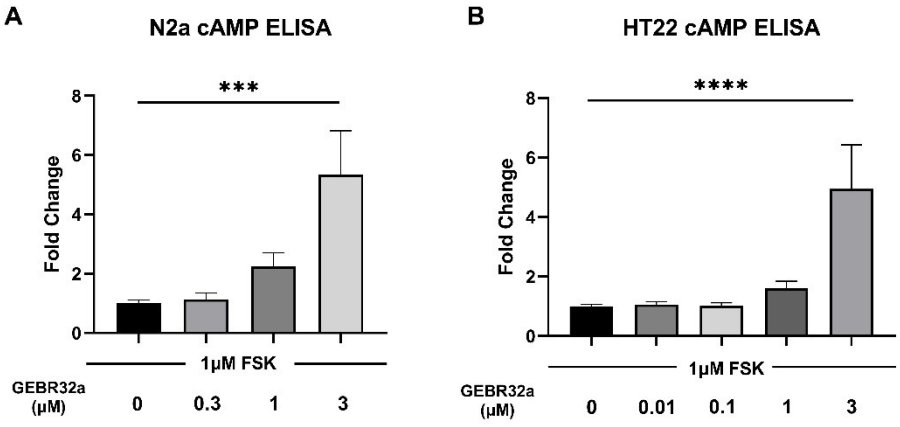

Supplementary Figure 2. Determination of intracellular cAMP concentration upon forskolin (FSK) stimulation to increase baseline cAMP levels, and concomitant GEBR32a treatment in N2a (A) and HT22 (B) cells (Dunnett's post-hoc: ***P<0.001, ****P<0.0001; n≥4/condition). Data is presented as mean + SEM.

Chapter 5

Computational investigation of the dynamic control of PDE4 isoform types on cAMP signaling

Published as:

Paes et al. (2022) *Biophys J.* Jul 19;121(14):2693-2711.
doi: 10.1016/j.bpj.2022.06.019

ABSTRACT

Cyclic adenosine monophosphate (cAMP) is a generic signaling molecule that, through precise control of its signaling dynamics, exerts distinct cellular effects. Consequently, aberrant cAMP signaling can have detrimental effects. Phosphodiesterase 4 (PDE4) enzymes profoundly control cAMP signaling and comprise different isoform types of which the enzymatic activity is modulated by differential feedback mechanisms. Because these feedback dynamics are non-linear and occur coincidentally, their effects are difficult to examine experimentally, but can be well simulated computationally. Through understanding the role of PDE4 isoform types in regulating cAMP signaling, PDE4-targeted therapeutic strategies can be better specified. Here, we established a computational model to study how feedback mechanisms on different PDE4 isoform types lead to dynamic, isoform-specific control of cAMP signaling. Ordinary differential equations describing cAMP dynamics were implemented in the VirtualCell (VCell) environment. Simulations indicated that long PDE4 isoforms exert the most profound control on oscillatory cAMP signaling, as opposed to the PDE4-mediated control of single cAMP input pulses. Moreover, elevating cAMP levels or decreasing PDE4 levels revealed different effects on downstream signaling. Together these results underline that cAMP signaling is distinctly regulated by different PDE4 isoform types and that this isoform-specificity should be considered in both computational and experimental follow-up studies to better define PDE4 enzymes as therapeutic targets in diseases in which cAMP signaling is aberrant.

AUTHOR SUMMARY

Cellular functioning relies on well-orchestrated intracellular signaling cascades. To sense and respond to the environment, cells relay extracellular signals to messenger molecules which can elicit adaptive responses. In response to different extracellular signals, cells often use the same messenger molecule, cyclic adenosine monophosphate (cAMP). By controlling the amplitude, duration and localization of this cAMP signaling, distinct messages can be relayed using the same signaling system. In disease, the well-orchestrated cAMP signaling can be impaired, causing unfavorable cellular responses. cAMP signaling is extensively controlled by phosphodiesterase 4 (PDE4) enzymes, which therefore provide a therapeutic target to restore aberrant cAMP signaling. PDE4 enzymes exist as different isoform types which control cAMP levels in similar, but distinct manners, as their enzymatic activity depends on dynamic feedback mechanisms. Experimentally, these highly dynamic feedback mechanisms and isoform-specific contribution to cAMP regulation are difficult to disentangle. Here, we investigated computationally which of the PDE4 isoform types exert(s) most control over cAMP signaling considering the aforementioned feedback mechanisms. Our results suggest that the so-called long PDE4 isoforms predominantly regulate cAMP signaling. Considering these findings, more specific targeting of long PDE4 types could achieve higher PDE4-mediated treatment efficacy in disease in which cAMP signaling is aberrant.

INTRODUCTION

Sensing the environment and responding in an adaptive manner is crucial to cell survival and proper cell functioning. Relaying extracellular signals intracellularly to elicit an adaptive response therefore has to be tightly regulated in a dynamic, spatiotemporal manner. The pivotal intracellular signaling molecule cyclic adenosine monophosphate (cAMP) is synthesized by conversion of adenosine triphosphate (ATP) by both transmembrane and soluble adenylyl cyclases (AC). Although AC activity is regulated by a wide variety of receptors, it is striking that these receptors, responding to different extracellular cues, all lead to the production of the generic signaling molecule cAMP, which subsequently can bind different effector proteins.
Among the cAMP effector proteins, protein kinase A (PKA) and exchange protein directly activated by cAMP (Epac) are most well-studied. PKA is a heterotetrametric protein complex that, upon binding cAMP, releases its catalytic subunits which can phosphorylate numerous target proteins (Herberg et al., 1996; Kim et al., 2007). Binding of cAMP to Epac releases the autoinhibitory conformation of Epac, which can initiate the activation of Rap1, a small GTPase of the Ras superfamily (de Rooij et al., 1998; Schmidt et al., 2013). Subsequently, Rap1 can influence a variety of cellular processes through modulation of various downstream proteins (Bos et al., 2001). Moreover, by binding Popeye domain containing proteins (POPDC) and cyclic nucleotide-gated channels (CNGC), cAMP signaling can modulate other biological functions (e.g. cell-cell adhesion and regulation of membrane potentials; reviewed in: (Kaupp and Seifert, 2002; Schindler and Brand, 2016)). Although these different effector proteins all respond to cAMP, through regulation of localization and the dynamics of the cAMP signal (e.g. its amplitude and duration), cAMP can distinctly influence different intracellular processes (Musheshe et al., 2018).

Intriguingly, the only way by which cAMP is enzymatically degraded, is via hydrolysis by phosphodiesterase (PDE) enzymes. In humans, eleven PDE gene families exist (PDE1-11) that can be classified based on their substrate selectivity;

some PDE types degrade cAMP selectively (PDE4,-7,-8) whilst others are selective to cyclic guanosine monophosphate (cGMP; PDE5,-6,-9). The remaining PDE types are dual-specific and degrade both cAMP and cGMP (PDE1,-2,-3,-10,-11). The different PDEs are heterogeneously distributed in a tissue- and cell-type specific manner (Baillie et al., 2019; Lakics et al., 2010). The PDE4 gene family comprises the largest amount of cAMP-specific PDEs and plays a critical role in shaping the dynamics and spatiotemporal control of cAMP signaling in many tissues and cell types (Baillie et al., 2019; Lakics et al., 2010). As pivotal regulators of cAMP signaling, PDE4 enzymes provide interesting pharmacological targets to modulate cAMP levels in a wide variety of disorders (Blokland et al., 2019; Paes et al., 2021; Peng et al., 2020). Consequently, PDE4 inhibition has been investigated as a therapeutic strategy to stimulate cAMP signaling. Although several PDE4 inhibitors are being used clinically, PDE4 inhibition may give rise to severe adverse effects (e.g. diarrhea, nausea, and emesis) for increasing doses. PDE4-mediated side effects are hypothesized to result, at least in part, from PDE4 inhibition in brainstem areas, and therefore more specific PDE4 inhibition is particularly required when, for the disease of interest, the therapeutic actions of PDE4 inhibition should occur in the brain (Paes et al., 2021). For example, in neurodegenerative disorder like Alzheimer's disease and multiple sclerosis, PDE4 inhibitors have to enter the central nervous system to exert therapeutic effect which makes these interventions also more prone to brainstem-mediated side effects (Blokland et al., 2019; Paes et al., 2021; Schepers et al., 2019). Therefore, a better understanding of how PDE4 mediates cAMP degradation is crucial to optimize PDE4 inhibition as a therapeutic strategy.

Human PDE4 enzymes are encoded by four genes (PDE4A-D) that each generate multiple isoforms (e.g. PDE4D1-9) through the use of alternative promoters and alternative splicing. Although the different isoforms are protein products with the same main biological function (i.e. cAMP hydrolysis), their protein sequence differences allow for isoform-specific localization and regulation of enzymatic activity

(Houslay, 2010; Paes et al., 2021). Specifically, PDE4 isoforms can be categorized as long, short, and supershort based on the presence of regulatory domains. These regulatory domains influence the functional effect of phosphorylation by different kinases including PKA and extracellular signal-regulated kinas (ERK) on PDE4 enzymatic activity (Paes et al., 2021). Long PDE4 isoforms are activated when phosphorylated by PKA (Alvarez et al., 1995; Hoffmann et al., 1998; MacKenzie et al., 2002; Sette and Conti, 1996; Sette et al., 1994), whilst being inhibited when phosphorylated by ERK (Baillie et al., 2000; Hoffmann et al., 1999; Lenhard et al., 1996; MacKenzie et al., 2000). In case of phosphorylation by both PKA and ERK, the ERK-mediated inhibition of long PDE4 forms will be relieved by concurrent phosphorylation by PKA (Hoffmann et al., 1999). Lacking the necessary regulatory domain, short PDE4 isoforms cannot be modulated by PKA but can be phosphorylated by ERK, resulting in enzyme activation. Similarly, supershort PDE4 isoforms can only be modulated by ERK, but in contrast to short isoforms, phosphorylation of ERK results in inhibition on supershort forms (Baillie et al., 2000). Importantly, while ERK may phosphorylate all PDE4 subtypes, this phosphorylation has only effects on the enzymatic activity of PDE4B, PDE4C, and PDE4D, but not PDE4A, forms due to the differences in amino acid sequence (Baillie et al., 2000; Lario et al., 2001; Paes et al., 2021). Interestingly, since PKA and ERK are activated downstream from cAMP signaling, their effects on PDE4 isoform activity act as feedback mechanisms on cAMP signaling (Figure 1). PKA is activated directly upon binding cAMP, whilst ERK is activated by intermediate signaling molecules downstream from cAMP. In fact, cAMP and ERK signaling are intricately linked in cell-type specific and cell-context dependent manners (reviewed in: (Stork and Schmitt, 2002)). Upon being activated by cAMP-bound Epac, Rap1 can initiate B-raf signaling which eventually activates ERK in specific cell types (Bos et al., 2001; Dugan et al., 1999; Hoy et al., 2020).

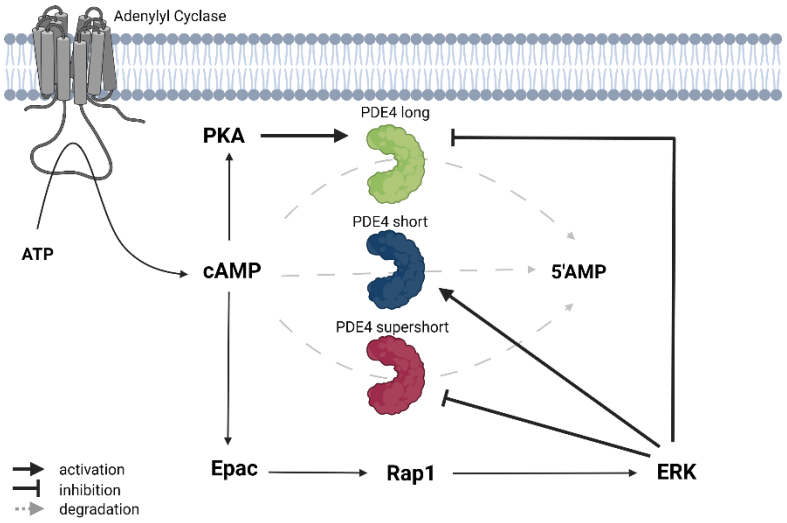

Figure 1. Schematic representation of cAMP signaling cascades that influence PDE4-mediated cAMP degradation. cAMP is created by conversion of ATP by adenylyl cyclases and is degraded by PDE4 enzymes to 5'-adenosine monophosphate (5'AMP). PDE4 enzymes comprise different isoform categories (i.e. long, short, and supershort) which are generated via the use of alternative promoters and alternative splicing from the four human PDE4 genes. The kinases PKA and ERK are activated downstream of cAMP and can influence the enzyme activity of PDE4 in an isoform-specific manner; long forms are activated upon phosphorylation by PKA, whilst phosphorylation by ERK causes inhibition of long and supershort PDE4 and activation of short PDE4. These feedback mechanisms contribute to the PDE4-mediated dynamic control of cAMP signaling. This figure was created with BioRender.com.

The fact that PDE4 isoforms show specific intracellular distribution patterns and their activity is dynamically and isoform-specifically regulated makes PDE4 isoforms crucial spatiotemporal regulators of cAMP signaling. Understanding the role of the different PDE4 isoform categories on this dynamic cAMP regulation will aid in determining which isoform type to inhibit to elicit the desired physiological effect. Consequently, inhibition of specific PDE4 isoforms may modulate cAMP signaling more effectively and may be therapeutically safer by inducing fewer or less severe side effects.

Signal termination, mediated by the different PDE4 isoform types, is critical in cAMP signaling and occurs very rapidly. This rapid termination makes experimental investigation of the role of specific PDE4 isoforms in spatiotemporal control of cAMP signaling difficult (Beavo and Brunton, 2002). Computational modeling of complex, dynamic biological mechanisms like cAMP signaling can overcome several experimental limitations while providing pivotal insights into the importance of specific molecules by considering cross-talk and feedback mechanisms. Various mechanistic computational models have been developed previously to understand cAMP signaling pathway dynamics. These models have investigated amongst others the diffusion and stochastic effects on the information flow through PKA signaling (Bhalla, 2004), the dynamics of calcium-induced cAMP signaling (Jędrzejewska-Szmek et al., 2017; Ohadi and Rangamani, 2019; Ohadi et al., 2019; Shumilov and Gotovtsev, 2021), the influence of receptor protein kinase and G-protein coupled receptor crosstalk (Getz et al., 2019), and the localization of cAMP signaling in subcellular domains (Kim et al., 2011; Oliveira et al., 2012; Stone et al., 2019; Tenner et al., 2020). Despite their important role in inactivating cAMP, cAMP-degrading PDE enzymes and their isoforms, which respond differently to feedback mechanisms, are not always included in the computational modeling efforts. Some models have studied the influence of PDE4 (Chay et al., 2016), PDE4 and PDE1 (Kim et al., 2011; Lindskog et al., 2006; Ohadi and Rangamani, 2019; Ohadi et al., 2019), and PDE1 and PDE10 (Oliveira et al., 2012). Others have investigated theoretically how a single PDE or PDE complexes can create cAMP nanocompartments and how these depend on the cAMP degradation rate, cAMP diffusion rate and geometrical and topological parameters (Lohse et al., 2017). Only the framework of Oliveira et al. specifically modeled two different subtypes of PDE4, i.e. PDE4B (located in the submembrane region) and PDE4D (located in the cytosol), the most prevalent isozymes in HEK293 cells (Oliveira et al., 2010). Their simulation results demonstrated that the generation of a cAMP microdomain required a pool of PDE4D anchored in the cytosol as well as

a PKA-mediated increase of PDE4D activity. Interestingly, cAMP microdomains did not require impeded diffusion of cAMP (Oliveira et al., 2010). To our knowledge, the influence of feedback mechanisms on general, but not isoform-specific, PDE4 activity has only been described by Song et al. (Song et al., 2013).

In this study, we model the dynamics of cAMP signaling and investigate the involvement of specific PDE4 isoform types, i.e. long, short and supershort, and the PKA/ERK feedback thereon, in the modulation of cAMP signaling dynamics. Using a computational approach we intend to better understand and conceptualize the signaling feedback mechanisms that differentially modulate the PDE4 isoform activity to determine which PDE4 isoform type may provide a more efficacious target in diseases in which PDE4 inhibition shows therapeutic potential.

MATERIALS AND METHODS

Mathematical model development

To simulate isoform-specific PDE4-mediated control of cAMP dynamics, a mathematical model was developed and implemented in the virtual cell environment VCell (http://vcell.org) (Slepchenko and Loew, 2010). Fifteen ordinary differential equations were established which describe the dynamics of cAMP, PDE4, PKA, Epac and RAP-1/ERK signaling in time. The following sections describe the mathematical framework of the model, the reactions and corresponding kinematic parameters. Figure 2 shows a schematic of the variables included in the model and their interactions.

Parameter values and initial conditions

Considering the high diffusion capability of free, unbound cAMP (Bock et al., 2020; Yang et al., 2016), we modelled the system as well-mixed using ordinary differential equations, which are listed, including initial concentrations, in Table 1. We also assume that all downstream, inactivated components are not present at the start of the simulation. All reactions and corresponding parameters are given in Tables 2 and 3. All reactions are assumed to be reversible, except the irreversible degradation of cAMP and phosphorylation-based actions on PDE4 isoforms.

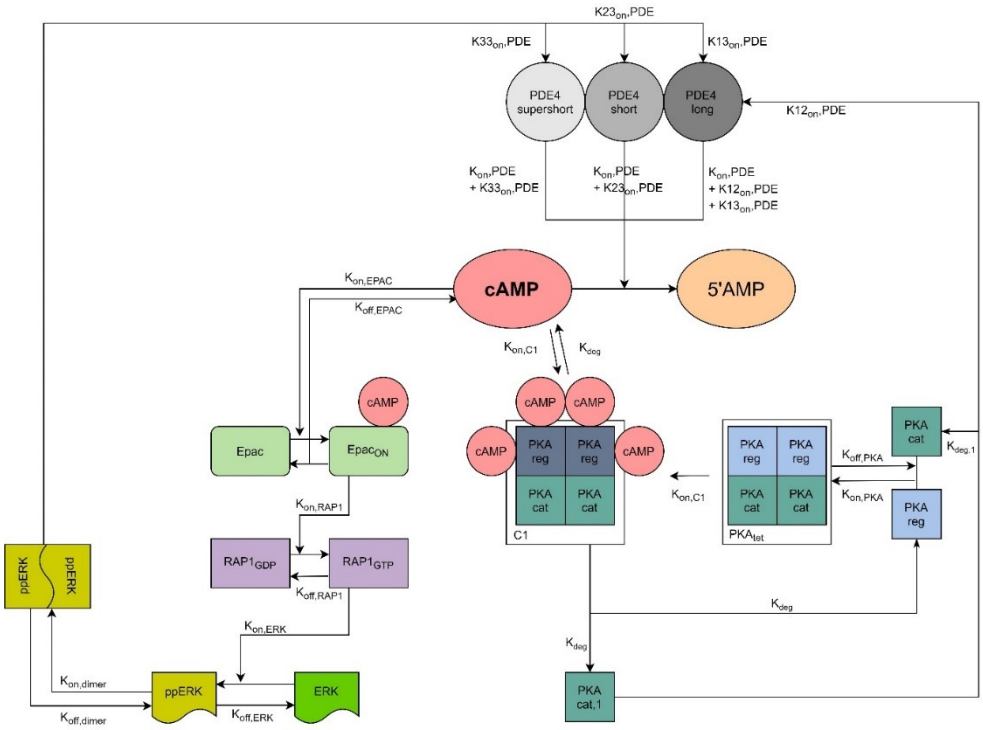

Figure 2: Schematic representation of the molecular reactions incorporated in the computational model. cAMP is modelled as an initial condition and is degraded to 5'AMP by different PDE4 isoforms (long, short, and supershort) that each can exhibit different degradation rates (e.g. $K12_{on}PDE$). If not degraded, cAMP can bind and activate the tetramer PKA (PKA_{tet}) to form C1, which causes PKA_{cat} subunits to be released ($PKA_{cat,1}$). Similarly, cAMP can bind and activate Epac to form $Epac_{ON}$, which can convert $RAP1_{GDP}$ into $RAP1_{GTP}$ to eventually elicit ERK phosphorylation and dimerization (ppERK). $PKA_{cat,1}$ and ppERK can modulate PDE4 isoform activity and thereby provide feedback mechanisms of cAMP signaling.

Table 1. Overview of reaction species, ordinary differential equations (ODE) and initial concentrations

#	Species	Description	Ordinary differential equation	Initial concentration (µM)	Reference for the used initial concentration
1	[cAMP]	cAMP concentration	$\frac{dcAMP}{dt} = -(k_{on,\ PDE} + k12_{on,\ PDE} + k13_{on,\ PDE}) \cdot cAMP \cdot PDE4_{long} - (k_{on,\ PDE} + k22_{on,\ PDE} + k23_{on,\ PDE}) \cdot cAMP \cdot PDE4_{short} - (k_{on,\ PDE} + k32_{on,\ PDE} + k33_{on,\ PDE}) \cdot cAMP \cdot PDE4_{supershort} - 4 \cdot k_{on,C1} \cdot \frac{PKA \cdot cAMP^{1.6}}{k_{mPKA}^{1.6} + cAMP^{1.6}} + 4 \cdot k_{deg} \cdot C_1 - k_{on,EPAC} \cdot \frac{EPAC \cdot cAMP}{k_{mEPAC} + cAMP} + k_{off\_Epac} \cdot Epac_{on}$	0.3 (standard) or cyclic input (see text)	(Agarwal et al., 2016), (Jedrzejewska-Szmek et al., 2017)
2	[AMP]	AMP concentration	$\frac{dAMP}{dt} = (k_{on,\ PDE} + k12_{on,\ PDE} + k13_{on,\ PDE}) \cdot cAMP \cdot PDE4_{long} + (k_{on,\ PDE} + k22_{on,\ PDE} + k23_{on,\ PDE}) \cdot cAMP \cdot PDE4_{short} + (k_{on,\ PDE} + k32_{on,\ PDE} + k33_{on,\ PDE}) \cdot cAMP \cdot PDE4_{supershort}$	0	(Neves et al., 2008)
3	[PDE4]	PDE4 concentration	constant	1 (standard) (hippocampal proportions, $PDE4_{long}$: 0.7; $PDE4_{short}$: 0.11; $PDE4_{supershort}$: 0.19)	(Neves et al., 2008) (**Supplementary Material**)
4	[PKA_{cat}]	PKA catalytic subunits	$\frac{dPKA_{cat}}{dt} = -2\ k_{on,PKA} \cdot PKA_{cat}^2 \cdot PKA_{reg}^2 + k_{deg,1} \cdot PKA_{cat,1} + 2k_{off\_PKA} \cdot PKA_{tet}$	0.023	(Oliveira et al., 2010)
5	[PKA_{reg}]	PKA regulatory subunits	$\frac{dPKA_{reg}}{dt} = -2k_{on,PKA} \cdot PKA_{reg}^2 \cdot PKA_{cat}^2 + 2k_{off\_PKA} \cdot PKA_{tet} + 2k_{deg} \cdot C_1$	0.048	(Oliveira et al., 2010)
6	[PKA_{tet}]	PKA tetramer	$\frac{dPKAtet}{dt} = k_{on\_PKA} \cdot PKA_{cat}^2 \cdot PKA_{reg}^2 - k_{off\_PKA} \cdot PKA_{tet} - k_{on,C1} \cdot \frac{PKAtet \cdot cAMP^{1.6}}{k_{mPKA}^{1.6} + cAMP^{1.6}}$	0.173	(Neves et al., 2008; Ohadi et al., 2019)
7	[C1]	cAMP-bound PKA tetramer	$\frac{dC1}{dt} = k_{on,C1} \cdot \frac{PKAtet \cdot cAMP^{1.6}}{k_{mPKA}^{1.6} + cAMP^{1.6}} - k_{deg} \cdot C1$	0	Model assumption
8	[PKA_{cat1}]	active PKA catalytic subunit	$\frac{dPKA_{cat1}}{dt} = 2k_{deg} \cdot C_1 - k_{deg,1} \cdot PKA_{cat,1}$	0	(Oliveira et al., 2010)
9	[EPAC]	inactivated Epac	$\frac{dEPAC}{dt} = -k_{on,EPAC} \cdot \frac{EPAC \cdot cAMP}{k_{mEPAC} + cAMP} + k_{off\_Epac} \cdot Epac_{on}$	0.488	(Jedrzejewska-Szmek et al., 2017; Salonikidis et al., 2008)

#	Species	Description	Ordinary differential equation	Initial concentration (µM)	Reference for the used initial concentration
10	[$EPAC_{on}$]	cAMP-bound, activated Epac	$\frac{dEPAC_{on}}{dt} = k_{on,EPAC} \cdot \frac{EPAC \cdot cAMP}{k_{mEPAC}+cAMP} - k_{off\_Epac} \cdot Epac_{on} - k_{onRAP1} \cdot Epac_{on} \cdot RAP1\_GDP + k_{offRAP1} \cdot RAP1_{GTP}$	0	(Jedrzejewska-Szmek et al., 2017)
11	[$RAP1_{GDP}$]	inactive Rap1	$\frac{dRAP1_{GDP}}{dt} = -k_{on,RAP1} \cdot Epac_{on} \cdot RAP1_{GDP} + k_{off,RAP1} \cdot RAP1_{GTP}$	0.2	(Sasagawa et al., 2005)
12	[$RAP1_{GTP}$]	active Rap1	$\frac{dRAP1_{GTP}}{dt} = k_{on,RAP1} \cdot Epac \cdot RAP1_{GDP} - k_{off,RAP1} \cdot RAP1_{GTP} - k_{on,ERK} \cdot RAP1_{GTP} \cdot ERK + k_{off} \cdot ppERK$	0	Model assumption
13	[ERK]	ERK concentration	$\frac{dERK}{dt} = -k_{on,ERK} \cdot ERK \cdot RAP1_{GTP} + k_{off,ERK} \cdot ppERK$	0.8	(Zhang et al., 2011)
14	[ppERK]	activated ERK	$\frac{dppERK}{dt} = k_{on,ERK} \cdot ERK \cdot RAP1_{GTP} - k_{off,ERK} \cdot ppERK + 2 \cdot k_{off,dimer} \cdot ERK_{dimer} - 2k_{on,dimer} \cdot ppERK^2$	0	Model assumption
15	[ERK_{dimer}]	dimerized ERK	$\frac{dERK_{dimer}}{dt} = k_{on,dimer} \cdot ppERK^2 - k_{off\ dimer} \cdot ERK_{dimer}$	0	Model assumption

cAMP and PDE4 dynamics

cAMP signaling is initiated by the synthesis of cAMP by activated adenylyl cyclases. Since the primary focus of this study is the role of different PDE4 isoforms on cAMP signaling, we investigate three types of initial cAMP conditions: 1) an initial pulse of 0.1, 0.3, 1 or 3 μM and 2) a continuous, cyclic input of cAMP specified as follows:

$$cAMP_{input} = 0.45 \,.\, |\sin(0.015t)| \,.\, (0.9998^{t}) + 0.3$$

which reflects the cAMP oscillations reported by Ohadi et al. (Ohadi et al., 2019) and 3) a ramp function of cAMP input defined as follows:

$$cAMP_{input} = 0.001.t \;(t < 300) + 0.3 \;(t > 300)$$

resulting in a gradual, time-dependent increase over 300s (Calebiro et al., 2009) until a constant input of 0.3 μM, mimicking a sustained plateau of adenylyl cyclase activation. Note that we do not model adenylyl activity explicitly here.

We simulate in the computational model the PDE4-mediated enzymatic inactivation of cAMP (Table 1: Equations 1-2). Moreover, we model the total initial amount of all PDE4 isoforms combined as constant and equal to 1 μM (Table 1: Equations 3) (Neves et al., 2008). The relative distribution of the PDE4 isoforms is modeled as follows: 70% long PDE4 isoform, 11% short PDE4 isoform and 19% supershort PDE4 isoform. These distributions are based on in-house measurements of rat hippocampal tissue to exemplify tissue-specific isoform proportions (see Supplementary Material). Since long PDE4 isoforms comprise 70% of the total in this tissue, the effect of long PDE4 isoforms on cAMP signaling may be biased by the fact that these long forms are most abundantly present. As such, we control for this potential bias by also investigating a scenario in which the isoforms have equal proportions. More specifically, one isoform is set to zero and the other isoforms are

both present at 0.5 μM concentration in order to keep the total PDE4 concentration constant at 1 μM (Figure 10). In the computational model, cAMP degradation is modelled with mass action kinetics, and has three contributions: 1) baseline degradation by PDE4 that is independent of isoform type, 2) isoform-specific modulation of the baseline degradation by the activated catalytic subunit of PKA ($PKA_{cat,1}$), and 3) isoform-specific modulation of the baseline degradation by activated ERK (ERK_{dimer}) (Table 1: Equations 1-2).

The activated catalytic subunit of PKA ($PKA_{cat,1}$) and activated ERK (ERK_{dimer}) are modeled to influence cAMP degradation rate by activating or inhibiting PDE4, depending on the PDE4 isoform involved (Paes et al., 2021). Therefore, $k12_{on,PDE}$, $k13_{on,PDE}$, $k22_{on,PDE}$, $k23_{on,PDE}$, $k32_{on,PDE}$ *and* $k33_{on,PDE}$ are not constant but depend on $PKA_{cat,1}$ or ERK_{dimer}, which can have an inhibitory (V_{max} is negative) or stimulating (V_{max} is positive) effect depending on the affected PDE4 isoform. These phosphorylation-based activity effects were modeled with a Michaelis-Menten function as:

$$ki2_{on,\,PDE} = \frac{v_{maxi} \cdot PKA_{cat1}}{k_{mi} + PKA_{cat1}} \quad and \quad ki3_{on,\,PDE} = \frac{v_{max1i} \cdot ERK_{dimer}}{k_{m1i} + ERK_{dimer}}$$

with i=1,2,3 *(Eq. 1)*

Phosphorylation by PKA or ERK changes the rate of cAMP hydrolysis by PDE4 by changing V_{max} without affecting k_m (Hoffmann et al., 1999; Hoffmann et al., 1998). Moreover, it has been reported that the k_m values for different PDE4 forms are similar (Bolger et al., 1996; Jin et al., 1992; Saldou et al., 1998). It has been reported that the measured basal V_{max} ($8.s^{-1}$) is increased to 272% due to phosphorylation by PKA and reduced by 75% due to phosphorylation by ERK in case of the long isoform (Hoffmann et al., 1999; Hoffmann et al., 1998). The basal activity of the short isoform and supershort isoforms are increased to 130% and reduced to 85% respectively due to phosphorylation by ERK (Baillie et al., 2000). We would like to highlight that some literature reports mention a % reduction in the Vmax value and others an overall

activity reduction with respect to the baseline value. Here we have chosen to adapt the basal Vmax value (taken as 8 s-1 based on (Bolger et al., 1997; Lim et al., 1999; Neves et al., 2008; Reeves et al., 1987)). For example, a 272% increase in the Vmax of long isoform mutated to mimic PKA phosphorylation has been reported (Hoffmann et al., 1999), which we captured via a Vmax of 21.76 (i.e. $k12_{on,PDE}$). A similar reasoning was made for the other Vmax values (Hoffmann et al., 1999; MacKenzie et al., 2000). Parameters used for each isoform are given in Table 2. We also implemented that $k13_{on,PDE}$ and $k33_{on,PDE}$ cannot become larger than the baseline PDE4 degradation rate ($k_{on,PDE}$: 0.15 $\mu M \cdot s^{-1}$), as this would result in 'negative degradation' and therefore 'production' of cAMP. The degradation of cAMP into AMP is assumed to be irreversible as cAMP can only be synthesized by conversion of ATP via ACs.

Table 2. Kinematic parameters used to model activity of PDE4 isoforms upon phosphorylation by PKA and ERK

Parameter	Description	k_m (μM)	Vmax ($\mu M^{-1} \cdot s^{-1}$)	Vmax %	References
$k_{on,PDE}$	Baseline PDE4 degradation rate	/	0.15 (mass action kinetics)		(Neves et al., 2008)
$k12_{on,PDE}$	PDE4 long PKA-phosphorylated	1.3	21.76	272%	(Hoffmann et al., 1999)
$k13_{on,PDE}$*	PDE4 long ERK-phosphorylated	1.3	-2	25%	(Hoffmann et al., 1999)
$k22_{on,PDE}$	PDE4 short PKA-phosphorylated	0	0		
$k23_{on,PDE}$	PDE4 short ERK-phosphorylated	1.3	10.4	130%	(MacKenzie et al., 2000)
$k32_{on,PDE}$	PDE4 supershort PKA-phosphorylated	0	0		
$k33_{on,PDE}$*	PDE4 supershort ERK-phosphorylated	1.3	-6.8	85%	(MacKenzie et al., 2000)

*$k13_{on,PDE}$ and $k33_{on,PDE}$ cannot become larger than $k_{on,PDE}$ (0.15 $\mu M.s^{-1}$), the baseline PDE4 degradation rate ($k_{on,PDE}$).

PKA dynamics

PKA activation by cAMP is modelled as a multistep process using mass action kinetics. The inactive tetramer PKA (PKA_{tet}) is formed by the association of two catalytic (PKA_{cat}) and two regulatory subunits (PKA_{reg}) with constant $k_{on,PKA}$. We assume that four cAMP molecules can bind cooperatively to the tetramer with a Hill coefficient of 1.6 (Kim et al., 2007; Zhang et al., 2015), to form a complex (C1). When C1 dissociates (with constant k_{deg}), the active catalytic subunits ($PKA_{cat,1}$) are released. Inactivation of the active catalytic subunits ($PKA_{cat,1}$) occurs at a constant rate $k_{deg,1}$, after which the catalytic subunits can re-associate with the regulatory subunits to form the PKA tetramer, PKA_{tet} (Fig. 2 and Table 1: Equations 4-8).

At basal cAMP levels PKA activity has been found to be absent (Koschinski and Zaccolo, 2017). We therefore assumed that cAMP was only able to significantly bind PKA when cAMP levels were higher than 5.2 µM (Koschinski and Zaccolo, 2017), which we modelled by putting k_{mPKA} to 5.2 µM (Table 1, Equation 7).

Epac-RAP1-ERK dynamics

Epac is a guanine nucleotide exchange factor (GEF) that aids in the activation of Rap1 (Bos et al., 2001; de Rooij et al., 1998; Schmidt et al., 2013). In the model, the binding of cAMP to Epac with rate constant $k_{on,Epac}$ releases Epac from its auto-inhibitory conformation (EPAC), producing $EPAC_{on}$ (Table 1: Equations 9-10). We assumed that Epac could only be significantly activated at cAMP concentrations higher than 30 µM, which we captured by setting k_{mEPAC} to 30 µM (Table 1, Equation 9) (Purves et al., 2009). Subsequently, $EPAC_{on}$ is able to activate Rap1, which is mathematically represented in Table 1: Equations 11-12. Rap1 can, through complex, cross-talking signaling cascades, modulate ERK activation (Bos et al., 2001; Dugan et al., 1999; Stork and Schmitt, 2002). Since PDE4 inhibitors that should exert therapeutic actions in the brain are also prone to induce PDE4-mediated side effects by actions in the brainstem, we sought to better understand PDE4-mediated cAMP degradation in neurons specifically. In neurons, cAMP increases ERK activity in an

Rap1/B-raf dependent manner (Dugan et al., 1999). Here, we assume that Rap1 directly activates ERK, as intermediate signaling via B-raf and MEK consists of linear reactions. ERK is activated after its dual phosphorylation and subsequent dimerization (Fig. 2 and Table 1: Equations 13-15). ERK dimerization is crucial for extranuclear/cytosolic actions, and PDE4 was found to associate with ERK2 dimers and not with monomers (Casar et al., 2008; Herrero et al., 2015). Subsequently, the ERK_{dimer} is able to phosphorylate PDE4 isoforms and stimulate or inhibit their rate isoform-specifically (Equation 1 and Table 2) (Houslay and Baillie, 2003).

Simulation settings

Simulations were run in VCell, for a duration of 500 or 1500s with a combined stiff solver (IDA/CVODE). The absolute and relative tolerance was set to $1 \cdot 10^{-9}$. The models for a single pulse and continuous input, can be accessed on the VCell public model repository https://vcell.org/vcell-published-models. The names of the models are as follows, for a single pulse: Carlier_cAMP_isoforms_v2; and for continuous, cyclic input: Carlier_cAMP_isoforms_cyclic_v2.

Details on running a model in VCell can be found in the quick start guide on the VCell website, https://vcell.org/support. Data was analyzed using GraphPad Prism V9.1.0.

Table 3: Reactions and kinetic parameters

#	Reaction	Rate constants	Value	Reference
1	$\xrightarrow{kon,PDE;\ PDE}$ cAMP → AMP	$k_{on,PDE}$	0.15 $\mu M^{-1} s^{-1}$	(Xin et al., 2008)
2	$2PKA_{cat} + 2PKA_{reg} \underset{koff,PKA}{\overset{kon,PKA}{\rightleftharpoons}} PKA$	$k_{on,PKA}$	10 $\mu M^{-3} s^{-1}$	Estimated
		$k_{off,PKA}$	$6 \cdot 10^{-4}$ s^{-1}	
3	$PKA + 4cAMP \xrightarrow{kon,C1} C_1$	$k_{on,C1}$	0.0261 s^{-1}	(Jedrzejewska-Szmek et al., 2017) (Koschinski and Zaccolo, 2017)
		$k_{m,PKA}$	5.2 µM	
4	$C1 \xrightarrow{kdeg} 2PKA_{cat,1} + 2PKA_{reg} + 4cAMP$	k_{deg}	0.21 s^{-1}	(Ohadi et al., 2019)
5	$PKA_{cat,1} \xrightarrow{kdeg,1} PKA_{cat}$	$k_{deg,1}$	0.0051 s^{-1}	(Jedrzejewska-Szmek et al., 2017)
6	$Epac + cAMP \underset{koff,Epac}{\overset{kon,Epac}{\rightleftharpoons}} Epac_{on}$	$k_{on,Epac}$	0.031 s^{-1} (estimated)	(Jedrzejewska-Szmek et al., 2017)
		$k_{off,Epac}$	0.00651 s^{-1}	
		$k_{m,Epac}$	30 µM	(Purves et al., 2009)
7	$Epac_{on} + RAP1_{GDP} \underset{koff,RAP1}{\overset{kon,RAP1}{\rightleftharpoons}} RAP1_{GTP}$	$k_{on,RAP1}$	0.05 $\mu M^{-1}/s^{-1}$ (estimated)	(Sasagawa et al., 2005)
		$k_{off,RAP1}$	$1.166 \cdot 10^{-4}$ s^{-1}	
8	$RAP1_{GTP} + ERK \underset{koff,ERK}{\overset{kon,ERK}{\rightleftharpoons}} ppERK$	$k_{on,ERK}$	0.88 $\mu M^{-1}/s^{-1}$	(Fujioka et al., 2006; Radhakrishnan et al., 2009)
		$k_{off,ERK}$	0.088 s^{-1}	
9	$ppERK + ppERK \underset{koff,dimer}{\overset{kon,dimer}{\rightleftharpoons}} ERK_{Dimer}$	$k_{on,dimer}$	0.2 $\mu M^{-1}/s^{-1}$	Estimated based on Kd=7.5nM (Khokhlatchev et al., 1998)
		$k_{off,dimer}$	0.0015 s^{-1}	

Sensitivity analysis

A sensitivity analysis was performed on the standard model where the Vmax parameter values were altered to investigate which Vmax was most influential on the average and maximal cAMP values over 1500 seconds for cyclic input (see Figure S3). The sensitivity was calculated as follows:

$$\text{Sensitivity} = \frac{|\text{cAMP}(\text{k}) - \text{cAMP}(\text{k} + \Delta\text{k})|}{\text{cAMP}(\text{k} + \Delta\text{k})} \Big/ \frac{\Delta\text{k}}{\text{k}}$$

where,

cAMP (k) = the maximal or average cAMP concentration over 1500 seconds for cyclic input using the standard model settings

cAMP (k+Δk)= the maximal or average cAMP concentration over 1500 seconds for cyclic input at + or - 10% of the standard Vmax model parameter values

Δk=varied parameter

k=standard model parameter value

RESULTS

Degradation dynamics of a single cAMP pulse

Different initial cAMP concentrations (0.1-3.0 μM) were used in the simulations to explore potential concentration-dependent effects on cAMP degradation (Figure 3). Irrespective of the initial cAMP concentration, single cAMP pulses were completely degraded within 25 s. Comparison of the degradation rates revealed that initial cAMP concentrations of 1.0 and 3.0 μM induced a higher degradation rate compared to lower initial cAMP concentrations (Fig 3A, insert). Note that increases in initial cAMP concentrations are not proportional to the amount of cAMP present over time (reflected by the areas under the curve (AUC), Fig 3B). For example, for a pulse of 3.0 μM cAMP, a fold change of 10 would be expected whilst a fold change of 8.17 is observed, which indicates that higher initial cAMP concentrations elicit additional effects to facilitate its own degradation.

A

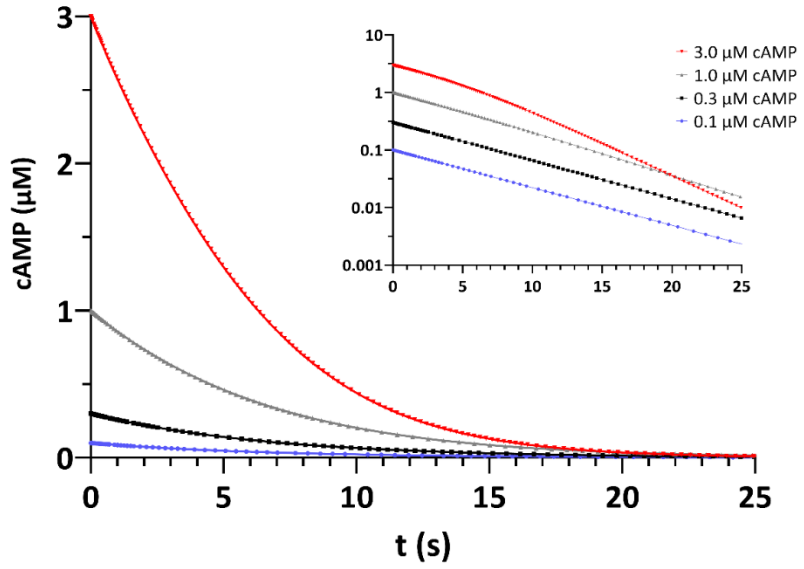

B

cAMP		Fold changes		
cAMP condition		Time to peak	Peak	AUC
0.1 µM cAMP	0.33	1	0.33	0.34
0.3 µM cAMP	1	1	1	1
1.0 µM cAMP	3.33	1	3.33	3.17
3.0 µM cAMP	10	1	10.00	8.17

Figure 3. Degradation dynamics of single cAMP pulses of different concentration predicted by the computational model. A) Single cAMP pulses in a concentration range of 0.1-3.0 µM are quickly degraded for all simulated concentrations. In the insert, degradation rates are compared by log-transformation of the y-axis showing equal degradation rates for cAMP concentration of 0.1-1.0 µM and profound increased degradation of cAMP in case of an initial concentration of 3 µM cAMP. B) Overview of plot characteristics per initial cAMP concentration. Fold changes in initial cAMP concentration, time to peak, peak value, and area under the curve (AUC) are shown compared to the 0.3 µM cAMP condition. These values indicate that the AUC does not change proportionally to the change in initial cAMP concentration. Simulations were run for 500 s considering estimated hippocampal PDE4 isoform proportions and a total initial (constant) amount of all PDE4 isoforms combined equal to 1 µM..

Effects of different cAMP concentrations on PKA, Epac, and ERK dynamics

Although distinct cAMP pulse concentrations were all found to be quickly degraded based on our initial simulations, we next sought to explore how downstream signaling cascades are affected by these different initial cAMP concentrations. In our computational model, we have focused on the downstream cAMP-PKA and cAMP-Epac-ERK pathways as PKA and ERK affect cAMP signaling using feedback mechanisms through the modulation of PDE4 enzyme activity. In the following sections, the mentioning of PKA, Epac, and ERK reflects concentrations of the species $PKA_{cat,1}$, $Epac_{ON}$, and ERK_{dimer}, respectively.

Simulations using single cAMP pulses of different concentrations revealed that PKA and Epac are differentially activated depending on the cAMP concentration. For example, cAMP pulses of 0.3 and 1.0 μM lead to slightly higher peak activation of Epac compared to PKA, whilst a cAMP pulse of 3.0 μM induces profoundly higher peaks of PKA compared to Epac (Fig 4A,B,D,E). Moreover, a distinction in PKA and Epac dynamics can be observed regarding their concentrations over time. Irrespective of the concentration cAMP, PKA levels subside more slowly compared to Epac (Fig 3A,B). ERK signaling is only activated if Epac is sufficiently activated (Fig 4 and Fig 2 in Material and Methods). Higher initial cAMP levels resulted profoundly higher ERK_{dimer} concentrations until the endpoint of the simulation (500 s) (Fig 4C,F).

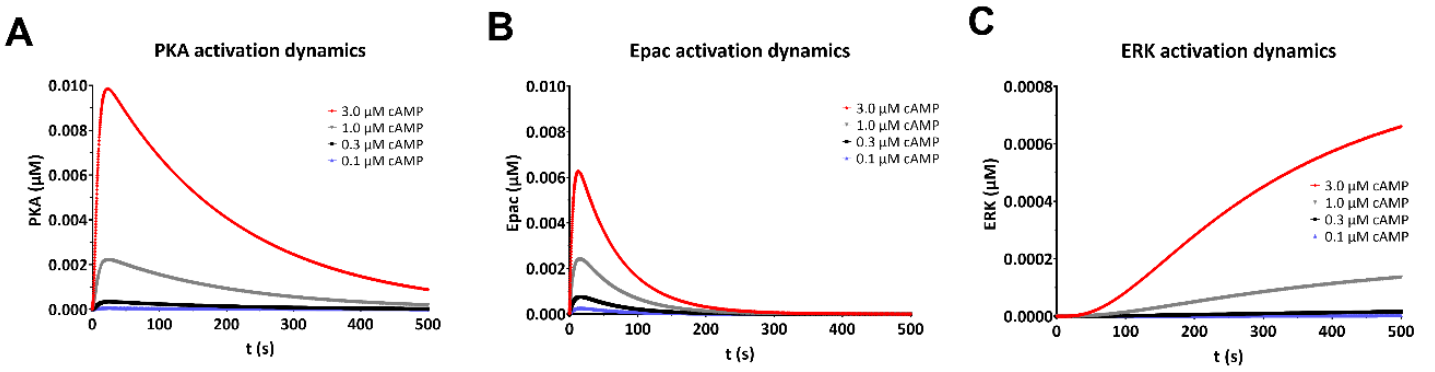

D

PKA		Fold changes		
cAMP condition		Time to peak	Peak	AUC
0.1 µM cAMP	0.33	1.03	0.17	0.17
0.3 µM cAMP	1	1	1	1
1.0 µM cAMP	3.33	1.04	6.43	6.41
3.0 µM cAMP	10	0.98	28.56	28.31

E

Epac		Fold changes		
cAMP condition		Time to peak	Peak	AUC
0.1 µM cAMP	0.33	0.95	0.34	0.34
0.3 µM cAMP	1	1	1	1
1.0 µM cAMP	3.33	0.97	3.18	3.13
3.0 µM cAMP	10	0.81	8.29	7.79

F

ERK		Fold changes		
cAMP condition		Time to peak	Peak	AUC
0.1 µM cAMP	0.33	1	0.12	0.12
0.3 µM cAMP	1	1	1	1
1.0 µM cAMP	3.33	1	8.61	8.93
3.0 µM cAMP	10	1	41.77	46.62

Figure 4. Activation dynamics of downstream signaling by different cAMP concentrations predicted by the computational model. Single cAMP pulses in a concentration range of 0.1-3.0 µM induced dose-dependent increases in PKA activation (A), Epac activation (B) and ERK activation (C). cAMP concentrations differentially affect PKA and Epac signaling as shown by differences in proportional peak height, time to peak and AUC differences for the various cAMP concentrations compared to the default model using 0.3 µM cAMP as initial concentration (D-E). ERK activation did not reach a plateau during the 500 s simulation, but shows non-linear increases as higher initial cAMP concentrations were simulated (C, F). PKA, Epac and ERK reflect the model species PKAcat,1, EpacON, and ERKdimer, respectively. Simulations were run for 500 s considering estimated hippocampal PDE4 isoform proportions.

Effects of PDE4 concentrations and isoform type on single pulse cAMP signaling

Corresponding to literature, cAMP is rapidly degraded in the computational model after a single cAMP pulse (Fig. 3). PDE4 enzymes play a pivotal role the regulation of cAMP signaling. To explore the effect of PDE4-mediated cAMP regulation, simulations were run using different concentrations of total PDE4 enzyme. Total PDE4 enzyme concentrations ranged from 0.1 to 10 μM, while taking into account the relative proportions of PDE4 isoform types as measured in the rat hippocampus as an example of organ-specific PDE4 isoform type expression (Supplementary Material). Relative proportions of long (0.70), short (0.11), and supershort (0.19) isoforms were kept constant for all total PDE4 concentrations. As expected, higher total PDE4 concentrations resulted in a more rapid degradation of a single 0.3 μM cAMP pulse (Fig. 5A). Dynamics of downstream PKA, Epac, and ERK signaling were highly non-linear for different PDE4 concentrations (Fig. 5B-D). For example, compared to the default total PDE4 concentration of 1 μM, higher PDE4 concentrations (3-10 μM) lead to 3- and 10-fold lower AUC values for cAMP, PKA and Epac. In contrast, lower PDE4 concentrations cause non-proportional increases in peak and AUC values for cAMP, PKA and Epac (Fig 5B,C,F). For example, a 10-fold higher initial cAMP pulse (3.0 μM) causes a 28.56- and 8.29-fold increase in the peak value for PKA and Epac, respectively. Regarding ERK activation, non-linear effects are observed for both lower and higher total PDE4 concentrations, implying ERK levels are particularly sensitive to the amount of PDE4 present (Fig 5D,F).

Interestingly, downstream signaling cascades appear to respond differently to increases in initial cAMP pulses versus reductions in the amount of PDE4 present when comparing to the default model in which an initial cAMP pulse of 0.3 μM is simulated with 1 μM PDE4 present. Specifically, a 10-fold increase in initial cAMP concentration causes a larger fold change in AUC value and peak value for PKA (PKA peak: 28.56 and AUC: 28.31; Fig 4D) compared to a 10-fold decrease in PDE4 concentration (PKA peak: 6.74 and AUC: 8.66; Fig 5F). In contrast, a 10-fold increase

in initial cAMP concentration causes a smaller fold change in AUC value for Epac (Epac AUC: 7.79; Fig 4E) compared to a 10-fold decrease in PDE4 concentration (Epac AUC: 8.89; Fig 5F). Moreover, changing the PDE4 concentration resulted into a more profound effect on the fold changes in time to peak for PKA and Epac (i.e. fold changes ranging 0.18-3.72; Fig 5F) compared to changes in cAMP input concentrations (i.e. fold changes ranging 0.81-1.04; Fig 4D,E). These findings indicate that changes in cAMP input or PDE4-mediated cAMP degradation differentially affect the amplitude and timing of activation of downstream signaling.

Because the enzyme activity of PDE4 isoform types is differentially altered by PKA and ERK feedback phosphorylation, we subsequently investigated whether the presence of a single PDE4 isoform type at a concentration of 1.0 μM, rather than a combination of them in specific proportions, resulted in isoform-specific dynamics of 0.3 μM cAMP pulse degradation. Unexpectedly, cAMP degradation was found to be identical irrespective of the PDE4 isoform type present (Fig. 5E). These results suggest that, for a single pulse, the rate of cAMP degradation is determined by the total isoform concentration rather than the isoform type present or the relative proportion of multiple types.

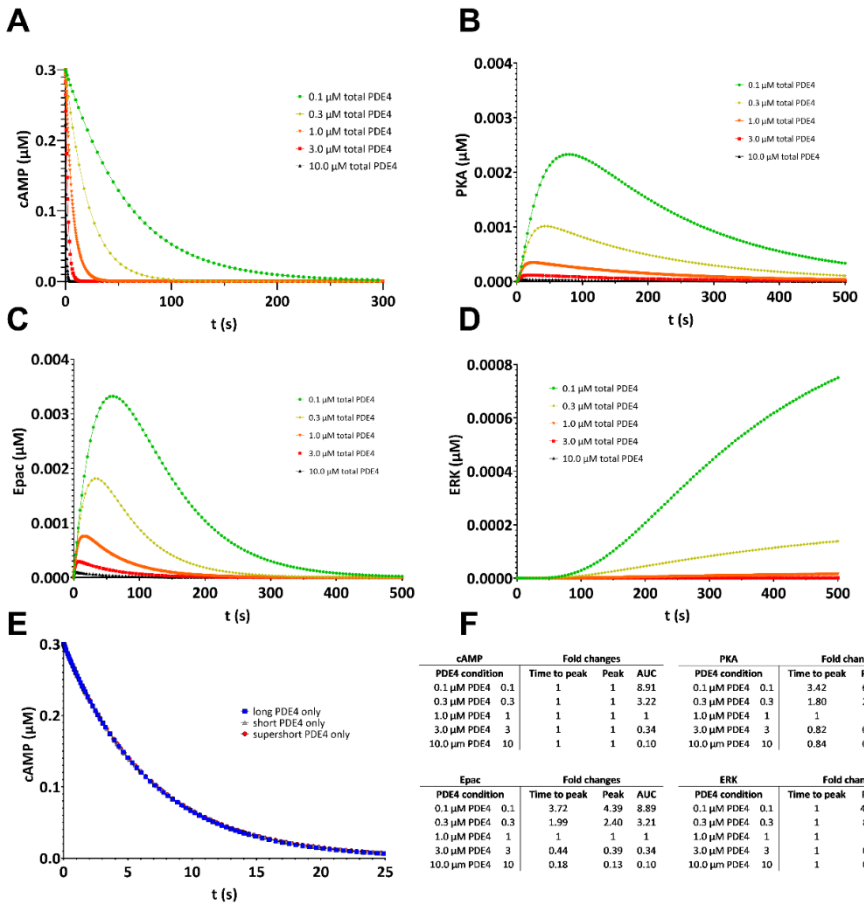

cAMP		Fold changes		
PDE4 condition		Time to peak	Peak	AUC
0.1 µM PDE4	0.1	1	1	8.91
0.3 µM PDE4	0.3	1	1	3.22
1.0 µM PDE4	1	1	1	1
3.0 µM PDE4	3	1	1	0.34
10.0 µm PDE4	10	1	1	0.10

PKA		Fold changes		
PDE4 condition		Time to peak	Peak	AUC
0.1 µM PDE4	0.1	3.42	6.74	8.66
0.3 µM PDE4	0.3	1.80	2.94	3.19
1.0 µM PDE4	1	1	1	1
3.0 µM PDE4	3	0.82	0.34	0.34
10.0 µm PDE4	10	0.84	0.10	0.10

Epac		Fold changes		
PDE4 condition		Time to peak	Peak	AUC
0.1 µM PDE4	0.1	3.72	4.39	8.89
0.3 µM PDE4	0.3	1.99	2.40	3.21
1.0 µM PDE4	1	1	1	1
3.0 µM PDE4	3	0.44	0.39	0.34
10.0 µm PDE4	10	0.18	0.13	0.10

ERK		Fold changes		
PDE4 condition		Time to peak	Peak	AUC
0.1 µM PDE4	0.1	1	47.53	45.15
0.3 µM PDE4	0.3	1	8.80	8.73
1.0 µM PDE4	1	1	1	1
3.0 µM PDE4	3	1	0.12	0.12
10.0 µm PDE4	10	1	0.01	0.01

Figure 5. The influence of PDE4 concentration and isoform type on single pulse cAMP signaling as predicted by the computational model. A) Degradation of a single 0.3 µM cAMP pulse is dependent on the concentration of total PDE4 present. Relative proportions of long, short and supershort PDE4 isoforms were kept constant. B-D) Lower total PDE4 concentrations induced higher peaks, increased time to peak and sustained activation of PKA, Epac and ERK. E) Simulations in which total PDE4 consists of only a specific PDE4 isoform type indicated that all PDE4 isoform types degrade a single 0.3 µM cAMP pulse identically. F) Fold changes in time to peak, peak and area under the curve (AUC) are listed for the different PDE4 concentration conditions, compared to the 1.0 µM PDE4 condition, for cAMP and for the downstream signaling molecules PKA, Epac, and ERK. PKA, Epac and ERK reflect the species $PKA_{cat,1}$, $Epac_{ON}$, and ERK_{dimer}, respectively. Simulations were run for 500 s considering, except for Fig 4E, estimated hippocampal PDE4 isoform proportions.

Dynamics of oscillatory cAMP signaling and isoform-specific control by PDE4

Following up on the unexpected finding that different PDE4 isoform types show identical dynamics of single cAMP pulse degradation when present at the same concentration, we hypothesized that single cAMP pulses may not be sufficient to elicit the PKA- and ERK-based feedback mechanisms on PDE4 activity as observed in cell-based experiments. Accordingly, under physiological conditions cAMP synthesis occurs in a prolonged, oscillatory manner rather than as the production of single cAMP pulses (Dyachok et al., 2006; Huff et al., 2020). Previous studies have shown that calcium oscillates spontaneously and that these oscillations influence the cAMP/PKA dynamics (Chen et al., 2013; Ohadi et al., 2019). In particular, computational work has shown that cAMP/PKA is a leaky integrator of calcium dynamics, meaning that cAMP/PKA senses the lower frequency of the calcium dynamics. Here, we wanted to explore how different PDE4 concentrations and isoform types regulate downstream signaling dynamics of oscillatory cAMP signaling.

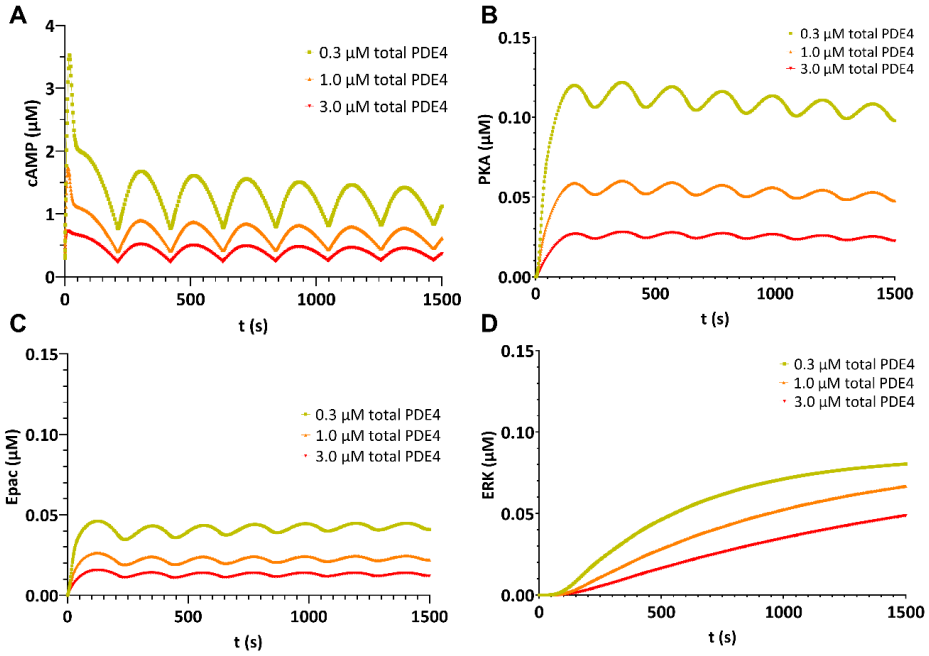

Figure 6. The influence of PDE4 concentration on oscillatory cAMP signaling as predicted by the computational model. A) Dynamic control of oscillatory cAMP pulses is dependent on the concentration of total PDE4 present. Relative proportions of long, short and supershort PDE4 isoforms were kept constant. B-D) Lower total PDE4 concentrations induced higher levels of activated PKA, Epac, and ERK. PKA, Epac and ERK reflect the species $PKA_{cat,1}$, $Epac_{ON}$, and ERK_{dimer}, respectively. Simulations were run for 1500 s considering estimated hippocampal PDE4 isoform proportions.

Similar as seen for a single cAMP pulse, the concentration of total PDE4 regulates oscillatory cAMP signaling and activation of downstream effectors (Fig 5 and 6). Higher (3.0 µM) and lower (0.3 µM) PDE4 concentrations resulted, respectively, in a faster and slower degradation of oscillatory cAMP (Fig 6A). Accordingly, activation of the effectors PKA ($PKA_{cat,1}$), Epac ($Epac_{ON}$) and ERK (ERK_{dimer}) was similarly changed and these effects were highly non-linear (Fig. 6B-D). Interestingly, and in contrast to a single pulse of cAMP, the isoform type or the relative proportion greatly influenced the rate of cAMP degradation in the simulated settings. More specifically, when keeping the total PDE4 concentration equal at 1 µM

but varying the type of isoform, Fig. 7 shows that the long and short isoforms maintain an oscillatory cAMP profile (albeit with a higher initial peak for the short isoform with respect to the long isoform, Fig. 7A), while the supershort isoform is not able to degrade the cyclic cAMP input at a sufficient rate, leading to a fast accumulation of cAMP (Fig. 7A insert). Also downstream signaling is distinct when only a specific PDE4 isoform type is present. For the short and long isoform, the steady state levels of activated PKA and Epac oscillate around 0.05 μM and 0.025 μM respectively, whereas for the supershort isoform, the steady state Epac and PKA levels are almost 10- and 5-fold higher (0.24 μM and 0.27 μM, Fig. 7B-C). A gradual increase in cAMP concentration followed by a sustained input resulted in similar findings to the cyclic cAMP input, i.e. the long and short isoforms maintain a stable cAMP profile, while the supershort isoform is not able to degrade the sustained cAMP input at a sufficient rate, leading to a fast accumulation of cAMP (see Supplementary Figure S2). As such, these results nicely correspond to the findings of the Conti laboratory in which sustained adenylyl cyclase activation as been shown to result in a transient increase in the intracellular cAMP concentration after which the intracellular cAMP concentrations reach a steady state level (for long isoform activation through PKA) (Rich et al., 2007). These simulations indicate that cAMP signaling is not effectively controlled in the presence of supershort PDE4 isoforms alone, suggesting that additional biological mechanisms would have to be employed to prevent cAMP levels from rising uncontrollably.

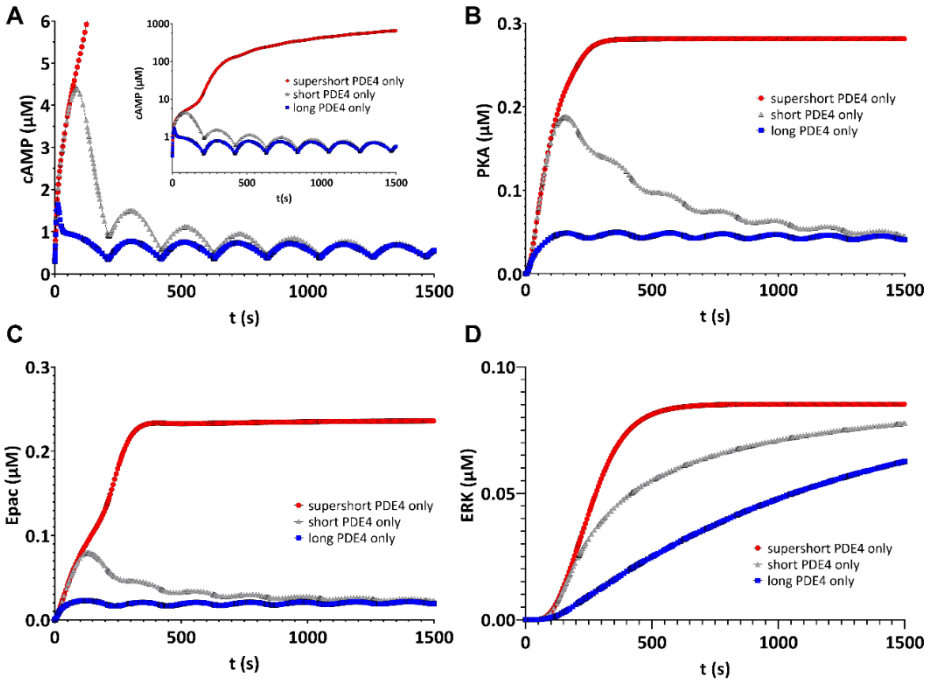

Figure 7. PDE4 isoform types differentially regulate oscillatory cAMP signaling. The effect of PDE4 isoform type on oscillatory cAMP signaling was simulated by including a single PDE4 isoform type only at a concentration of 1 µM. A) Dynamic control of oscillatory cAMP signaling is distinct for different PDE4 isoform types. Presence of supershort PDE4 isoforms only leads to profound accumulation of cAMP (insert). When only short or long PDE4 isoforms are present, cAMP levels can be stabilized in a concentration range after an initial peak. B-C) Similar to the effect on oscillatory cAMP control, PKA and Epac are most profoundly activated when only supershort PDE4 isoforms are present. In case only short PDE4 isoforms are present, an initial increase can be observed after which activation levels stabilize. D) Similar to PKA and Epac activation, ERK activation increased mainly when only supershort isoforms were present. Presence of only short PDE4 isoforms led to a higher ERK activation compared to long PDE4 isoforms only. PKA, Epac and ERK reflect the species $PKA_{cat,1}$, $Epac_{ON}$, and ERK_{dimer}, respectively. Simulations were run for 1500 s with oscillatory cAMP input (0.3 µM).

PDE4 activity changes over time in an isoform-specific manner

To understand why the type of PDE4 isoform only has an important impact for cyclic cAMP pulses and not for a single cAMP pulse in the computational model, we looked in detail at Equation 1 in Table 1 (Material and Methods). The activity, i.e.

the degradation rate, of the PDE4 isoform types is differentially affected upon phosphorylation events by activated PKA and ERK. As PKA and ERK themselves are dynamically regulated over time (Fig 7B,D), we next sought to investigate how the degradation rates for the different PDE4 isoform types change over time as a response to oscillatory cAMP signaling.

For a single cAMP pulse, the degradation rates overlap for all isoforms types (Figure 5E) which can be explained by the fact that the elevations in activated PKA and ERK concentrations are small (Figure 5B-D) resulting in no or negligible differences between the enzymatic activity of different PDE4 isoforms. In contrast, for cyclic cAMP pulses there is a continuous generation of activated ERK and PKA, leading to higher overall degradation rates by means of biological feedbacks loops impacting upon PDE4 activity (Fig 6A). For the long isoform, of which the activity is regulated by both PKA and ERK, the activation rate is higher than the inhibition rate, which reflects the Vmax settings (i.e. 21.76 for activation, -2 for inhibition), resulting in net increased activation (Fig 8A and Supplemental Figure S1). In other words, the activation of the long isoform by PKA keeps the PKA concentration under control, since a higher degradation rate of cAMP results in less PKA formation (a negative feedback loop), resulting in a compensatory $k12_{on,PDE}$ rate. The short isoform is activated by ERK. Since the activation of ERK is slower than of PKA (Fig 6B,D), the increase in k_{on}short (i.e. $k_{on,PDE}$ + $k23_{on,PDE}$) is slower than the increase of k_{on}long (i.e. $k_{on,PDE}$ + $k12_{on,PDE}$ + $k13_{on,PDE}$) and overall a lower activation rate is reached for short PDE4 compared to long PDE4. Consequently, the cAMP has a larger initial peak when only the short isoform is present in comparison to when all (Fig 6A), or only the long isoform (Fig 7A) is present.

The supershort isoform is inhibited by ERK, which represents a positive feedback loop. More specifically, a high ERK concentration inhibits the degradation of cAMP by long and supershort PDE4 forms, leading to downstream activation of ERK. Consequently, in the simulations of cyclic cAMP input with only the supershort

isoform present, the k_{on}supershort (i.e. $k_{on,PDE}$ + $k33_{on,PDE}$) rate flattens out already after 500s (Fig 8A-B), implying that there is no degradation of cAMP anymore (all PDE4 supershort isoforms are inhibited) resulting in a massive build-up of the cAMP concentration (Fig. 7A). These simulations show that, in cases where only the supershort isoform is present, other mechanisms should be activated to limit the cAMP concentration increase, and in particular mechanisms that limit the activation of the ERK pathway or increase the cAMP degradation in an PDE4-independent mechanism.

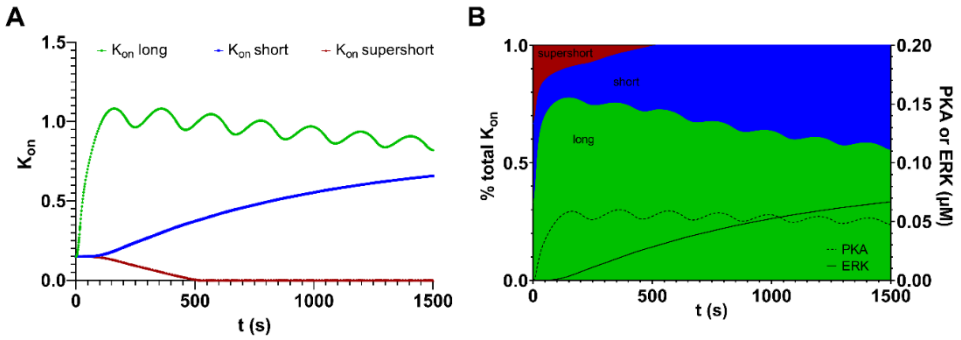

Figure 8. Degradation rates of cAMP by PDE4 long, short, and supershort isoforms change differentially over time. The degradation rates of long (K_{on}long), short (K_{on}short) and supershort (K_{on}supershort) forms are shown in green, blue and red, respectively. Degradation rates per PDE4 isoform are dependent on the baseline degradation rate and modulation by PKA and/or ERK and are calculated based on Tables 1 and Table 2 (K_{on}long = $k_{on,PDE}$ + $k12_{on,PDE}$ + $k13_{on,PDE}$; K_{on}short = $k_{on,PDE}$ + $k22_{on,PDE}$ + $k23_{on,PDE}$; K_{on}supershort = $k_{on,\ PDE}$ + $k32_{on,\ PDE}$ + $k33_{on,\ PDE}$). A) Changes in absolute degradation rates per PDE4 isoform type are plotted over time. B) The contribution of different PDE4 isoform types to the total degradation changes over time. Changes in degradation rate correspond to changes in PKA and ERK levels as shown by the dashed (PKA) and solid (ERK) black line. PKA and ERK reflect the species $PKA_{cat,1}$ and ERK_{dimer}, respectively. Simulations were run for 1500 s considering estimated hippocampal PDE4 isoform proportions (total 1 μM) and oscillatory cAMP input (0.3 μM).

The degradation rates of long and supershort PDE4 isoforms start to go down once ERK becomes activated while short forms are activated (Fig 8A-B). This implies that, in case ERK is already activated and PDE4 long and supershort forms

are thus initially inhibited before cAMP synthesis is started, PDE4-mediated cAMP degradation could be diminished. This means that preceding ERK activation, by inhibition of long and supershort PDE4, could have 'permissive and facilitating' actions on cAMP signaling.

To investigate the influence of Vmax parameter values on the model outcome, we performed a sensitivity analysis in which we varied the Vmax values +/- 10% and looked at the average and maximum cAMP value over 1500 seconds (see Supplementary Figure S3). As can be appreciated from these results, the sensitivity of the model is similar for all Vmax values, with the highest for kon12PDE which captures the effect of the long isoform phosphorylation by PKA. In this respect, the sensitivity analysis is in line with the other reported results that highlight the important effect of the long isoform. Importantly, we highlight here that due to the scarcity of quantitative data, the baseline Vmax values are based on measures in different cell types using different assays.

Initial PKA and ERK concentrations influence PDE4-mediated cAMP degradation

Despite the large influence of PKA and ERK on PDE4-mediated cAMP degradation, our prior simulations did not take into account the initial presence of PKA and/or ERK and may therefore not fully represent the biological situation in which these species may modulate PDE4 activity already before cAMP is synthesized. Therefore, we also explored the influence of the activated PKA and ERK concentration on PDE4-mediated cAMP degradation by using non-zero initial concentrations (0.05 and 0.066 µM, respectively) based on their final values in the simulations shown in Figure 6B and -D. The following simulations were run using a single pulse only, since cyclic pulses lead to continuous degradation and production which overrules the effect of different initial PKA and ERK conditions.

Figure 9 shows the degradation dynamics of a single 0.3 µM cAMP pulse for different initial concentrations of PKA and ERK. Similar to above, these results

indicate that the initial PKA concentration has an important influence on cAMP degradation by increasing the activity of long PDE4 isoforms and overruling a potential influence of initial ERK concentrations (i.e. note that the curves of the green diamonds and blue triangles overlap in Figure 9). In case no PKA is initially present, non-zero initial concentrations of ERK also influence cAMP degradation by inhibiting long and supershort PDE4 isoforms while activating short PDE4 isoforms. Depending on the intracellular distribution of the different PDE4 isoform types and their relative proportions, these initial PKA and ERK concentrations may give rise to specific intracellular cAMP gradients by distinctly influencing PDE4 activity.

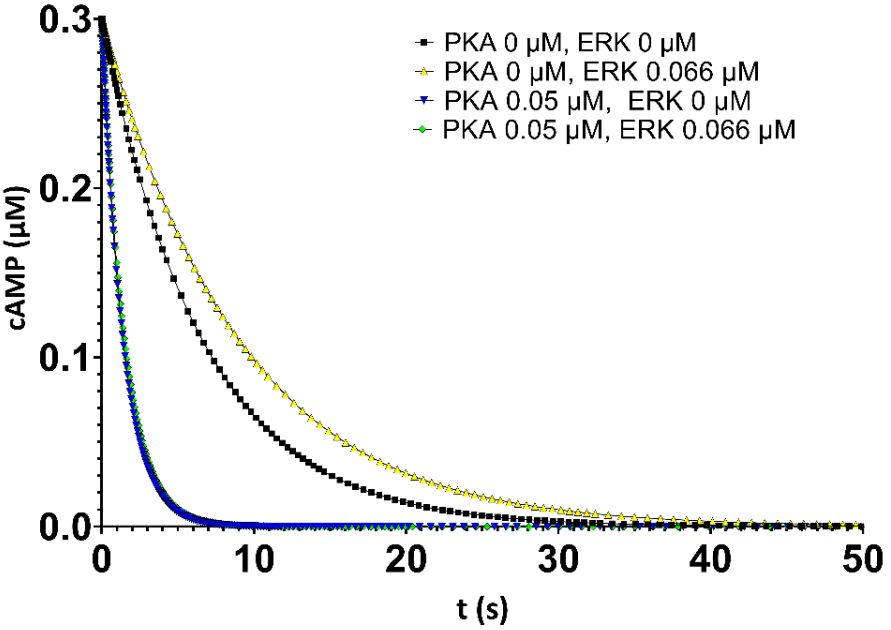

Figure 9. The initial concentrations of PKA and ERK influence degradation of a single cAMP pulse. Elevated initial PKA levels lead to quicker degradation of a single 0.3 µM cAMP pulse (blue triangles), while increased initial ERK levels diminish degradation (yellow triangles) compared to the default simulation in which PKA and ERK are initially absent (black squares). When both PKA and ERK are initially present, PKA overrules the effect of ERK indicating that PKA, by activating long PDE4 isoforms, has a major influence on PDE4-mediated cAMP degradation (green diamonds). PKA and ERK reflect the species $PKA_{cat,1}$ and ERK_{dimer}, respectively. Simulations were run considering estimated hippocampal PDE4 isoform proportions (total 1 µM) with a single cAMP pulse input (0.3 µM).

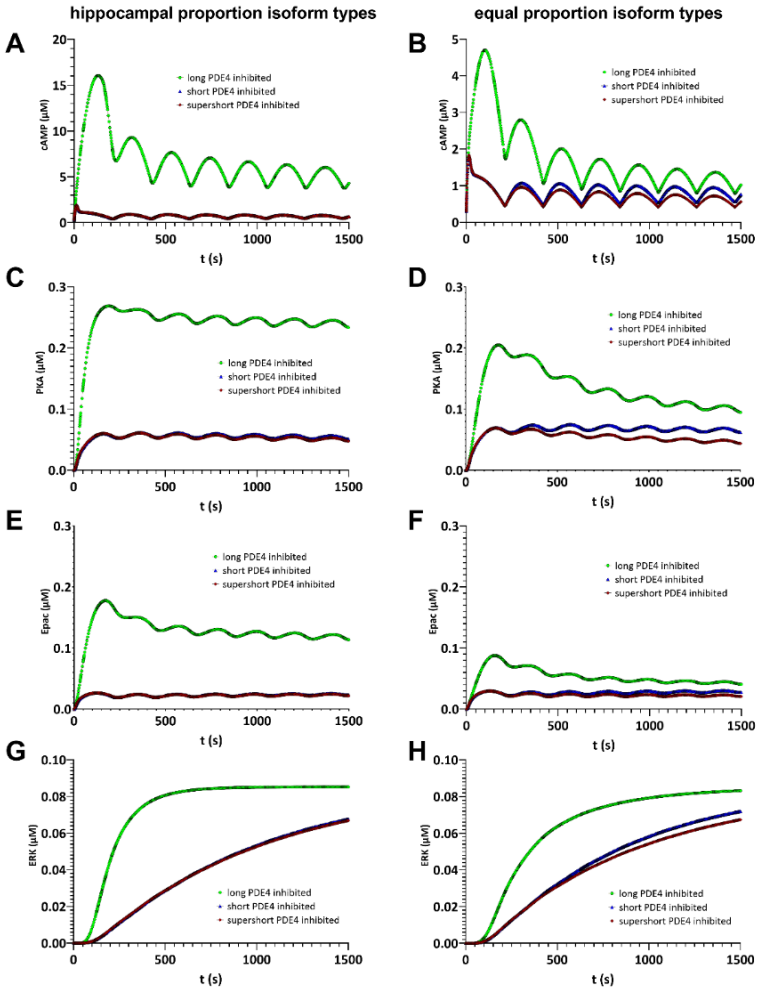

Figure 10. **Effects of isoform-type specific PDE4 inhibition on cAMP and downstream signaling.** The effect of isoform-specific PDE4 inhibition on cAMP signaling was tested while considering the relative proportions of isoform types measured in the hippocampus (panels A, C, E and G) or considering equal expression proportions of the different PDE4 isoform types (panels B, D, F and H) for a cyclic input of cAMP. Inhibition of long PDE4 isoforms (green lines) produced the largest elevations in cAMP (A-B), PKA (C-D), Epac (E-F), and ERK levels (G-H) irrespective of the proportion of isoform types. Inhibition of short forms (blue lines) led to higher levels of cAMP and downstream molecules than inhibition of supershort forms (red lines) when considering equal isoform type proportions (B,D,F,H) but not in case of hippocampal proportions (A,C,E,G) indicating relative proportions determine the functional importance of isoform types. PKA, Epac and ERK reflect the species $PKA_{cat,1}$, $Epac_{ON}$, and ERK_{dimer}, respectively. Simulations were run for 1500 s with oscillatory cAMP input (0.3 μM).

Inhibition of PDE4 long isoforms has the most profound effect on cAMP signaling

Based on the observations that cAMP signaling is best kept under control when long PDE4 isoforms are present (Fig 7), long isoforms contribute largely to the total PDE4-mediated cAMP degradation (Fig 8), and the dominant effect of PKA over ERK in modulating PDE4 activity by acting on long PDE4 forms specifically (Fig 9), we sought to investigate whether inhibition of long PDE4 isoforms specifically impacts cAMP signaling most profoundly compared to inhibition of the other isoform types.

Inhibition of single PDE4 isoform types was simulated by setting this isoform to zero while leaving the other two types unaffected. In prior simulations we have used the relative proportions of long, short, and supershort PDE4 isoforms based on those measured in the hippocampus as an example of tissue-specific expression, i.e. 0.7 long, 0.11 short, 0.19 supershort. Since long PDE4 isoforms comprised 70% of the total in this tissue, the observations that long PDE4 isoforms exert a large control on cAMP signaling may have been biased by the fact that these long forms are most abundantly present. To control for this potential bias we also simulated the inhibition of an isoform type while keeping the remaining forms in equal proportions, i.e. one isoform is set to zero and the other isoforms are both present at 0.5 μM concentration in order to keep the total PDE4 concentration constant at 1 μM.

Figure 10 visualizes the effect of PDE4 isoform type inhibition on cAMP signaling considering both the hippocampal proportion of isoform types as well as equal proportions. Irrespective of the proportions considered, inhibition of long PDE4 forms led, compared to inhibition of short or supershort isoforms, to higher levels of cAMP (green curve, Fig 10A,B), PKA (green curve, Fig 10C,D), Epac (green curve, Fig 10E,F), and ERK signaling (green curve, Fig 10G,H). Inhibition of short isoforms differed from the inhibition of supershort forms only when considering equal proportion of isoform types (Fig 10B,D,F,H) which demonstrates that unequal abundance of PDE4 isoform types (e.g. in the case of the hippocampus) influences the functional importance of a particular isoform type.

DISCUSSION

Various intra- and extracellular stimuli all induce the synthesis of cAMP but eventually evoke distinct cellular effects. This 'repurposing' of the same signaling machinery by controlling its dynamics is beneficial from an evolutionary perspective compared to developing separate pathways for each stimulus, receptor or response (Purvis and Lahav, 2013). Accordingly, by means of compartmentalization and multiple (dynamic) feedback mechanisms, cAMP can convey signals from multiple different sources to induce distinct responses. By degrading cAMP, PDE4 enzymes exert profound control over cAMP signaling dynamics. Specifically, PDE4 enzymes consist of multiple isoform types of which the enzyme activity is dynamically regulated in a feedback-based manner in response to downstream cAMP signaling. Here, we constructed a computational model to explore the role of PDE4 and its different isoforms in the control of cAMP dynamics.

Based on our model, we explored the effects of different concentrations cAMP and PDE4 on activation of the downstream cAMP-PKA and cAMP-Epac pathways. It was identified that PKA activation was mainly influenced by the concentration of cAMP, whilst Epac activation was more sensitive to the amount of PDE4 present. Moreover, simulations using different total PDE4 concentrations caused substantial changes in PKA and Epac activation dynamics by changing time to peak values, whilst simulation using different cAMP concentrations did not. Changes in PDE4 concentration led to non-linear changes in the dynamics of cAMP and downstream effectors, which provides an estimation of the magnitude of effect of experimentally observed changes in PDE4 expression. For example, the 1.5-4.0 fold increases in PDE4 at the mRNA, protein, and enzyme activity level that have been reported in physiological and disease-associated conditions do affect cAMP and downstream signaling based on our model (Levallet et al., 2007; Paes et al., 2020; Peter et al., 2007).

In light of investigating the effect of PKA- and ERK-based feedback on PDE4 isoform activity, our simulations indicated that oscillatory cAMP signaling, as opposed to single cAMP input pulses, is necessary to induce downstream effector activation that can influence PDE4 isoform activity. As the change in enzyme activity upon phosphorylation by PKA and/or ERK is PDE4 isoform-specific, we examined how oscillatory cAMP signaling affects the activity of these PDE4 isoform types. The results indicated long PDE4 isoforms exert the largest control on dynamics of cAMP and downstream effector signaling (Fig. 7) and that long PDE4 isoforms contribute most to total PDE4-mediated cAMP degradation (Fig 8). These long-dominant effects may have been biased by the fact that we considered PDE4 isoform proportions based on measurements in rat hippocampal tissue, in which long forms were predominantly (i.e. 70%) present. However, simulations in which each of the PDE4 isoform type were present in equal amount and were separately inhibited, long forms also exhibited the largest impact on cAMP and downstream signaling dynamics (Fig 10). This seemingly importance of long PDE4 forms is supported by the fact that the four PDE4 genes (*PDE4A-D*) encode more long isoforms than short and supershort isoforms (Paes et al., 2021), which may imply that long forms are involved in a broader array of cellular functions. Indeed, these various long PDE4 isoforms are known to localize to specific intracellular compartments owing to their unique N-terminus amino acid stretches to engage in specific protein-protein interactions (Houslay, 2010; Paes et al., 2021). As such, long PDE4 isoforms can control cAMP signaling in a precisely located and efficient manner as their activity can be quickly increased upon phosphorylation by PKA.

In contrast to long forms, supershort PDE4 forms were found to inadequately control oscillatory cAMP signaling (Fig 7). These isoforms cannot be phosphorylated, and activated, by PKA, but are only affected by ERK phosphorylation. However, phosphorylation by ERK actually decreases enzyme activity of supershort PDE4 while modestly increasing the activity of short PDE4 forms. Thus, phosphorylation-based

feedback mechanisms appear insufficient in increasing supershort PDE4 isoform activity. This may imply that cAMP levels could become uncontrollable in compartments where only supershort PDE4 forms are present. However, early studies have reported the transcription-based upregulation of (super)short PDE4 in response to cAMP signaling activation as an alternative feedback mechanism (Conti, 2000; Liu et al., 2000; Swinnen et al., 1991b). Moreover, (super)short forms have been shown to localize throughout the cytosol where they may control cAMP signaling globally compared to cAMP control by long PDE4 forms in specific locations (Bolger et al., 1997; Cheung et al., 2007; Huston et al., 1997).

The results of this study, which indicate the effects of PDE4 isoform types on cAMP signaling dynamics, should be interpreted in the light of the following assumptions and limitations. Firstly and most importantly, The model simulations predict that all cAMP is degraded in approximately 15 seconds (single cAMP pulse), which differs from the reported cAMP measurements in live cells (i.e. 100-300 seconds (Violin et al., 2008). Although this discrepancy may be cell-dependent, we hypothesize that this might be due to the ODE formalism we are using as such do not fully account for the spatial regulation of cAMP signaling via cAMP compartmentalization and local subcellular cAMP gradients. More specifically, precise subcellular localization of PDE isoforms is proposed to be important for shaping cAMP gradients (Barnes et al., 2005; Feinstein et al., 2012; Xin et al., 2015). Here, we provide a very rough approximation of how different isoforms of a certain PDE4 subtype may be proportionally expressed in (parts of) an organ. As such, our approximation of the ratio of different PDE4 isoform categories by means of a Western blot of just the PDE4D subtype does not reflect or provide information on the expression of all PDE4 subtypes and isoforms in specific cell types and their localization within these cells. Interestingly, of the 21 reported human PDE4 isoforms, 15 are long (70%), 2 are short (10%), and 4 are supershort isoforms (20%) which reflects very similar proportions as reported for PDE4D isoforms here (Paes et al.,

2021). As soon as isoform-specific intracellular expression patterns are determined, these details can be included in future models. In addition, local production by ACs, cAMP buffering (by e.g. PKA), physical barriers (i.e. the cytoskeleton), export by multidrug resistance proteins and cell shape are also believed to contribute to cAMP compartmentalization (Saucerman et al., 2014). Importantly, recent insights indicated that cAMP is primarily buffered by PKA regulatory subunit condensates and that PDEs effectively reduce cAMP signaling in highly localized, nanometer-sized compartments (Bock et al., 2020; Jackson, 2020; Zhang et al., 2020). Also, A-kinase anchoring proteins (AKAPs) have the ability to anchor PKA, Epac and PDE4 to specific subcellular locations, to form local signaling complexes with high signaling specificity and efficacy (Dema et al., 2015; Omar and Scott, 2020). By tethering PKA to specific subcellular locations, it can specifically activate effector proteins in its vicinity. Besides, AKAPs can also directly bind effector proteins, to spatially and temporally influence the signal transduction (Dema et al., 2015; Omar and Scott, 2020). AKAPs are thus important players in establishing compartmentalized cAMP signaling by contributing to the subcellular localization of signaling components, but it is not yet completely understood how the intracellular positioning of cAMP effector proteins (i.e. PDE4, Epac, PKA) by AKAPs shapes cellular cAMP signaling.

Secondly, considering the short time scales that we model, we assume a constant amount of protein, thus ignoring potential production and degradation processes. For example, the transcriptional upregulation of (super)short PDE4 as feedback mechanism may take longer than 1500 s as simulated here, but could be implicated in future models. as well as transcriptional or epigenetic regulation (Paes et al., 2020; Paes et al., 2021; Tilley and Maurice, 2005). For example, the transcriptional upregulation of (super)short PDE4 as feedback mechanism may take longer than 1500 s as simulated here, but could be implicated in future models. Earlier studies reported large increases in (super)short transcripts, but these were observed after a period of multiple hours (Swinnen et al., 1989; Swinnen et al., 1991a).

Because of this difference in time frames and the difficulty of translating cAMP increases to downstream transcriptional upregulation, we opted to not include transcription-regulated feedback in this model yet. Thirdly, this study focuses on PDE4, whereas other cAMP degrading PDEs also play an important role in the spatiotemporal dynamics of cAMP signaling. Similarly, the PDE4 activity can be modulated through a wide variety of post-translational modifications and interactions with partner proteins (Paes et al., 2021), which are not all captured in the current model. For example, the effect of phosphatases, which would remove phosphorylation of PDE4 or undo effects of PKA in Raf-1 expressing cells on phosphorylation of Raf1 and its downstream signaling to ERK (Stork and Schmitt, 2002), providing yet other cell-specific routes for cAMP and ERK signaling pathways to interact, could be incorporated in future work. Finally, the parameter values of the model (e.g. proportional/relative concentrations of included signaling molecules and the way they influence each other) are highly cell type-, context-, and compartment-specific (Dodge-Kafka et al., 2005; Dugan et al., 1999; Stork and Schmitt, 2002). Future work should focus on acquiring these cell-type and context-specific experimental data (e.g. using next-generation cAMP-sensing techniques (Bock et al., 2020)) in order to better calibrate the computational models (including, if necessary, stochastic simulation techniques such as reported in {Jędrzejewska-Szmek, 2017 #908}) and simulate these dedicated scenarios.

The current study pointed out that different PDE4 isoforms distinctly regulate cAMP and downstream signaling dynamics and that these isoform-specific differences should be considered in future computational and experimental work on PDE4/cAMP signaling. Computational follow-up studies could focus on PDE4/cAMP signaling in specific cellular compartments or cell types by adapting the model presented here. Moreover, this model can provide insights in PDE4 drug design by simulating how PDE4 inhibitors, with different affinities to the different isoform types, impact overall cAMP signaling. Experimentally, future computational work should

validate the influence of specific PDE4 isoforms on cell-type specific cAMP-regulated processes by using, for example, RNA silencing or (epi)genetic editing.

ACKNOWLEDGMENTS

We thank Zeynep Karagöz for independently confirming our simulation results. AC gratefully acknowledges the financial support of the Dutch province of Limburg in the LINK (FCL67723) ("Limburg INvesteert in haar Kenniseconomie") knowledge economy project and a VENI grant (number 15075). This work was supported by Alzheimer Nederland [Grant WE.03-2016-07]. TV and JP have a proprietary interest in selective PDE4D inhibitors for the treatment of demyelinating disorders. JP has a proprietary interest in the PDE4 inhibitor roflumilast for the treatment of cognitive impairment as well as PDE4D inhibitors for the treatment of Alzheimer's disease.

CONTRIBUTIONS

DP, SH, and AC developed the computational model. DP, SH and AC analyzed its results. DP, TV, JP, and AC contributed to the design and conception of the study. DP, SH, and AC drafted the manuscript. DP, SH, DvdH, TV, and JP contributed to manuscript revision, read, and approved the submitted version.

REFERENCES

Agarwal SR, Clancy CE and Harvey RD (2016) Mechanisms Restricting Diffusion of Intracellular cAMP. *Sci Rep* **6**:19577.

Alvarez R, Sette C, Yang D, Eglen RM, Wilhelm R, Shelton ER and Conti M (1995) Activation and selective inhibition of a cyclic AMP-specific phosphodiesterase, PDE-4D3. *Mol Pharmacol* **48**:616-622.

Argyrousi EK, Heckman PR, van Hagen BT, Muysers H, van Goethem NP and Prickaerts J (2020) Pro-cognitive effect of upregulating cyclic guanosine monophosphate signalling during memory acquisition or early consolidation is mediated by increased AMPA receptor trafficking. *Journal of psychopharmacology (Oxford, England)* **34**:103-114.

Baillie GS, MacKenzie SJ, McPhee I and Houslay MD (2000) Sub-family selective actions in the ability of Erk2 MAP kinase to phosphorylate and regulate the activity of PDE4 cyclic AMP-specific phosphodiesterases. *Br J Pharmacol* **131**:811-819.

Baillie GS, Tejeda GS and Kelly MP (2019) Therapeutic targeting of 3',5'-cyclic nucleotide phosphodiesterases: inhibition and beyond. *Nat Rev Drug Discov* **18**:770-796.

Barnes AP, Livera G, Huang P, Sun C, O'Neal WK, Conti M, Stutts MJ and Milgram SL (2005) Phosphodiesterase 4D Forms a cAMP Diffusion Barrier at the Apical Membrane of the Airway Epithelium*. *Journal of Biological Chemistry* **280**:7997-8003.

Beavo JA and Brunton LL (2002) Cyclic nucleotide research—still expanding after half a century. *Nature reviews Molecular cell biology* **3**:710-717.

Bhalla US (2004) Signaling in Small Subcellular Volumes. I. Stochastic and Diffusion Effects on Individual Pathways. *Biophysical Journal* **87**:733-744.

Blokland A, Heckman P, Vanmierlo T, Schreiber R, Paes D and Prickaerts J (2019) Phosphodiesterase Type 4 Inhibition in CNS Diseases. *Trends Pharmacol Sci* **40**:971-985.

Bock A, Annibale P, Konrad C, Hannawacker A, Anton SE, Maiellaro I, Zabel U, Sivaramakrishnan S, Falcke M and Lohse MJ (2020) Optical Mapping of cAMP Signaling at the Nanometer Scale. *Cell* **182**:1519-1530.e1517.

Bolger GB, Erdogan S, Jones RE, Loughney K, Scotland G, Hoffmann R, Wilkinson I, Farrell C and Houslay MD (1997) Characterization of five different proteins produced by alternatively spliced mRNAs from the human cAMP-specific phosphodiesterase PDE4D gene. *Biochem J* **328 (Pt 2)**:539-548.

Bolger GB, McPhee I and Houslay MD (1996) Alternative splicing of cAMP-specific phosphodiesterase mRNA transcripts. Characterization of a novel tissue-specific isoform, RNPDE4A8. *J Biol Chem* **271**:1065-1071.

Bos JL, de Rooij J and Reedquist KA (2001) Rap1 signalling: adhering to new models. *Nature Reviews Molecular Cell Biology* **2**:369-377.

Calebiro D, Nikolaev VO, Gagliani MC, de Filippis T, Dees C, Tacchetti C, Persani L and Lohse MJ (2009) Persistent cAMP-signals triggered by internalized G-protein-coupled receptors. *PLoS Biol* **7**:e1000172-e1000172.

Casar B, Pinto A and Crespo P (2008) Essential role of ERK dimers in the activation of cytoplasmic but not nuclear substrates by ERK-scaffold complexes. *Molecular cell* **31**:708-721.

Chay A, Zamparo I, Koschinski A, Zaccolo M and Blackwell KT (2016) Control of βAR- and N-methyl-D-aspartate (NMDA) Receptor-Dependent cAMP

Dynamics in Hippocampal Neurons. *PLOS Computational Biology* **12**:e1004735.
Chen X, Rochefort Nathalie L, Sakmann B and Konnerth A (2013) Reactivation of the Same Synapses during Spontaneous Up States and Sensory Stimuli. *Cell Reports* **4**:31-39.
Cheung YF, Kan Z, Garrett-Engele P, Gall I, Murdoch H, Baillie GS, Camargo LM, Johnson JM, Houslay MD and Castle JC (2007) PDE4B5, a novel, super-short, brain-specific cAMP phosphodiesterase-4 variant whose isoform-specifying N-terminal region is identical to that of cAMP phosphodiesterase-4D6 (PDE4D6). *J Pharmacol Exp Ther* **322**:600-609.
Conti M (2000) Phosphodiesterases and cyclic nucleotide signaling in endocrine cells. *Molecular endocrinology (Baltimore, Md)* **14**:1317-1327.
de Rooij J, Zwartkruis FJT, Verheijen MHG, Cool RH, Nijman SMB, Wittinghofer A and Bos JL (1998) Epac is a Rap1 guanine-nucleotide-exchange factor directly activated by cyclic AMP. *Nature* **396**:474-477.
Dema A, Perets E, Schulz MS, Deák VA and Klussmann E (2015) Pharmacological targeting of AKAP-directed compartmentalized cAMP signalling. *Cell Signal* **27**:2474-2487.
Dodge-Kafka KL, Soughayer J, Pare GC, Carlisle Michel JJ, Langeberg LK, Kapiloff MS and Scott JD (2005) The protein kinase A anchoring protein mAKAP coordinates two integrated cAMP effector pathways. *Nature* **437**:574-578.
Dugan LL, Kim JS, Zhang Y, Bart RD, Sun Y, Holtzman DM and Gutmann DH (1999) Differential Effects of cAMP in Neurons and Astrocytes: ROLE OF B-RAF*. *Journal of Biological Chemistry* **274**:25842-25848.
Dyachok O, Isakov Y, Sågetorp J and Tengholm A (2006) Oscillations of cyclic AMP in hormone-stimulated insulin-secreting beta-cells. *Nature* **439**:349-352.
Feinstein WP, Zhu B, Leavesley SJ, Sayner SL and Rich TC (2012) Assessment of cellular mechanisms contributing to cAMP compartmentalization in pulmonary microvascular endothelial cells. *American journal of physiology Cell physiology* **302**:C839-852.
Fujioka A, Terai K, Itoh RE, Aoki K, Nakamura T, Kuroda S, Nishida E and Matsuda M (2006) Dynamics of the Ras/ERK MAPK cascade as monitored by fluorescent probes. *Journal of biological chemistry* **281**:8917-8926.
Getz M, Swanson L, Sahoo D, Ghosh P and Rangamani P (2019) A predictive computational model reveals that GIV/girdin serves as a tunable valve for EGFR-stimulated cyclic AMP signals. *Molecular Biology of the Cell* **30**:1621-1633.
Herberg FW, Taylor SS and Dostmann WR (1996) Active site mutations define the pathway for the cooperative activation of cAMP-dependent protein kinase. *Biochemistry* **35**:2934-2942.
Herrero A, Pinto A, Colón-Bolea P, Casar B, Jones M, Agudo-Ibáñez L, Vidal R, Tenbaum SP, Nuciforo P and Valdizán EM (2015) Small molecule inhibition of ERK dimerization prevents tumorigenesis by RAS-ERK pathway oncogenes. *Cancer cell* **28**:170-182.
Hoffmann R, Baillie GS, MacKenzie SJ, Yarwood SJ and Houslay MD (1999) The MAP kinase ERK2 inhibits the cyclic AMP-specific phosphodiesterase HSPDE4D3 by phosphorylating it at Ser579. *The EMBO journal* **18**:893-903.
Hoffmann R, Wilkinson IR, McCallum JF, Engels P and Houslay MD (1998) cAMP-specific phosphodiesterase HSPDE4D3 mutants which mimic activation and changes in rolipram inhibition triggered by protein kinase A

phosphorylation of Ser-54: generation of a molecular model. *Biochem J* **333 (Pt 1)**:139-149.
Houslay M and Baillie G (2003) The role of ERK2 docking and phosphorylation of PDE4 cAMP phosphodiesterase isoforms in mediating cross-talk between the cAMP and ERK signalling pathways, Portland Press Ltd.
Houslay MD (2010) Underpinning compartmentalised cAMP signalling through targeted cAMP breakdown. *Trends Biochem Sci* **35**:91-100.
Hoy JJ, Salinas Parra N, Park J, Kuhn S and Iglesias-Bartolome R (2020) Protein kinase A inhibitor proteins (PKIs) divert GPCR-Gαs-cAMP signaling toward EPAC and ERK activation and are involved in tumor growth. *The FASEB Journal* **34**:13900-13917.
Huff TC, Camarena V, Sant DW, Wilkes Z, Van Booven D, Aron AT, Muir RK, Renslo AR, Chang CJ, Monje PV and Wang G (2020) Oscillatory cAMP signaling rapidly alters H3K4 methylation. *Life science alliance* **3**.
Huston E, Lumb S, Russell A, Catterall C, Ross AH, Steele MR, Bolger GB, Perry MJ, Owens RJ and Houslay MD (1997) Molecular cloning and transient expression in COS7 cells of a novel human PDE4B cAMP-specific phosphodiesterase, HSPDE4B3. *Biochem J* **328 (Pt 2)**:549-558.
Jackson PK (2020) cAMP Signaling in Nanodomains. *Cell* **182**:1379-1381.
Jędrzejewska-Szmek J, Damodaran S, Dorman DB and Blackwell KT (2017) Calcium dynamics predict direction of synaptic plasticity in striatal spiny projection neurons. *European Journal of Neuroscience* **45**:1044-1056.
Jedrzejewska-Szmek J, Luczak V, Abel T and Blackwell K (2017) β-adrenergic signaling broadly contributes to LTP induction. *PLoS computational biology* **13**:e1005657.
Jin SL, Swinnen JV and Conti M (1992) Characterization of the structure of a low Km, rolipram-sensitive cAMP phosphodiesterase. Mapping of the catalytic domain. *J Biol Chem* **267**:18929-18939.
Kaupp UB and Seifert R (2002) Cyclic nucleotide-gated ion channels. *Physiol Rev* **82**:769-824.
Khokhlatchev AV, Canagarajah B, Wilsbacher J, Robinson M, Atkinson M, Goldsmith E and Cobb MH (1998) Phosphorylation of the MAP kinase ERK2 promotes its homodimerization and nuclear translocation. *Cell* **93**:605-615.
Kim C, Cheng CY, Saldanha SA and Taylor SS (2007) PKA-I Holoenzyme Structure Reveals a Mechanism for cAMP-Dependent Activation. *Cell* **130**:1032-1043.
Kim M, Park AJ, Havekes R, Chay A, Guercio LA, Oliveira RF, Abel T and Blackwell KT (2011) Colocalization of Protein Kinase A with Adenylyl Cyclase Enhances Protein Kinase A Activity during Induction of Long-Lasting Long-Term-Potentiation. *PLOS Computational Biology* **7**:e1002084.
Koschinski A and Zaccolo M (2017) Activation of PKA in cell requires higher concentration of cAMP than in vitro: implications for compartmentalization of cAMP signalling. *Sci Rep* **7**:14090.
Lakics V, Karran EH and Boess FG (2010) Quantitative comparison of phosphodiesterase mRNA distribution in human brain and peripheral tissues. *Neuropharmacology* **59**:367-374.
Lario PI, Bobechko B, Bateman K, Kelly J, Vrielink A and Huang Z (2001) Purification and characterization of the human PDE4A catalytic domain (PDE4A330-723) expressed in Sf9 cells. *Archives of biochemistry and biophysics* **394**:54-60.

Lenhard JM, Kassel DB, Rocque WJ, Hamacher L, Holmes WD, Patel I, Hoffman C and Luther M (1996) Phosphorylation of a cAMP-specific phosphodiesterase (HSPDE4B2B) by mitogen-activated protein kinase. *Biochem J* **316 (Pt 3)**:751-758.

Levallet G, Levallet J, Bouraïma-Lelong H and Bonnamy P-J (2007) Expression of the cAMP-Phosphodiesterase PDE4D Isoforms and Age-Related Changes in Follicle-Stimulating Hormone-Stimulated PDE4 Activities in Immature Rat Sertoli Cells1. *Biology of Reproduction* **76**:794-803.

Lim J, Pahlke G and Conti M (1999) Activation of the cAMP-specific phosphodiesterase PDE4D3 by phosphorylation. Identification and function of an inhibitory domain. *J Biol Chem* **274**:19677-19685.

Lindskog M, Kim M, Wikström MA, Blackwell KT and Kotaleski JH (2006) Transient Calcium and Dopamine Increase PKA Activity and DARPP-32 Phosphorylation. *PLOS Computational Biology* **2**:e119.

Liu H, Palmer D, Jimmo SL, Tilley DG, Dunkerley HA, Pang SC and Maurice DH (2000) Expression of Phosphodiesterase 4D (PDE4D) Is Regulated by Both the Cyclic AMP-dependent Protein Kinase and Mitogen-activated Protein Kinase Signaling Pathways: A POTENTIAL MECHANISM ALLOWING FOR THE COORDINATED REGULATION OFPDE4D ACTIVITY AND EXPRESSION IN CELLS*. *Journal of Biological Chemistry* **275**:26615-26624.

Lohse C, Bock A, Maiellaro I, Hannawacker A, Schad LR, Lohse MJ and Bauer WR (2017) Experimental and mathematical analysis of cAMP nanodomains. *PLOS ONE* **12**:e0174856.

MacKenzie SJ, Baillie GS, McPhee I, Bolger GB and Houslay MD (2000) ERK2 mitogen-activated protein kinase binding, phosphorylation, and regulation of the PDE4D cAMP-specific phosphodiesterases. The involvement of COOH-terminal docking sites and NH2-terminal UCR regions. *J Biol Chem* **275**:16609-16617.

MacKenzie SJ, Baillie GS, McPhee I, MacKenzie C, Seamons R, McSorley T, Millen J, Beard MB, van Heeke G and Houslay MD (2002) Long PDE4 cAMP specific phosphodiesterases are activated by protein kinase A-mediated phosphorylation of a single serine residue in Upstream Conserved Region 1 (UCR1). *Br J Pharmacol* **136**:421-433.

Musheshe N, Schmidt M and Zaccolo M (2018) cAMP: From Long-Range Second Messenger to Nanodomain Signalling. *Trends in Pharmacological Sciences* **39**:209-222.

Nelissen E, De Vry J, Antonides A, Paes D, Schepers M, van der Staay FJ, Prickaerts J and Vanmierlo T (2017) Early-postnatal iron deficiency impacts plasticity in the dorsal and ventral hippocampus in piglets. International Journal of Developmental Neuroscience 59:47-51.

Neves SR, Tsokas P, Sarkar A, Grace EA, Rangamani P, Taubenfeld SM, Alberini CM, Schaff JC, Blitzer RD, Moraru, II and Iyengar R (2008) Cell shape and negative links in regulatory motifs together control spatial information flow in signaling networks. *Cell* **133**:666-680.

Ohadi D and Rangamani P (2019) Geometric Control of Frequency Modulation of cAMP Oscillations due to Calcium in Dendritic Spines. *Biophysical Journal* **117**:1981-1994.

Ohadi D, Schmitt DL, Calabrese B, Halpain S, Zhang J and Rangamani P (2019) Computational Modeling Reveals Frequency Modulation of Calcium-cAMP/PKA Pathway in Dendritic Spines. *Biophysical Journal* **117**:1963-1980.

Oliveira RF, Kim M and Blackwell KT (2012) Subcellular Location of PKA Controls Striatal Plasticity: Stochastic Simulations in Spiny Dendrites. *PLOS Computational Biology* **8**:e1002383.

Oliveira RF, Terrin A, Di Benedetto G, Cannon RC, Koh W, Kim M, Zaccolo M and Blackwell KT (2010) The Role of Type 4 Phosphodiesterases in Generating Microdomains of cAMP: Large Scale Stochastic Simulations. *PLOS ONE* **5**:e11725.

Omar MH and Scott JD (2020) AKAP Signaling Islands: Venues for Precision Pharmacology. *Trends in Pharmacological Sciences* **41**:933-946.

Paes D, Lardenoije R, Carollo RM, Roubroeks JAY, Schepers M, Coleman P, Mastroeni D, Delvaux E, Pishva E, Lunnon K, Vanmierlo T, van den Hove D and Prickaerts J (2020) Increased isoform-specific phosphodiesterase 4D expression is associated with pathology and cognitive impairment in Alzheimer's disease. *Neurobiol Aging* **97**:56-64.

Paes D, Schepers M, Rombaut B, van den Hove D, Vanmierlo T and Prickaerts J (2021) The Molecular Biology of Phosphodiesterase 4 Enzymes as Pharmacological Targets: An Interplay of Isoforms, Conformational States, and Inhibitors. *Pharmacol Rev* **73**:1016-1049.

Peng T, Qi B, He J, Ke H and Shi J (2020) Advances in the Development of Phosphodiesterase-4 Inhibitors. *J Med Chem* **63**:10594-10617.

Peter D, Jin SLC, Conti M, Hatzelmann A and Zitt C (2007) Differential Expression and Function of Phosphodiesterase 4 (PDE4) Subtypes in Human Primary CD4⁺ T Cells: Predominant Role of PDE4D. *The Journal of Immunology* **178**:4820.

Purves GI, Kamishima T, Davies LM, Quayle JM and Dart C (2009) Exchange protein activated by cAMP (Epac) mediates cAMP-dependent but protein kinase A-insensitive modulation of vascular ATP-sensitive potassium channels. *The Journal of physiology* **587**:3639-3650.

Purvis JE and Lahav G (2013) Encoding and decoding cellular information through signaling dynamics. *Cell* **152**:945-956.

Radhakrishnan K, Edwards JS, Lidke DS, Jovin TM, Wilson BS and Oliver JM (2009) Sensitivity analysis predicts that the ERK-pMEK interaction regulates ERK nuclear translocation. *IET Syst Biol* **3**:329-341.

Reeves ML, Leigh BK and England PJ (1987) The identification of a new cyclic nucleotide phosphodiesterase activity in human and guinea-pig cardiac ventricle. Implications for the mechanism of action of selective phosphodiesterase inhibitors. *Biochem J* **241**:535-541.

Rich TC, Xin W, Mehats C, Hassell KA, Piggott LA, Le X, Karpen JW and Conti M (2007) Cellular mechanisms underlying prostaglandin-induced transient cAMP signals near the plasma membrane of HEK-293 cells. *American journal of physiology Cell physiology* **292**:C319-C331.

Saldou N, Obernolte R, Huber A, Baecker PA, Wilhelm R, Alvarez R, Li B, Xia L, Callan O, Su C, Jarnagin K and Shelton ER (1998) Comparison of Recombinant Human PDE4 Isoforms: Interaction with Substrate and Inhibitors. *Cellular Signalling* **10**:427-440.

Salonikidis PS, Zeug A, Kobe F, Ponimaskin E and Richter DW (2008) Quantitative Measurement of cAMP Concentration Using an Exchange Protein Directly Activated by a cAMP-Based FRET-Sensor. *Biophysical Journal* **95**:5412-5423.

Sasagawa S, Ozaki Y-i, Fujita K and Kuroda S (2005) Prediction and validation of the distinct dynamics of transient and sustained ERK activation. *Nature cell biology* **7**:365-373.

Saucerman JJ, Greenwald EC and Polanowska-Grabowska R (2014) Mechanisms of cyclic AMP compartmentation revealed by computational models. *J Gen Physiol* **143**:39-48.

Schepers M, Tiane A, Paes D, Sanchez S, Rombaut B, Piccart E, Rutten BPF, Brone B, Hellings N, Prickaerts J and Vanmierlo T (2019) Targeting Phosphodiesterases-Towards a Tailor-Made Approach in Multiple Sclerosis Treatment. *Front Immunol* **10**:1727.

Schindler RF and Brand T (2016) The Popeye domain containing protein family--A novel class of cAMP effectors with important functions in multiple tissues. *Prog Biophys Mol Biol* **120**:28-36.

Schmidt M, Dekker FJ and Maarsingh H (2013) Exchange protein directly activated by cAMP (epac): a multidomain cAMP mediator in the regulation of diverse biological functions. *Pharmacol Rev* **65**:670-709.

Sette C and Conti M (1996) Phosphorylation and activation of a cAMP-specific phosphodiesterase by the cAMP-dependent protein kinase. Involvement of serine 54 in the enzyme activation. *J Biol Chem* **271**:16526-16534.

Sette C, Vicini E and Conti M (1994) The ratPDE3/IVd phosphodiesterase gene codes for multiple proteins differentially activated by cAMP-dependent protein kinase. *J Biol Chem* **269**:18271-18274.

Shumilov AV and Gotovtsev PM (2021) Modeling the activity of the dopamine signaling pathway by combination of analog electrical circuit and mathematical approaches. *Heliyon* **7**:e05879.

Slepchenko BM and Loew LM (2010) Use of virtual cell in studies of cellular dynamics. *Int Rev Cell Mol Biol* **283**:1-56.

Song RS, Massenburg B, Wenderski W, Jayaraman V, Thompson L and Neves SR (2013) ERK regulation of phosphodiesterase 4 enhances dopamine-stimulated AMPA receptor membrane insertion. *Proceedings of the National Academy of Sciences* **110**:15437-15442.

Stone N, Shettlesworth S, Rich TC, Leavesley SJ and Phan AV (2019) A two-dimensional finite element model of cyclic adenosine monophosphate (cAMP) intracellular signaling. *SN Applied Sciences* **1**:1713.

Stork PJS and Schmitt JM (2002) Crosstalk between cAMP and MAP kinase signaling in the regulation of cell proliferation. *Trends in Cell Biology* **12**:258-266.

Swinnen JV, Joseph DR and Conti M (1989) The mRNA encoding a high-affinity cAMP phosphodiesterase is regulated by hormones and cAMP. *Proc Natl Acad Sci U S A* **86**:8197-8201.

Swinnen JV, Tsikalas KE and Conti M (1991a) Properties and hormonal regulation of two structurally related cAMP phosphodiesterases from the rat Sertoli cell. *Journal of Biological Chemistry* **266**:18370-18377.

Swinnen JV, Tsikalas KE and Conti M (1991b) Properties and hormonal regulation of two structurally related cAMP phosphodiesterases from the rat Sertoli cell. *J Biol Chem* **266**:18370-18377.

Tenner B, Getz M, Ross B, Ohadi D, Bohrer CH, Greenwald E, Mehta S, Xiao J, Rangamani P and Zhang J (2020) Spatially compartmentalized phase regulation of a Ca2+-cAMP-PKA oscillatory circuit. *eLife* **9**:e55013.

Tilley DG and Maurice DH (2005) Vascular Smooth Muscle Cell Phenotype-Dependent Phosphodiesterase 4D Short Form Expression: Role of

Differential Histone Acetylation on cAMP-Regulated Function. *Molecular Pharmacology* **68**:596.
Violin JD, DiPilato LM, Yildirim N, Elston TC, Zhang J and Lefkowitz RJ (2008) beta2-adrenergic receptor signaling and desensitization elucidated by quantitative modeling of real time cAMP dynamics. *J Biol Chem* **283**:2949-2961.
Xin W, Feinstein WP, Britain AL, Ochoa CD, Zhu B, Richter W, Leavesley SJ and Rich TC (2015) Estimating the magnitude of near-membrane PDE4 activity in living cells. *American journal of physiology Cell physiology* **309**:C415-424.
Xin W, Tran TM, Richter W, Clark RB and Rich TC (2008) Roles of GRK and PDE4 activities in the regulation of beta2 adrenergic signaling. *J Gen Physiol* **131**:349-364.
Yang P-C, Boras BW, Jeng M-T, Docken SS, Lewis TJ, McCulloch AD, Harvey RD and Clancy CE (2016) A Computational Modeling and Simulation Approach to Investigate Mechanisms of Subcellular cAMP Compartmentation. *PLOS Computational Biology* **12**:e1005005.
Zhang JZ, Lu T-W, Stolerman LM, Tenner B, Yang JR, Zhang J-F, Falcke M, Rangamani P, Taylor SS, Mehta S and Zhang J (2020) Phase Separation of a PKA Regulatory Subunit Controls cAMP Compartmentation and Oncogenic Signaling. *Cell* **182**:1531-1544.e1515.
Zhang P, Kornev AP, Wu J and Taylor SS (2015) Discovery of Allostery in PKA Signaling. *Biophys Rev* **7**:227-238.
Zhang Y, Liu R-Y, Heberton G, Smolen P, Baxter D, Cleary L and Byrne J (2011) Computational Design of Enhanced Learning Protocols. *Nature neuroscience* **15**:294-297.

SUPPLEMENTARY MATERIAL

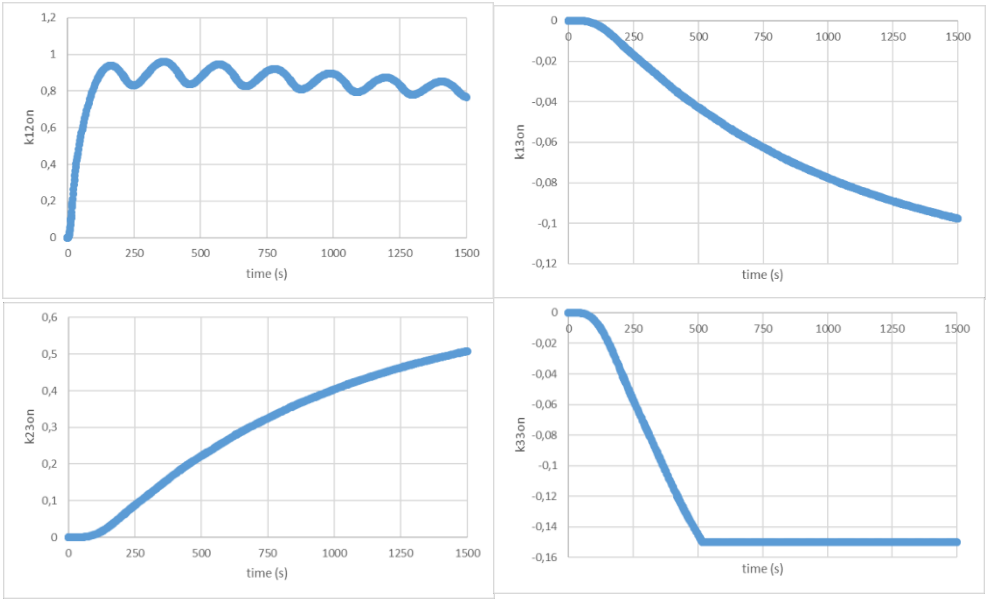

Figure S1. Changes in degradation rates $k12_{on,PDE}$, $k13_{on,PDE}$, $k23_{on,PDE}$, and $k33_{on,PDE}$ over time. $k12_{on,PDE}$ reflects the activating effect of phosphorylation by PKA on long PDE4 isoform activity (top left). $k13_{on,PDE}$ and $k33_{on,PDE}$ reflect the inhibiting effects of phosphorylation by ERK on long and supershort PDE4 isoform activity, respectively (top right and bottom right). $k23_{on,PDE}$ reflects the activating effect of phosphorylation by ERK on short PDE4 isoform activity (bottom left). Note the differences in y-axes. Simulations were run for 1500 s considering estimated hippocampal PDE4 isoform proportions (total 1 µM) and oscillatory cAMP input (0.3 µM).

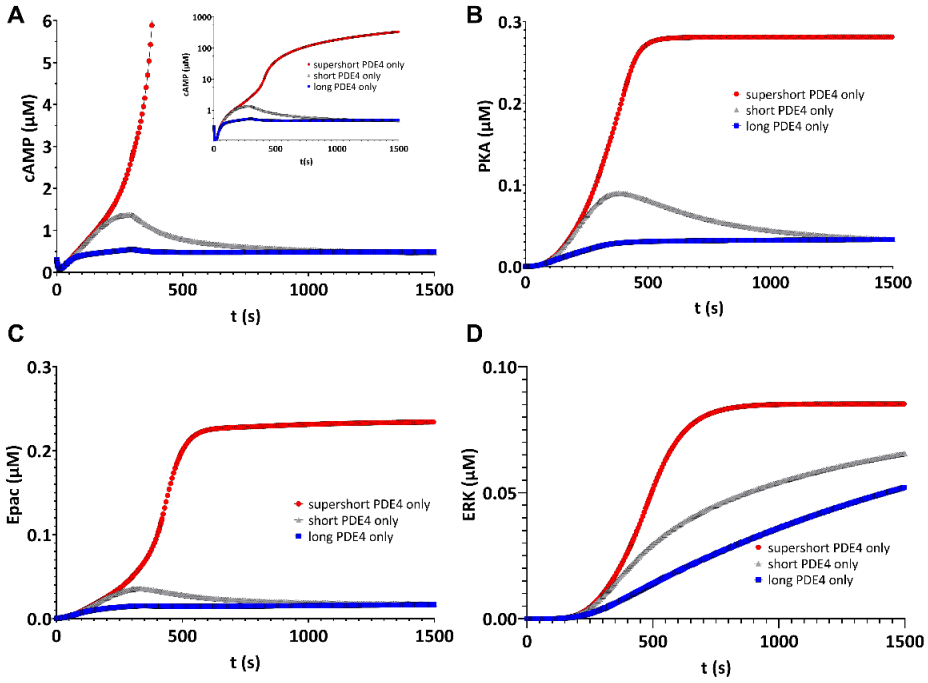

Figure S2. PDE4 isoform types differentially regulate sustained cAMP signaling. The effect of PDE4 isoform type on sustained cAMP signaling was simulated by including a single PDE4 isoform type only at a concentration of 1 µM. A) Dynamic control of sustained cAMP signaling is distinct for different PDE4 isoform types. Presence of supershort PDE4 isoforms only leads to profound accumulation of cAMP (insert). When only short or long PDE4 isoforms are present, cAMP levels can be stabilized in a concentration range after an initial peak. B-C) PKA and Epac are most profoundly activated when only supershort PDE4 isoforms are present. In case only short PDE4 isoforms are present, an initial increase can be observed after which activation levels stabilize. D) Similar to PKA and Epac activation, ERK activation increased mainly when only supershort isoforms were present. Presence of only short PDE4 isoforms led to a higher ERK activation compared to long PDE4 isoforms only. PKA, Epac and ERK reflect the species PKAcat,1, EpacON, and ERKdimer, respectively. Simulations were run for 1500 s with gradual increase and then constant cAMP input (0.3 µM).

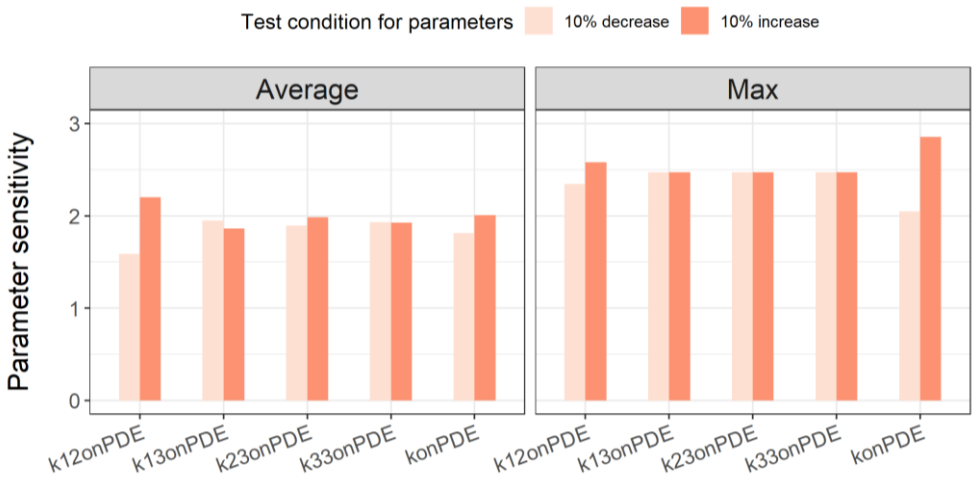

Figure S3. Local sensitivity analysis of the cAMP model. Parameter sensitivity values on the y-axis indicate how a 10% increase (light orange) or decrease (dark orange) in each parameter [vmax parameter values, see also Table 2] affects the average (left) and maximum (right) cAMP value over 1500 seconds for a oscillatory input of cAMP and considering estimated hippocampal PDE4 isoform proportions (total 1 μM).

Estimation of proportional PDE4 isoform type expression in rat hippocampus tissue

Sample preparation and western blotting methodology was performed as previously described (Argyrousi et al., 2020; Nelissen et al., 2017). Briefly, hippocampal tissue of a 4-month-old male Wistar rat was used. Approximately 20 mg of the left hippocampus was homogenized in 400 μl lysis buffer (100 mM Tris-HCl, 200 mM NaCl, 1 mM EDTA, 2 mMDTT, 0.05% Triton, 1 tablet complete protease inhibitor mix/20 ml buffer (Roche, Vilvoorde, Belgium), 1 tablet PhosSTOP phosphatase inhibitor cocktail/10 ml buffer (Roche) using a mini-Bead-Beater (BioSpec products, Bartlesville, OK, USA). Samples were homogenized three times for 30 s with 5 min cooling on ice between runs. After 30 min cooling on ice, samples were centrifuged at 16,000 x g for 20 min. (4 °C), and the supernatant was divided into aliquots and stored at−80 °C until further use. Protein concentrations were determined with the Bio-Rad DC™ protein assay (Bio-Rad Laboratories, Inc.).

Brain homogenate (total protein input, 20 µg was resolved in 10% SDS polyacrylamide gel electrophoresis and then transferred onto nitrocellulose membranes (Bio-Rad Laboratories). The membranes were blocked (50% Odyssey blocking buffer in PBS; Li-Cor, Lincoln, NE) for one hour at room temperature, followed by overnight incubation with the primary antibodies at 4°C. The primary antibodies consisted of rabbit anti-PDE4D (1:500, ab14613; Abcam) and mouse anti-GAPDH (1:1,000,000, #10R-G109A; Fitzgerald Industries, Acton, MA) as loading control. Membranes were subsequently incubated with secondary antibodies for one hour at room temperature: goat anti-rabbit IRDye 800 (1:10,000; Li-Cor) and donkey anti-mouse IRDye 680 (1:10,000; Li-Cor). Membranes were visualised using the Odyssey Infrared Imaging System (Li-Cor), and protein bands were quantified using ImageJ by means of densitometry (National Institutes of Health, Bethesda, MD). Protein bands of ~55 kDa were considered to be supershort PDE4D isoforms, bands of ~65 kDa were considered to be PDE4D short isoforms and band >75 kDa were considered to be long PDE4D isoforms (Supplemental Figure 4).

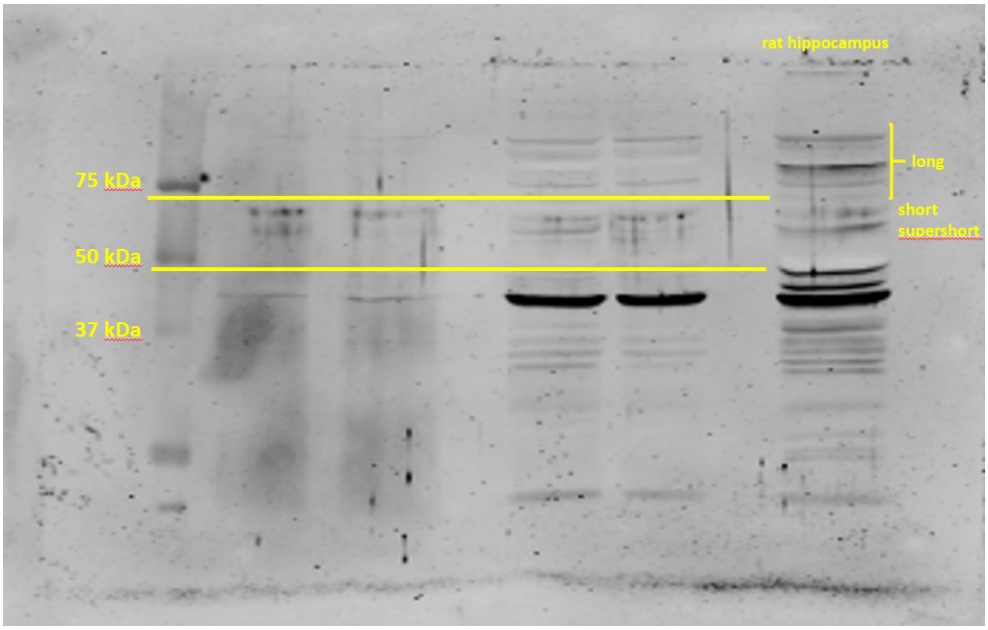

Figure S4. Western blot image of rat hippocampal tissue (right column) stained for PDE4D. Protein bands of ~55 kDa were considered to be supershort PDE4D isoforms, bands of ~65 kDa were considered to be PDE4D short isoforms and band >75 kDa were considered to be long PDE4D isoforms.

Chapter 6

Inhibition of PDE2 and PDE4 synergistically improves memory consolidation processes

Published as:

Paes et al. (2021) *Neuropharmacology*. Feb 15;184:108414.
doi: 10.1016/j.neuropharm.2020.108414

ABSTRACT

Phosphodiesterases (PDE) are the only enzymes that degrade cAMP and cGMP which are second messengers crucial to memory consolidation. Different PDE inhibitors have been developed and tested for their memory-enhancing potential, but the occurrence of side effects has hampered clinical progression. As separate inhibition of the PDE2 and PDE4 enzyme family has been shown to enhance memory, we investigated whether concurrent treatment with a PDE2 and PDE4 inhibitor can have synergistic effects on memory consolidation processes. We found that combined administration of PF-999 (PDE2 inhibitor) and roflumilast (PDE4 inhibitor) increases the phosphorylation of the AMPA receptor subunit GluR1 and induces CRE-mediated gene expression. Moreover, when combined sub-effective and effective doses of PF-999 and roflumilast were administered after learning, time-dependent forgetting was abolished in an object location memory task. Pharmacokinetic assessment indicated that combined treatment does not alter exposure of the individual compounds. Taken together, these findings suggest that combined PDE2 and PDE4 inhibition has synergistic effects on memory consolidation processes at sub-effective doses, which could therefore provide a therapeutic strategy with an improved safety profile.

INTRODUCTION

Cyclic nucleotides are second messengers that convey extracellular signals to adaptive changes within the cell. In the central nervous system, cyclic adenosine monophosphate (cAMP) and cyclic guanosine monophosphate (cGMP) have been suggested to play a crucial role in neuronal signal transduction and memory consolidation processes. Downstream targets of cAMP and cGMP include protein kinases (e.g. PKA and PKG), nucleotide exchange factors (Epac1 and Epac2), popeye-domain containing proteins (POPDC) and cyclic nucleotide gated channels (CNGC). Via these downstream targets, cAMP and cGMP can modulate a multitude of processes involved in synaptic plasticity mechanisms like long-term potentiation (LTP). LTP takes place in two distinct phases: short-lasting early LTP (E-LTP) during which no gene transcription or translation is induced and enduring late LTP (L-LTP) which does involve gene expression and protein synthesis. As such, E-LTP consists of post-translational modifications (e.g. phosphorylation) by which the localization and functionality of proteins can be adapted. For example, phosphorylation of specific residues on the AMPA receptor subunit GluR1 induces receptor trafficking and conductivity changes which then facilitate synaptic plasticity (Lee, 2006). L-LTP involves transcription of plasticity genes regulated by the transcription factor CREB (Barco et al., 2002; Kida, 2012; Suzuki et al., 2011). Cyclic nucleotide levels modulate both E-LTP and L-LTP through activation of downstream effectors which can subsequently phosphorylate different substrates (e.g. CREB) and induce gene transcription.

Intracellular cyclic nucleotides are degraded exclusively by phosphodiesterases (PDE). The PDE enzyme family comprises 11 gene families (PDE1-11) that specifically target cAMP (PDE4, -7, -8), cGMP (PDE5, -6, -9) or have specificity to both (PDE1, -2, -3, -10, -11) (Bender and Beavo, 2006). Since PDEs are the sole enzymes regulating cyclic nucleotide levels, pharmacological inhibition of PDEs provides an approach to modulate cyclic nucleotide concentrations and

subsequently influence neuronal plasticity and memory processes. Accordingly, preclinical studies indicated that inhibition of different PDE subtypes can improve neuronal plasticity and memory functioning. Inhibition of PDE2, PDE4, PDE5, PDE9 and PDE10 has been demonstrated to enhance cognitive functioning, including memory, in rodent preclinical studies (reviewed in: (Heckman et al., 2017)). For example, treatment with the PDE2 inhibitor BAY60-7550 improves hippocampal long-term potentiation and object recognition memory in rats (Boess et al., 2004; Domek-Lopacinska and Strosznajder, 2008; Rutten et al., 2007). Chronic oral administration of this compound (0.3 mg/kg) improved memory in a transgenic AD mouse model (Sierksma et al., 2013). These studies indicate the therapeutic potential of PDE2 inhibition, but poor pharmacokinetic properties of BAY60-7550 make this molecule unsuitable for clinical development. Hence, efforts have been made to develop new, selective PDE2 inhibitors (reviewed in: (Gomez and Breitenbucher, 2013)). The PDE2 inhibitor PF-05180999 (PF-999) showed better pharmacokinetics but Phase I clinical trials (NCT01981486, NCT01429740 and NCT01981499) testing its use in schizophrenia and migraine were discontinued (Helal et al., 2017). Selective PDE4 inhibitors and their effect on plasticity and memory processes have been described more extensively. PDE4 inhibition by rolipram or FFPM restores memory performance in transgenic AD mice as well as models using natural ageing or streptozotocin to induce cognitive impairments (Gong et al., 2004; Guo et al., 2017; Kumar and Singh, 2017). PDE4 inhibitors have been reported to produce emetic side effects, which would hamper clinical use of non-selective PDE4 inhibitors (Vanmierlo et al., 2016). The PDE4 gene family contains four genes (PDE4A-D), each encoding multiple isoforms using different promoters and alternative splicing. Targeted inhibition of individual PDE4 genes or isoforms can also increase neuroplasticity and memory functioning (Li et al., 2011; Sierksma et al., 2014; Zhang et al., 2018; Zhang et al., 2017). Specific inhibition of PDE4D using the compound GEBR-7b (0.001 mg/kg, s.c.) improved spatial memory in APPswe/PS1dE9 mice (Sierksma et al., 2014).

As PDE4D inhibition is thought to be underlying emetic side effects (Mori et al., 2010), approaches may be necessary to circumvent the occurrence of side effects. Similarly, as found upon PDE2 and PDE4 inhibition, object memory is improved by PDE5 inhibition using sildenafil, vardenafil or icariin (Jin et al., 2014; Prickaerts et al., 2002; Puzzo et al., 2008; Puzzo et al., 2009; Reneerkens et al., 2012; Zhang et al., 2013). In addition, PDE5 inhibition has protective actions against striatal degeneration through stimulation of neuronal survival pathways (Puerta et al., 2010). Two different PDE9 inhibitors (BAY-73-6691 and PF-04447943) were found to have enhancing effects in healthy rodents and disease models in a variety of cognitive behavioral tasks (Hutson et al., 2011; van der Staay et al., 2008; Verhoest et al., 2012) and inhibition of PDE10 by papaverine or PQ-10 improves memory functioning in MK-801 and scopolamine-deficit models and a mouse model of Huntington's disease (Giralt et al., 2013; Reneerkens et al., 2013).

Although the inhibition of PDE2, PDE4, PDE5, PDE9 and PDE10 shows potential to enhance cognitive function in preclinical studies, inconsistent effects are found in clinical studies investigating the memory-enhancing effects of PDE inhibitors (Heckman et al., 2015; Heckman et al., 2017). As of yet, no PDE inhibitor has been clinically approved to improve cognitive functioning which can be attributed to unacceptable side-effects (in the case of PDE4), or a lack of efficacy (e.g. (Schwam et al., 2014)). Hence, alternative therapeutic approaches utilizing PDE inhibition should be explored to enhance efficacy and improve the safety profile. More recently, combined administration of a PDE4 (roflumilast) and PDE5 (vardenafil) inhibitor at sub-effective doses was found to improve memory in transgenic AD mice (Gulisano et al., 2018). Since PDEs are localized to specific compartments within the cell (Baillie, 2009), more subtle inhibition of different 'PDE microdomains' may collectively still facilitate signal transduction and LTP to produce memory-enhancing effects.

In the human brain, and in particular in memory-associated brain regions, PDE2 and PDE4 make up a large proportion of PDE activity (Lakics et al., 2010). Both PDE2 and PDE4 can regulate pre- and postsynaptic processes, making them interesting targets to enhance plasticity (Fernandez-Fernandez et al., 2015; Liu et al., 2017; Polito et al., 2013). Based on their regional and intracellular expression and the fact that separate inhibition of PDE2 or PDE4 promotes memory formation, we sought to investigate whether combined inhibition of PDE2 and PDE4 yields additive or synergistic effects to improve the treatment's safety profile and efficacy. To study potential synergistic effects of inhibition, we tested the effect of PDE2 and PDE4 inhibitors on processes underlying synaptic plasticity and spatial memory performance, and we established a pharmacokinetic profile of combined treatment.

METHODS

Animals

All experimental procedures were approved by the local ethical committee of Maastricht University for animal experiments and met governmental guidelines. Two batches of twenty-four 3-4-month-old male Wistar rats (Charles River, Sulzfeld, Germany) were used (average body weight at the beginning of the study: 346 g (batch 1) and 357 g (batch 2). The animals were housed individually in standard cages on sawdust bedding in an air-conditioned room (about 20°C). They were kept under a reversed 12/12 h light/dark cycle (lights on from 20.00 to 08.00) and had free access to food and water. Rats were housed and tested in the same room. A radio, which was playing softly, provided background noise in the room. All testing was done between 10.00 and 18.00.

Materials

PF-999 and roflumilast were supplied by Dart NeuroScience as a white powder. Methyl 2-hydroxyethyl cellulose (Tylose® MH300) and Tween80 (polyoxyethylenesorbitan monooleate) were purchased from Sigma-Aldrich Chemie bv (Steinheim, Germany). For behavioral and PK experiments compound dilutions were freshly prepared on every experimental day and were dissolved in 0.5% tylose solution (98% of the end volume) with 2% Tween80. P-GluR1 (S845) antibody was obtained from Cell Signaling Technology (#8084). GluR1 antibody was purchased from Millipore Sigma (MAB2263). IRDye® Secondary Antibodies were purchased from LI-COR Biosciences.

Vectors used in CRE-mediated transcription

We generated a ratiometric CRE-mediated gene expression reporter. Nuclear localized mCherry expressed under the control of a tandem repeat of CREs and a nuclear localized GFP was inserted downstream of the neuron-specific promoter Synapsin I. These two reporters drove expression in opposite directions with a DNA

insulator sequence nestled between. The ratiometric expression cassette was then packaged into AAV8 virus which infected 100% of the neurons in culture. The level of mCherry in the nucleus, a read-out of CRE-mediated gene expression, was normalized by the GFP level, which indicates the reporter infection efficiency. Thus, the mCherry:GFP ratio reads out the specific level of CRE-mediated gene expression in each neuron.

Rat Brain Section Preparations and Treatments

Male Sprague-Dawley rats (8–12 weeks old) were anesthetized by isoflurane. The brains were rapidly removed and placed in ice-cold, oxygenated Krebs-HCO3 buffer (124 mM NaCl, 4 mM KCl, 26 mM NaHCO3, 1.5 mM CaCl2, 1.25 mM KH2PO4, 1.5 mM MgSO4 and 10 mM D-glucose, pH 7.4). Coronal slices (350 µm) were prepared using a vibrating blade microtome, VT1200 (Leica Microsystems, Nussloch, Germany). Neocortical and striatal sections were punched out from the slices in ice-cold Krebs-HCO3 buffer. Three sections were placed in one incubation chamber of BSK6-6 brain slice keeper (Scientific Systems Design Inc.) with 4 mL of fresh Krebs-HCO3 buffer containing adenosine deaminase (10 µg/mL, Roche Diagnostics, Indianapolis, USA). The slices were preincubated at 30 °C under constant oxygenation with 95% O2/5% CO2 for 30 min. The buffer was then replaced with fresh Krebs-HCO3 buffer without adenosine deaminase after 30 min of pre-incubation. Slices were treated with Krebs-HCO3 buffer containing either vehicle (0.1% DMSO) or compound(s) for 30 min at 30°C under constant oxygenation. To terminate the stimulation, each single slice was transferred to microcentrifuge tube, flashed frozen in liquid nitrogen and stored at -80 °C.

Immunoblotting

Frozen tissue samples were sonicated in cell extraction buffer (LT FNN0011, Thermo Fisher Scientific, Carlsbad, US) containing complete protease inhibitor cocktail (Roche Diagnostics, Indianapolis, USA) and phosphatase inhibitor cocktail 1

and 2 (Sigma-Aldrich Corp., St. Louis, USA). The homogenate was centrifuged at 10,000×g for 15 min at 4 °C. Protein concentration in the supernatant was determined by the BCA using bovine serum albumin as standard protein assay method (Pierce, Rockford, IL, USA). Equal amount of protein samples were denatured in NuPAGE LDS sample buffer supplemented with NuPAGE Sample Reducing Agent, incubated at 75°C for 10 min, resolved by Bolt 10 % Bis-Tris Plus gels (Thermo Fisher Scientific, Carlsbad, US) transferred onto PVDF membrane subjected to immunoblot analysis with iBind™ Flex Fluorescent Detection kit. The membranes were immunoblotted using specific antibodies using Odyssey fluorescence detection system. Antibody bindings were revealed by incubation with IRDye 680RD donkey anti-mouse and IRDye 800CW Donkey anti-Rabbit secondary antibodies and imaged with Odyssey CLx near-infrared fluorescence imaging system. Images were processed and band intensity were quantified using Image Studio software (Licor-Odyssey, Lincoln, USA). For each experiment, values obtained for treated slices were calculated relative to the value for the control slices. Normalized data from multiple experiments were averaged and statistical analysis was carried out as described in the figure legends.

Cell culture and transfection

Primary cortical cultures were prepared from E18 C57Bl/6 mice (Jackson Laboratories, Bar Harbor, ME, USA). Cortical tissue was dissociated using the Neural Tissue Dissociation Kit and the gentleMACS™ Octo Dissociator (Miltenyi Biotec, Auburn, CA, USA) as per manufacturer's instructions. Neurons were plated in BioCoat PDL-coated 96-well plates (Becton Dickinson, Franklin Lakes, NJ, USA) and maintained in Neurobasal medium (Thermo Fisher Scientific, Waltham, MA, USA) supplemented with MACS® NeuroBrew® -21 (Miltenyi Biotec, Auburn, CA, USA). Neurons were infected on DIV7 and experiments were performed on DIV9 or DIV10. Cultures were fixed in 4% PFA after overnight stimulation (18 hrs), immunostained

with an anti-Maps2 Ab (HM-2; Sigma Aldrich, St. Louis, MO) and anti-mouse Alexa-647 secondary antibody, and nuclei stained with Hoechst 33342 (Thermo Fisher Scientific, Waltham, MA, USA). We measured Hoechst, GFP, mCherry and Map2 on a Cell InSight high content imager (Thermo Fisher Scientific, Waltham, MA, USA). Automated algorithms identified the Hoechst-stained nuclei and with that mask, average pixel intensities for the GFP and mCherry channels were determined.

Object location task

The object location test (OLT) was performed as described elsewhere using an identical apparatus and objects as those described previously (Akkerman et al., 2012a). Briefly, the effect of PF-999 and roflumilast on the consolidation processes of long-term memory was investigated using a 24 h interval between the OLT learning- and test-trials (T1 and T2, respectively). In the first two weeks, the animals were handled daily and were allowed to get accustomed to the test setup in two days, i.e. they were allowed to explore the apparatus (without any objects) twice for 3 min each day. Then the rats were adapted to the testing routine until they showed a stable discrimination performance, i.e. a good discrimination at 1 h interval and no discrimination at 24 h interval (data not shown). After this, the experiments were performed in which PF-999 and roflumilast were tested. PF-999 and roflumilast were tested at 0.03, 0.1 and 0.3 mg/kg and were administered p.o. (2 ml/kg), 3 h after T1 to investigate the effects on late memory consolidation. More specifically, dose-response curves were constructed for each of the compounds using the first batch of animals and subsequently the highest ineffective doses were combined to test their effectiveness on memory consolidation. Subsequently, using a second batch of rats, dose-response curves for both PF-999 and roflumilast were validated followed by combination treatments of suboptimal and optimal doses of both compounds. The vehicle condition was tested by means of a single injection for the dose-response curves and two vehicle injections were used as an ultimate control for the

combination treatments. Because rats were retested with different compound doses using a randomized crossover design, test sessions were scheduled to allow at least a two-day wash-out period. The order of the treatments was balanced to prevent the data from being distorted by potential object- and side-preferences of the animals.

Rat Pharmacokinetics Determination

Pharmacokinetic properties of PF-999, roflumilast, roflumilast N-oxide, and their combination in male SD rats were determined using standardized procedures as described previously with the exception of vehicle and doses tested (Santora et al., 2018). Briefly, pharmacokinetics properties in male SD rats (300–350 g) were determined following oral (PO) administration (N = 3, 0.1 mg/kg). Rats were catheterized in femoral vein. PF-999 and roflumilast were formulated in 0.5% Methyl 2-hydroxyethyl cellulose (Tylose® MH300) and 2% Tween80. Rats were not fasted during this study. Blood was sampled at 0 (pre-dose), 0.25, 0.5, 1, 2, 4, and 8 h following PO dosing. Plasma was isolated by centrifugation, and all samples were frozen at −80 °C. Calibration standards were prepared by the addition of known concentrations of test article to blank rat plasma to provide a calibration range of 0.5–2000 ng/mL. Then 50 µL plasma samples or calibration standard was added to 250 µL of internal standard solution in acetonitrile. Samples were vortex mixed and centrifuged at 12000 rpm for 5 min at 4 °C. Supernatant (100 µL) was transferred to labeled autosampler vials containing 300 µL of mobile phase (water/acetonitrile/formic acid, 90/10/0.2%), vortex mixed, and analyzed by LC-MS/MS. A bioanalytical method was developed for the quantification of test article in rat plasma. Method development and sample analysis was conducted using a Waters Quattro Premier LC-MS/MS system equipped with Waters Acquity UPLC system. Then 5 µL of the samples were analyzed using a Waters Acquity UPLC system equipped with a C 18 reversed-phase column (Phenomenex Kinetex C18, 1.7 µm, 2.1 mm × 50.0 mm). Mobile phase consisted of 0.1% formic acid in water and of 0.1%

formic acid in acetonitrile with a flow rate of 0.7 mL/min. Eluent was directed to a Waters Quattro Premier mass spectrometer equipped with a turbo electrospray interface. Multiple reaction monitoring (MRM) transition in positive ion mode was used.

For CNS penetration studies male SD rats (300–350 g) were dosed PO (N = 3, 10 mg/kg). PF-999 was formulated in NMP:PEG400:water (10:30:60), and roflumilast was formulated in PEG400:water (20:80). Animals were anesthetized, and approximately 0.3 mL of blood from each rat was collected via cardiac puncture into tubes containing lithium heparin as the anticoagulant at 1 h post dose. Plasma was isolated by centrifugation. Animals were then decapitated and brains were removed. All samples were stored frozen at approximately −80 °C until analysis. Plasma analysis was performed as described above. One hemisphere of each brain sample was weighed. One to five dilutions (w/v) were prepared by addition of 1:1 mixture of water/2-propanol (4-fold of the brain weight) to each brain sample. Brains were homogenized by Fast Prep Calibration standards (ranging from 0.500 to 2000 ng/mL), quality control samples, and test samples containing the internal standard (IS) were separated from rat brain preparations via protein precipitation by addition of 100 µL of 75:25 acetonitrile/water solvent containing analyte calibrants and 300 µL of acetonitrile/IS solution mix (40 ng/mL in acetonitrile) to 100 µL brain homogenate. Following vortex mixing and centrifugation, 20 µL aliquots of the supernatants were diluted with 580 µL of 20:80 acetonitrile/water containing 0.2% formic acid and mixed for the 10 mg/kg study. Following vortex mixing and centrifugation, 100 µL aliquots of the supernatants were diluted with 300 µL of 10:90 acetonitrile/water containing 0.2% formic acid and mixed for the 1.0 mg/kg study. Then 5 µL of each sample was applied to a Kinetex 1.7 µm C18, 100 Å, 50 mm × 2.1 mm column (Phenomenex, Torrance, CA) and eluted with a mobile phase gradient (initial 10% B hold for 0.1 min, then 10% B to 90% B in 1.0 min) consisting of solution A (0.1% formic acid in water) and solution B (0.1% formic acid in acetonitrile). The

column temperature was maintained at 30 °C. The column eluent was subjected to positive-mode electrospray ionization (ES+), and the analytes were detected with a QTrap 5500 quadrupole/ion trap mass spectrometer (AB Sciex, Framingham, MA). Plasma binding and brain tissue binding was determined as described previously (Santora et al., 2018).

Statistical analysis

The ratio of p-GluR1 and GluR1 fluorescence intensity was calculated for striatal and cortical slices (n=3/condition). One-way ANOVA was performed to test for differences among conditions, followed by Bonferroni post-hoc t-tests. Quantification of p-GluR1/GluR1 was performed similarly in the experiment using fixed concentrations of either PF-999 or roflumilast combined with different doses of the other compound. After one-way ANOVA, Dunnett's post-hoc tests were performed comparing combined treatment conditions to the condition that was treated with only the fixed concentration of either PF-999 or roflumilast. In all analyses, an α level of 0.05 was considered statistically significant.

Fluorescence induced by CRE-mediated transcription was quantified using a Cell InSight cell-content imager (Thermo Fisher Scientific) which automatically determined nuclear CRE-mCherry and SynapsinI-GFP levels for individual neurons. The ratio of mCherry to GFP was calculated for each individual neuron in 9 fields per well over triplicate wells used for each experiment. We performed 3 independent experiments and the normalized fluorescence values were then averaged (n=3/condition). One-way ANOVA was performed to test for differences in forskolin EC_{50} values among conditions, followed by Dunnett's post-hoc t-tests.

For the object location task, the basic measures were the times spent by rats exploring an object during T1 and T2. The time spent in exploring the two identical samples will be represented by 'a1' and 'a2'. The time spent in T2 in exploring the sample and moved object will be represented by 'a3' and 'b', respectively. The

following variables were calculated: e1 = a1 + a2, e2 = a3 + b, and d2 = (b – a3) / e2. e1 and e2 are measures of the total exploration time of both objects during T1 and T2 respectively. Animals that exhibited e1 and e2 values of less than 5 or 8 seconds were excluded from the analysis, since no reliable conclusions can be drawn from short exploration times (Akkerman et al., 2012b). The d2 index is a relative measure of discrimination corrected for exploratory activity in the test-trial (e2). Thus, even if a treatment would affect exploratory behavior, the d2 index will be comparable between conditions. One-sample t-statistics were performed in order to assess per treatment condition whether d2 differed from zero. However, comparison of the mean d2 value with the value zero may not be the most suitable way for analyzing memory performance (increased chance of making a type I error). Results were therefore also assessed using one-way ANOVA. In case of a significant difference between treatment conditions, pairwise post-hoc comparisons were performed using Bonferroni t-tests.

RESULTS

Synergistic actions of PDE2 and PDE4 inhibition on striatal and cortical GluR1 phosphorylation

Phosphorylation of the AMPA receptor GluR1 subunit by PKA or PKG can promote synaptic plasticity by trafficking of the receptor to the membrane and increasing receptor conductance. Here we tested whether PDE2 and PDE4 inhibition affects GluR1 phosphorylation at Ser845 in rat striatal and cortical slices and whether combined treatment has additive effects. Slices were treated with PF-999, roflumilast, or both (1 μM), and the ratio of phosphorylated GluR1 (p-GluR1 Ser845) and total GluR1 was measured.

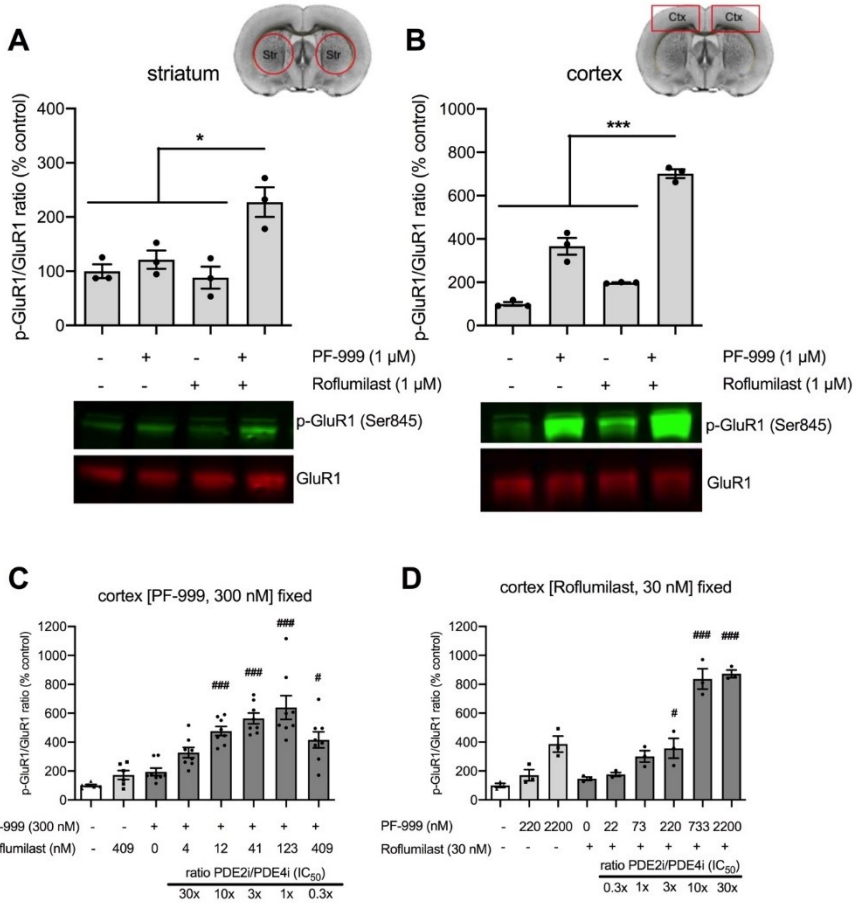

Figure 1. Effects of PDE2 and PDE4 inhibition on GluR1 phosphorylation. A-B) The ratio of phosphorylation GluR1 (p-GluR1) and total GluR1 was measured in striatal and cortical rat brain slices treated with PF-999, roflumilast or both (1 μM; n=3/condition). One-way ANOVA followed by Bonferroni post-hoc t-tests revealed that combined treatment significantly increased p-GluR1 compared to vehicle or individual treatment with PF-999 or roflumilast in both striatal and cortical slices (*:P<0.05, ***:P<0.0001). In cortical slices, treatment with PF-999 alone increased p-GluR1 compared to the vehicle and roflumilast condition (P<0.001 and P<0.01, respectively. Not indicated in graph). C-D) Concentration-dependent effects of combined treatment were tested in cortical slices by using a fixed concentration of either PF-999 (300 nM, panel C) or roflumilast (30 nM, panel D) combined with increasing concentration of the other compound. One-way ANOVA followed by Dunnett's post-hoc t-tests revealed that administration of 12-409 nM roflumilast combined with 300 nM PF-999 significantly increases p-GluR1/GluR1 compared to treatment with PF-999 in absence of roflumilast (#:P<0.05, ###: P<0.001). Vice versa, when using a fixed roflumilast concentration combined with increasing concentrations of PF-999, one-way ANOVA and Dunnett's post-hoc t-tests shows that PF-999 can potentiate the effect of roflumilast in the 220-2200 nM concentration range (#:P<0.05, ###: P<0.001).

In striatum, one-way ANOVA revealed significant differences in p-GluR1/GluR1 ratio between conditions ($F(3,8) = 10.13$, $P < 0.01$; Fig 1A). Bonferroni post-hoc t-tests indicate increased p-GluR1/GluR1 ratio in the PF-999 and roflumilast condition compared to vehicle ($P < 0.0001$) and PF-999 or roflumilast alone ($P < 0.05$). Similarly, in cortex one-way ANOVA revealed significant differences in p-GluR1/GluR1 ratio between conditions ($F(3,8) = 140.2$, $P < 0.0001$; Fig 1B). Bonferroni post-hoc t-tests indicate a significant higher p-GluR1/GluR1 ratio in the PF-999 condition compared to vehicle ($P < 0.001$, not shown in Fig 1B), and a non-significant trend with roflumilast alone ($P = 0.09$, not shown in Fig 1B). Additionally, combined treatment with PF-999 and roflumilast was found to significantly increase p-GluR1/GluR1 ratio compared to vehicle (***:$P < 0.0001$) and PF-999 or roflumilast alone (***:$P < 0.0001$ for both). These findings indicate that PF-999 can increase cortical p-GluR1 and that combined administration of PF-999 and roflumilast has additive effects on p-GluR1/GluR1 ratio in both striatal and cortical slices.

To test whether these additive effects are concentration-dependent, we established concentration-response curves by pairing increasing concentrations of either PF-999 or roflumilast with a low dose of the other compound that only causes minimal increases in pGluR1 by itself (Fig 1C and 1D). When combining a fixed concentration of PF-999 (300 nM) with increasing doses of roflumilast (0-409 nM), a dose-dependent effect on cortical p-GluR1/GluR1 ratio is observed (Fig 1C). One-way ANOVA of PF-999 conditions in combination with roflumilast (0-409 nM, black bars) revealed significant differences in p-GluR1/GluR1 ratio between conditions ($F(5,42) = 11.08$, $P < 0.0001$). Compared to treatment with PF-999 alone, significant increases in p-GluR1/GluR1 ratio were found when roflumilast (12-409 nM) was added (12-123 nM, ###:$P < 0.001$; 409 nM, #:$P < 0.05$; Dunnett's post-hoc t-tests). No significant effect was found upon combined treatment of 300 nM PF-999 with 4 nM roflumilast. Treatment with roflumilast (409 nM) or PF-999 (300 nM, Fig 1C) alone was ineffective (Fig 1C), as was treatment with lower doses of roflumilast (4-123 nM, data not shown). These findings indicate that PDE4 inhibition in addition to PDE2 inhibition significantly increases the amount of phosphorylated GluR1.

Vice versa, when using a fixed concentration of roflumilast (30 nM) in combination with increasing PF-999 concentrations (0-2200 nM), concentration-dependent effects on p-GluR1/GluR1 were observed as well (Fig 1D). One-way ANOVA of roflumilast conditions in combination with PF-999 (0-2200 nM, black bars) revealed significant differences in p-GluR1/GluR1 ratio between conditions ($F(5,12) = 11.08$, $P < 0.0001$). Compared to treatment with roflumilast alone, significant increases in p-GluR1/GluR1 ratio were found when PF-999 (220-2200 nM) was added (220 nM, #:$P < 0.05$; 733-2200, ###:$P < 0.001$; Dunnett's post-hoc t-tests). No significant increase was found upon combined treatment of 30 nM roflumilast with 22-73 nM PF-999. Thus, synergy was seen with combined administration of PF-999 and roflumilast at a variety of drug concentrations, with PDE2 to PDE4 IC_{50} ratios ranging from 1-30x.

PDE2 and PDE4 inhibition synergistically increases CRE-mediated gene expression

As long-term memory critically depends on gene transcription mediated by CREB, we investigated whether inhibition of PDE2 and PDE4 synergistically induces CRE-mediated expression in primary cortical cultures. After infection with ratiometric fluorescent reporter, the effect of PDE2 and PDE4 inhibition on CRE-mediated gene expression was studied by measuring CRE-mCherry fluorescence intensity upon exposure to a concentration range of forskolin (0-10 ·M) to stimulate cAMP production and treatment with PF-999, roflumilast or their combination (Fig 2). One-way ANOVA revealed significant differences between EC_{50} values for forskolin ($F(3,8) = 7.22$, $P < 0.05$). Dunnett's post-hoc t-tests indicated a significantly lower EC_{50} of forskolin for the combined PF-999 and roflumilast condition (EC_{50} = 0.70 μM) compared to vehicle (EC_{50} = 1.62 μM; $P < 0.01$, not indicated in Fig 2A). Roflumilast treatment, but not PF-999, augmented CRE-reporter expression in the presence of forskolin, while combination of both inhibitors greatly increased the overall signal (Fig 2B/C. These findings indicate that combined treatment with PF-999 and roflumilast facilitates CRE-mediated gene expression upon stimulation with lower levels of forskolin.

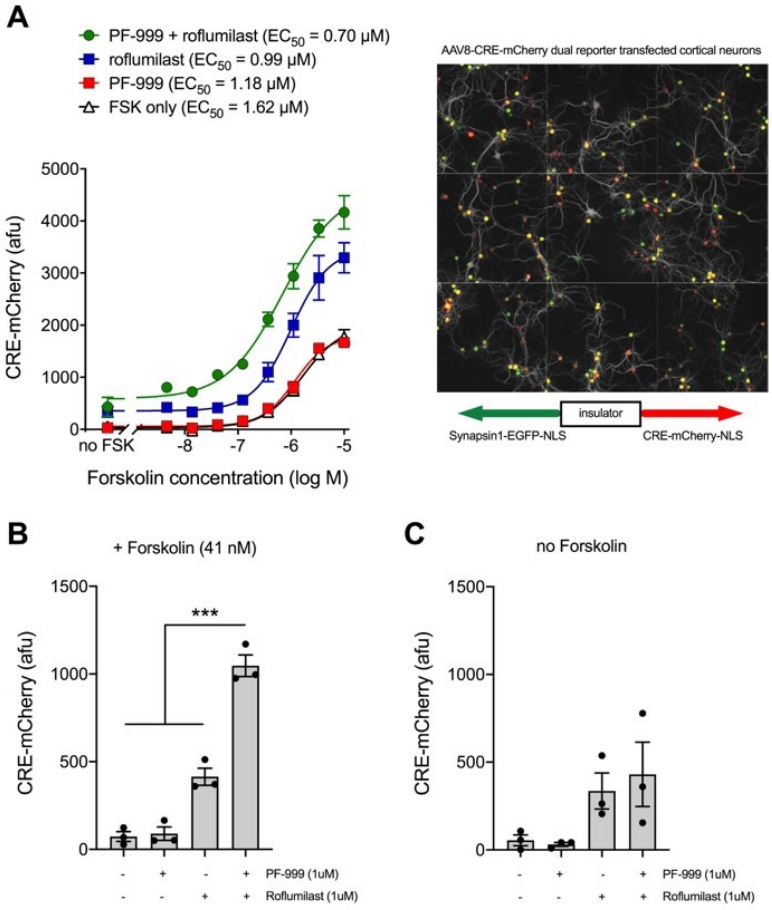

Figure 2. Effect of PDE2 and PDE4 inhibition on forskolin-induced CRE-mediated gene expression. The effect of PDE2 and PDE4 inhibition on CRE-mediated gene expression was investigated in cortical neurons infected with a ratiometric fluorescent reporter of CRE-mediated transcription. Neurons were stimulated with forskolin (0-10 µM) and additionally treated with PF-999, roflumilast or both compounds (1 µM) and the nuclear mCherry:GFP ratio indicated the amount of CRE-mediated gene expression. A) Forskolin dose response (left panel), and a representative image is shown of Map-2(+) cortical neurons (white) expressing both GFP and mCherry fluorescence as well as a schematic depiction of the fluorescent reporter (right panel). B/C) Significantly higher fluorescence intensities were measured for combined treatment with PF-999 and Roflumilast compared to vehicle and PF-999 or roflumilast alone in the presence of Forskolin (ANOVA at 42 nM Forskolin: $F(3,8) = 98.40$, $P < 0.0001$, Bonferroni post-hoc test $P < 0.001$ for PF-999 + Roflumilast vs. all other conditions; ANOVA without Forskolin: $F(3,8) = 3.56$, $P = 0.07$). Without Forskolin, PDE4 inhibition had small but non-significant effect on CRE-reporter expression. No effect was seen for PDE2 inhibition alone.

Combined administration of roflumilast and PF-999 improves spatial object memory in rats

The previous experiments indicated that combined PDE2 and PDE4 inhibition modulates neuronal signaling intricately linked with synaptic plasticity and long-term memory. Hence, we sought to investigate whether PDE2 and PDE4 inhibition can facilitate memory consolidation *in vivo*. By means of oral administration of different doses PF-999 or roflumilast to rats 3 h after the training trial of an object location task, effective doses of each of the compounds were determined. The delay interval between the first and second trial was 24 h. Memory performance, as indicated by the discrimination index (d2), was significantly different from chance (zero) in animals that received 0.3 mg/kg PF-999 or 0.3 mg/kg roflumilast, as indicated by one-sample t-tests (Fig 3, left and middle panel). No significant effect on memory was detected with lower doses of PF-999 or roflumilast. For PF-999, one-way ANOVA revealed significant differences in d2 between treatment conditions (d2: $F(3, 68) = 3.94$, $P < 0.05$). Post-hoc Bonferroni t-tests revealed that rats treated with 0.3 mg/kg PF-999 showed significantly better object discrimination when compared to vehicle ($P < 0.05$) and 0.1 mg/kg PF-999 ($P < 0.05$). For roflumilast, one-way ANOVA also revealed significant differences in d2 between treatment conditions (d2: $F(3, 44) = 6.97$, $P < 0.001$). Rats receiving 0.3 mg/kg roflumilast showed significantly better object discrimination when compared to vehicle ($P < 0.001$) and 0.1 mg/kg roflumilast ($P < 0.01$; Bonferroni post-hoc t-test). This indicates that post-trial administration of doses 0.3 mg/kg PF-999 or roflumilast 3 hrs after learning enhanced memory measured 24 hours later in our NOL paradigm.

After determining effective doses of PF-999 and roflumilast we asked if combined administration of highest ineffective doses (i.e. 0.1 mg/kg) of both compounds can exert synergistic effects on memory consolidation. We treated rats with vehicle, roflumilast or PF-999 alone, or a combination of both. When memory recall was tested 24-hrs after training, the discrimination index (d2) significantly differed from chance in animals that received the combined administration of 0.1

mg/kg PF-999 and roflumilast, but not in rats treated with vehicle or either compound alone (Fig 3, right panel). One-way ANOVA revealed significant differences between treatment conditions (d2: $F(3, 77) = 5.29$, $P < 0.01$). Post-hoc Bonferroni t-tests revealed that rats treated with the combination of PF-999 and roflumilast (0.1 mg/kg for both compound) showed significantly higher object discrimination compared to vehicle ($P < 0.001$) and 0.1 mg/kg roflumilast condition ($P < 0.05$).

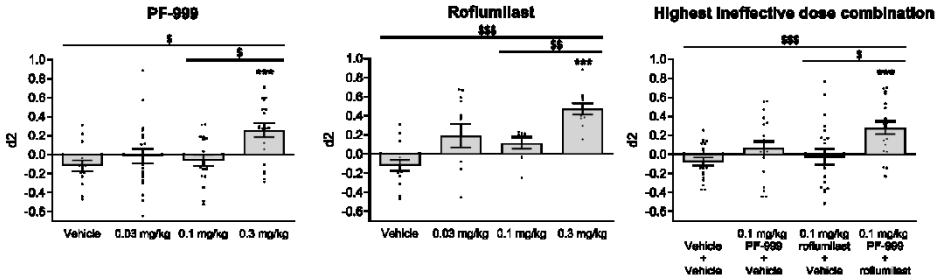

Figure 3. Effects of increasing doses PF-999 and roflumilast and the combination of highest ineffective doses on spatial memory consolidation. Compared to the vehicle condition, both PF-999 (left panel) and roflumilast (middle panel) injected p.o. 3 h after T1, improved memory performance at a dose of 0.3 mg/kg. A difference from chance is depicted with asterisks (one sample t-tests, ***: $P < 0.001$). One-way ANOVA revealed significant differences for the discrimination index d2 between treatment conditions for PF-999 (d2: $F(3, 68) = 3.94$, $P < 0.05$) as well as for roflumilast (d2: $F(3, 44) = 6.97$, $P < 0.001$). Combination of the highest ineffective dose of 0.1 mg/kg (right panel) improved memory compared to vehicle, and yielded memory performance significantly different from chance. Differences between conditions are indicated with dollar signs (Bonferroni post-hoc t-test, $: $P < 0.05$, $$: $P < 0.01$, $$$: $P < 0.001$).

Combined administration of effective and ineffective doses of PF-999 and roflumilast

In a second study, we aimed to confirm our finding of synergy and determine dose-responses for the drug combination using a second batch of animals. Here again, memory performance was significantly higher than zero in animals that received 0.3 mg/kg PF-999 or 0.3 mg/kg roflumilast, as indicated by one-sample t-

tests, but not at 0.1 mg/kg of either drug (Fig 4, left and middle panel). Then, combined administration of subeffective and effective doses PF-999 and roflumilast was tested at doses 0.03, 0.1, and 0.3 mg/kg. We found that animals that received 0.1 or 0.3 mg/kg of both PF-999 and roflumilast showed significant memory recall 24 hours after testing (Fig 4, right panel; one-sample t-test vs. chance). One-way ANOVA revealed significant differences between treatment conditions (d2: $F(3, 77) = 5.23$; $P < 0.01$). Bonferroni post-hoc analysis showed that the combination of PF-999 and roflumilast at doses of 0.1 or 0.3 mg/kg administered 3 h after T1 significantly improved object discrimination performance when compared to the vehicle condition ($P < 0.05$). Thus, treatment with PF-999 and roflumilast at doses of 0.1 or 0.3 mg/kg prevents time-dependent forgetting of rats. As 0.1 mg/kg was a subefficacious dose for both compounds when administered separately, these results demonstrate synergistic effects of combined PDE2 and PDE4 inhibition on memory consolidation.

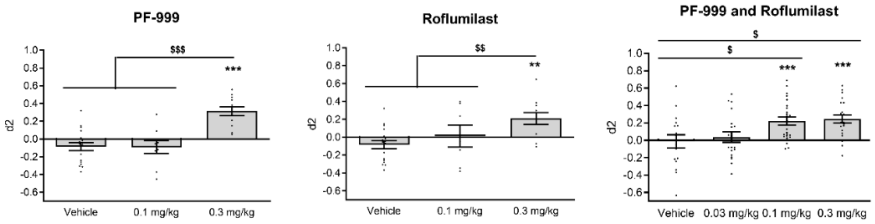

Figure 4. Effects of increasing doses PF-999 and roflumilast and their combined administration on spatial memory consolidation. Compared to the vehicle condition and zero, single administration of either PF-999 (left) or roflumilast (middle) at a dose of 0.3 mg/kg improved memory performance. One-way ANOVA revealed significant differences for the discrimination index d2 between treatment conditions in the PF-999 dose-response curve (d2: $F(2, 36) = 18.57$; $P < 0.001$) and roflumilast dose-response curve (d2: $F(2, 33) = 5.75$; $P < 0.01$). The combination of PF-999 and roflumilast (right) at doses of 0.1 and 0.3 mg/kg injected 3 h after T1, improved memory performance compared to the vehicle condition. A difference from zero is depicted with asterisks (one sample t-tests, **: $P < 0.01$, ***: $P < 0.001$). One-way ANOVA revealed significant differences for the discrimination index d2 between treatment conditions (d2: $F(3, 77) = 5.23$, $P < 0.01$). Differences between conditions are indicated with dollar signs (Bonferroni post-hoc t-tests, $: $P < 0.05$).

Pharmacokinetics of individual and combined administration of PF-999 and roflumilast

Since combined treatments may influence the pharmacokinetics of individual compounds, a pharmacokinetic profile was established for PF-999 and roflumilast upon individual and combined administration in rats. Plasma concentrations were determined at doses of 0.1 mg/kg p.o. (N=3; Table 1). These measurements indicated that both compounds yielded similar plasma C_{max}, T_{max}, and $AUC_{0\text{-}inf}$ when administered alone or in combination. We also evaluated exposures of N-oxide metabolite of roflumilast, which potently inhibited PDE4D3 (IC_{50} = 0.75nM), and there was no difference. Thus, combined administration of our inhibitors did not change oral absorption or metabolism of roflumilast to the bio-active *N*-oxide. Estimated brain concentrations for PF-999 were 0.334 and 0.420 ng/ml when dosed individually or in combination with roflumilast, corresponding to 1.8-2.4 times the IC_{50} for PDE2 inhibition. For roflumilast, brain concentrations of 0.112 and 0.106 ng/ml were estimated upon individual or combined dosing with PF-999. With an IC_{50} of 0.234 nM roflumilast at PDE4D3, these estimated brain concentrations are 1.1-1.2 fold higher than the IC_{50}. Estimated brain exposure of the N-oxide was 1.9-fold higher than the IC_{50} to inhibit PDE4D3. Thus, the sub-efficacious 0.1 mg/kg dose yielded relative exposures of 1-2x IC_{50} to inhibit PDE2 or PDE4, respectively.

Table 1 Pharmacokinetic properties of PF-999 and roflumilast when administered individually and combined.

PF-999		**Individual**	**Combined**
MW: 414 IC_{50} (PDE2A): 0.44 nM Br/P: 0.58 Free fraction [brain]: 12.7% Free fraction [plasma]: 31.5%	T_{max}	0.25	0.25
	C_{max} (ng/ml)	0.973 (±0.425)	0.724 (±0.361)
	$AUC_{0\text{-}inf}$ (ng*hr/ml)	0.922 (±0.447)	0.996 (±0.595)
	Est. Brain (ng/ml)	0.334	0.420
	Est Brain / IC_{50}	1.83	2.31
Roflumilast			
MW: 403 IC_{50} (PDE4D3): 0.234 nM Br/P: 1.2 Free fraction [brain]: 1.1% Free fraction [plasma]: 1.4%	T_{max}	0.25	0.25
	C_{max} (ng/ml)	0.0934 (±0.0279)	0.0883 (±0.0107)
	$AUC_{0\text{-}inf}$ (ng*hr/ml)	0.146 (±0.017)	0.123 (±0.031)
	Est. Brain (ng/ml)	0.112	0.106
	Est Brain / IC_{50}	1.19	1.12
Roflumilast, *N*-oxide			
MW: 419 IC_{50} (PDE4D3): 0.746 nM Br/P: 0.2 Free fraction: not determined	T_{max}	0.84 (0.29)	0.67 (0.29)
	C_{max} (ng/ml)	3.13 (±0.968)	3.04 (±0.727)
	$AUC_{0\text{-}inf}$ (ng*hr/ml)	9.44 (±0.52)	9.27 (±2.06)
	Est. Brain (ng/ml)	0.613	0.596
	Est Brain / IC_{50}	1.96	1.91

DISCUSSION

In the current study, we investigated whether combined inhibition of PDE2 and PDE4 can improve memory consolidation processes. First, the effect of PDE2 and PDE4 inhibition, using PF-999 and roflumilast respectively, on GluR1 phosphorylation was tested in striatal and cortical rat brain slices. Ser845 phosphorylated GluR1 subunits have been found to specifically localize to learning-associated synapses (Matsuo et al., 2008). In striatal slices, combined application of PF-999 and roflumilast significantly promoted GluR1 phosphorylation. In cortical slices, application of PF-999 alone was found to significantly increase GluR1 phosphorylation. This effect was augmented by combined treatment of PF-999 and roflumilast. Earlier studies indicated that separate inhibition of PDE2 or PDE4 can increase GluR1 trafficking to the membrane (Park et al., 2016; Song et al., 2016); a process dependent on serine 845 phosphorylation (Oh et al., 2006). Also, membrane insertion of calcium-permeable AMPA receptors involved in hippocampal LTP is reported to be dependent on PKA signaling (Park et al., 2016). As GluR1 can be phosphorylated by both PKA and PKG, combined PDE2 and PDE4 inhibition may significantly increase both PKA and PKG activity leading to higher p-GluR1/GluR1 ratios. Taken together, these findings suggest that PF-999 and roflumilast increase GluR1 phosphorylation through synergistic actions.

In addition, the effect of PDE2 and PDE4 inhibition on forskolin-stimulated CRE-mediated expression was tested in cortical neurons. CRE-mediated expression is activated by PKA- and PKG-signaling to CREB (Kandel, 2012), which in turn is stimulated by elevated cyclic nucleotide levels. We found that CRE-mediated expression is stimulated by significantly lower concentrations of forskolin when treated with PF-999 and roflumilast, but not when treated with either inhibitor alone. These seemingly synergistic actions of dual inhibition are comparable to those found for GluR1 phosphorylation as inhibition of one PDE family induces effects which are potentiated by additional inhibition of the other PDE family. The current findings are

consistent with previous studies showing that inhibition of PDE4 and PDE2 can increase CREB phosphorylation (Asanuma et al., 1996; Feng et al., 2019; Lueptow et al., 2016; Soares et al., 2017; Zhong et al., 2016). Another study found that PDE2 inhibition does not increase CREB phosphorylation but restores corticosterone-induced decreases in CREB binding protein (CBP) in mouse hippocampal neurons (Xu et al., 2013). CBP serves as a co-activator of CREB and may thus stimulate CREB-mediated transcription upon increased CREB phosphorylation induced by PDE4 inhibition.

To demonstrate synergistic effects *in vivo*, an object location task was used to test the effects of PF-999 and roflumilast on spatial memory performance in rats. Specifically, the effects of both compounds were investigated on late memory consolidation by means of oral administering 3 h after the learning trial. A dose of 0.3 mg/kg was found to be effective for both compounds when administered individually. Subsequently, sub-effective and effective doses were combined (0.1 and 0.3 mg/kg, respectively for both PF-999 and roflumilast) to investigate potential synergistic effects on memory consolidation. Delay-dependent forgetting could be fully prevented by treating animals with combinations of both sub-effective and effective doses. Thus, combining doses of PF-999 and roflumilast, which by themselves are ineffective, can improve spatial memory performance in rats suggesting cooperative actions on underlying molecular mechanisms. Additional pharmacokinetic profiling of PF-999 and roflumilast upon individual or combined administration indicated that combined administration does not influence exposure to either PF-999 or roflumilast. Determined IC_{50} concentrations were consistent with previously reported values for PF-999 (Helal et al., 2017) and roflumilast (Hatzelmann et al., 2010). Brain concentrations [free+bound] ranged from 1-2x the IC_{50} (i.e. 50% enzyme inhibition) after a dose of 0.1 mg/kg. However, because of high protein binding, we anticipate that free brain concentrations of roflumilast are well below IC_{50} at efficacious exposures. However, brain levels of the active roflumilast N-oxide

metabolite were higher, and the estimated free brain concentration of PF-999 was 0.7x IC_{50}[PDE2] at the efficacious dose of 0.3 mg/kg, and 0.29x IC_{50} [PDE2] at the 0.1 mg/kg sub-effective dose. Our findings are in accordance with studies in nonhuman primates and humans in which memory-enhancing doses led to low brain PDE4 occupancy levels (Takano et al., 2018; Van Duinen et al., 2018). Furthermore, while higher doses would occupy more PDE4 sites, these doses do not show memory enhancing effects in mice (Vanmierlo et al., 2016). Similarly, receptor occupancy as measured by PET is below the detectable level after PF-999 doses of 0.1-0.3 mg/kg (Gu et al., 2019). The latter finding is consistent with observations on PDE2 inhibitor TAK-915, a compound that reverses NMDA receptor antagonist induced memory impairment at brain occupancy levels of 46-63%, but enhances object recognition memory in intact rats at doses that are 30- to 100-fold lower (Mikami et al., 2017). Overall, these results indicate that PDE2 and PDE4 inhibitors can exert profound effects on behavior even at low brain concentrations. Our *in vitro* studies in cortical slices tested fixed drug concentrations of either 300 nM PF-999 or 30 nM roflumilast with varying concentrations of the PDE4 and PDE2 inhibitors, respectively. Inhibitor concentrations were set to induce a minimal pGluR1 signal that could be facilitated by adding the corresponding inhibitor for the other PDE. The lowest concentration of roflumilast required for elevating pGluR1 in cortical slices when PDE2 was inhibited by PF-999 was 12 nM (51x IC_{50}), and the lowest dose of PF-999 required for elevating pGluR1 was between 73 nM and 220 nM (166–500x IC_{50}). These drug concentrations are much higher than what was measured in brain post memory enhancing doses *in vivo*. Here again, a disconnect between biochemical surrogate measures of memory (pGluR1 in our study) and *in vivo* exposures in memory models has also been observed with TAK-915. The latter compound potently inhibits PDE2 (IC_{50} = 0.61 nM) and enhances memory in intact young rats at oral doses of 0.1 mg/kg, but it requires doses of 10 mg/kg with corresponding brain concentrations of 331 ng/ml (723 nM) for enhancing hippocampal and cortical pGluR1 and cGMP *in vivo* (Mikami et al.,

2017; Nakashima et al., 2018). It is likely that neuromodulatory input and Ca^{2+}-signaling resulting from synaptic activity during memory encoding are not preserved in the slice system, and inadequately modelled when animals are exposed to drug in the absence of behavior *in vivo*. Our exploration focused on GluR1 Ser845 phosphorylation and CRE-mediated gene-expression as exemplary cyclic nucleotide regulated mechanisms linked to memory consolidation and synaptic plasticity in the hippocampus and neocortex. However, PDE2 and PDE4 may have additional effects on transmitter release (Fernandez-Fernandez et al., 2015), dopaminergic receptor signaling (Polito et al., 2013), and excitation/inhibition balance in dopaminergic systems (Liu et al., 2017) not explored here. Thus, simultaneous augmentation of multiple mechanism may underlie the increased sensitivity to PDE inhibition *in vivo*.

The phosphorylation of the AMPA receptor GluR1 subunit is required for synaptic plasticity and retention of spatial memory (Lee et al., 2003). The synergistic effects of PDE2 and PDE4 inhibition on GluR1 phosphorylation paired with increased CREB phosphorylation may therefore have contributed to the improved spatial memory performance. Interestingly, inhibition of PDE5 - rather than PDE4 - increased GluR1 trafficking to the membrane in mice (Argyrousi et al., 2020). Subeffective dose combination of rolipram (PDE4 inhibitor) and vardenafil (PDE5 inhibitor) at different time points can also improve memory performance in rats (Bollen et al., 2015). More recently, combined treatment for three weeks with subeffective doses of roflumilast (0.01 mg/kg) and vardenafil (0.1 mg/kg) was found to restore memory impairments in APPswe mice (Gulisano et al., 2018). These studies support our finding that inhibition of different PDE families may jointly exert memory enhancing effects. Through partial activation of multiple distinct mechanisms, which may act sequentially or concurrently, behavioral plasticity is effectively enhanced. We focused here on two key mechanism of memory formation, AMPA receptor phosphorylation and CRE-mediated gene expression. While combined inhibition greatly enhanced both, we cannot be entirely sure that effects on GluR1 phosphorylation was more

sensitive to PDE2 and CRE-mediated transcription more sensitive to PDE4 inhibition. These findings may imply that the PDEs regulate cyclic nucleotide levels in different intracellular compartments. PDE2 and PDE4 have been implicated in the regulation of both pre- and postsynaptic signaling (Fernandez-Fernandez et al., 2015; Liu et al., 2017; Polito et al., 2013). PDE2A protein is detected in pyramidal neurons and interneurons of rat neocortex, and it is highly concentrated in axons and nerve terminals of the mossy fiber pathway in hippocampus (Stephenson et al., 2009). Elevations in cGMP and cAMP levels upon NMDA receptor activation are regulated by respectively PDE2 and PDE4 (Suvarna and O'Donnell, 2002). As certain PDE2 and PDE4 transcript variants are known to associate with the membrane, they may be positioned within signaling complexes that regulate the phosphorylation of pre- and post-synaptic targets, including AMPA receptors (Bender and Beavo, 2006). The PDE2A3 isoform is localized to presynaptic membranes and may mediate the effect of PDE2A inhibitors on presynaptic plasticity (Fernandez-Fernandez et al., 2015; Russwurm et al., 2009). The PDE4D3 and PDE4D5 isoforms are localized to the perinuclear region and within the nucleus, respectively, which enables PDE4 to predominantly exert control on the cAMP-PKA-CREB signaling axis which eventually leads to CRE-mediated transcription (Boczek et al., 2019; Clister et al., 2019). PDE2 and PDE4 may thus be involved in distinct but partly overlapping or cross-talking signaling cascades which, upon combined inhibition, can produce synergistic effects on plasticity. Correspondingly, PDE2 and PDE4 inhibition can both inhibit endothelial cell proliferation, but exert these effects through different mechanisms (Favot et al., 2004).

An open question remains whether combined inhibition of PDE2 and PDE4 is efficacious and synergy is seen in models of memory impairment. An interesting finding in this context was reported by Gulisano et al., who found that combined PDE4 and PDE5 inhibition can improve memory in transgenic AD mice only with chronic dosing (Gulisano et al., 2018). In addition, much higher concentrations of

PDE2 inhibitors may be required to reverse memory impairment than tested here in normal adult rats (Gu et al., 2019; Mikami et al., 2017; Nakashima et al., 2018). Hence, the memory-enhancing effect of combined PDE2 and PDE4 inhibition in disease models remains to be investigated. Nevertheless, the fact that subeffective doses PF-999 and roflumilast can synergistically increase memory consolidation through modulation of plasticity processes may provide a new therapeutic strategy. CNS expression of PDE2 is largely conserved between rat, primates, and humans (Stephenson et al., 2009), whereas human expression of the many PDE4 isoforms may vary substantially when compared to preclinical species. Thus, combining two targets with well characterized effects on memory in preclinical models may de-risk clinical translation of PDE biology arising from complications associated with variation of gene expression between species. Furthermore, because efficacy is achieved at lower levels of PDE4 inhibition, target related side effects such as emesis may be minimized. More generally, dual inhibitors of phosphodiesterases may open significant new avenues for the development of plasticity enhancers with improved efficacy.

ACKNOWLEDGEMENTS

We would like to thank Laurent Gomez for critical discussions, Finley Serneo and Yan Beaver for CRE-luci studies, and John Nikpur for help with DMPK studies.

FUNDING AND DISCLOSURES

The authors declare that this study was funded by Dart Neuroscience, LLC. The funder was not involved in the study design or collection, analysis, or interpretation of the data. MP, DGW, KX, and DZ are former employees of Dart Neuroscience, LLC. JP has a proprietary interest in selective PDE4D inhibitors for the treatment of neurodegenerative disorders.

REFERENCES

Akkerman S, Blokland A, Reneerkens O, van Goethem NP, Bollen E, Gijselaers HJ, Lieben CK, Steinbusch HW and Prickaerts J (2012a) Object recognition testing: methodological considerations on exploration and discrimination measures. *Behav Brain Res* **232**:335-347.

Akkerman S, Prickaerts J, Steinbusch HW and Blokland A (2012b) Object recognition testing: statistical considerations. *Behav Brain Res* **232**:317-322.

Argyrousi EK, Heckman PR, van Hagen BT, Muysers H, van Goethem NP and Prickaerts J (2020) Pro-cognitive effect of upregulating cyclic guanosine monophosphate signalling during memory acquisition or early consolidation is mediated by increased AMPA receptor trafficking. *Journal of psychopharmacology (Oxford, England)* **34**:103-114.

Asanuma M, Nishibayashi S, Iwata E, Kondo Y, Nakanishi T, Vargas MG and Ogawa N (1996) Alterations of cAMP response element-binding activity in the aged rat brain in response to administration of rolipram, a cAMP-specific phosphodiesterase inhibitor. *Brain Res Mol Brain Res* **41**:210-215.

Baillie GS (2009) Compartmentalized signalling: spatial regulation of cAMP by the action of compartmentalized phosphodiesterases. *FEBS J* **276**:1790-1799.

Barco A, Alarcon JM and Kandel ER (2002) Expression of constitutively active CREB protein facilitates the late phase of long-term potentiation by enhancing synaptic capture. *Cell* **108**:689-703.

Bender AT and Beavo JA (2006) Cyclic nucleotide phosphodiesterases: molecular regulation to clinical use. *Pharmacol Rev* **58**:488-520.

Boczek T, Cameron EG, Yu W, Xia X, Shah SH, Castillo Chabeco B, Galvao J, Nahmou M, Li J, Thakur H, Goldberg JL and Kapiloff MS (2019) Regulation of Neuronal Survival and Axon Growth by a Perinuclear cAMP Compartment. *J Neurosci* **39**:5466-5480.

Boess FG, Hendrix M, van der Staay FJ, Erb C, Schreiber R, van Staveren W, de Vente J, Prickaerts J, Blokland A and Koenig G (2004) Inhibition of phosphodiesterase 2 increases neuronal cGMP, synaptic plasticity and memory performance. *Neuropharmacology* **47**:1081-1092.

Bollen E, Akkerman S, Puzzo D, Gulisano W, Palmeri A, D'Hooge R, Balschun D, Steinbusch HW, Blokland A and Prickaerts J (2015) Object memory enhancement by combining sub-efficacious doses of specific phosphodiesterase inhibitors. *Neuropharmacology* **95**:361-366.

Clister T, Greenwald EC, Baillie GS and Zhang J (2019) AKAP95 Organizes a Nuclear Microdomain to Control Local cAMP for Regulating Nuclear PKA. *Cell chemical biology* **26**:885-891.e884.

Domek-Lopacinska K and Strosznajder JB (2008) The effect of selective inhibition of cyclic GMP hydrolyzing phosphodiesterases 2 and 5 on learning and memory processes and nitric oxide synthase activity in brain during aging. *Brain Res* **1216**:68-77.

Favot L, Keravis T and Lugnier C (2004) Modulation of VEGF-induced endothelial cell cycle protein expression through cyclic AMP hydrolysis by PDE2 and PDE4. *Thromb Haemost* **92**:634-645.

Feng H, Wang C, He W, Wu X, Li S, Zeng Z, Wei M and He B (2019) Roflumilast ameliorates cognitive impairment in APP/PS1 mice via cAMP/CREB/BDNF

signaling and anti-neuroinflammatory effects. *Metab Brain Dis* **34**:583-591.
Fernandez-Fernandez D, Rosenbrock H and Kroker KS (2015) Inhibition of PDE2A, but not PDE9A, modulates presynaptic short-term plasticity measured by paired-pulse facilitation in the CA1 region of the hippocampus. *Synapse* **69**:484-496.
Giralt A, Saavedra A, Carreton O, Arumi H, Tyebji S, Alberch J and Perez-Navarro E (2013) PDE10 inhibition increases GluA1 and CREB phosphorylation and improves spatial and recognition memories in a Huntington's disease mouse model. *Hippocampus* **23**:684-695.
Gomez L and Breitenbucher JG (2013) PDE2 inhibition: potential for the treatment of cognitive disorders. *Bioorg Med Chem Lett* **23**:6522-6527.
Gong B, Vitolo OV, Trinchese F, Liu S, Shelanski M and Arancio O (2004) Persistent improvement in synaptic and cognitive functions in an Alzheimer mouse model after rolipram treatment. *J Clin Invest* **114**:1624-1634.
Gu G, Scott T, Yan Y, Warren N, Zhang A, Tabatabaei A, Xu H, Aertgeerts K, Gomez L, Morse A, Li Y-W, Breitenbucher JG, Massari E, Vivian J and Danks A (2019) Target Engagement of a Phosphodiesterase 2A Inhibitor Affecting Long-Term Memory in the Rat. *Journal of Pharmacology and Experimental Therapeutics* **370**:399-407.
Gulisano W, Tropea MR, Arancio O, Palmeri A and Puzzo D (2018) Sub-efficacious doses of phosphodiesterase 4 and 5 inhibitors improve memory in a mouse model of Alzheimer's disease. *Neuropharmacology* **138**:151-159.
Guo H, Cheng Y, Wang C, Wu J, Zou Z, Niu B, Yu H, Wang H and Xu J (2017) FFPM, a PDE4 inhibitor, reverses learning and memory deficits in APP/PS1 transgenic mice via cAMP/PKA/CREB signaling and anti-inflammatory effects. *Neuropharmacology* **116**:260-269.
Hatzelmann A, Morcillo EJ, Lungarella G, Adnot S, Sanjar S, Beume R, Schudt C and Tenor H (2010) The preclinical pharmacology of roflumilast--a selective, oral phosphodiesterase 4 inhibitor in development for chronic obstructive pulmonary disease. *Pulm Pharmacol Ther* **23**:235-256.
Heckman PR, Wouters C and Prickaerts J (2015) Phosphodiesterase inhibitors as a target for cognition enhancement in aging and Alzheimer's disease: a translational overview. *Curr Pharm Des* **21**:317-331.
Heckman PRA, Blokland A and Prickaerts J (2017) From Age-Related Cognitive Decline to Alzheimer's Disease: A Translational Overview of the Potential Role for Phosphodiesterases. *Adv Neurobiol* **17**:135-168.
Helal CJ, Arnold EP, Boyden TL, Chang C, Chappie TA, Fennell KF, Forman MD, Hajos M, Harms JF, Hoffman WE, Humphrey JM, Kang Z, Kleiman RJ, Kormos BL, Lee CW, Lu J, Maklad N, McDowell L, Mente S, O'Connor RE, Pandit J, Piotrowski M, Schmidt AW, Schmidt CJ, Ueno H, Verhoest PR and Yang EX (2017) Application of Structure-Based Design and Parallel Chemistry to Identify a Potent, Selective, and Brain Penetrant Phosphodiesterase 2A Inhibitor. *J Med Chem* **60**:5673-5698.
Hutson PH, Finger EN, Magliaro BC, Smith SM, Converso A, Sanderson PE, Mullins D, Hyde LA, Eschle BK, Turnbull Z, Sloan H, Guzzi M, Zhang X, Wang A, Rindgen D, Mazzola R, Vivian JA, Eddins D, Uslaner JM, Bednar R, Gambone C, Le-Mair W, Marino MJ, Sachs N, Xu G and Parmentier-Batteur S (2011) The selective phosphodiesterase 9 (PDE9) inhibitor PF-04447943 (6-[(3S,4S)-4-methyl-1-(pyrimidin-2-ylmethyl)pyrrolidin-3-yl]-1-(tetrahydro-2H-py ran-4-yl)-1,5-dihydro-4H-pyrazolo[3,4-d]pyrimidin-4-

one) enhances synaptic plasticity and cognitive function in rodents. *Neuropharmacology* **61**:665-676.
Jin F, Gong QH, Xu YS, Wang LN, Jin H, Li F, Li LS, Ma YM and Shi JS (2014) Icariin, a phosphodiesterase-5 inhibitor, improves learning and memory in APP/PS1 transgenic mice by stimulation of NO/cGMP signalling. *Int J Neuropsychopharmacol* **17**:871-881.
Kandel ER (2012) The molecular biology of memory: cAMP, PKA, CRE, CREB-1, CREB-2, and CPEB. *Mol Brain* **5**:14.
Kida S (2012) A Functional Role for CREB as a Positive Regulator of Memory Formation and LTP. *Exp Neurobiol* **21**:136-140.
Kumar A and Singh N (2017) Inhibitor of Phosphodiestearse-4 improves memory deficits, oxidative stress, neuroinflammation and neuropathological alterations in mouse models of dementia of Alzheimer's Type. *Biomed Pharmacother* **88**:698-707.
Lakics V, Karran EH and Boess FG (2010) Quantitative comparison of phosphodiesterase mRNA distribution in human brain and peripheral tissues. *Neuropharmacology* **59**:367-374.
Lee HK (2006) Frontiers in Neuroscience
AMPA Receptor Phosphorylation in Synaptic Plasticity: Insights from Knockin Mice, in *The Dynamic Synapse: Molecular Methods in Ionotropic Receptor Biology* (Kittler JT and Moss SJ eds), CRC Press/Taylor & Francis
Taylor & Francis Group, LLC., Boca Raton (FL).
Lee HK, Takamiya K, Han JS, Man H, Kim CH, Rumbaugh G, Yu S, Ding L, He C, Petralia RS, Wenthold RJ, Gallagher M and Huganir RL (2003) Phosphorylation of the AMPA receptor GluR1 subunit is required for synaptic plasticity and retention of spatial memory. *Cell* **112**:631-643.
Li YF, Cheng YF, Huang Y, Conti M, Wilson SP, O'Donnell JM and Zhang HT (2011) Phosphodiesterase-4D knock-out and RNA interference-mediated knock-down enhance memory and increase hippocampal neurogenesis via increased cAMP signaling. *J Neurosci* **31**:172-183.
Liu X, Zhong P, Vickstrom C, Li Y and Liu QS (2017) PDE4 Inhibition Restores the Balance Between Excitation and Inhibition in VTA Dopamine Neurons Disrupted by Repeated In Vivo Cocaine Exposure. *Neuropsychopharmacology* **42**:1991-1999.
Lueptow LM, Zhan CG and O'Donnell JM (2016) Cyclic GMP-mediated memory enhancement in the object recognition test by inhibitors of phosphodiesterase-2 in mice. *Psychopharmacology (Berl)* **233**:447-456.
Matsuo N, Reijmers L and Mayford M (2008) Spine-type-specific recruitment of newly synthesized AMPA receptors with learning. *Science* **319**:1104-1107.
Mikami S, Nakamura S, Ashizawa T, Nomura I, Kawasaki M, Sasaki S, Oki H, Kokubo H, Hoffman ID, Zou H, Uchiyama N, Nakashima K, Kamiguchi N, Imada H, Suzuki N, Iwashita H and Taniguchi T (2017) Discovery of Clinical Candidate N-((1S)-1-(3-Fluoro-4-(trifluoromethoxy)phenyl)-2-methoxyethyl)-7-methoxy-2-oxo-2,3-dihydropyrido[2,3-b]pyrazine-4(1H)-carboxamide (TAK-915): A Highly Potent, Selective, and Brain-Penetrating Phosphodiesterase 2A Inhibitor for the Treatment of Cognitive Disorders. *Journal of Medicinal Chemistry* **60**:7677-7702.
Mori F, Perez-Torres S, De Caro R, Porzionato A, Macchi V, Beleta J, Gavalda A, Palacios JM and Mengod G (2010) The human area postrema and other

nuclei related to the emetic reflex express cAMP phosphodiesterases 4B and 4D. *J Chem Neuroanat* **40**:36-42.
Nakashima M, Imada H, Shiraishi E, Ito Y, Suzuki N, Miyamoto M, Taniguchi T and Iwashita H (2018) Phosphodiesterase 2A Inhibitor TAK-915 Ameliorates Cognitive Impairments and Social Withdrawal in N-Methyl-d-Aspartate Receptor Antagonist–Induced Rat Models of Schizophrenia. *Journal of Pharmacology and Experimental Therapeutics* **365**:179-188.
Oh MC, Derkach VA, Guire ES and Soderling TR (2006) Extrasynaptic membrane trafficking regulated by GluR1 serine 845 phosphorylation primes AMPA receptors for long-term potentiation. *J Biol Chem* **281**:752-758.
Park P, Sanderson TM, Amici M, Choi SL, Bortolotto ZA, Zhuo M, Kaang BK and Collingridge GL (2016) Calcium-Permeable AMPA Receptors Mediate the Induction of the Protein Kinase A-Dependent Component of Long-Term Potentiation in the Hippocampus. *J Neurosci* **36**:622-631.
Polito M, Klarenbeek J, Jalink K, Paupardin-Tritsch D, Vincent P and Castro LR (2013) The NO/cGMP pathway inhibits transient cAMP signals through the activation of PDE2 in striatal neurons. *Front Cell Neurosci* **7**:211.
Prickaerts J, van Staveren WC, Sik A, Markerink-van Ittersum M, Niewohner U, van der Staay FJ, Blokland A and de Vente J (2002) Effects of two selective phosphodiesterase type 5 inhibitors, sildenafil and vardenafil, on object recognition memory and hippocampal cyclic GMP levels in the rat. *Neuroscience* **113**:351-361.
Puerta E, Hervias I, Barros-Minones L, Jordan J, Ricobaraza A, Cuadrado-Tejedor M, Garcia-Osta A and Aguirre N (2010) Sildenafil protects against 3-nitropropionic acid neurotoxicity through the modulation of calpain, CREB, and BDNF. *Neurobiol Dis* **38**:237-245.
Puzzo D, Sapienza S, Arancio O and Palmeri A (2008) Role of phosphodiesterase 5 in synaptic plasticity and memory. *Neuropsychiatr Dis Treat* **4**:371-387.
Puzzo D, Staniszewski A, Deng SX, Privitera L, Leznik E, Liu S, Zhang H, Feng Y, Palmeri A, Landry DW and Arancio O (2009) Phosphodiesterase 5 inhibition improves synaptic function, memory, and amyloid-beta load in an Alzheimer's disease mouse model. *J Neurosci* **29**:8075-8086.
Reneerkens OA, Rutten K, Akkerman S, Blokland A, Shaffer CL, Menniti FS, Steinbusch HW and Prickaerts J (2012) Phosphodiesterase type 5 (PDE5) inhibition improves object recognition memory: indications for central and peripheral mechanisms. *Neurobiol Learn Mem* **97**:370-379.
Reneerkens OAH, Rutten K, Bollen E, Hage T, Blokland A, Steinbusch HWM and Prickaerts J (2013) Inhibition of phoshodiesterase type 2 or type 10 reverses object memory deficits induced by scopolamine or MK-801. *Behav Brain Res* **236**:16-22.
Russwurm C, Zoidl G, Koesling D and Russwurm M (2009) Dual Acylation of PDE2A Splice Variant 3: TARGETING TO SYNAPTIC MEMBRANES*. *Journal of Biological Chemistry* **284**:25782-25790.
Rutten K, Prickaerts J, Hendrix M, van der Staay FJ, Sik A and Blokland A (2007) Time-dependent involvement of cAMP and cGMP in consolidation of object memory: studies using selective phosphodiesterase type 2, 4 and 5 inhibitors. *Eur J Pharmacol* **558**:107-112.
Santora VJ, Almos TA, Barido R, Basinger J, Bellows CL, Bookser BC, Breitenbucher JG, Broadbent NJ, Cabebe C, Chai C-K, Chen M, Chow S, Chung DM, Crickard L, Danks AM, Freestone GC, Gitnick D, Gupta V,

Hoffmaster C, Hudson AR, Kaplan AP, Kennedy MR, Lee D, Limberis J, Ly K, Mak CC, Masatsugu B, Morse AC, Na J, Neul D, Nikpur J, Peters M, Petroski RE, Renick J, Sebring K, Sevidal S, Tabatabaei A, Wen J, Yan Y, Yoder ZW and Zook D (2018) Design and Synthesis of Novel and Selective Glycine Transporter-1 (GlyT1) Inhibitors with Memory Enhancing Properties. *Journal of Medicinal Chemistry* **61**:6018-6033.

Schwam EM, Nicholas T, Chew R, Billing CB, Davidson W, Ambrose D and Altstiel LD (2014) A multicenter, double-blind, placebo-controlled trial of the PDE9A inhibitor, PF-04447943, in Alzheimer's disease. *Curr Alzheimer Res* **11**:413-421.

Sierksma AS, Rutten K, Sydlik S, Rostamian S, Steinbusch HW, van den Hove DL and Prickaerts J (2013) Chronic phosphodiesterase type 2 inhibition improves memory in the APPswe/PS1dE9 mouse model of Alzheimer's disease. *Neuropharmacology* **64**:124-136.

Sierksma AS, van den Hove DL, Pfau F, Philippens M, Bruno O, Fedele E, Ricciarelli R, Steinbusch HW, Vanmierlo T and Prickaerts J (2014) Improvement of spatial memory function in APPswe/PS1dE9 mice after chronic inhibition of phosphodiesterase type 4D. *Neuropharmacology* **77**:120-130.

Soares LM, Meyer E, Milani H, Steinbusch HW, Prickaerts J and de Oliveira RM (2017) The phosphodiesterase type 2 inhibitor BAY 60-7550 reverses functional impairments induced by brain ischemia by decreasing hippocampal neurodegeneration and enhancing hippocampal neuronal plasticity. *Eur J Neurosci* **45**:510-520.

Song RS, Tolentino R, Sobie EA and Neves-Zaph SR (2016) Cross-regulation of Phosphodiesterase 1 and Phosphodiesterase 2 Activities Controls Dopamine-mediated Striatal alpha-Amino-3-hydroxy-5-methyl-4-isoxazolepropionic Acid (AMPA) Receptor Trafficking. *J Biol Chem* **291**:23257-23267.

Stephenson DT, Coskran TM, Wilhelms MB, Adamowicz WO, O'Donnell MM, Muravnick KB, Menniti FS, Kleiman RJ and Morton D (2009) Immunohistochemical localization of phosphodiesterase 2A in multiple mammalian species. *The journal of histochemistry and cytochemistry : official journal of the Histochemistry Society* **57**:933-949.

Suvarna NU and O'Donnell JM (2002) Hydrolysis of N-methyl-D-aspartate receptor-stimulated cAMP and cGMP by PDE4 and PDE2 phosphodiesterases in primary neuronal cultures of rat cerebral cortex and hippocampus. *J Pharmacol Exp Ther* **302**:249-256.

Suzuki A, Fukushima H, Mukawa T, Toyoda H, Wu LJ, Zhao MG, Xu H, Shang Y, Endoh K, Iwamoto T, Mamiya N, Okano E, Hasegawa S, Mercaldo V, Zhang Y, Maeda R, Ohta M, Josselyn SA, Zhuo M and Kida S (2011) Upregulation of CREB-mediated transcription enhances both short- and long-term memory. *J Neurosci* **31**:8786-8802.

Takano A, Uz T, Garcia-Segovia J, Tsai M, Lahu G, Amini N, Nakao R, Jia Z and Halldin C (2018) A Nonhuman Primate PET Study: Measurement of Brain PDE4 Occupancy by Roflumilast Using (R)-[(11)C]Rolipram. *Mol Imaging Biol* **20**:615-622.

van der Staay FJ, Rutten K, Barfacker L, Devry J, Erb C, Heckroth H, Karthaus D, Tersteegen A, van Kampen M, Blokland A, Prickaerts J, Reymann KG, Schroder UH and Hendrix M (2008) The novel selective PDE9 inhibitor BAY 73-6691 improves learning and memory in rodents. *Neuropharmacology* **55**:908-918.

Van Duinen MA, Sambeth A, Heckman PRA, Smit S, Tsai M, Lahu G, Uz T, Blokland A and Prickaerts J (2018) Acute administration of roflumilast enhances immediate recall of verbal word memory in healthy young adults. *Neuropharmacology* **131**:31-38.

Vanmierlo T, Creemers P, Akkerman S, van Duinen M, Sambeth A, De Vry J, Uz T, Blokland A and Prickaerts J (2016) The PDE4 inhibitor roflumilast improves memory in rodents at non-emetic doses. *Behav Brain Res* **303**:26-33.

Verhoest PR, Fonseca KR, Hou X, Proulx-Lafrance C, Corman M, Helal CJ, Claffey MM, Tuttle JB, Coffman KJ, Liu S, Nelson F, Kleiman RJ, Menniti FS, Schmidt CJ, Vanase-Frawley M and Liras S (2012) Design and discovery of 6-[(3S,4S)-4-methyl-1-(pyrimidin-2-ylmethyl)pyrrolidin-3-yl]-1-(tetrahydro-2H-pyr an-4-yl)-1,5-dihydro-4H-pyrazolo[3,4-d]pyrimidin-4-one (PF-04447943), a selective brain penetrant PDE9A inhibitor for the treatment of cognitive disorders. *J Med Chem* **55**:9045-9054.

Xu Y, Pan J, Chen L, Zhang C, Sun J, Li J, Nguyen L, Nair N, Zhang H and O'Donnell JM (2013) Phosphodiesterase-2 inhibitor reverses corticosterone-induced neurotoxicity and related behavioural changes via cGMP/PKG dependent pathway. *Int J Neuropsychopharmacol* **16**:835-847.

Zhang C, Xu Y, Chowdhary A, Fox D, 3rd, Gurney ME, Zhang HT, Auerbach BD, Salvi RJ, Yang M, Li G and O'Donnell JM (2018) Memory enhancing effects of BPN14770, an allosteric inhibitor of phosphodiesterase-4D, in wild-type and humanized mice. *Neuropsychopharmacology* **43**:2299-2309.

Zhang C, Xu Y, Zhang HT, Gurney ME and O'Donnell JM (2017) Comparison of the Pharmacological Profiles of Selective PDE4B and PDE4D Inhibitors in the Central Nervous System. *Sci Rep* **7**:40115.

Zhang J, Guo J, Zhao X, Chen Z, Wang G, Liu A, Wang Q, Zhou W, Xu Y and Wang C (2013) Phosphodiesterase-5 inhibitor sildenafil prevents neuroinflammation, lowers beta-amyloid levels and improves cognitive performance in APP/PS1 transgenic mice. *Behav Brain Res* **250**:230-237.

Zhong Y, Zhu Y, He T, Li W, Yan H and Miao Y (2016) Rolipram-induced improvement of cognitive function correlates with changes in hippocampal CREB phosphorylation, BDNF and Arc protein levels. *Neurosci Lett* **610**:171-176.

Chapter 7

General Discussion

The inhibition of PDE4 and, in particular, PDE4D has previously been investigated as a therapeutic strategy to treat memory problems associated with Alzheimer's disease (AD) (Cheng et al., 2010; Feng et al., 2019; Sierksma et al., 2014; Wang et al., 2020a; Zhang et al., 2018). While PDE4(D) inhibitors can potently increase neuroplasticity processes *in vitro* and *in vivo*, the progression of these molecules into the clinic has been hampered by severe adverse effects, including nausea, emesis and diarrhea. As such, more specific PDE4(D) inhibitory treatments might be of great added value, maximizing their therapeutic effects while minimizing or preventing side effects. Interestingly, PDE4 enzymes consist of several subtypes and isoforms which are expressed in tissue-specific and cell-type specific patterns (Miró et al., 2002a; Miró et al., 2002b; Paes et al., 2021; Pérez-Torres et al., 2000). Moreover, within distinct cell types, PDE4D isoforms can locate to specific intracellular compartments to control cAMP signaling with high spatial resolution. As such, targeting of specific PDE4D isoforms can provide the necessary treatment selectivity to prevent PDE4(D)-mediated side effects of non-specific PDE4(D) inhibitors, while conserving the therapeutic effects.

Picking the best isoform as therapeutic target in AD

Since PDE4D isoforms potentially provide better targets, an understanding of the differently described isoforms had to be established. As also outlined in **Chapter 2** (Paes et al., 2021), the nomenclature of PDE4 isoforms is complicated due to the existence of both mRNA transcript variants and protein isoforms that are differentially annotated within and across online genome browsers. Moreover, naming of PDE4 isoforms may not be consistent across species (see Supplementary Table 1 in **Chapter 2**). Building on the understanding of isoform-specific sequences at the DNA, mRNA, and protein level, PDE4D isoform-specific expression was measured in post-mortem brain tissue of Alzheimer's disease (AD) patients and matched healthy controls. As described in **Chapter 3**, mRNA expression of specific

PDE4D isoforms (PDE4D1, -D3, -D5, and –D8) was found to be upregulated in AD brains and these expression changes were found to be associated with altered DNA methylation of isoform-specific promoter regions in the *PDE4D* gene (Paes et al., 2020a). Moreover, these changes in expression and DNA methylation correlated significantly with measures of AD pathology (amyloid-β plaques, tau tangles, and Braak staging) and cognitive impairment (Mini-Mental State Examination score, MMSE). Similar findings were gathered in experiments described in **Chapter 4**, in which isoform-specific PDE4D expression increases were found in the hippocampus and frontal cortex of transgenic AD mice (Paes et al., 2023). Whilst intriguingly translational between men and mice, these correlations between AD phenotype and PDE4D expression do not automatically imply causality. In addition, the directionality of a possible causal relationship between PDE4D isoform expression and AD pathology cannot be inferred directly from this work. In platelets, increasing cAMP levels inhibits the production of amyloid-β (Sepúlveda et al., 2019). A similar mechanism may exist in the AD brain in which elevated PDE4D isoform expression would decrease cyclic adenosine monophosphate (cAMP) levels leading to increased amyloid-β production. Vice versa, cells exposed to inflammatory stimuli can upregulate PDE4 expression (Konrad et al., 2015), which may explain how AD pathology would increase PDE4D isoform expression. Indeed, in **Chapter 4**, it was described that hippocampal neurons acutely exposed to amyloid-β show increased expression of certain PDE4D isoforms (Paes et al., 2023). If both causal directionalities exist in the (AD) brain, AD pathology could upregulate PDE4D expression, which increases amyloid-β production, leading to a self-propagating cycle. Promisingly, a recent conference abstract suggests that pharmacological PDE4D inhibition can lead to reduced amyloid-β synthesis and increased amyloid-β degradation (Xu, 2022). The interesting finding that PDE4D isoform expression is altered in AD should be seen as a first step as certain limitations in the associated study setup described in **Chapters 3** and **4** have to be considered. Importantly, since homogenized human and mouse

brain tissues were used in **Chapters 3** and **4** respectively, information regarding cell-type specific expression or even intracellular localization of PDE4D isoforms could not be determined. The yielded findings using homogenized tissues thus demonstrate the overall changes in PDE4D expression across many cells of different lineage; future studies could determine changes in expression, function, and intracellular localization of PDE4D isoforms in specific cell types. Moreover, PDE4D expression was measured at the mRNA level and can therefore not be directly translated to changes in protein levels or activity. Due to a lack of suitable commercial and non-commercial antibodies and the co-migration of multiple PDE4D isoforms on SDS-PAGE, it is extremely challenging, work intensive and expensive to assess protein expression levels of all specific PDE4D isoforms. Moreover, intracellular PDE4D isoform activity can also be altered via mechanisms independent of expression (e.g. through post-translational modifications as summarized in **Chapter 2**). Nevertheless, the studies described in **Chapters 3** and **4** indicate that certain PDE4D isoforms seem to be affected more or seem to be more important than others in the context of AD.

PDE4D isoforms in the regulation of neuronal plasticity

Concurrent with altered PDE4D isoform expression, aberrant cAMP-PKA-CREB signaling was observed in the hippocampus of transgenic AD mice (**Chapter 4**), which will negatively impact neuroplasticity processes like neurite outgrowth (Batty et al., 2017; Mingorance-Le Meur and O'Connor, 2009). To validate the modulating role of PDE4D in regulating neuroplasticity, the effect of the PDE4D-selective inhibitor GEBR32a on neurite outgrowth was assessed in neuronal cell lines. In both a neuroblastoma (N2a) and hippocampal (HT22) cell line, exposure to GEBR32a elicited a concentration-dependent increase in neurite length (**Chapter 4**). Although it is convincing that GEBR32a can inhibit PDE4D based on the observations in this thesis and prior reports (Brullo et al., 2016; Cavalloro et al., 2020; Prosdocimi

et al., 2018; Ricciarelli et al., 2017), its selectivity towards PDE4D may not apply to studies using mice and murine cell lines. The putative binding mode by which GEBR32a achieves its PDE4D-selectivity involves an interaction with a PDE4D-specific phenylalanine present in the UCR2 region of long PDE4 isoforms (Cavalloro et al., 2020; Prosdocimi et al., 2018); PDE4A, -4B, and -4C, have a tyrosine instead. However, this phenylalanine residue represents a polymorphism that is present in primates, but not in mice (Burgin et al., 2010; Johnson et al., 2010). Therefore, PDE4D-selective binding of GEBR32a through interactions with a phenylalanine in UCR2 can likely not be achieved in murine cells like N2a and HT22 cells. It thus remains to be validated whether GEBR32a acts as a PDE4D-selective inhibitor in mice and murine cells. However, using a CRISPR-mediated genetic knockdown approach, the role of individual PDE4D isoforms in the regulation of neurite growth could be assessed in these murine cells (**Chapter 4**). It was found that all long PDE4D isoforms that are expressed in HT22 cells are involved in neurite growth regulation (i.e. PDE4D3, -D5, -D7, and –D9)(Paes et al., 2023). Specifically, genetic knockdown of these isoforms promoted neurite outgrowth and could protect against the neurotoxic, neurite-shortening effects of amyloid-β. Interestingly, knockdown of PDE4D3 or PDE4D9 could completely overcome the neurotoxic effects of amyloid-β on neurite growth and even induced longer neurites in those cells when compared to cells not exposed to amyloid-β. Thus, ablation of specific long PDE4D isoforms can promote plasticity in neurons *in vitro*. It remains to be determined whether inhibition or genetic ablation of these specific isoforms improves neuroplasticity *in vivo* as well. Since neuroplasticity is a result of the spatiotemporal interaction of different cell types (e.g., neurons, astrocytes, microglia, and oligodendrocytes), it remains to be determined if the net effect of PDE4D isoform inhibition in different cell types will yield a functional improvement in neuroplasticity depending on the role of these PDE4D isoforms in other cell types.

Moreover, while genetic knockdown experiments indicate a clear involvement of specific long PDE4D isoforms in neuronal plasticity, it is not clear if these isoforms regulate the same cellular process. Isoform-specific adaptor proteins result in a distribution of isoforms to distinct intracellular compartments (**Chapter 2**, (Boczek et al., 2019a; Boczek and Kapiloff, 2020; Clister et al., 2019; Paes et al., 2021)). Based on this distinct localization, different PDE4D isoforms likely influence cAMP signaling in different compartments, while all long isoforms regulate neurite growth. Considering that different long PDE4D isoforms may regulate neurite growth in different compartments or signaling domains, it remains to be investigated whether simultaneous knockdown of more than one expressed long isoforms has an additive effect on promoting neurite growth. As mentioned for ablating a single isoform, the effect of inhibiting multiple isoforms on general neuroplasticity remains to be validated taking into account the different roles PDE4D isoforms play in different cell types.

Furthermore, the genetic knockdown experiments presented in this thesis have looked into relatively acute effects on neuroplasticity. In general, changes in intracellular signaling are followed by compensatory mechanisms to 'reset' the system. This principle also applies to PDE4-mediated signaling. The cAMP-PKA-CREB signaling axis, which would be stimulated upon PDE4(D) inhibition, regulates the transcription of several PDE4 isoforms (Le Jeune et al., 2002; Seybold et al., 1998; Swinnen et al., 1989). Inhibition of PDE4(D) can consequently induce cAMP-mediated compensatory mechanisms that would counteract the effects of the initial PDE4(D) activity inhibition. Therefore, in addition to the acute PDE4D isoform knockout experiments reported here, the chronic effects of PDE4D isoform knockout await to be determined. Of note in this respect, as PDE4 inhibition is known to have anti-inflammatory effects in different organs (Li et al., 2018), chronic PDE4(D) inhibition may also dampen neuro-inflammation in the AD brain which may actually contribute to overall therapeutic, memory-enhancing or memory-restoring effects.

Considering isoform-specific PDE4 activity dynamics

In addition to transcription-based feedback, cAMP signaling is also dynamically regulated by a feedback mechanism at the protein level. More precisely, upon increasing cAMP levels, the downstream kinase protein kinase A (PKA) is activated which subsequently can phosphorylate and thereby enhance the enzymatic activity of long PDE4 isoforms specifically. By means of increased cAMP hydrolysis by these activated long PDE4 isoforms, elevated cAMP levels can be restored to baseline concentrations. Enzymatic activity modulation through, for example, phosphorylation by PKA, enables the dynamic control of cAMP levels by PDE4. As outlined in **Chapter 2**, several post-translational modifications like phosphorylation by PKA or interactions with other proteins can influence the enzymatic activity of specific PDE4(D) isoforms. As PDE4 activity regulation is a dynamic process as a result of positive and negative feedback loops, experimental investigation of the influence of isoform types on cAMP signaling using molecular biology techniques can be difficult. Therefore, a computational model was established to investigate the involvement of (activity modulation of) the different PDE4 isoform types in controlling cAMP levels (**Chapter 5**) (Paes et al., 2022). Taking into account the different proportions by which long, short, and supershort isoforms may be present, the simulations of the computational model indicated that long PDE4 isoforms exert the most profound control on cAMP signaling. The prominent effect of long isoforms is likely a result of the fact that their enzymatic activity is considerably increased upon phosphorylation by PKA. Consequently, inhibition of long isoforms specifically will yield the most substantial increase in cAMP levels. Thus, long PDE4(D) isoforms may be the most interesting pharmacological targets from a therapeutic perspective.

While a computational model can provide great insights into dynamic processes that are hard to disentangle in a biological system, a model is inherently limited to the parameters that are being considered. Several factors that are known to shape cAMP signaling and its control by PDE4 enzymes were not included in the

model described in this thesis. Firstly, PDE4 subtypes, PDE4 isoform types, and specific PDE4 isoforms within these type categories localize to specific intracellular compartments rather than exhibiting a homogeneous distribution throughout the cell (Anton et al., 2022; Blackman et al., 2011). Secondly, while the effects of phosphorylation by PKA and ERK on PDE4 activity are most extensively studied and included in the model, the effects other modulators of (isoform-specific) PDE4 enzymatic activity as listed in **Chapter 2** were not simulated. Lastly, current simulations have only considered cAMP signaling during a relatively short timescale (i.e. several minutes). Other feedback mechanisms that occur at a larger timescale like the aforementioned transcription-based feedback of upregulation PDE4 isoforms are therefore not considered yet. Thus, as computational models become better in simulating the spatiotemporal control of cAMP signaling by PDE4 subtypes and isoforms based on increasing knowledge of the localization, activity and cell-type specific expression of these enzymes, these *in silico* approaches can provide a useful way to define new or better-specified therapeutic targets.

Long PDE4D isoforms as suitable therapeutic targets

Several lines of evidence presented in this thesis indicate that specific targeting of long PDE4D isoforms provides an effective therapeutic strategy to promote neuroplasticity in the context of AD. A pivotal role for long isoforms in regulation neuroplasticity is supported by prior studies. It has been shown that inhibition of high-affinity rolipram binding sites (HARBS), which are predominantly provided by long isoforms, enhances neurite outgrowth and spatial memory (Boomkamp et al., 2014; Egawa et al., 1997). In addition, pharmacological and shRNA-based inhibition of long PDE4D isoforms has been demonstrated to improve memory function (Li et al., 2011; Ricciarelli et al., 2017; Zhang et al., 2018). Based on abovementioned mRNA expression analyses, the long isoforms PDE4D3 and PDE4D5 were found to be upregulated in hippocampal cells exposed to amyloid-β, transgenic

mouse brains showing amyloid-β pathology as well as in post-mortem human brain tissue of AD patients. Moreover, in these human brain samples, epigenetic signatures in the PDE4D3 and PDE4D5 promoters were found to be altered, which supports the observation of altered transcription. Moreover, through the use of isoform-specific CRISPR-Cas9 knockdown experiments, specific long PDE4D isoforms were found to regulate neurite length in mouse hippocampal neurons. Genetic knockdown of only those long PDE4D isoforms that were expressed by these cells led to a significant increase in neuronal plasticity (i.e. PDE4D3, -D5, -D7, and -D9). Provided the pivotal role of long PDE4 isoforms in regulating cAMP signaling, as validated using a computational model, inhibiting these forms will likely exert the most profound therapeutic effect. The question remains which of these long isoforms poses the ideal therapeutic target. An important aspect is that the exact involvement of these long PDE4D isoforms in PDE4-associated side effects remains to be determined. However, based on PDE4D isoform expression analysis presented in **Chapter 4**, it is clear that not all long PDE4D isoforms that regulate neuronal plasticity are expressed in the mouse stomach and therefore likely do not mediate peripherally regulated gastro-intestinal side effects upon systemic PDE4(D) inhibition. Specifically, PDE4D7 and PDE4D9 are not highly expressed in the mouse stomach, while their genetic ablation does improve neuronal plasticity.

Looking into the robustness of findings, for several reasons, PDE4D3 may be the isoform to investigate in detail first. Firstly, PDE4D3 consistently showed increased expression within the human temporal lobe and mouse hippocampus and frontal cortex tissue displaying amyloid-β pathology and mouse hippocampal neurons exposed to amyloid-β. In fact, PDE4D3 expression correlated most strongly with levels of AD pathology and cognitive decline in the human material. Secondly, genetic PDE4D3 knockdown had the most profound effect on stimulating neurite outgrowth in mouse hippocampal cells and this knockdown could fully counter the neurite-shortening effect of amyloid-β exposure. Thirdly, in different experimental

setups, Boczek et al. found that disrupting PDE4D3 from its perinuclear compartment resulted in enhanced neuronal survival and increased neurite outgrowth (Boczek et al., 2019b). Thus, PDE4D3-specific targeting may be an efficacious approach to stimulate neuroplasticity. However, as mentioned, side effects may still arise and, in particular for PDE4D3, cardiac side effects could occur considering the role of PDE4D3 in regulating ryanodine receptor functioning in the heart (Lehnart et al., 2005). Next to PDE4D3, PDE4D7 may be of interest as its role in gastro-intestinal side effects may be limited considering relatively low expression in the mouse stomach (**Chapter 4**) and in neurons of the human area postrema, which is involved in the central regulation of emesis (Vanmierlo, 2019). Moreover, the increase in enzyme activity upon phosphorylation by PKA is higher for PDE4D7 than any other long PDE4D isoform (Richter et al., 2005). This may imply that the relatively largest cAMP increase can be induced by inhibiting PDE4D7, considering equal expression of long isoforms.

Inhibitors selective for long PDE4D isoforms

Irrespective whether inhibition of PDE4D3, PDE4D7, other long isoforms, or all long PDE4D isoforms contributes to the side effects observed upon non-specific PDE4 inhibition, targeting of long PDE4D isoforms may enhance therapeutic efficacy. The target specification towards specific isoforms has important implications for drug development. In order to develop PDE4 inhibitors that are selective towards the PDE4D subtype and long isoforms specifically, the sequence differences among subtypes and isoforms categories can be exploited (Blokland et al., 2019; Burgin et al., 2010; Paes et al., 2021). Because of their sequence, long PDE4D isoforms can dimerize which results in the capping of the regulatory UCR2 domain of one monomer across the catalytic domain of the other monomer (Cedervall et al., 2015; Houslay and Adams, 2010). Because of this configuration, specific amino acid residues of UCR2 extend into the catalytic domain with which inhibitor molecules can

interact to achieve specificity towards long isoforms. In fact, this trans-capping can be modulated when long isoforms are phosphorylated by PKA, which results in conformational changes that actually can increase the affinity of UCR2-engaging inhibitors (**Chapter 2, Table 4**). With long forms exerting most profound control on cAMP levels, UCR2-engaging long form inhibitors will create a positive feedback loop regarding their binding as the inhibition causes PKA activation, which in turn changes the enzyme conformation to promote inhibitor binding. However, it has also been described that as a result of dimerization, which is specific to long isoforms, UCR2-engaging inhibitors cannot achieve complete inhibition, as binding of the inhibitor to one monomer changes the enzyme's conformation which prevents proper inhibition of the other monomer (Burgin et al., 2010; Cedervall et al., 2015). As such, according to their binding mode, these types of inhibitor can be regarded as UCR2-engaging, long form-specific, PKA-activated specific, partial inhibitors.

While exploitation of these long form-specific structural features allows the development of long form-specific inhibitors, PDE4D selectivity is not yet achieved in this manner. However, as mentioned earlier, primates express a phenylalanine in the transcapping UCR2 region of PDE4D as opposed to a tyrosine for PDE4A, -4B, and -4C. Non-primate mammals express a tyrosine for all four PDE4 subtypes. Hence, inhibitors that specifically engage with this PDE4D-specific phenylalanine can achieve PDE4D selectivity (for primate PDE4 enzymes). This concept is described in detail by Burgin et al. and has led to the development of a PDE4D-selective inhibitor preferentially binding long isoforms. This molecule, called D159797, BPN14770 or Zatolmilast has been tested for its neuroplasticity-enhancing and memory-improving effects in *in vitro* and (pre)clinical *in vivo* studies (Berry-Kravis et al., 2021; Cui et al., 2019; Sutcliffe et al., 2014; Wang et al., 2020b; Zhang et al., 2018)[NCT03817684]. Although PDE4D inhibition has been associated with severe side effects through actions in brainstem areas like the area postrema that regulate emesis, this PDE4D-selective inhibitor did not show any adverse effects in behavioral

correlate measures of emetic behavior in humanized PDE4D mice at doses 300-fold higher than the therapeutic dose (Zhang et al., 2018). These humanized PDE4D mice express the human PDE4D sequence with a phenylalanine instead of tyrosine in the UCR2 region, which allows the engagement of PDE4D-specific inhibitors to exploit phenylalanine-dependent binding. In primates, emetic side effects were observed at orally administered doses of 1.5 mg/kg (Sutcliffe et al., 2014), which can be extrapolated to an emetic dose of 0.32 mg/kg for a human adult weighing 60 kg (Reagan-Shaw et al., 2008). Accordingly, administrating 19.2 mg in humans is expected to be emetic, but a Phase I clinical study using BPN14770/zatolmilast showed no adverse effects upon administration of doses up to 40 mg, though at 100 mg vomiting was observed ([NCT02840279], https://www.alzforum.org/news/conference-coverage/running-trial-results-ctad-conference). The use of BPN14770 as pharmacological intervention against AD-associated memory deficits was further investigated in a Phase II clinical trial [NCT03817684]. While experimental outcomes have not been disclosed at the time of writing (August 2022), a press release indicated that, although no clinically significant safety issues were observed, no significant improvement in the primary endpoint, i.e. the composite score of the neuropsychological test battery RBANS-DMI, was observed at a dose of 25 mg (twice daily) in this clinical trial (https://www.shionogi.com/global/en/news/2020/05/20200526.html). The absence of safety issues is in accordance with recent studies looking into the role of PDE4 subtypes in gastro-intestinal side effects associated with PDE4 inhibition. The Richter laboratory indicated that inhibition of more than one subtype will elicit specific side effects (i.e. gastroparesis and hypothermia) but that subtype-selective inhibition will not (Boyd et al., 2021; McDonough et al., 2020). Thus, the inability of meeting the primary endpoint in the Phase II trial using BPN14770 likely resulted, despite seeming target engagement (Wakabayashi et al., 2020), from a lack of efficacy rather than due

to adverse side effects. The question remains whether this lack of efficacy would be a compound-specific or mechanism-dependent effect.

Other PDE4D-selective compounds have been developed and are reported to enhance neuroplasticity and memory processes (e.g., V11294, GEBR7b and GEBR32a)(Brullo et al., 2014; Brullo et al., 2016; Bruno et al., 2011; Cavalloro et al., 2020; Gale et al., 2003; Gale et al., 2002; Prosdocimi et al., 2018; Ricciarelli et al., 2017)**(Chapter 4)**. It still remains to be determined whether different classes of molecules will show efficacy without side effects in clinical trials. Nevertheless, in preclinical studies, GEBR32a did not induce emetic-like behavior for doses 1000-fold higher than the memory-enhancing dose (Ricciarelli et al., 2017). Compound-specific effects could involve suboptimal dosing regimens, while mechanism-dependent effects may relate to the inability of UCR2-engaging long form PDE4(D) inhibitors to achieve full inhibition as outlined above. Importantly, different classes of PDE4(D) inhibitors may have additional PDE4(D)-independent actions based on their specific pharmacophores.

Interestingly, GEBR32a shows structural similarities to the clinically used anti-Alzheimer drug donepezil. Donepezil is regarded mainly as an acetylcholinesterase inhibitor but it also acts a potent agonist of the σ_1-receptor (Ishikawa et al., 2009; Solntseva et al., 2014). Moreover, the structural resemblance between donepezil and GEBR32a is also seen for the selective σ_1-receptor agonist SA4503 or cutamesine (**Figure 1A**). Based on this structural similarity, GEBR32a may, like donepezil and SA5403, bind σ_1-receptors. Molecular docking of GEBR32a, donepezil, and SA5403 in a crystal structure of the σ_1-receptor reveals a potential similar binding mode for all three compounds (**Figure 1B-C**). Interestingly, a central nitrogen atom that is reported to be crucial for σ_1-receptor binding is present in each compound and (almost) overlays (Bolshakova et al., 2016). Intriguingly, GEBR32a's memory-enhancing effects may thus be due to PDE4(D) inhibition and potentially additional effects such as σ_1-receptor activation. Agonism of the σ_1-receptor by donepezil and

SA5403 can promote neurite outgrowth (Ishima et al., 2008; Li et al., 2017); observations that were also described in **Chapter 4** for GEBR32a. Thus, while still speculative and to be investigated, the neuronal plasticity enhancement by GEBR32a may, in addition to its inhibitory effect on PDE4(D), be induced by activation of σ_1-receptor.

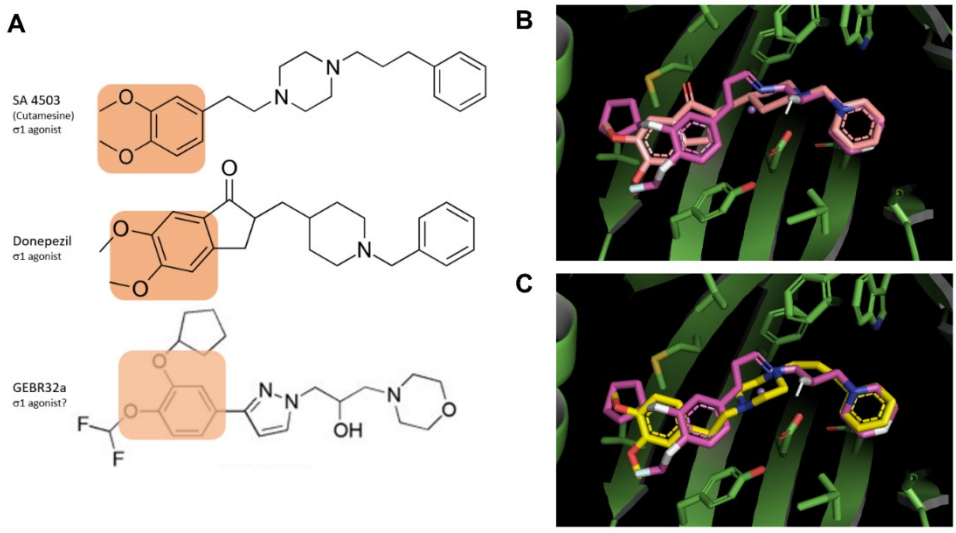

Figure 1. Structural comparison of GEBR32a with σ_1-receptor agonists. A) Chemical structures of SA4503 (cutamesine), donepezil and GEBR32a with their 3,4-dialkoxyphenyl moiety indicated in the orange square. B) Binding poses of GEBR32a (purple) and donepezil (pink) in a crystal structure of the σ_1-receptor based on molecular docking. Striking is the overlay of the rings of both GEBR32a and donepezil and close proximity of the central nitrogen atom. C) Binding poses of GEBR32a (purple) and SA4503/cutamesine (pink). Striking is the overlay of the central nitrogen atom and rings of both GEBR32a and SA4503.

Considering the effects of PDE4D inhibition in different brain regions

In general, while the role of PDE4(D) in neuroplasticity processes has been reported in a substantial amount of scientific literature as mentioned above, its effects on human cognition, and especially in an AD context, has not been thoroughly explored. A possible explanation of the relative lack of efficacy of BPN14770 in AD is the fact that global PDE4D inhibition in multiple brain regions simultaneously may have less potent cognition-enhancing effects than local PDE4D

inhibition in, for example, the hippocampus specifically. Linked to this, the work of the Arnsten laboratory has indicated that PDE4D expression during aging in the frontal cortex of rats actually decreases, which is concurrent with increased phosphorylation of tau protein, which could promote AD-associated pathology, and worsen working memory (Leslie et al., 2020). Consequently, in elderly subjects, PDE4D inhibition may improve hippocampus-dependent memory processes while impairing frontal cortex-based functions like working memory. Importantly, across different brain regions, intracellular localization of PDE4D and its isoforms may be differentially regulated. For example, PDE4D can localize presynaptically at hippocampal pyramidal neurons (Montenegro-Venegas et al., 2022), whilst PDE4D is localized predominantly postsynaptically, at pyramidal neurons in the prefrontal cortex (Datta et al., 2020). The region-specific localization of PDE4D may result from a difference in expression of PDE4D-binding partner proteins (as summarized in **Chapter 2**) across regions. PDE4D may be localized presynaptically to modulate cAMP levels that regulate plasticity-promoting hyperpolarization-activated cation channel signaling (Beaumont and Zucker, 2000), while postsynaptic PDE4D can modulate synaptic plasticity through, for example, cAMP-PKA-CREB signaling (Kandel, 2012). Thus, PDE4D inhibition may have to be regional to exert sufficiently potent therapeutic effects.

Different strategies can be explored to achieve this increased spatial specificity. Firstly, assuming most memory-enhancing effects of PDE4D inhibition are exerted in the hippocampus, PDE4D isoforms that are specifically enriched in this brain region could be targeted. For example, **Chapter 4** described that PDE4D8 is highly expressed in the mouse hippocampus, but not in the frontal cortex, nor in the mouse neuronal HT22 cell line. As such, its hippocampal expression may be a result of expression in non-neuronal cell types. Whether targeting PDE4D8 could provide a means to establish hippocampus-specific and plasticity-enhancing PDE4D inhibition remains to be determined. As described above, it is possible to develop

inhibitors that exploit binding to conformational states that are specific to long isoforms but targeting one long isoform specifically (e.g., PDE4D8) cannot be achieved using this rationale. Interestingly, the highly localized cAMP-hydrolyzing actions of specific PDE4D isoforms can be deregulated by means of disrupting protein-protein interactions of the specific isoform and its partner protein(s) (Baillie et al., 2019; Lee et al., 2013). The potential of this approach has been demonstrated *in vivo* as well (Martin et al., 2014). However, the interactome of distinct PDE4D isoforms is currently incomplete and partner proteins may be cell type-specific and context-specific. Thus, while providing high spatial specificity within cells, the precise interaction that is to be disrupted remains to be verified.

Secondly, increased spatial specificity of pharmacological targeting can be achieved by using synergistic interventions that both act on regionally expressed targets. More concretely, the synergism of two treatments minimizes the induction of side effects by one of the treatments in 'off-target areas' as, owing to the synergism, lower concentrations for each of the treatments are required. Consequently, effects are conditional on both targets being expressed in the brain region where therapeutic effects should be elicited.

Synergistic PDE inhibition to achieve more localized therapeutic effects without side effects

The concept of synergistic PDE inhibition to promote neuronal plasticity and memory consolidation was described in **Chapter 6**. Here, the synergistic effects of PDE4 and PDE2 inhibition in neuronal plasticity processes *in vitro* and memory consolidation *in vivo* were validated (Paes et al., 2020b). While these data robustly show that synergistic PDE4 and PDE2 inhibition can improve memory processes, the ability to translate *in vitro* to *in vivo* findings in these type of studies should be addressed. Specifically, the potential mismatch between inhibitor concentrations and doses used in *in vitro* and *in vivo* assays, respectively, requires discussion. In **Chapter**

6, the half-maximum inhibitory concentrations (IC_{50}) of the PDE4 inhibitor roflumilast and PDE2 inhibitor PF-05180999 are reported to be 0.234 nM and 0.440 nM respectively, while the 1 µM concentrations used to investigate AMPA receptor GluR1 subunit phosphorylation in brain slices were >2000-fold higher.

This apparent discrepancy in functional concentrations can be attributed to several factors. Firstly, the reported IC_{50} values usually are reported on the compound's ability to inhibit the activity of purified enzymes rather than enzymes in a cell context. As outlined in **Chapter 2** and summarized in that chapter's **Table 1**, several post-translational modifications and protein partner interactions can influence PDE4 enzyme activity and inhibitor affinity (Paes et al., 2021). Since these modifications and interactors are not present in inhibitor affinity assays using purified enzymes, these assays cannot accurately reflect affinities of PDE4 inhibitors in cells. Moreover, the purified PDE4 that is used in these assays often comprises a single PDE4 subtype and often only considers the PDE4 catalytic domain. As elaborately outlined in **Tables 2-4** of **Chapter 2**, PDE4 inhibitors can exhibit distinct affinities towards different PDE4 subtypes and especially show different binding to full-length enzymes compared to catalytic domains only (Paes et al., 2021). Abovementioned arguments are supported by experimental evidence as described by Wunder and colleagues (Wunder et al., 2013). In their study, it was found that IC_{50} values for roflumilast were 89-fold higher in cell-based assays compared to IC_{50} values determined using purified enzymes. Similar observations were done for other PDE4 inhibitors. Interestingly, the ratio between cellular and purified enzyme IC_{50} values seems to depend on the binding modes of PDE4 inhibitors in the catalytic domain as the conformation-dependent, UCR2-engaging PDE4 inhibitors tested actually show lower IC_{50} values in cells compared to purified enzymes. This suggests that PDE4 enzymes may adopt distinct conformations in the different assays which can favor binding of either UCR2-engaging or purely catalytic domain-binding inhibitors. Secondly, although relatively high concentrations have been applied

extracellularly, functional concentrations in the relevant intracellular PDE2 and PDE4 signaling microdomains may be lower depending on cell penetrance and intracellular diffusion. Thirdly, it is important to consider the specific experimental setup and its associated cellular signaling when determining PDE4 inhibitor concentrations that induce a particular effect. For the experiments using brain slices described in **Chapter 6**, cAMP signaling was not promoted by any exogenous trigger (e.g. cAMP synthesis stimulation by forskolin). Thus, in the absence of high levels of cAMP, their breakdown can also not be prevented by inhibition of PDE2 and/or PDE4. In order to elicit cellular effects downstream of cAMP-PKA signaling in the absence of signals triggering this cascade, profound inhibition of PDE2 and PDE4 is required to elevate basal cAMP levels. This would require higher levels of the corresponding inhibitors. However, as indicated by the cell-based experiments in **Chapter 6**, in the absence of forskolin, even relatively high concentrations of roflumilast and/or PF-05180999 (i.e. 1 µM) could not significantly stimulate CRE-mediated transcription. Lastly, despite the use of relatively high concentrations of roflumilast and/or PF-05180999, conclusions on the involved mechanisms can still be drawn as long as the selectivity of their inhibition can be guaranteed. Encouragingly, roflumilast and PF-05180999 exhibit >1000-fold selective binding towards respectively PDE4 and PDE2 compared to other PDE families (Hatzelmann et al., 2010; Helal et al., 2017). It is therefore unlikely that these compounds exerted effects through other targets than PDE4 and PDE2.

While the abovementioned factors can help explain the discrepancy between the IC_{50} values of roflumilast and PF-05180999 and the functional concentrations required to elicit effects in cells, the translation of IC_{50} values to therapeutic doses *in vivo* is even more complex. Taking into account the ability of roflumilast and PF-05180999 to be bound to plasma albumin and their brain penetrance, it is obvious that IC_{50} values derived from enzyme kinetic assays cannot accurately be extrapolated to *in vivo* settings. *In vivo*, a compound's net effect will also be

dependent on its affinity towards different isoforms and the relative expression ratio of these isoforms in the cells that are to be targeted. Moreover, determining free fractions of inhibitors in the brain may not reflect the compound concentration that is able to bind targets, but may rather reflect the compound concentration that is not (yet) bound to the target.

Thus, taking into account the difficulties in translating functional *in vitro* compound concentrations to *in vivo* doses, assays should be performed at the enzyme, cell, brain region, and organism level to properly validate the therapeutic potential of a treatment strategy. The studies described in **Chapter 6** robustly showed that PDE4 and PDE2 inhibition using suboptimal doses for each compound acts synergistically to promote cellular neuroplasticity processes and memory consolidation. The potential of synergistically acting treatments is supported by the pro-cognitive effects of synergistic PDE4 and PDE5 inhibition as reported by Gulisano and co-workers (Gulisano et al., 2018). As PDEs from different gene families show different intracellular distribution patterns, relatively subtle inhibition of two different types (e.g., PDE4 and PDE2 or PDE4 and PDE5) may promote a broader and/or prolonged cAMP diffusion in the cells to elicit downstream signaling responses. While the memory-enhancing effects of combined PDE4 and PDE5 inhibition have been validated after chronic treatment in a transgenic AD model (Gulisano et al., 2018), the synergistic actions of PDE4 and PDE2 inhibition presented here were only investigated upon acute exposure in wild-type mice. Thus, it remains to be verified whether these acute effects can be extrapolated to chronic treatments in an AD context.

Looking ahead

In light of the findings and conclusions described above, future experiments and "backup plans" can be devised. Important next steps would be to determine what the effects are of chronic knockdown of PDE4D (long) isoforms on neuronal

plasticity and whether knockdown of multiple (long) PDE4D isoforms has additive effects. Crucial would be the comparison of cell-type specific, region-specific and brain-general PDE4D knockdown and elucidating which PDE4D isoforms are involved in side effects mediated by either the brainstem and/or gastrointestinal organs. The function and intracellular localization of individual isoforms in specific cell types could be investigated using isoform knockdown or dominant-negative PDE4 isoforms coupled with the use of FRET-based cAMP sensors to determine isoform-regulated cAMP nanodomains (Bock et al., 2020; Bolger et al., 2020). These experiments should provide additional insights into the PDE4D isoforms that should be targeted for a more efficacious and/or safer treatment. While both strategies outlined in the thesis (i.e. more specific targeting of PDE4 subtypes or isoforms and synergistic inhibition of PDE4 and another PDE type) can be investigated further to treat memory problems in AD, additional promise could lay in combining these strategies. This would mean that a PDE4 inhibitor specific towards certain subtypes/isoforms (e.g., the PDE4D-selective inhibitor GEBR32a) can be combined with an inhibitor of another PDE type (e.g., the PDE2 inhibitor PF-05180999). This combination will minimize off-target effects by using a more selective PDE4 inhibitor and, owing to the synergistic actions, lower doses of each inhibitor are required, which will minimize the occurrence of side effects. Although it is to be expected, it remains to be validated experimentally whether synergistically acting treatments are less likely to evoke side effects. In addition to combining two PDE-inhibiting compounds that have synergistic actions, single molecules can be explored further that have dual actions on PDE4 and another target. For example, molecules have been described that can inhibit both PDE4 and acetylcholinesterase (AChE) enzymes (Liu et al., 2022). As most of the clinically used AD medication belongs to the class of AChE inhibitors (i.e. donepezil, galantamine, and rivastigmine; see **Chapter 1**), therapeutic effects of dual PDE4/AChE are to be expected. Dual PDE4/AChE inhibitors can potently increase intracellular cAMP signaling by simultaneously elevating

extracellular acetylcholine levels, which can promote cAMP synthesis, and inhibiting PDE4-mediated cAMP breakdown. This synergistic mechanism may require lower doses, which could translate to a lower likelihood of side effects. It is interesting to envision drug development/optimization efforts of dual PDE4/AChE inhibitors to achieve PDE4 subtype selectivity while retaining AChE inhibitory actions. Importantly, as the use of AChE inhibitors is associated with side effects that overlap with those observed for PDE4 inhibitors (i.e. nausea, emesis, diarrhea) (Imbimbo, 2001), the safety of dual PDE4/AChE inhibitors should be examined.

Generally, side effects associated with the use of PDE4 inhibitors are arguably the main reason PDE4 inhibitors are not yet clinically used for the treatment of AD. Thus, efforts should be taken to minimize or prevent PDE4-mediated side effects. Next to the approaches undertaken in this thesis, other strategies can be further explored to reduce side effects. By formulating the prototypical PDE4 inhibitor rolipram with fusogenic lipid vesicles, Gobejishvili et al. decreased rolipram's ability to cross the blood-brain barrier, which was concurrent with a reduction in emetic-like behavior in mice (Gobejishvili et al., 2022). Since therapeutic actions of PDE4 inhibitors are required in the brain as well, this strategy cannot be pursued for the treatment of AD. Interestingly, the PDE4 inhibitor LEO-29102 has low emetic potential and was designed as a 'soft drug', which means that it creates few, long-lasting, metabolites (Felding et al., 2014). LEO-29102, formulated as a cream, has been tested in a Phase II clinical trial for the treatment of atopic dermatitis [NCT01037881]. It remains to be determined whether the low emetogenicity of LEO-29102 is related to the route of administration and whether administration routes that optimize brain exposure would not result in side effects, despite the rapid metabolism of the compound. Furthermore, LEO-29102 interacts with amino acids in the C-terminus of PDE4 that are conserved across PDE4 subtypes as opposed to PDE4(D) long-form, UCR2-enganging inhibitors that have shown to be efficacious in

stimulating neuroplasticity. Thus, considering its different binding mode, its subtype-selectivity and efficacy await to be examined.

As recent reports by the Richter laboratory have indicated that subtype-selective PDE4 inhibition can prevent certain PDE4-mediated side effects, subtype-specific inhibition rather than PDE4D-selective inhibition may be sufficient to reduce side effects. While inhibition of PDE4D rather than PDE4B seems to exert the most profound memory-enhancing effects (Zhang et al., 2017), the precise role of non-PDE4D subtypes and isoforms in molecular memory mechanisms that are affected in AD remain to be fully explored experimentally. Similarly, PDE4 is not the only cAMP-selective PDE. Provided the pivotal role of cAMP-PKA-CREB signaling in memory formation, other cAMP-selective PDEs and their isoforms provide novel therapeutic targets. As a proof-of-principle, we have shown that PDE7 inhibition also promotes spatial memory consolidation (McQuown et al., 2021). Thus, the same target-specifying strategies as described in this thesis can be applied to other cAMP-modulating therapeutic targets.

All in all, the work in this thesis shows that more specific targeting of PDE4D isoforms can retain the therapeutic neuroplasticity-enhancing effects that are observed upon non-selective PDE4(D) inhibition. Moreover, synergistic inhibition of PDE4 and PDE2 shows therapeutic potential and likely reduces side effects as lower doses of each of the inhibitors are required. Thus, new strategies have been validated that provide new avenues to optimize PDE4-inhibiting strategies with improved efficacy and/or safety for the treatment of memory deficits in AD.

REFERENCES

Anton SE, Kayser C, Maiellaro I, Nemec K, Möller J, Koschinski A, Zaccolo M, Annibale P, Falcke M, Lohse MJ and Bock A (2022) Receptor-associated independent cAMP nanodomains mediate spatiotemporal specificity of GPCR signaling. *Cell* **185**:1130-1142.e1111.

Baillie GS, Tejeda GS and Kelly MP (2019) Therapeutic targeting of 3',5'-cyclic nucleotide phosphodiesterases: inhibition and beyond. *Nat Rev Drug Discov* **18**:770-796.

Batty NJ, Fenrich KK and Fouad K (2017) The role of cAMP and its downstream targets in neurite growth in the adult nervous system. *Neuroscience Letters* **652**:56-63.

Beaumont V and Zucker RS (2000) Enhancement of synaptic transmission by cyclic AMP modulation of presynaptic Ih channels. *Nat Neurosci* **3**:133-141.

Berry-Kravis EM, Harnett MD, Reines SA, Reese MA, Ethridge LE, Outterson AH, Michalak C, Furman J and Gurney ME (2021) Inhibition of phosphodiesterase-4D in adults with fragile X syndrome: a randomized, placebo-controlled, phase 2 clinical trial. *Nature medicine* **27**:862-870.

Blackman BE, Horner K, Heidmann J, Wang D, Richter W, Rich TC and Conti M (2011) PDE4D and PDE4B function in distinct subcellular compartments in mouse embryonic fibroblasts. *J Biol Chem* **286**:12590-12601.

Blokland A, Heckman P, Vanmierlo T, Schreiber R, Paes D and Prickaerts J (2019) Phosphodiesterase Type 4 Inhibition in CNS Diseases. *Trends Pharmacol Sci* **40**:971-985.

Bock A, Annibale P, Konrad C, Hannawacker A, Anton SE, Maiellaro I, Zabel U, Sivaramakrishnan S, Falcke M and Lohse MJ (2020) Optical Mapping of cAMP Signaling at the Nanometer Scale. *Cell* **182**:1519-1530.e1517.

Boczek T, Cameron EG, Yu W, Xia X, Shah SH, Castillo Chabeco B, Galvao J, Nahmou M, Li J, Thakur H, Goldberg JL and Kapiloff MS (2019a) Regulation of Neuronal Survival and Axon Growth by a Perinuclear cAMP Compartment. *The Journal of neuroscience : the official journal of the Society for Neuroscience* **39**:5466-5480.

Boczek T, Cameron EG, Yu W, Xia X, Shah SH, Castillo Chabeco B, Galvao J, Nahmou M, Li J, Thakur H, Goldberg JL and Kapiloff MS (2019b) Regulation of Neuronal Survival and Axon Growth by a Perinuclear cAMP Compartment. *J Neurosci* **39**:5466-5480.

Boczek T and Kapiloff MS (2020) Compartmentalization of local cAMP signaling in neuronal growth and survival. *Neural Regen Res* **15**:453-454.

Bolger GB, Smoot LHM and van Groen T (2020) Dominant-Negative Attenuation of cAMP-Selective Phosphodiesterase PDE4D Action Affects Learning and Behavior. *Int J Mol Sci* **21**.

Bolshakova AV, Kukanova EO, Gainullina AN, Zhemkov VA, Korban SA and Bezprozvanny IB (2016) Sigma-1 receptor as a potential pharmacological target for the treatment of neuropathology. *St Petersburg Polytechnical University Journal: Physics and Mathematics* **2**:31-40.

Boomkamp SD, McGrath MA, Houslay MD and Barnett SC (2014) Epac and the high affinity rolipram binding conformer of PDE4 modulate neurite outgrowth and myelination using an in vitro spinal cord injury model. *Br J Pharmacol* **171**:2385-2398.

Boyd A, Aragon IV, Rich J, McDonough W, Oditt M, Irelan D, Fiedler E, Abou Saleh L and Richter W (2021) Assessment of PDE4 Inhibitor-Induced Hypothermia as a Correlate of Nausea in Mice. *Biology* **10**.

Brullo C, Massa M, Rocca M, Rotolo C, Guariento S, Rivera D, Ricciarelli R, Fedele E, Fossa P and Bruno O (2014) Synthesis, biological evaluation, and molecular modeling of new 3-(cyclopentyloxy)-4-methoxybenzaldehyde O-(2-(2,6-dimethylmorpholino)-2-oxoethyl) Oxime (GEBR-7b) related phosphodiesterase 4D (PDE4D) inhibitors. *J Med Chem* **57**:7061-7072.

Brullo C, Ricciarelli R, Prickaerts J, Arancio O, Massa M, Rotolo C, Romussi A, Rebosio C, Marengo B, Pronzato MA, van Hagen BTJ, van Goethem NP, D'Ursi P, Orro A, Milanesi L, Guariento S, Cichero E, Fossa P, Fedele E and Bruno O (2016) New insights into selective PDE4D inhibitors: 3-(Cyclopentyloxy)-4-methoxybenzaldehyde O-(2-(2,6-dimethylmorpholino)-2-oxoethyl) oxime (GEBR-7b) structural development and promising activities to restore memory impairment. *Eur J Med Chem* **124**:82-102.

Bruno O, Fedele E, Prickaerts J, Parker LA, Canepa E, Brullo C, Cavallero A, Gardella E, Balbi A, Domenicotti C, Bollen E, Gijselaers HJ, Vanmierlo T, Erb K, Limebeer CL, Argellati F, Marinari UM, Pronzato MA and Ricciarelli R (2011) GEBR-7b, a novel PDE4D selective inhibitor that improves memory in rodents at non-emetic doses. *Br J Pharmacol* **164**:2054-2063.

Burgin AB, Magnusson OT, Singh J, Witte P, Staker BL, Bjornsson JM, Thorsteinsdottir M, Hrafnsdottir S, Hagen T, Kiselyov AS, Stewart LJ and Gurney ME (2010) Design of phosphodiesterase 4D (PDE4D) allosteric modulators for enhancing cognition with improved safety. *Nat Biotechnol* **28**:63-70.

Cavalloro V, Russo K, Vasile F, Pignataro L, Torretta A, Donini S, Semrau MS, Storici P, Rossi D, Rapetti F, Brullo C, Parisini E, Bruno O and Collina S (2020) Insight into GEBR-32a: Chiral Resolution, Absolute Configuration and Enantiopreference in PDE4D Inhibition. *Molecules* **25**.

Cedervall P, Aulabaugh A, Geoghegan KF, McLellan TJ and Pandit J (2015) Engineered stabilization and structural analysis of the autoinhibited conformation of PDE4. *Proc Natl Acad Sci U S A* **112**:E1414-1422.

Cheng Y-F, Wang C, Lin H-B, Li Y-F, Huang Y, Xu J-P and Zhang H-T (2010) Inhibition of phosphodiesterase-4 reverses memory deficits produced by Aβ25–35 or Aβ1–40 peptide in rats. *Psychopharmacology* **212**:181-191.

Clister T, Greenwald EC, Baillie GS and Zhang J (2019) AKAP95 Organizes a Nuclear Microdomain to Control Local cAMP for Regulating Nuclear PKA. *Cell chemical biology* **26**:885-891.e884.

Cui S-Y, Yang M-X, Zhang Y-H, Zheng V, Zhang H-T, Gurney ME, Xu Y and O'Donnell JM (2019) Protection from amyloid β peptide-induced memory, biochemical and morphological deficits by a phosphodiesterase-4D (PDE4D) allosteric inhibitor. *Journal of Pharmacology and Experimental Therapeutics*:jpet.119.259986.

Datta D, Enwright JF, Arion D, Paspalas CD, Morozov YM, Lewis DA and Arnsten AFT (2020) Mapping Phosphodiesterase 4D (PDE4D) in Macaque Dorsolateral Prefrontal Cortex: Postsynaptic Compartmentalization in Layer III Pyramidal Cell Circuits. *Front Neuroanat* **14**:578483.

Egawa T, Mishima K, Matsumoto Y, Iwasaki K, Iwasaki K and Fujiwara M (1997) Rolipram and its optical isomers, phosphodiesterase 4 inhibitors,

attenuated the scopolamine-induced impairments of learning and memory in rats. *Japanese journal of pharmacology* **75**:275-281.

Feng H, Wang C, He W, Wu X, Li S, Zeng Z, Wei M and He B (2019) Roflumilast ameliorates cognitive impairment in APP/PS1 mice via cAMP/CREB/BDNF signaling and anti-neuroinflammatory effects. *Metab Brain Dis* **34**:583-591.

Felding J, Sørensen MD, Poulsen TD, Larsen J, Andersson C, Refer P, Engell K, Ladefoged LG, Thormann T, Vinggaard AM, Hegardt P, Søhoel A and Nielsen SF (2014) Discovery and Early Clinical Development of 2-{6-[2-(3,5-Dichloro-4-pyridyl)acetyl]-2,3-dimethoxyphenoxy}-N-propylacetamide (LEO 29102), a Soft-Drug Inhibitor of Phosphodiesterase 4 for Topical Treatment of Atopic Dermatitis. *Journal of Medicinal Chemistry* **57**:5893-5903.

Gale DD, Hofer P, Spina D, Seeds EA, Banner KH, Harrison S, Douglas G, Matsumoto T, Page CP, Wong RH, Jordan S, Smith F, Banik N, Halushka PV, Cavalla D, Rotshteyn Y, Kyle DJ, Burch RM and Chasin M (2003) Pharmacology of a new cyclic nucleotide phosphodiesterase type 4 inhibitor, V11294. *Pulm Pharmacol Ther* **16**:97-104.

Gale DD, Landells LJ, Spina D, Miller AJ, Smith K, Nichols T, Rotshteyn Y, Tonelli A, Lacouture P, Burch RM, Page CP and O'Connor BJ (2002) Pharmacokinetic and pharmacodynamic profile following oral administration of the phosphodiesterase (PDE)4 inhibitor V11294A in healthy volunteers. *British journal of clinical pharmacology* **54**:478-484.

Gobejishvili L, Rodriguez WE, Bauer P, Wang Y, Soni C, Lydic T, Barve S, McClain C and Maldonado C (2022) Novel Liposomal Rolipram Formulation for Clinical Application to Reduce Emesis. *Drug design, development and therapy* **16**:1301-1309.

Gulisano W, Tropea MR, Arancio O, Palmeri A and Puzzo D (2018) Sub-efficacious doses of phosphodiesterase 4 and 5 inhibitors improve memory in a mouse model of Alzheimer's disease. *Neuropharmacology* **138**:151-159.

Hatzelmann A, Morcillo EJ, Lungarella G, Adnot S, Sanjar S, Beume R, Schudt C and Tenor H (2010) The preclinical pharmacology of roflumilast--a selective, oral phosphodiesterase 4 inhibitor in development for chronic obstructive pulmonary disease. *Pulm Pharmacol Ther* **23**:235-256.

Helal CJ, Arnold EP, Boyden TL, Chang C, Chappie TA, Fennell KF, Forman MD, Hajos M, Harms JF, Hoffman WE, Humphrey JM, Kang Z, Kleiman RJ, Kormos BL, Lee CW, Lu J, Maklad N, McDowell L, Mente S, O'Connor RE, Pandit J, Piotrowski M, Schmidt AW, Schmidt CJ, Ueno H, Verhoest PR and Yang EX (2017) Application of Structure-Based Design and Parallel Chemistry to Identify a Potent, Selective, and Brain Penetrant Phosphodiesterase 2A Inhibitor. *J Med Chem* **60**:5673-5698.

Houslay MD and Adams DR (2010) Putting the lid on phosphodiesterase 4. *Nat Biotechnol* **28**:38-40.

Imbimbo BP (2001) Pharmacodynamic-Tolerability Relationships of Cholinesterase Inhibitors for Alzheimer's Disease. *CNS Drugs* **15**:375-390.

Ishikawa M, Sakata M, Ishii K, Kimura Y, Oda K, Toyohara J, Wu J, Ishiwata K, Iyo M and Hashimoto K (2009) High occupancy of σ1 receptors in the human brain after single oral administration of donepezil: a positron emission tomography study using [11C]SA4503. *International Journal of Neuropsychopharmacology* **12**:1127-1131.

Ishima T, Nishimura T, Iyo M and Hashimoto K (2008) Potentiation of nerve growth factor-induced neurite outgrowth in PC12 cells by donepezil: Role of sigma-1 receptors and IP3 receptors. *Progress in Neuro-Psychopharmacology and Biological Psychiatry* **32**:1656-1659.

Johnson KR, Nicodemus-Johnson J and Danziger RS (2010) An evolutionary analysis of cAMP-specific Phosphodiesterase 4 alternative splicing. *BMC evolutionary biology* **10**:247.

Kandel ER (2012) The molecular biology of memory: cAMP, PKA, CRE, CREB-1, CREB-2, and CPEB. *Mol Brain* **5**:14.

Konrad FM, Bury A, Schick MA, Ngamsri K-C and Reutershan J (2015) The Unrecognized Effects of Phosphodiesterase 4 on Epithelial Cells in Pulmonary Inflammation. *PLOS ONE* **10**:e0121725.

Le Jeune IR, Shepherd M, Van Heeke G, Houslay MD and Hall IP (2002) Cyclic AMP-dependent transcriptional up-regulation of phosphodiesterase 4D5 in human airway smooth muscle cells. Identification and characterization of a novel PDE4D5 promoter. *J Biol Chem* **277**:35980-35989.

Lee LC, Maurice DH and Baillie GS (2013) Targeting protein-protein interactions within the cyclic AMP signaling system as a therapeutic strategy for cardiovascular disease. *Future medicinal chemistry* **5**:451-464.

Lehnart SE, Wehrens XHT, Reiken S, Warrier S, Belevych AE, Harvey RD, Richter W, Jin SLC, Conti M and Marks AR (2005) Phosphodiesterase 4D Deficiency in the Ryanodine-Receptor Complex Promotes Heart Failure and Arrhythmias. *Cell* **123**:25-35.

Leslie SN, Datta D, Christensen KR, van Dyck CH, Arnsten AFT and Nairn AC (2020) Phosphodiesterase PDE4D Is Decreased in Frontal Cortex of Aged Rats and Positively Correlated With Working Memory Performance and Inversely Correlated With PKA Phosphorylation of Tau. *Front Aging Neurosci* **12**:576723.

Li D, Zhang S-Z, Yao Y-H, Xiang Y, Ma X-Y, Wei X-L, Yan H-T and Liu X-Y (2017) Sigma-1 receptor agonist increases axon outgrowth of hippocampal neurons via voltage-gated calcium ions channels. *CNS Neuroscience & Therapeutics* **23**:930-939.

Li H, Zuo J and Tang W (2018) Phosphodiesterase-4 Inhibitors for the Treatment of Inflammatory Diseases. *Front Pharmacol* **9**:1048.

Li YF, Cheng YF, Huang Y, Conti M, Wilson SP, O'Donnell JM and Zhang HT (2011) Phosphodiesterase-4D knock-out and RNA interference-mediated knock-down enhance memory and increase hippocampal neurogenesis via increased cAMP signaling. *J Neurosci* **31**:172-183.

Liu J, Liu L, Zheng L, Feng KW, Wang HT, Xu JP and Zhou ZZ (2022) Discovery of novel 2,3-dihydro-1H-inden-1-ones as dual PDE4/AChE inhibitors with more potency against neuroinflammation for the treatment of Alzheimer's disease. *Eur J Med Chem* **238**:114503.

Martin TP, Hortigon-Vinagre MP, Findlay JE, Elliott C, Currie S and Baillie GS (2014) Targeted disruption of the heat shock protein 20-phosphodiesterase 4D (PDE4D) interaction protects against pathological cardiac remodelling in a mouse model of hypertrophy. *FEBS open bio* **4**:923-927.

McDonough W, Aragon IV, Rich J, Murphy JM, Abou Saleh L, Boyd A, Koloteva A and Richter W (2020) PAN-selective inhibition of cAMP-phosphodiesterase 4 (PDE4) induces gastroparesis in mice. *FASEB J.*

McQuown S, Paes D, Baumgartel K, Prickaerts J and Peters M (2021) Pharmacological inhibition of phosphodiesterase 7 enhances consolidation processes of spatial memory. *Neurobiol Learn Mem* **177**:107357.

Mingorance-Le Meur A and O'Connor TP (2009) Neurite consolidation is an active process requiring constant repression of protrusive activity. *The EMBO journal* **28**:248-260.

Miró X, Pérez-Torres S, Artigas F, Puigdomènech P, Palacios JM and Mengod G (2002a) Regulation of cAMP phosphodiesterase mRNAs expression in rat brain by acute and chronic fluoxetine treatment. An in situ hybridization study. *Neuropharmacology* **43**:1148-1157.

Miró X, Pérez-Torres S, Puigdomènech P, Palacios JM and Mengod G (2002b) Differential distribution of PDE4D splice variant mRNAs in rat brain suggests association with specific pathways and presynaptical localization. *Synapse* **45**:259-269.

Montenegro-Venegas C, Guhathakurta D, Pina-Fernandez E, Andres-Alonso M, Plattner F, Gundelfinger ED and Fejtova A (2022) Bassoon controls synaptic vesicle release via regulation of presynaptic phosphorylation and cAMP. *EMBO reports* **23**:e53659.

Paes D, Hermans S, van den Hove D, Vanmierlo T, Prickaerts J and Carlier A (2022) Computational investigation of the dynamic control of cAMP signaling by PDE4 isoform types. *Biophys J* **121**:2693-2711.

Paes D, Lardenoije R, Carollo RM, Roubroeks JAY, Schepers M, Coleman P, Mastroeni D, Delvaux E, Pishva E, Lunnon K, Vanmierlo T, van den Hove D and Prickaerts J (2020a) Increased isoform-specific phosphodiesterase 4D expression is associated with pathology and cognitive impairment in Alzheimer's disease. *Neurobiol Aging* **97**:56-64.

Paes D, Schepers M, Rombaut B, van den Hove D, Vanmierlo T and Prickaerts J (2021) The Molecular Biology of Phosphodiesterase 4 Enzymes as Pharmacological Targets: An Interplay of Isoforms, Conformational States, and Inhibitors. *Pharmacol Rev* **73**:1016-1049.

Paes D, Schepers M, Willems E, Rombaut B, Tiane A, Solomina Y, Tibbo A, Blair C, Kyurkchieva E, Baillie GS, Ricciarelli R, Brullo C, Fedele E, Bruno O, van den Hove D, Vanmierlo T and Prickaerts J (2023) Ablation of specific long PDE4D isoforms increases neurite elongation and conveys protection against amyloid-beta pathology. *Cell Mol Life Sci* **80**:178.

Paes D, Xie K, Wheeler DG, Zook D, Prickaerts J and Peters M (2020b) Inhibition of PDE2 and PDE4 synergistically improves memory consolidation processes. *Neuropharmacology* **184**:108414.

Pérez-Torres S, Miró X, Palacios JM, Cortés R, Puigdoménech P and Mengod G (2000) Phosphodiesterase type 4 isozymes expression in human brain examined by in situ hybridization histochemistry and [3H]rolipram binding autoradiography: Comparison with monkey and rat brain. *Journal of Chemical Neuroanatomy* **20**:349-374.

Prosdocimi T, Mollica L, Donini S, Semrau MS, Lucarelli AP, Aiolfi E, Cavalli A, Storici P, Alfei S, Brullo C, Bruno O and Parisini E (2018) Molecular Bases of PDE4D Inhibition by Memory-Enhancing GEBR Library Compounds. *Biochemistry* **57**:2876-2888.

Reagan-Shaw S, Nihal M and Ahmad N (2008) Dose translation from animal to human studies revisited. *Faseb j* **22**:659-661.

Ricciarelli R, Brullo C, Prickaerts J, Arancio O, Villa C, Rebosio C, Calcagno E, Balbi M, van Hagen BT, Argyrousi EK, Zhang H, Pronzato MA, Bruno O and

Fedele E (2017) Memory-enhancing effects of GEBR-32a, a new PDE4D inhibitor holding promise for the treatment of Alzheimer's disease. *Sci Rep* **7**:46320.

Richter W, Jin SL and Conti M (2005) Splice variants of the cyclic nucleotide phosphodiesterase PDE4D are differentially expressed and regulated in rat tissue. *Biochem J* **388**:803-811.

Sepúlveda C, Hernández B, Burgos CF, Fuentes E, Palomo I and Alarcón M (2019) The cAMP/PKA Pathway Inhibits Beta-amyloid Peptide Release from Human Platelets. *Neuroscience* **397**:159-171.

Seybold J, Newton R, Wright L, Finney PA, Suttorp N, Barnes PJ, Adcock IM and Giembycz MA (1998) Induction of Phosphodiesterases 3B, 4A4, 4D1, 4D2, and 4D3 in Jurkat T-cells and in Human Peripheral Blood T-lymphocytes by 8-Bromo-cAMP and G_s-coupled Receptor Agonists: POTENTIAL ROLE IN β₂-ADRENORECEPTOR DESENSITIZATION *. *Journal of Biological Chemistry* **273**:20575-20588.

Sierksma AS, van den Hove DL, Pfau F, Philippens M, Bruno O, Fedele E, Ricciarelli R, Steinbusch HW, Vanmierlo T and Prickaerts J (2014) Improvement of spatial memory function in APPswe/PS1dE9 mice after chronic inhibition of phosphodiesterase type 4D. *Neuropharmacology* **77**:120-130.

Solntseva EI, Kapai NA, Popova OV, Rogozin PD and Skrebitsky VG (2014) The involvement of sigma1 receptors in donepezil-induced rescue of hippocampal LTP impaired by beta-amyloid peptide. *Brain Research Bulletin* **106**:56-61.

Sutcliffe JS, Beaumont V, Watson JM, Chew CS, Beconi M, Hutcheson DM, Dominguez C and Munoz-Sanjuan I (2014) Efficacy of selective PDE4D negative allosteric modulators in the object retrieval task in female cynomolgus monkeys (Macaca fascicularis). *PLoS One* **9**:e102449.

Swinnen JV, Joseph DR and Conti M (1989) The mRNA encoding a high-affinity cAMP phosphodiesterase is regulated by hormones and cAMP. *Proc Natl Acad Sci U S A* **86**:8197-8201.

VANMIERLO T, PRICKAERTS, J., WIERINGA, P. (2019) SELECTIVE PDE4D INHIBITORS AGAINST DEMYELINATING DISEASES, (UNIVERSITEIT HASSELT UM, ACADEMISCH ZIEKENHUIS MAASTRICHT ed).

Wakabayashi Y, Telu S, Dick RM, Fujita M, Ooms M, Morse CL, Liow JS, Hong JS, Gladding RL, Manly LS, Zoghbi SS, Mo X, D'Amato EC, Sindac JA, Nugent RA, Marron BE, Gurney ME, Innis RB and Pike VW (2020) Discovery, Radiolabeling, and Evaluation of Subtype-Selective Inhibitors for Positron Emission Tomography Imaging of Brain Phosphodiesterase-4D. *ACS Chem Neurosci* **11**:1311-1323.

Wang H, Zhang F-f, Xu Y, Fu H-r, Wang X-d, Wang L, Chen W, Xu X-y, Gao Y-f, Zhang J-g and Zhang H-T (2020a) The Phosphodiesterase-4 Inhibitor Roflumilast, a Potential Treatment for the Comorbidity of Memory Loss and Depression in Alzheimer's Disease: A Preclinical Study in APP/PS1 Transgenic Mice. *International Journal of Neuropsychopharmacology* **23**:700-711.

Wang Y, Gao S, Zheng V, Chen L, Ma M, Shen S, Qu J, Zhang H, Gurney ME, O'Donnell JM and Xu Y (2020b) A Novel PDE4D Inhibitor BPN14770 Reverses Scopolamine-Induced Cognitive Deficits via cAMP/SIRT1/Akt/Bcl-2 Pathway. *Front Cell Dev Biol* **8**:599389.

Wunder F, Quednau R, Geerts A, Barg M and Tersteegen A (2013) Characterization of the cellular activity of PDE 4 inhibitors using two novel PDE 4 reporter cell lines. *Mol Pharm* **10**:3697-3705.
Xu Y (2022) PDE4D inhibitor: a novel weapon against mild cognitive impairment and Alzheimer's disease? *The FASEB Journal* **36**.
Zhang C, Xu Y, Chowdhary A, Fox D, 3rd, Gurney ME, Zhang HT, Auerbach BD, Salvi RJ, Yang M, Li G and O'Donnell JM (2018) Memory enhancing effects of BPN14770, an allosteric inhibitor of phosphodiesterase-4D, in wild-type and humanized mice. *Neuropsychopharmacology* **43**:2299-2309.
Zhang C, Xu Y, Zhang HT, Gurney ME and O'Donnell JM (2017) Comparison of the Pharmacological Profiles of Selective PDE4B and PDE4D Inhibitors in the Central Nervous System. *Sci Rep* **7**:40115.

Chapter 8

Summary

The goals of this thesis were 1) to identify which PDE4D isoforms are involved in neuroplasticity processes that are impaired by AD-associated pathology, and 2) to investigate the therapeutic potential of using combined treatments to reduce the therapeutic dose of PDE4(D) inhibitors. In light of these goals, this thesis presents a comprehensive literature review and four experimental studies using *in silico, in vitro*, and *in vivo* approaches.

In order to identify which PDE4D isoforms are involved in neuroplasticity processes that are impaired by AD-associated pathology, an extensive overview was established on the molecular biology of PDE4 enzymes and their utility as pharmacological targets in **Chapter 2**. It was outlined that PDE4 enzymes are encoded by four different genes (*PDE4A-D*) that each give rise to multiple isoforms owing to the use of alternative promoters and alternative splicing. Confusion can arise when referring to these isoforms as their nomenclature may differ across online databases, species and depending on whether one refers to the isoform's mRNA or protein. Hence, an overview figure of all known isoforms (page 41) and a comparison of human and rodent isoforms (page 126) were established to clarify the nomenclature and classification to the scientific field and to easily refer to the multitude of isoforms in upcoming chapters. This chapter also summarized how differences in protein sequence across PDE4 subtypes and isoforms result in different properties in view of enzymatic activity regulation, protein-protein interactions and inhibitor binding by changing the enzyme's conformation. The amino acids involved in all reported post-translational modifications and interactions with other proteins were illustrated in an overview figure (page 51). Moreover, the effect of these modifications and interactions on enzymatic activity of PDE4 subtypes or isoforms and their affinity to PDE4 inhibitors was reported. This overview provided the rationale to establish a thorough analysis of the approaches to determine affinities of PDE4 inhibitors. Therefore, a comprehensive list of PDE4 inhibitors was compiled indicating affinity per PDE4 subtype (page 69), isoform (page 75) or conformation

(page 79). Lastly, potential mechanisms underlying the adverse side effects associated with PDE4 inhibition were described in relation to the therapeutic dose ranges of several PDE4 inhibitors.

Next, using the gained knowledge on human PDE4D isoform sequences, promoter DNA (hydroxy)methylation and mRNA expression of PDE4D isoforms were measured in post-mortem material of the middle temporal lobe of AD patients and healthy controls (**Chapter 3**). Specific isoforms (PDE4D1, -D3, -D5, and -D8) displaying increased expression in AD were identified, concomitant with changes in the DNA methylation signatures of associated promoter regions. Moreover, increased PDE4D1 and PDE4D3 expression was associated with higher levels of plaque and tangles and lower cognitive performance. This study indicated that, although stemming from the same gene, expression regulation of PDE4D is impacted in an isoform-specific manner in AD.

To follow up on and complement these findings using human material, studies using animal models and cell lines were conducted in **Chapter 4**. In correspondence to the observations in human tissue, an upregulation of the same PDE4D isoforms was found in brain material of transgenic AD mice that exhibit amyloid-β pathology as well as in cultured hippocampal neurons exposed to amyloid-β. The notion that pharmacological PDE4D inhibition can promote neuronal plasticity was validated in the same mouse hippocampal neuronal cell line. Making use of CRISPR-Cas9 mediated gene-editing, it was determined in the same cell line that specific knockdown of one of the long PDE4D isoforms (i.e. PDE4D3, PDE4D5, PDE4D7, and PDE4D9) is sufficient to enhance neuronal plasticity processes. Moreover, knockdown of one of these isoforms could protect against plasticity-impairing effect of amyloid-β. Lastly, this chapter indicated which of the long PDE4D isoforms may not be involved in stomach-associated side effects of PDE4(D) inhibition by describing the isoform-specific expression in the mouse stomach.

Since knockdown of long-form PDE4D isoforms specifically was found to promote neuronal plasticity, the understanding of the molecular biology of the different PDE4D isoforms described in **Chapter 2** could be used to put these findings into a mechanistic perspective. The enzyme activity of PDE4D isoforms is differentially altered by phosphorylation by protein kinase A (PKA) and/or extracellular signal-regulated kinase (ERK) depending on the isoform category (i.e. long, short, and supershort). In order to understand why genetic knockdown of long isoforms specifically enhanced neuronal plasticity, an *in silico* computational model was established to simulate how the different isoform categories regulate cyclic adenosine monophosphate (cAMP) levels and control downstream signaling over time (**Chapter 5**). Here, it was described that long PDE4D isoforms specifically exert the largest control on cAMP and its downstream signaling. Hence, supporting the experimental data of the previous chapter, inhibition of long PDE4D isoforms may provide the most profound approach to increase cAMP signaling involved in neuronal plasticity processes.

In view of the first goal of this thesis, inhibition of specific PDE4D isoforms involved in (AD-associated) memory processes could provide a more efficacious and/or safer therapeutic strategy. Besides this approach, the safety of PDE4(D) inhibitors can be improved by lowering the required therapeutic dose to reduce the risk of adverse side effects. Following up on the second goal of this thesis, **Chapter 6** demonstrates the potential of combining PDE2 and PDE4 inhibitors to promote neuroplasticity *in vitro* and stimulate memory consolidation *in vivo*. As it was found that PDE2 and PDE4 inhibitors exert synergistic actions, the therapeutic doses of each inhibitor could be lowered, which would minimize the risk of PDE4-mediated adverse side effects.

Concludingly, the work in this thesis has established the potential of PDE4D isoform-specific inhibition and synergistic PDE4/PDE2 inhibition as new strategies to

make PDE4-targeting therapies more efficacious and/or safer for the benefit of treating memory deficits in AD.

Chapter 9

Samenvatting

De doelstellingen van deze thesis waren 1) het identificeren welke PDE4D-isovormen betrokken zijn bij de processen van neuroplasticiteit die door AD-gerelateerde pathologie aangedaan worden, en 2) het onderzoeken van het therapeutische potentieel van gecombineerde behandelingen gericht op het verlagen van de therapeutische dosis van PDE4(D)-inhibitoren. In het kader van deze doelstellingen worden in deze thesis een uitgebreide literatuurreview uiteengezet, alsmede vier experimentele studies waarin gebruik is gemaakt van *in silico, in vitro* en *in vivo*-methoden.

Om te kunnen identificeren welke PDE4D-isovormen betrokken zijn bij de processen van neuroplasticiteit die aangetast worden door AD-gerelateerde pathologie, wordt in **Hoofdstuk 2** een uitgebreid overzicht gepresenteerd die de moleculaire biologie van PDE4-enzymen uiteenzet en het potentieel van deze enzymen als effectief farmacologisch doelwit. In dit hoofdstuk wordt beschreven dat PDE4-enzymen door vier verschillende genen worden gecodeerd (*PDE4A-D*) die elk, door middel van alternatieve promoters en alternatieve splicing, meerdere isovormen tot expressie kunnen brengen. Bij het refereren naar deze isovormen kan er onduidelijkheid ontstaan doordat er verschillen bestaan in de gebruikte nomenclatuur binnen online databases, binnen diersoorten en of er wordt gerefereerd naar het mRNA of het eiwit van de isovorm. Derhalve is een overzicht van alle tot dusver bekende isovormen samengesteld (pagina 41) samen met een vergelijking van humane isovormen en isovormen bij knaagdieren (pagina 126) ter verduidelijking van de nomenclatuur en classificatie voor het wetenschappelijke veld en om makkelijker te kunnen refereren naar de veelvuldige isovormen in de volgende hoofdstukken. In dit hoofdstuk wordt ook samengevat hoe verschillen in eiwitsequentie tussen PDE4-subtypen en -isovormen leiden tot verschillende eigenschappen met betrekking tot regulatie van enzymactiviteit, eiwit-eiwitinteracties en het binden van inhibitoren door veranderingen in de conformatie van het enzym. Welke aminozuren betrokken zijn bij alle in de literatuur beschreven

post-translationele modificaties en interacties met andere eiwitten is weergegeven in de figuur op pagina 51. Eveneens wordt het effect van deze modificaties en interacties op enzymatische activiteit van PDE4-subtypen of -isovormen en PDE4-inhibitoraffiniteit beschreven. Dit overzicht heeft de aanleiding gevormd om een grondige analyse uit te voeren naar de wijze waarop de affiniteit van een PDE4-inhibitor wordt bepaald. Daartoe is een uitgebreid overzicht van PDE4-inhibitoren samengesteld waarbij affiniteit wordt weergegeven per PDE4-subtype (pagina 69), isovorm (pagina 75) en conformatie (pagina 79). Tenslotte worden de potentiële onderliggende mechanismen beschreven die geassocieerd worden met de negatieve bijwerkingen door PDE4-inhibitie en hoe deze zich verhouden tot therapeutische doses van verscheidene PDE4-inhibitoren.

Vervolgens, gebruikmakend van de opgedane inzichten omtrent humane PDE4D isovorm sequenties, werden promoter DNA (hydroxy)methylatie en mRNA expressie van PDE4D isovormen gemeten in post-mortem hersenmateriaal van de middelste slaapwending van AD patiënten en gezonde controles (**Hoofdstuk 3**). Specifieke isovormen (PDE4D1, -D3, -D5 en -D8) werden geïdentificeerd die een verhoogde expressie in AD lieten zien, welke geassocieerd was met veranderingen in het DNA methylatieprofiel van de corresponderende promoter-regio's. Bovendien was verhoogde PDE4D1 en PDE4D3 expressie geassocieerd met verhoogde niveaus van amyloïde plaques en neurofibrillaire tangles en een lager cognitief vermogen. Deze studie toonde aan dat, hoewel isovormen voortkomen uit hetzelfde gen, expressieregulatie van PDE4D in AD wordt beïnvloed op een isovorm-specifieke wijze.

Om voort te borduren op de gedane bevindingen in humaan materiaal en deze bevindingen aan te vullen werden er in **Hoofdstuk 4** experimenten verricht gebruikmakend van diermodellen en cellijnen. In overeenstemming met de observaties in human weefsel werd er een expressieverhoging van dezelfde PDE4D isovormen gevonden in hersenmateriaal van transgene AD muizen die β-amyloïd

pathologie vertonen alsmede in gekweekte hippocampale neuronen blootgesteld aan β-amyloïd. Het idee dat farmacologische inhibitie van PDE4D neuronale plasticiteit kan bevorderen werd gevalideerd in dezelfde muriene hippocampale neuroncellijn. Gebruikmakend van CRISPR-Cas9 gemedieerde genbewerking werd in dezelfde cellijn bepaald dat specifieke knock-down van één van de lange PDE4D isovormen (i.e. PDE4D3, PDE4D5, PDE4D7 en PDE4D9) voldoende is om neuronale plasticiteitsprocessen te verbeteren. Bovendien kon knock-down van één van deze isovormen bescherming verschaffen tegen het plasticiteit-aantastende effect van β-amyloïd. Ten slotte gaf dit hoofdstuk, door het beschrijven van isovorm-specifieke expressie in de muizenmaag, aan welke van de lange PDE4D isovormen wellicht niet betrokken zijn bij het induceren van maag-geassocieerde bijwerkingen van PDE4(D) inhibitie.

Aangezien het werd gevonden dat knock-down van lange PDE4D isovormen neuronale plasiticteit bevordert, kon het inzicht in de moleculaire biologie van de verschillende PDE4D isovormen zoals beschreven in **Hoofdstuk 2** gebruikt worden om deze bevindingen in een mechanistisch perspectief te plaatsen. De enzymactiviteit van PDE4D isovormen wordt differentieel beïnvloed door fosforylering door 'protein kinase A' (PKA) en/of 'extracellular signal-regulated kinase' (ERK) afhankelijk van de isovorm-categorie (i.e. lang, kort en superkort). Om te begrijpen waarom genetische knock-down van specifiek lange isovormen neuronale plasticiteit bevorderde, werd er een *in silico* computationeel model gecreëerd om te simuleren hoe de verschillende isovorm-categorieën cyclisch adenosine monofosfaat (cAMP) niveaus reguleren en hoe deze de vervolgsignalering beïnvloeden gedurende de tijd (**Hoofdstuk 5**). In dit hoofdstuk werd beschreven dat specifiek lange PDE4D isovormen het grootste effect uitoefenen op cAMP signalering en de signalering die daarop volgt. De experimentele data uit het vorige hoofdstuk wordt hierdoor ondersteund en daardoor kan gesuggereerd worden dat

inhibitie van lange PDE4D isovormen de meest effectieve aanpak is om de cAMP signalering die betrokken is in neuronale plasticiteitsprocessen te bevorderen.

Betreffende de eerste doelstelling van deze thesis kan inhibitie van specifieke PDE4D isovormen betrokken bij (AD-geassocieerde) geheugenprocessen een effectievere en/of veiligere behandelstrategie verschaffen. Naast deze aanpak kan de veiligheid van PDE4(D) inhibitoren ook verbeterd worden door het verlagen van de therapeutische dosis om het risico op nadelige bijwerkingen te reduceren. In lijn met de tweede doelstelling van deze thesis, laat **Hoofdstuk 6** het potentieel zien van het combineren van PDE2 en PDE4 inhibitoren om neuroplasticiteit *in vitro* en geheugenvorming *in vivo* te stimuleren. Aangezien werd bevonden dat PDE2 en PDE4 synergistische acties vertonen, zouden therapeutische doses van iedere inhibitor verlaagd kunnen worden wat er vervolgens voor zou kunnen zorgen dat het risico op PDE4-gemedieerde nadelige bijwerkingen geminimaliseerd wordt.

Concluderend, het werk in deze thesis heeft de potentie van PDE4D isovorm-specifieke inhibitie en synergistische PDE4/PDE2 inhibitie vastgesteld als nieuwe strategieën om behandelingen gericht op PDE4 doeltreffender en/of veiliger te maken ten bate van de behandeling van geheugenproblemen in AD.

Appendix

Impact Paragraph

Scientific impact

An increasing prevalence of Alzheimer's disease (AD) has greatly stimulated the urge to increase the amount of more and better treatments. However, the progression to the clinic of pharmacological treatments that treat memory problems associated with AD has stagnated since the development of acetylcholinesterase inhibitors (i.e., rivastigmine, galantamine, and donepezil) and memantine. Although the drug aducanumab was recently approved by the Food and Drug Administration (FDA), yet rejected by the European Medicines Agency (EMA), the severe adverse effects associated with this treatment has caused a lot of controversy. Therefore, the efficacy and safety of aducanumab remain to be better defined. In general, the efficacy and safety of current AD medication can be regarded as suboptimal as therapeutic actions are often short lasting, patient-specific and/or concurrent with adverse effects like headaches, nausea, vomiting, and diarrhea. Thus, there is an urgent need for new pharmacological treatment strategies to combat AD-associated memory problems.

As outlined in this thesis, insights into the molecular biology of PDE4 as pharmacological target opens up avenues to improve PDE4-targeting therapies for the treatment of Alzheimer's disease (AD). While the potential of PDE4 inhibition to stimulate memory consolidation has been studied extensively, adverse side effects associated with PDE4 inhibition required this treatment strategy to become more specific. Since the PDE4 enzyme family comprises several subtypes and isoforms (**Chapter 2**), target specification can be performed in order to make PDE4-targeting therapeutic more efficacious and/or safer. From a scientific perspective, the work in this thesis has provided the insight that long PDE4D isoforms in particular are involved in the regulation of neuronal plasticity, also in presence of AD-associated pathology. This insight has implications for the design and development of PDE4 inhibitors, which can eventually translate into pharmacological treatments for memory problems in AD patients. Since long isoforms can adopt distinct conformational states compared to (super)short isoforms and PDE4D expresses

subtype-unique amino acids, PDE4 inhibitors can be developed that exploit these features to obtain long PDE4D isoform binding specificity. Since potential PDE4 inhibitors are often solely screened for their affinity of binding the PDE4 catalytic domain rather than affinity towards specific PDE4 subtype and/or isoforms (**Chapter 2**), many small molecules may have been disregarded as lowly potent inhibitors whilst they may actually be able to selectively bind certain subtype or isoform specific conformations. Thus, since targeting specific subtypes or isoforms may be therapeutically more efficacious or safer, potential subtype-selectively or conformation-selectivity of (disregarded) PDE4 inhibitors may have to be reconsidered.

Accordingly, based on a molecular docking screening approach, the ability of PDE4 inhibitors (n=3013) to bind different PDE4 subtypes and conformations was modeled. In **Figure 1**, the affinity of these inhibitors towards the PDE4D catalytic domain and PDE4D catalytic domain with its C-terminus capped is shown, indicating that certain inhibitors bind with higher affinity to C-terminus capped conformations. Thus, based on the insights from this thesis that certain isoforms provide a more promising therapeutic target than others, PDE4 inhibitors can be selected or designed to selectively bind the isoform of interest. A preliminary selection of inhibitors could be based on *in silico* screenings, as exemplified here, to provide multiple small molecules that can be tested and validated as subtype-specific or isoform-specific PDE4 inhibitor to treat cognitive problems in AD.

In addition to a more precise targeting of PDE4 subtypes and isoforms, this thesis has provided a proof-of-principle set of experiments that highlight the therapeutic potential of the synergistic actions of PDE4 and PDE2 inhibition on memory consolidation processes (**Chapter 6**). Further characterization of the efficacy and safety of this treatment strategy in preclinical disease models and subsequent clinical studies may eventually lead to a clinically safe pharmacological intervention that can alleviate memory problems in patients suffering from AD.

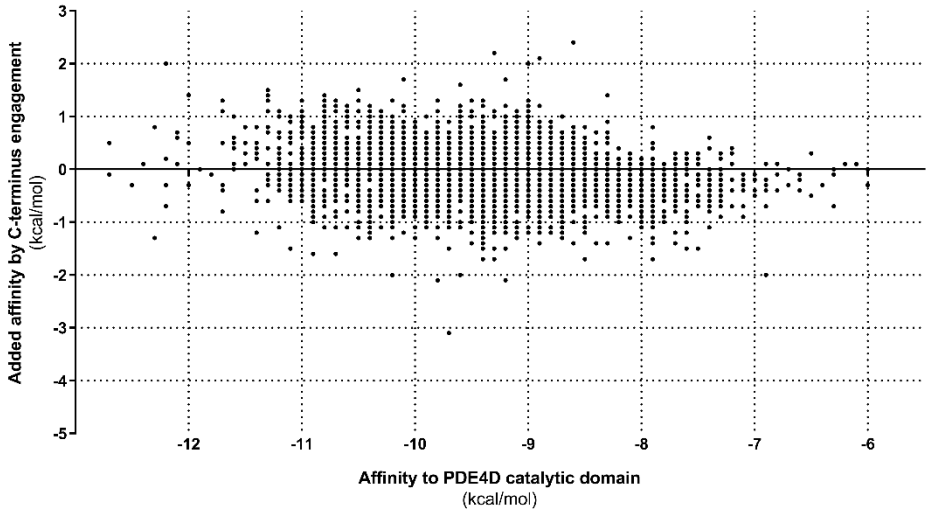

Figure 1. Binding affinities of PDE4 inhibitors (n=3013) for PDE4D catalytic domain and PDE4D catalytic domain with the C-terminus capped based on molecular docking *in silico* screening using crystal structures of different PDE4D conformations available on RCSB Protein Data Bank.

Beyond AD, the principles of subtype/isoform specific PDE4 inhibition and synergistic PDE4 and PDE2 inhibition as therapeutic strategies has also implications for the research into PDE4 as a therapeutic target in other disorders. Since PDE4-mediated cAMP signaling occurs in any cell type, PDE4 enzymes provide interesting targets in a myriad of diseases. Since PDE4 inhibitors, depending on administration route and dose, can be associated with severe adverse effects, target specification towards PDE4 subtypes and/or isoforms is key to optimize efficacy and safety. Thus, similar approaches as taken to optimize PDE4 inhibition to treat AD as delineated in this thesis, could, and perhaps should, be applied to other diseases in which PDE4 inhibition has shown promise. In **Table 1**, several illustrative disorders are listed for which PDE4-targeting treatment strategies could be optimized by means of target specification.

Table 1. Illustrative list of diseases that may benefit from PDE4 target specification.

Type of condition	Disease	Reference
Neurological	Parkinson's disease	(Chen et al., 2022; Dong et al., 2021)
	Multiple Sclerosis	(Schepers et al., 2019)
	(Ischemic) stroke	(Cai et al., 2022; Kaur et al., 2022)
	Fragile X syndrome	(Berry-Kravis et al., 2021)
	Neuropathic pain	(Zhang et al., 2022)
Dermatological	Psoriasis	(Aljefri et al., 2022)
Gastro-intestinal	Inflammatory Bowel Syndrome	(Liu et al., 2022)
Pulmonary	Idiopathic Pulmonary Fibrosis	(Herrmann et al., 2022)
Hepatic	Non-alcoholic fatty liver disease	(Tao et al., 2022; Yu et al., 2021)
Metabolic	Obesity	(Irelan et al., 2022)
Addictive	Methamphetamine reinforcement	(Honeywell et al., 2022)
Cancer	Breast cancer	(Mukherjee et al., 2022)
	Prostate cancer	(Powers et al., 2015; Xie et al., 2021)

Considering the potential of improving therapeutic strategies for these disorders by targeting specific PDE4 isoforms as outlined in this thesis, identifying the PDE4 isoforms involved in each particular disease is crucial. Determining the most promising PDE4 subtype and/or isoform could be determined by testing subtype-specific and isoform-specific PDE4 inhibitors, but also through measuring PDE4 subtype and isoform expression in disease states, insight can be acquired about which subtypes/isoforms could provide the best therapeutic target. The classification and comparison of the different PDE4 subtypes and isoforms has brought the insight that each of the PDE4 genes displays a characteristic exon architecture (**Chapter 2**). Each PDE4 isoform can be distinguished by sequences coming from an isoform-unique exon. As described in **Chapter 3** and **Chapter 4**, disease-associated mRNA expression of PDE4 isoforms can be measured using qPCR primers that amplify sequences stemming from these isoform-specific exons. Since the isoform-specific exons and the associated sequences are known, this information can be used to extract PDE4 isoform-specific expression patterns from (freely accessible) online data repositories of exon array and RNAseq experiments. As these data are available for

many diseases/experimental designs, also those in which PDE4 inhibition may have therapeutic effects, target specification towards PDE4 subtypes and/or isoforms could be explored be re-analyzing these datasets at the isoform level. Exon array datasets are particularly suitable for this approach as the expression of isoform-specific exons will give a direct indication of the expression of the associated isoform. Given the distinct roles of specific PDE4 isoforms, it is crucial to measure expression differences at the isoform level as general PDE4 expression may 'dilute' and mask isoform-specific expression differences. As a proof of principle, several publicly available exon array datasets were re-analyzed to investigate PDE4 isoform expression differences. As an example, in **Figure 2** the PDE4 isoform-specific expression is shown as measured by means of exon array analysis in post-mortem material of the entorhinal cortex of AD patients and healthy controls (based on GEO accession ID: GSE26972, (Berson et al., 2012)).

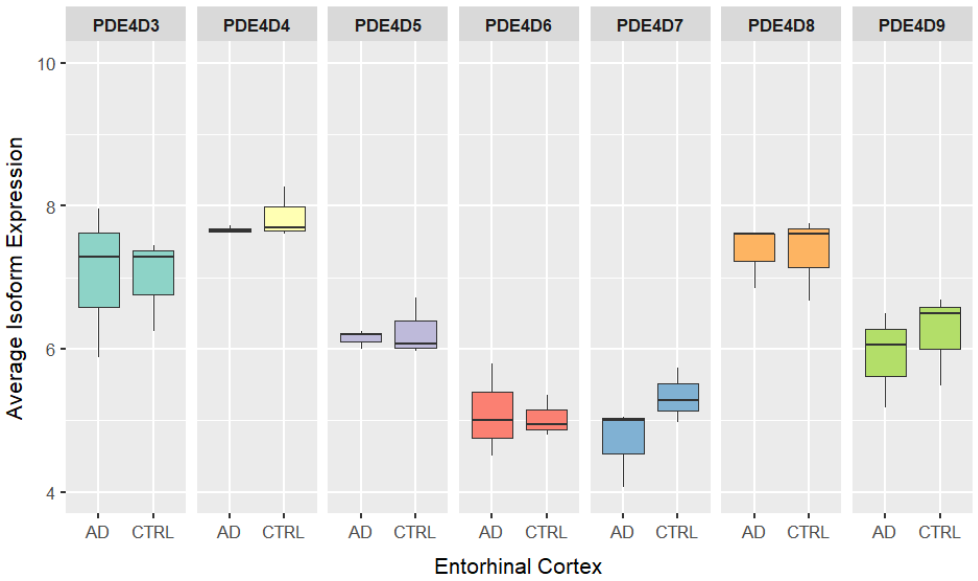

Figure 2. Proof-of-principle indicating that knowledge of PDE4 isoform-specific sequences can be used to determine PDE4 isoform-specific expression by means of re-analyzing publicly available Exon Array datasets. Note that the expression of isoforms PDE4D1 and PDE4D2 cannot be specifically and reliably assessed using the specific exon array probes used in this dataset.

Overall, oriented towards AD, the major scientific implications of the work in this thesis are the validation of new avenues to treat memory problems in AD by means of more specific PDE4 inhibition at the level of PDE4D isoforms or combined treatment with a PDE4 and PDE2 inhibitor. More generally and rather focused on PDE4 as therapeutic targets, this thesis has provided several *in silico*, *in vitro*, and *in vivo* research strategies that can be utilized to optimize PDE4-targeting therapies in a multitude of diseases.

Societal impact

The fundamental insights into the role of specific PDE4D isoforms in the regulation of neuronal plasticity processes will be of use in developing more efficacious and safer therapies to treat memory deficits in AD. Although there is a long trajectory ahead until the treatment strategies explored here are validated in a clinical setting, the societal impact of this thesis will be most evident upon the development of isoform-specific PDE4D inhibitors and/or the validation of synergistic PDE4-PDE2 inhibition. Upon validation, patients suffering from AD-associated memory problems can be effectively treated and by mitigating their symptoms, the quality of life of patients, their family and caretakers will be greatly improved. More generally, society as a whole will benefit from improved PDE4-mediating therapeutics, as AD-associated burden on the healthcare system will be alleviated. Similarly, as highlighted in the previous section, the scientific insights into PDE4's molecular biology can also improve the treatment of other diseases which will benefit many other patient populations and associated families and caretakers.
Despite the fact that it is hard to predict whether the outlined treatment strategies will be validated in a clinical setting, the scientific advancements presented here are sought to provide hope to patients, their families, caretakers and contributors to funding agencies like Alzheimer Nederland, as it shows that new treatment strategies can be created but only await to be proven successful.

REFERENCES

Aljefri YE, Ghaddaf AA, Alkhunani TA, Alkhamisi TA, Alahmadi RA, Alamri AM and Alraddadi AA (2022) Efficacy and safety of apremilast monotherapy in moderate-to-severe plaque psoriasis: A systematic review and meta-analysis. *Dermatologic therapy* **35**:e15544.

Berry-Kravis EM, Harnett MD, Reines SA, Reese MA, Ethridge LE, Outterson AH, Michalak C, Furman J and Gurney ME (2021) Inhibition of phosphodiesterase-4D in adults with fragile X syndrome: a randomized, placebo-controlled, phase 2 clinical trial. *Nature medicine* **27**:862-870.

Berson A, Barbash S, Shaltiel G, Goll Y, Hanin G, Greenberg DS, Ketzef M, Becker AJ, Friedman A and Soreq H (2012) Cholinergic-associated loss of hnRNP-A/B in Alzheimer's disease impairs cortical splicing and cognitive function in mice. *EMBO Mol Med* **4**:730-742.

Cai N, Xu B, Li X, Qin Y, Li M, Chen K, Xu J and Wang H (2022) Roflumilast, a cyclic nucleotide phosphodiesterase 4 inhibitor, protects against cerebrovascular endothelial injury following cerebral ischemia/reperfusion by activating the Notch1/Hes1 pathway. *Eur J Pharmacol* **926**:175027.

Chen JY, Zhu Q, Cai CZ, Luo HB and Lu JH (2022) α-mangostin derivative 4e as a PDE4 inhibitor promote proteasomal degradation of alpha-synuclein in Parkinson's disease models through PKA activation. *Phytomedicine : international journal of phytotherapy and phytopharmacology* **101**:154125.

Dong WL, Zhong JH, Chen YQ, Xie JF, Qin YY, Xu JP, Cai NB, Li MF, Liu L and Wang HT (2021) Roflupram protects against rotenone-induced neurotoxicity and facilitates α-synuclein degradation in Parkinson's disease models. *Acta Pharmacol Sin* **42**:1991-2003.

Herrmann FE, Hesslinger C, Wollin L and Nickolaus P (2022) BI 1015550 is a PDE4B Inhibitor and a Clinical Drug Candidate for the Oral Treatment of Idiopathic Pulmonary Fibrosis. *Front Pharmacol* **13**:838449.

Honeywell KM, Doren EV and Szumlinski KK (2022) Selective Inhibition of PDE4B Reduces Methamphetamine Reinforcement in Two C57BL/6 Substrains. *Int J Mol Sci* **23**.

Irelan D, Boyd A, Aragon I, Fiedler E and Richter W (2022) Pharmacologic or Genetic PDE4 Inactivation Reduces Obesity and Improves Glucose Handling in Mice. *The FASEB Journal* **36**.

Kaur A, Singh TG, Khan H, Kumar M, Singh N and Abdel-Daim MM (2022) Neuroprotective Effect of Piclamilast-Induced Post-Ischemia Pharmacological Treatment in Mice. *Neurochemical research* **47**:2230-2243.

Liu H, Wang Q, Huang Y, Deng J, Xie X, Zhu J, Yuan Y, He YM, Huang YY, Luo HB and He X (2022) Discovery of novel PDE4 inhibitors targeting the M-pocket from natural mangostanin with improved safety for the treatment of Inflammatory Bowel Diseases. *Eur J Med Chem* **242**:114631.

Mukherjee P, Bagchi A, Banerjee A, Roy H, Bhattacharya A, Biswas A and Chatterji U (2022) PDE4 inhibitor eliminates breast cancer stem cells via noncanonical activation of mTOR. *Journal of cellular biochemistry*.

Powers GL, Hammer KD, Domenech M, Frantskevich K, Malinowski RL, Bushman W, Beebe DJ and Marker PC (2015) Phosphodiesterase 4D inhibitors limit prostate cancer growth potential. *Molecular cancer research : MCR* **13**:149-160.

Schepers M, Tiane A, Paes D, Sanchez S, Rombaut B, Piccart E, Rutten BPF, Brône B, Hellings N, Prickaerts J and Vanmierlo T (2019) Targeting Phosphodiesterases-Towards a Tailor-Made Approach in Multiple Sclerosis Treatment. *Front Immunol* **10**:1727.

Tao X, He H, Peng J, Xu R, Fu J, Hu Y, Li L, Yang X, Feng X, Zhang C, Zhang L, Yu X, Shen A, Huang K and Fu Q (2022) Overexpression of PDE4D in mouse liver is sufficient to trigger NAFLD and hypertension in a CD36-TGF-β1 pathway: therapeutic role of roflumilast. *Pharmacol Res* **175**:106004.

Xie C, Lin PJ and Hao J (2021) Eggmanone Effectively Overcomes Prostate Cancer Cell Chemoresistance. *Biomedicines* **9**.

Yu Y, He C, Tan S, Huang M, Guo Y, Li M and Zhang Q (2021) MicroRNA-137-3p Improves Nonalcoholic Fatty Liver Disease through Activating AMPKα. *Analytical cellular pathology (Amsterdam)* **2021**:4853355.

Zhang FF, Wang H, Zhou YM, Yu HY, Zhang M, Du X, Wang D, Zhang F, Xu Y, Zhang JG and Zhang HT (2022) Inhibition of phosphodiesterase-4 in the spinal dorsal horn ameliorates neuropathic pain via cAMP-cytokine-Cx43 signaling in mice. *CNS Neurosci Ther* **28**:749-760.

Appendix

Curriculum Vitae | About the author

Dean Paes was born on the 8th of July 1993 in Geleen, the Netherlands. Growing up in Obbicht, he attended secondary school at the Gymnasium of Trevianum Scholengroep in Sittard. In this period, he also completed two academic courses (Evolution and Physiology) at the Open University in Heerlen. Upon graduating secondary school, Dean enrolled into the bachelor program Molecular Life Sciences at Maastricht University in 2011. During this program, he followed the MaRBLe^{+} honors program and performed an internship under the supervision of Dr. Nicole Leibold and Prof. dr. Daniël van den Hove before obtaining the Bachelor Degree in 2014. In September 2014, he started the two-year Research Master Fundamental Neuroscience at Maastricht University. As part of this research master, he conducted a research internship at HiQScreen Sàrl in Geneva, Switzerland. During this internship, Dean investigated nicotinic acetylcholine receptors as pharmacological targets under supervision of Prof. dr. Daniel Bertrand. The associated Research Master Degree was obtained in July 2016. Continuing research in neuropharmacology, he then started working as a research assistant in the department of Psychiatry and Neuropsychology at Maastricht University to study the effects of phosphodiesterase (PDE) inhibitors on memory performance in rats.

Upon obtaining a Kootstra Talent Fellowship from the Maastricht University Medical Centre, Dean began his PhD research to investigate the role of PDE4D isoforms as pharmacological targets in the treatment of Alzheimer's disease at Maastricht University and Hasselt University in June 2017. This work was performed under supervision of promotores Prof. dr. Daniël van den Hove (Maastricht University) and Dr. Tim Vanmierlo (Hasselt University) and co-promotor Prof. dr. Niels Hellings (Hasselt University). Next to the PhD research, he supervised research projects of more than 20 bachelor, (research) master and Erasumus exchange students. Dean has also been a PhD representative and member of the educational committee of the School for Mental Health and Neuroscience (MHeNS) at Maastricht University from 2017 up until 2021. From 2020 until 2021, he was also a PhD

representative of the European Graduate School of Neuroscience (EURON). During his PhD trajectory, he also (co-)organized local and international symposia within the framework of MHeNS and EURON. Moreover, Dean attended and presented at several (inter)national conferences and symposia (e.g. Dutch Neuroscience Meeting and Gordon Research Conference/Seminar). Looking for innovative ways to approach the research questions of his PhD research, Dean initiated several collaborations. By means of a Young European Research University Network (YERUN) mobility award, he visited the lab of Prof. Eduardo Eyras at Pompeu Fabra Universidad in Barcelona, Spain in 2018 to learn how to analyze whole exome sequencing and RNA-seq data. From 2019 onwards, these insights would later be used to start a collaboration with Dr. Lars Eijssen (Maastricht University) to measure PDE isoform-specific expression from publicly available datasets. Parallel to the main PhD project, Dean initiated *in silico* screening approaches to (re-)evaluate existing and new compound as PDE4 inhibitors. After the PhD project, Dean started working as a scientist at Mosa Meat, a pioneering company in the cultivated meat industry. Currently, as a senior scientist, he is applying his insights in pharmacology and molecular cell biology there to develop cost-efficient culture media.

Appendix

List of publications

LIST OF PUBLICATIONS

Reviews

Paes D, Schepers M, Rombaut B, van den Hove D, Vanmierlo T, Prickaerts J. The Molecular Biology of Phosphodiesterase 4 Enzymes as Pharmacological Targets: An Interplay of Isoforms, Conformational States, and Inhibitors. *Pharmacol Rev*. 2021 Jul;73(3):1016-1049. doi: 10.1124/pharmrev.120.000273.

Rombaut B, Kessels S, Schepers M, Tiane A, **Paes D**, Solomina Y, Piccart E, van den Hove D, Brône B, Prickaerts J, Vanmierlo T. PDE inhibition in distinct cell types to reclaim the balance of synaptic plasticity. *Theranostics*. 2021 Jan 1;11(5):2080-2097. doi: 10.7150/thno.50701.

Blokland A, Heckman P, Vanmierlo T, Schreiber R, **Paes D**, Prickaerts J. Phosphodiesterase Type 4 Inhibition in CNS Diseases. *Trends Pharmacol Sci*. 2019 Dec;40(12):971-985. doi: 10.1016/j.tips.2019.10.006.

Schepers M, Tiane A, **Paes D**, Sanchez S, Rombaut B, Piccart E, Rutten BPF, Brône B, Hellings N, Prickaerts J, Vanmierlo T. Targeting Phosphodiesterases-Towards a Tailor-Made Approach in Multiple Sclerosis Treatment. *Front Immunol*. 2019 Jul 24;10:1727. doi: 10.3389/fimmu.2019.01727.

Research articles

Paes D, Schepers M, Willems E, Rombaut B, Tiane A, Solomina Y, Tibbo A, Blair C, Kyurkchieva E, Baillie GS, Ricciarelli R, Brullo C, Fedele E, Bruno O, van den Hove D, Vanmierlo T, Prickaerts J. Ablation of specific long PDE4D isoforms increases neurite elongation and conveys protection against amyloid-β pathology. *Cell Mol Life Sci*. 2023 Jun 12;80(7):178. doi: 10.1007/s00018-023-04804-w.

Schepers M, **Paes D**, Tiane A, Rombaut B, Piccart E, van Veggel L, Gervois P, Wolfs E, Lambrichts I, Brullo C, Bruno O, Fedele E, Ricciarelli R, Ffrench-Constant C, Bechler ME, van Schaik P, Baron W, Lefevere E, Wasner K, Grünewald A, Verfaillie C, Baeten P, Broux B, Wieringa P, Hellings N, Prickaerts J, Vanmierlo T. Selective PDE4 subtype inhibition provides new opportunities to intervene in neuroinflammatory versus

myelin damaging hallmarks of multiple sclerosis. *Brain Behav Immun*. 2023 Mar;109:1-22. doi: 10.1016/j.bbi.2022.12.020.

Nelissen E, van Hagen BTJ, Argyrousi EK, van Goethem NP, Heckman PRA, **Paes D**, Mulder-Jongen DAJ, Ramaekers JG, Blokland A, Schmidt HHHW, Prickaerts J. Soluble guanylate cyclase stimulator riociguat improves spatial memory in mice via peripheral mechanisms. *Neurosci Lett*. 2022 Sep 25;788:136840. doi: 10.1016/j.neulet.2022.136840.

Paes D, Hermans S, van den Hove D, Vanmierlo T, Prickaerts J, Carlier A. Computational investigation of the dynamic control of cAMP signaling by PDE4 isoform types. Biophys J. 2022 Jun 18:S0006-3495(22)00478-7. doi: 10.1016/j.bpj.2022.06.019. PMID: 35717559.

van Hagen BTJ, van Goethem NP, Nelissen E, **Paes D**, Koymans K, van Hoof S, Schreiber R, Varney M, Newman-Tancredi A, Prickaerts J. Biased 5-HT1A receptor agonists F13714 and NLX-101 differentially affect pattern separation and neuronal plasticity in rats after acute and chronic treatment. *Mol Cell Neurosci*. 2022 Mar 10;120:103719. doi: 10.1016/j.mcn.2022.103719.

Paes D, Xie K, Wheeler DG, Zook D, Prickaerts J, Peters M. Inhibition of PDE2 and PDE4 synergistically improves memory consolidation processes. *Neuropharmacology*. 2021 Feb 15;184:108414. doi: 10.1016/j.neuropharm.2020.108414.

McQuown S, **Paes D**, Baumgärtel K, Prickaerts J, Peters M. Pharmacological inhibition of phosphodiesterase 7 enhances consolidation processes of spatial memory. *Neurobiol Learn Mem*. 2021 Jan;177:107357. doi: 10.1016/j.nlm.2020.107357.

Paes D, Lardenoije R, Carollo RM, Roubroeks JAY, Schepers M, Coleman P, Mastroeni D, Delvaux E, Pishva E, Lunnon K, Vanmierlo T, van den Hove D, Prickaerts J. Increased isoform-specific phosphodiesterase 4D expression is associated with pathology and cognitive impairment in Alzheimer's disease. *Neurobiol Aging*. 2021 Jan;97:56-64. doi: 10.1016/j.neurobiolaging.2020.10.004.

van Goethem NP*, **Paes D***, Puzzo D*, Fedele E*, Rebosio C, Gulisano W, Palmeri A, Wennogle LP, Peng Y, Bertrand D, Prickaerts J. Antagonizing α7 nicotinic receptors with methyllycaconitine (MLA) potentiates receptor activity and memory acquisition. *Cell Signal*. 2019 Oct;62:109338. doi: 10.1016/j.cellsig.2019.06.003.

Barkhuizen M, van Mechelen R, Vermeer M, Chedraui P, **Paes D**, van den Hove DLA, Vaes B, Mays RW, Steinbusch HWM, Robertson NJ, Kramer BW, Gavilanes AWD. Systemic multipotent adult progenitor cells improve long-term neurodevelopmental outcomes after preterm hypoxic-ischemic encephalopathy. *Behav Brain Res*. 2019 Apr 19;362:77-81. doi: 10.1016/j.bbr.2019.01.016.

Nelissen E, De Vry J, Antonides A, **Paes D**, Schepers M, van der Staay FJ, Prickaerts J, Vanmierlo T. Early-postnatal iron deficiency impacts plasticity in the dorsal and ventral hippocampus in piglets. *Int J Dev Neurosci*. 2017 Jun;59:47-51. doi: 10.1016/j.ijdevneu.2017.03.006.

Book chapters

Published:

Paes D, van Hagen BTJ and Prickaerts J (2018) Chapter 3 - Object Novelty Memory Tests: Methods, Test Procedures and Measurements, in *Handbook of Behavioral Neuroscience* (Ennaceur A and de Souza Silva MA eds) pp 39-51, Elsevier.

In press:

Paes D, Altuntaş E, Mall E, Jackish L, Doğan A, Post M (2023) Chapter: Cell Nutrition and Growth Media, in *Technological and Scientific Foundations of Cellular Agriculture*, Elsevier.

Mall E, Andriessen V, Jackish L, Doğan A, **Paes D**, Altuntaş E, Post M (2023) Chapter: Introduction to Cultured Meat, in *Technological and Scientific Foundations of Cellular Agriculture*, Elsevier.

Appendix

Acknowledgments | Dankwoord | Dankbetuuging

There is no end to the minuteness, which you can unveil through physical investigation, for the simple reason that the investigation itself is what is chopping things into pieces.

- Alan Watts